# Towards a thermally complete study of inflationary predictions

Inaugural dissertation
of the Faculty of Science,
University of Bern

presented by

**Simona Procacci**

from Oberburg BE

Supervisor of the doctoral thesis
**Prof. Dr. Mikko Laine**

**Albert Einstein Center for Fundamental Physics**
**Institute for Theoretical Physics, University of Bern**

Accepted by the Faculty of Science.

Bern, 01.09.2023

The Dean
Prof. Dr. Marco Herwegh

source: https://doi.org/10.48549/4522 | downloaded: 3.7.2025

*Dedicated to the memory of*
*my grandfather Jürg Joss.*

This work is licensed under the Creative Commons Attribution 4.0 International License.
http://creativecommons.org/licenses/by/4.0/

**Abstract**

This monograph presents theoretical efforts aiming at precision probes for the model of cosmological inflation. The latter is considered for its virtue of explaining the origin of primordial perturbations. However, the description of the transition from a vacuum- to a radiation-dominated universe is not yet robust. Asking for a realistic framework, we study the effects of including interactions among the inflaton field and a thermal plasma.

The concrete setup is the one of [1], where we investigate the dynamics of inflation in the presence of a heat bath. In [3] real-time lattice simulations are used to improve on the estimation of the thermal friction felt by the inflaton field. We compute the contributions to the gravitational wave signal from the warming-up period after inflation [2], and implement thermal corrections to tensor fluctuations produced during inflation [4]. Depending on the maximal temperature reached after inflation, the high-frequency part of [2] can be constrained with $N_{\rm eff}$, whereas the low-frequency part of [4] may be probed with LISA or ET. To explore these prospects, in [5] we study the dependence of the temperature evolution on the confinement scale of the gauge plasma.

The text presented here shows partial overlap with the published material. Nonetheless, the exposition commits to be self-contained, including a pedagogical review of cosmological perturbation theory and inflation, and deriving results through detailed calculations.

**List of publications**

[1] M. Laine and S. Procacci, *Minimal warm inflation with complete medium response*, JCAP 06 (2021), 031 [2102.09913].

[2] P. Klose, M. Laine and S. Procacci, *Gravitational wave background from non-Abelian reheating after axion-like inflation*, JCAP 05 (2022), 021 [2201.02317].

[3] M. Laine, L. Niemi, S. Procacci and K. Rummukainen, *Shape of the hot topological charge density spectral function*, JHEP 11 (2022), 126 [2209.13804].

[4] P. Klose, M. Laine and S. Procacci, *Gravitational wave background from vacuum and thermal fluctuations during axion-like inflation*, JCAP 12 (2022), 020 [2210.11710].

[5] H. Kolesova, M. Laine and S. Procacci, *Maximal temperature of strongly-coupled dark sectors*, JHEP 05 (2023), 239 [2303.17973].

# Contents

**Notation** **iv**

**List of symbols** **v**

**1 Introduction** **1**

**2 Dynamics of small perturbations in cosmology** **3**
2.1 Flat FLRW metric perturbations . . . . . 6
2.2 Energy-momentum tensor perturbations . . . . . 9
2.3 Einstein's equations . . . . . 12

**3 Origin of primordial perturbations from vacuum fluctuations** **16**
3.1 Cosmological inflation . . . . . 17
3.2 Scalar perturbations . . . . . 20
3.3 Tensor perturbations . . . . . 26
3.4 Observational constraints . . . . . 30

**4 A thermal treatment of the inflationary epoch** **36**
4.1 Inflaton evolution in the presence of a thermal bath . . . . . 37
4.2 Perturbative thermodynamics for a thermalized inflaton . . . . . 40
4.3 Heat bath equation of motion . . . . . 42

**5 Example: axion-like inflation** **44**
5.1 CMB constraints on inflaton mass and decay constant . . . . . 47
5.2 Friction coefficient and mass correction . . . . . 49
5.3 Non-perturbative thermodynamics for a radiation bath . . . . . 52
5.4 Numerical results and parameter scan . . . . . 54

**6 Gravitational waves from thermal processes** **58**
6.1 During inflation . . . . . 59
6.2 During reheating . . . . . 66

**7 Conclusions** **75**
7.1 Overview . . . . . 75
7.2 Outlook . . . . . 77

**Appendix** **78**

**A Cosmological perturbation theory** **78**
A.1 Coordinate transformations . . . . . 78
A.2 Computing the Einstein tensor for a FLRW metric . . . . . 80
A.3 Simplifying Einstein's equations for scalar perturbations at inflation . . . . . 85
A.4 Statistical properties of small perturbations . . . . . 86

**B The retarded pseudoscalar correlator** **92**
B.1 Imaginary part: Chern-Simons diffusion rate . . . . . 92
B.2 Real part: thermal mass correction . . . . . 99

**C Gravitational wave production via scatterings** **104**
C.1 Feynman rules . . . . . 104
C.2 Matrix elements . . . . . 107

**Bibliography** **113**

**Acknowledgements** **120**

# Notation and conventions

Indices denoted by Greek letters run from 0 to 3, describing the components on the four-dimensional space-time. Roman letters are used for spatial indices and run from 1 to 3. Repeated indices are summed over. Analytical computations are performed using natural units, where

$$c = \hbar = k_{\rm B} = 1 \ ,$$

but retaining the Planck mass $m_{\rm pl}$. For any physical quantity $Q$ we denote:

| Symbol | Definition | Page |
|---|---|---|
| $\boldsymbol{Q}$ | $= (Q_1, Q_2, Q_3)$, 3-dimensional vector | 4 |
| $\dot{Q}$ | $= \partial_t Q$ derivative with respect to time in standard FRLW coordinates | 4 |
| $Q'$ | $= \partial_\tau Q$ derivative with respect to conformal time | 4 |
| $Q_{,i}$ | $= \partial_i Q$ derivative with respect to $i$-th spatial direction | 4 |
| $Q_{;\mu}$ | $= D_\mu Q$, covariant derivative with respect to $x^\mu$ | 4 |
| $\bar{Q}$ | Unperturbed quantity | 5 |
| $\delta Q$ | First order perturbation | 5 |
| $Q^{\rm t}_{ij}$ | Symmetric, transverse and traceless tensor $Q^{{\rm t},i}_{ij} = Q^{{\rm t}\,i}_{i} = 0$ | 6 |
| $\tilde{Q}$ | Gauge transformed quantity | 7 |
| $\widehat{Q}$ | $= aQ$, where $a$ is the scale factor | 22 |

For classical computations in comoving momentum space we use the Minkowski metric $\eta_{\mu\nu}$ with sign convention $\eta_{00} = -1$. The Fourier expansion is carried out in spatial coordinates,

$$Q(\tau,\mathbf{x}) = \int_{\mathbf{k}} Q(\tau,\mathbf{k})\, e^{i\mathbf{k}\cdot\mathbf{x}} \ , \qquad \int_{\mathbf{k}} \equiv \int \frac{{\rm d}^3k}{(2\pi)^3} \ ,$$
$$Q(\tau,\mathbf{k}) = \int_{\mathbf{x}} Q(\tau,\mathbf{x})\, e^{-i\mathbf{k}\cdot\mathbf{x}} \ , \qquad \int_{\mathbf{x}} \equiv \int {\rm d}^3x \ .$$

Fields are quantized in a local Minkowski frame denoted by $\mathcal{X} = (t,\mathbf{x})$, where the sign convention is $\eta_{00} = +1$, and the Fourier expansion is defined in four dimensions, $\mathcal{K} = (\omega,\mathbf{k})$,

$$Q(\mathcal{X}) = \int_{\mathcal{K}} Q(\mathcal{K})\, e^{i(\omega t - \mathbf{k}\cdot\mathbf{x})} \ , \qquad \int_{\mathcal{K}} \equiv \int \frac{{\rm d}\omega}{2\pi} \int_{\mathbf{k}} \ ,$$
$$Q(\mathcal{K}) = \int_{\mathcal{X}} Q(\mathcal{X})\, e^{-i(\omega t - \mathbf{k}\cdot\mathbf{x})} \ , \qquad \int_{\mathcal{X}} \equiv \int {\rm d}t \int_{\mathbf{x}} \ .$$

In general we omit hats on quantum operators (hats are rather used as in the last entry of the table above), with the exceptions of the Hamiltonian $\hat{H}$ (to be distinguished from the Hubble parameter) and the density matrix $\hat{\rho}$.

For some computations it is useful to analytically continue from Minkowski to Euclidean space-time, $t \to -it_{\rm E}$, denoting $X = (t_{\rm E},\mathbf{x})$. The compact time direction is then transformed to a discrete frequency space,

$$Q(X) = \sum\!\!\!\!\!\!\int_{K} Q(K)\, e^{i(\omega_n t_{\rm E} - \mathbf{k}\cdot\mathbf{x})} \ , \qquad \sum\!\!\!\!\!\!\int_{K} \equiv T\sum_{\omega_n} \int_{\mathbf{k}} \ ,$$
$$Q(K) = \int_{X} Q(X)\, e^{-i(\omega_n t_{\rm E} - \mathbf{k}\cdot\mathbf{x})} \ , \qquad \int_{X} \equiv \int_0^\beta {\rm d}t_{\rm E} \int_{\mathbf{x}} \ ,$$

where $\omega_n \equiv 2\pi n T$ are the Matsubara modes, and $\beta \equiv 1/T$ is the Boltzmann factor.

# List of globally defined symbols

The symbols introduced in the different chapters (separated by a horizontal line) and used throughout the entire document are listed below.

| Symbol | Value (SI units) and definition | Page |
|---|---|---|
| $c$ | $\approx 3.00 \times 10^{8}\ \mathrm{m\,s^{-1}}$, velocity of light | iv |
| $\hbar$ | $\approx 1.05 \times 10^{-34}\ \mathrm{kg\,m^{2}\,s^{-1}}$, reduced Planck's constant | iv |
| $k_{\mathrm{B}}$ | $\approx 1.38 \times 10^{-23}\ \mathrm{kg\,m^{2}\,s^{-2}\,K^{-1}}$, Boltzmann constant | iv |
| $m_{\mathrm{pl}}$ | $\approx 2.18 \times 10^{-8}\ \mathrm{kg} \approx 1.22 \times 10^{19}\ \mathrm{GeV\,c^{-2}}$, Planck mass | iv |
| $t_{\mathrm{pl}}$ | $\approx 5.39 \times 10^{-44}$ s, Planck time | 1 |
| $T_{\mathrm{dec}}$ | $\sim 3000$ K, temperature at decoupling | 1 |
| $t_{\mathrm{dec}}$ | $\sim 10^{12}$ s $\sim 3 \times 10^{5}$ y, time at decoupling | 1 |
| $T_0$ | $\approx 2.73$ K, CMB temperature today | 1 |
| $d_{\mathrm{dec}}$ | $\sim 3 \times 10^{23}$ m $\sim 100$ Mpc, size of visible universe at decoupling | 1 |
| $d_0$ | $\sim 4 \times 10^{25}$ m $\sim 14$ Gpc, size of visible universe today | 1 |
| $t$ | Physical time coordinate | 3 |
| $\kappa$ | Spatial curvature | 3 |
| $a$ | Scale factor | 3 |
| $H$ | Hubble constant (time dependent) | 3 |
| $\tau$ | Conformal time | 4 |
| $\eta_{\mu\nu}$ | Minkowski metric | 4 |
| $\mathcal{H}$ | Conformal Hubble constant | 4 |
| $\mathcal{M}_\tau$ | Submanifold of constant conformal time $\tau$ | 4 |
| $n_\mu, t^\mu$ | Normal and tangent vector defining time slicing and space threading | 4 |
| $g_{\mu\nu}, g$ | Metric tensor and its determinant | 4 |
| $\nabla^2$ | $= \eta^{ij}\partial_i\partial_j$ | 4 |
| $\Box_H, \Box_{\mathcal{H}}$ | $\equiv \bar{g}^{\mu\nu} D_\mu D_\nu$, D'Alembert operator in FLRW standard/conformal coordinates | 4 |
| $G^\mu{}_\nu$ | Einstein tensor | 5 |
| $T^\mu{}_\nu$ | Energy-momentum tensor | 5 |
| $G$ | $\approx 6.67 \times 10^{-11}\ \mathrm{m^{3}\,kg^{-1}\,s^{-2}}$, gravitational constant, $G = m_{\mathrm{pl}}^{-2}$ in natural units | 5 |
| $h_{\mu\nu}$ | Perturbations of the Minkowski metric | 6 |
| $\xi^\mu$ | Parameter of coordinate transformation | 7 |
| $\phi, \psi$ | Scalar metric perturbations in Newtonian gauge | 8 |
| $\vartheta_{ij}$ | Tensor metric perturbations in Newtonian gauge | 8 |
| $\Gamma^\rho_{\mu\nu}$ | Christoffel symbols | 8 |
| $R_{\mu\nu}, R$ | Ricci tensor and Ricci scalar | 8 |
| $e$ | Energy density | 10 |
| $p$ | Fluid pressure | 10 |
| $c_s$ | Speed of sound | 10 |
| $u^\mu, v^i$ | Fluid velocity and physical fluid velocity | 10 |
| $\Pi^i{}_j$ | Anisotropic stress tensor | 10 |
| $\mathcal{R}$ | Curvature perturbation | 12 |
| $\Delta$ | Relative energy density perturbation | 12 |
| $k, k/a$ | Comoving momentum and physical momentum | 16 |
| $\varphi$ | Inflaton field | 18 |
| $V(\varphi)$ | Inflaton self-interacting potential | 18 |

| | | |
|---|---|---|
| $\epsilon_V, \eta_V$ | Slow-roll parameters | 19 |
| $N$ | Number of e-folds during inflation | 19 |
| $m$ | Inflaton mass | 18 |
| $f$ | Inflaton perturbation in spatially flat gauge | 22 |
| $\mathrm{w}_{\mathbf{k}}$ | Annihilation (and creation) operator | 23 |
| $\|0\rangle$ | Vacuum state with respect to $\mathrm{w}_{\mathbf{k}}$ | 23 |
| $H_*$ | Hubble constant at horizon exit | 25 |
| $\mathcal{P}_{\mathcal{R}}$ | Primordial power spectrum of curvature perturbations | 25 |
| $\epsilon_{ij}^{\lambda}$ | Tensors of helicity $\lambda \in \{+, \times\}$ building helicity basis | 26 |
| $h_\lambda$ | Tensor perturbation of helicity $\lambda$ | 26 |
| $\mathbb{L}_{\alpha\beta;\mu\nu}$ | Projection operator onto transverse and traceless tensor components | 27 |
| $\mathbb{K}_{\alpha\beta}$ | Projection operator onto perpendicular vectors | 27 |
| $\mathcal{P}_{\mathrm{T}}$ | Tensor perturbation spectrum | 27 |
| $h_{<,>}$ | Short and long-distance fluctuations | 28 |
| $G_{\mathrm{R}}$ | Retarded Green's function | 29 |
| $\mathcal{T}$ | Transfer function | 31 |
| $A_s$ | Amplitude of primordial power spectrum of scalar perturbations | 33 |
| $n_s$ | Tilt of primordial power spectrum of scalar perturbations | 33 |
| $r$ | Ratio of tensor and scalar spectral amplitudes | 33 |
| $\Omega_{\mathrm{GW}}$ | Observable power spectrum for gravitational waves today | 34 |
| $f_0$ | Physical frequency today | 34 |
| $N_{\mathrm{eff}}$ | Effective number of neutrino species | 35 |
| $\mathcal{L}$ | Lagrangian | 36 |
| $V_0(\varphi)$ | Tree-level inflaton potential | 36 |
| $J$ | Coupling of heat bath to the inflaton field | 36 |
| $\Upsilon$ | Friction coefficient | 36 |
| $m_{\mathrm{T}}$ | Thermal mass | 37 |
| $\hat{H}$ | Hamiltonian | 38 |
| $\mathcal{Z}$ | Partition function | 41 |
| $\epsilon_k$ | $= \sqrt{k^2 + m^2}$ | 40 |
| $t_{\mathrm{E}}$ | $\equiv it$ imaginary time coordinate | 41 |
| $n_{\mathrm{B}}(x)$ | $\equiv 1/(e^{x/T} - 1)$ Bose distribution | 41 |
| $s$ | Entropy density | 42 |
| $g_*, h_*$ | Number of relativistic degrees of freedom | 43 |
| $T_c$ | Critical temperature | 43 |
| $u$ | Volume fraction in mixed phase | 43 |
| $f_a$ | Decay constant of axion-like particle | 44 |
| $\alpha$ | $\equiv g^2/(4\pi)$ coupling constant of gauge sector | 45 |
| $F_{\mu\nu}^a$ | Non-Abelian Yang-Mills field strength tensor | 45 |
| $\Lambda_{\mathrm{UV}}$ | $\sim \sqrt{m f_a}$ confinement scale of broken gauge group | 45 |
| $\Lambda_{\mathrm{IR}}$ | Confinement scale of unbroken $SU(N_c)$ | 45 |
| $Q, \chi$ | Topological charge and susceptibility from non-Abelian gauge sector | 45 |
| $d_A$ | $\equiv N_c^2 - 1$ color factor | 49 |
| $c_\chi$ | $\equiv 1/(64\pi^2)$ | 50 |
| $t_{\mathrm{ref}}$ | Reference time given by the Hubble parameter at the beginning of inflation | 54 |
| $\eta, \zeta$ | Shear and bulk viscosity | 60 |
| $\delta(\mathcal{P})$ | Normalized $\delta$-distribution so that $\int_{\mathcal{P}} \delta(\mathcal{P}) \equiv 1$ | 68 |

# Chapter 1

# Introduction

Any history of the universe begins with something we do not properly understand, let us simply call this moment in space and time the *initial singularity*, and assume the immediately subsequent cosmos to be in an initial quantum state until $t_{\rm pl} \sim 10^{-44}\,\mathrm{s}$ [6]. The present work enters the plethora of modern efforts to grasp the gap between the initial quantum state and the beginning of the, theoretically more established, thermal history of the early universe.

The latter starts at $t \sim 10^{-10}\,\mathrm{s}$ [7, p.35], when Standard Model particles filled the universe, forming an extremely hot and dense environment, that was expanding and cooling (see fig. 1.1 for an illustration). In these conditions we expect to find a plasma, where radiation interacts with fully ionised matter via Thomson scatterings [8]. As the universe cools down to $T_{\rm dec} \sim 3000\,\mathrm{K}$,

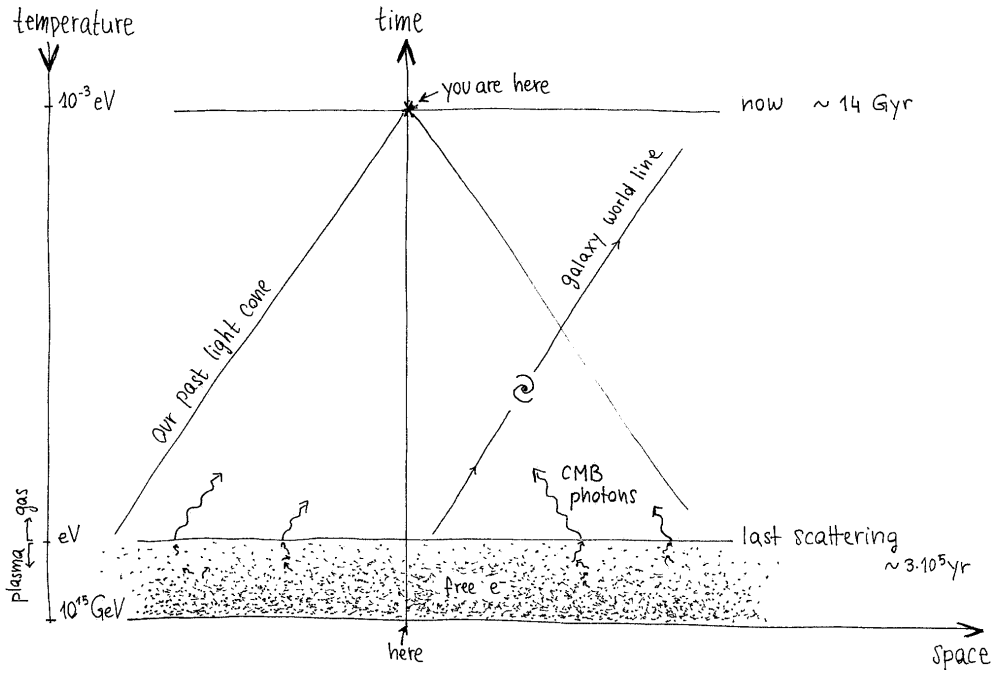


Figure 1.1: Sketch of the different processes involved in the origin of the CMB.

around $t_{\rm dec} \sim 300'000$ years after $t_{\rm pl}$, matter and radiation decouple as the free electrons combine with the positive particles in the plasma to form a gas [9]. The universe becomes thus transparent to photons, that from this moment on travel freely across space and time, allowing us to sample

our universe at $t \geq t_{\rm dec}$.

In particular, the radiation that decoupled at $t_{\rm dec}$ is observed today as a background signal in the microwave frequency range, redshifted to a black-body temperature of $T_0 = 2.73$ K [10]. We call this the Cosmic Microwave Background (CMB).

Thanks to the CMB, we learn that the universe is homogeneous and isotropic on scales that correspond to 1% of the visible size.[1] Temperature fluctuations of the order of $\delta T/\bar{T} \sim 10^{-5}$ are observed at smaller scales [11]. The large-scale structure in the present universe may have formed via gravitational collapse of these early density perturbations. Their evolution can be studied following a perturbative approach within general relativity, as long as they are small. For the origin of primordial perturbations standard cosmology does however not provide an explanation.

The model of inflation suggests how the perturbations in the CMB could result from vacuum fluctuations in an early epoch of exponential expansion. Inflationary predictions can be tested experimentally not only thanks to the CMB and the study of the large-scale structure of the universe, but also by measuring the abundance of light elements. Another important probe is expected in the next decades by the detection of a gravitational wave background signal. On the theoretical side, a realistic and robust framework for inflation is not yet established, and we should pursue it as meticulously as required for the construction of a new generation of detectors.

In this spirit, here we study the impact of interactions between the inflaton field and a thermal plasma, seeking to identify a plausible mechanism for transitioning from an epoch of exponential expansion to one of radiation domination.

## Structure of this work

While it may seem more natural to first explore the origin of perturbations and then move onto their evolution, our approach is to start in chapter 2 with a review of classical perturbations and their dynamics in cosmology. This provides a natural framework for the introduction of inflation, which we review in sec. 3.1 in its simplest realization. A step-by-step derivation of standard results for the primordial power spectrum of scalar and tensor perturbations is presented in secs. 3.2 and 3.3, offering a fresh perspective on the topic. Appendix A supplies additional material, while observational implications are briefly discussed in sec. 3.4.

Chapter 4 introduces our specific scenario, in which a generic thermal plasma is weakly coupled to the inflaton. An effective evolution equation for the inflaton field is derived in sec. 4.1. In sec. 4.2, we explore the possibility of the inflaton field undergoing thermalization, and analyze its impact on the thermodynamic functions of the system. Finally, sec. 4.3 deals with the evolution equations governing the behavior of the heat bath, distinguishing the case where a phase transition occurs within the plasma. The example of axion-like inflation is used in chapter 5 to present a viable inflationary scenario, that is capable of dynamically implementing a heating-up period. The details on the evaluation of the friction coefficient $\Upsilon$ and the mass correction entering the dynamics are left for appendix B. While secs. 5.1, 5.2 and 5.3 are dedicated to the determination of the coefficients entering the evolution equations, sec. 5.4 presents benchmark results.

The implications of our framework for the generation of gravitational waves are studied in chapter 6, both for the inflationary phase (sec. 6.1) and the reheating phase (sec. 6.2). The calculations for the latter are presented in appendix C. Chapter 7 provides a summary of the main findings and concluding remarks.

[1] While the CMB radiation was travelling to us, the size of our visible universe has been expanding from $d_{\rm dec} \sim 100$ Mpc $\sim 3 \times 10^{26}$cm to today's value of $d_0 \sim 14$ Gpc $\sim 4 \times 10^{28}$ cm, and it is homogeneous at scales $\sim 200$ Mpc.

# Chapter 2

# Dynamics of small perturbations in cosmology

The present chapter aims to evaluate Einstein's equations for small perturbations around the homogeneous and isotropic background.

The general procedure in cosmology assumes that, as long as the inhomogeneities are relatively small, we call them *perturbations* and study their evolution using linear *perturbation theory*, where higher powers of small quantities are neglected.[2] General relativity inevitably leads to an ambiguity in the choice of the coordinates, considered in appendix A.1. The perturbative method is applied in secs. 2.1 and 2.2, where respectively we define metric and energy-momentum tensor perturbations. The resulting Einstein's equations are presented in sec. 2.3. A step by step derivation of the Einstein tensor can be found in appendix A.2.

All the computations in this chapter are performed using flat ($\kappa = 0\ \mathrm{m}^{-2}$) conformal FLRW coordinates, cf. eq. (2.3). The assumption of flatness is justified empirically for all observable epochs in the history of the universe [12]. These do not include the inflationary epoch. Therefore, when we present the model of inflation in chapter 3, we allow for non-flat initial conditions and show how, independently of them, the universe becomes flat after inflation.

The gravitational growth depends on the equation of state and the streaming lengths[3] of the stuff filling the early universe [12]. Since the precise nature of the dominant components to the energy density remains an open question, here we use a general equation of state, cf. eq. (2.72).

## The background, homogeneous and isotropic universe

Before analysing perturbations, let us introduce the unperturbed background universe. An expanding homogeneous and isotropic universe is described by the Friedmann-Lemaître-Robertson-Walker (FLRW) metric

$$\mathrm{d}s^2_{\mathrm{FLRW}} = -\mathrm{d}t^2 + a^2(t)\,\mathrm{d}\mathbf{x}^2_\kappa\ , \qquad \mathrm{d}\mathbf{x}^2_\kappa = \frac{\mathrm{d}r^2}{1-\kappa r^2} + r^2\,\mathrm{d}\mathbf{\Omega}^2\ , \tag{2.1}$$

where $\kappa$ is a constant representing the curvature of space, $\kappa = 0\ \mathrm{m}^{-2}$ for the flat case, and $\mathrm{d}\mathbf{\Omega}^2 = \mathrm{d}\theta^2 + \sin^2\theta\mathrm{d}\phi^2$ is the unit solid angle. The parameter $a(t)$ is the (dimensionless) scale factor, and its relative change in time is called the Hubble parameter,

$$H \equiv \frac{\dot{a}}{a}\ , \tag{2.2}$$

[2] More details can be found in [13]. For generalisations to the second order see e.g. [14].

[3] Particle mean free paths between interactions. In addition, the growth is also affected by pressure forces.

where dots denote time derivatives. Conformal coordinates are defined via the conformal time $\tau$,

$$\mathrm{d}\tau \equiv \frac{\mathrm{d}t}{a(t)} \qquad \Rightarrow \quad \mathrm{d}s^2_{\mathrm{FLRW}} = a^2(\tau)\left[\, -\mathrm{d}\tau^2 + \mathrm{d}\mathbf{x}^2_\kappa \,\right] . \tag{2.3}$$

Choosing a positive-definite cosmic time $t \in [0, \infty)$, the conformal time coordinate $\tau$ takes also negative values. For $\kappa = 0\ \mathrm{m}^{-2}$, the metric in eq. (2.3) is related to the Minkowski metric by a conformal transformation. For classical computations we adopt the sign convention

$$\eta_{\mu\nu} = \mathrm{diag}(-1,\ 1,\ 1,\ 1) . \tag{2.4}$$

Let us denote derivatives with respect to conformal time with primes, $\partial_\tau \equiv {}'$, and introduce

$$\mathcal{H} \equiv \frac{a'}{a} , \tag{2.5}$$

the conformal Hubble parameter. From eq. (2.3) we obtain relations between the Hubble parameter and its conformal counterpart, where $Q$ is an arbitrary physical quantity,

$$\mathcal{H} = aH , \qquad \mathcal{H}' = a^2(H^2 + \dot{H}) = a\ddot{a} , \tag{2.6}$$

$$\mathcal{H}^{-1}Q' = H^{-1}\dot{Q} , \qquad Q'' = a^2(H\dot{Q} + \ddot{Q}) . \tag{2.7}$$

The so defined space-time manifold for the background universe can be conveniently *sliced* into a family of space-like submanifolds $\mathcal{M}_\tau$ of constant conformal time $\tau$.[4] In a homogeneous and isotropic universe all physical quantities only depend on $\tau$. Therefore, on each $\mathcal{M}_\tau$, unperturbed quantities reduce to constants.

Spatial coordinates give the threading of the space-time into $x^i = \mathrm{const}$ threads, as illustrated in figure 2.1. At each space-time point $p$ we find a covector $n_\mu$ normal to the corresponding time slice $\mathcal{M}_\tau$, and a vector $t^\mu$ tangent to the thread passing through $p$,

$$n_\mu = |n|\,(1, \mathbf{0}) , \qquad t^\mu = |t|\,(1, \mathbf{0}) . \tag{2.8}$$

They can be normalized to unit length with $g^{\mu\nu}n_\mu n_\nu = g_{\mu\nu}t^\mu t^\nu = -1$ (see eqs. (2.33) and (2.34)).

For the unperturbed universe, computations are performed in a locally conformally flat frame, where for any (symmetric) tensorial quantity $Q$ we denote

$$Q^i = \delta^{ij}Q_j = Q_i \ , \ \ldots \ , \qquad \nabla^2 Q \equiv \partial^i\partial_i Q , \qquad \mathrm{tr}\ Q_{ij} = \mathrm{tr}\ Q^{ij} \equiv Q^i_i . \tag{2.9}$$

It is useful to distinguish the d'Alembert (box) operator with respect to the background metric in standard and conformal FRLW coordinates. Denoting by $\bar{g}_{\mu\nu}$ the background metric given by eq. (2.1) or eq. (2.3), and $\bar{g} \equiv \det \bar{g}_{\mu\nu}$, we obtain respectively,

$$\begin{aligned} \Box_H Q \equiv \bar{g}^{\mu\nu} D_\mu D_\nu Q &= \frac{1}{\sqrt{-\bar{g}}}\partial_\mu\left(\sqrt{-\bar{g}}\bar{g}^{\mu\nu}\partial_\nu Q\right) = a^{-3}\left[\partial_t(-a^3\dot{Q}) + \partial_i(aQ^{,i})\right] \\ &= -\ddot{Q} - 3H\dot{Q} + a^{-2}\nabla^2 Q , \end{aligned} \tag{2.10}$$

$$\Box_{\mathcal{H}} Q = a^{-4}\left[\partial_\tau(-a^2Q') + \partial_i(a^2Q^{,i})\right] = a^{-2}\left(-Q'' - 2\mathcal{H}Q' + \nabla^2 Q\right) . \tag{2.11}$$

Derivatives are denoted by $\partial_\mu Q = Q_{,\mu}$, while $D_\mu Q = Q_{;\mu}$ is the covariant derivative.

[4] An introduction to the topic of time-foliation can be found e.g. in [15].

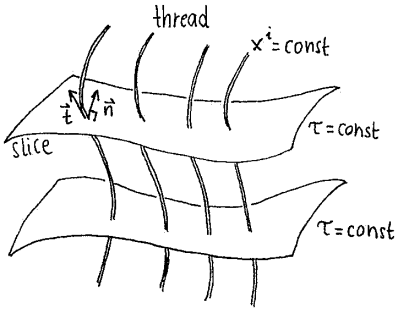


Figure 2.1: Sketch of the time slicing and spatial threading of the space-time in $D = 2{+}1$ dimensions.

## Components of perturbations

We now switch on spatial fluctuations on top of the constant background on $\mathcal{M}_\tau$ and assume that any physical quantity $Q(x)$ can be decomposed into the sum

$$Q(\tau, \mathbf{x}) = \bar{Q}(\tau) + \delta Q(\tau, \mathbf{x}) + \mathcal{O}(\delta^2) \tag{2.12}$$

of a homogeneous and isotropic quantity $\bar{Q}(\tau)$, and a small (linear) perturbation $\delta Q(\tau, \mathbf{x})$. The same procedure should be applied to the metric tensor describing the geometry of space-time, whose zeroth order part is given by eq. (2.3). Therefore, indices are raised and lowered using the perturbed metric. However, at linear order metric perturbations only act on background quantities $\bar{Q}$, so that for $\delta Q$ we maintain the notation introduced in eqs. (2.9)–(2.11).

Within the perturbative method, the laws of physics are linearized around the background. Subtracting the Einstein equations of general relativity at zeroth order from the ones for the full theory we obtain the first-order equations,

$$\delta G^\mu{}_\nu = 8\pi G \delta T^\mu{}_\nu \ , \tag{2.13}$$

where $G$ denotes the gravitational constant. This set of equations describes the evolution of primordial perturbations towards the large-scale structures we observe today.

### Scalars

The first-order decomposition of a scalar quantity $A(\tau, \mathbf{x})$ accordingly to eq. (2.12) gives

$$A(\tau, \mathbf{x}) = \bar{A}(\tau) + \delta A(\tau, \mathbf{x}) + \mathcal{O}(\delta^2) \ . \tag{2.14}$$

### Vectors

An arbitrary 4-(co)vector $B^\mu = (B^0, B^i)$ is made of a scalar temporal component $B^0$ and of a spatial 3-vector component on $\mathcal{M}_\tau$. Applying the decomposition introduced in (2.12), note that spatial components of background quantities vanish as there is no preferred direction,

$$B^\mu(\tau, \mathbf{x}) = \bar{B}^\mu(\tau) + \delta B^\mu(\tau, \mathbf{x}) + \mathcal{O}(\delta^2) \ , \qquad \bar{B}^\mu = (\bar{B}^0, \ \mathbf{0} \ ) \ , \quad \delta B^\mu = (b^0, \delta B^i) \ , \quad b^0 \equiv \delta B^0 \ , \tag{2.15}$$

and $\partial_i \bar{B}^0 = 0$ for all spatial directions $i = 1, 2, 3$. With respect to the flat-space metric, $\delta B^i$ can be further decomposed into a curl-free and a divergence-free part,

$$b^i \equiv \delta B^i = b^i_{\rm s} + b^i_{\rm v} \ , \qquad b^i_{\rm s} = -\partial^i b = -b^{,i} \ , \quad \partial_i b^i_{\rm v} = 0 \ , \tag{2.16}$$

denoted as the *scalar* $b^{\rm s}_i$ ($b$ is a scalar) and *vector* $b^{\rm v}_i$ parts of the spatial perturbations $\delta B^i$ [16]. In Euclidean space, this decomposition follows from Helmoltz's theorem [17, p.97]. All together we have two scalars $\{b^0, b\}$ and one divergenceless 3-vector $b^i_{\rm v}$.

**Higher order tensors**

For the purposes of the present treatise, it is enough to consider rank-2 tensors $C_{\mu\nu}$. Restricting moreover to symmetric tensors $C_{\mu\nu} = C_{\nu\mu}$, in four dimensions we are dealing with ten independent components. We define

$$C_{\mu\nu}(\tau,\mathbf{x}) = \bar{C}_{\mu\nu}(\tau) + \underbrace{\delta C_{\mu\nu}(\tau,\mathbf{x})}_{\left.\begin{array}{l}\delta C_{00} \equiv -2c_0 \\ \delta C_{0i} = \delta C_{i0} \equiv -c_i \\ \delta C_{ij} \equiv -2\delta_{ij}c_{\rm D} + 2\gamma_{ij}\end{array}\right\} \Rightarrow \quad \delta C_{\mu\nu} = \left(\begin{array}{c|c} -2c_0 & -c_i \\ \hline -c_i & -2\delta_{ij}c_{\rm D} + 2\gamma_{ij}\end{array}\right)} + \mathcal{O}(\delta^2) \ , \tag{2.17}$$

where $\gamma_{ij} = \gamma_{ji}$ is traceless, $\gamma^i_i = 0$. For the homogeneous and isotropic background it holds

$$\bar{C}_{0i} = \bar{C}_{i0} = 0 \ , \quad \bar{C}_{ij} = \bar{C}\delta_{ij} \ , \qquad \partial_i\bar{C} = \partial_i\bar{C}_{00} = 0 \ \ \forall i = 1,2,3 \ . \tag{2.19}$$

The 3-vector $c_i$ can be decomposed as discussed above,

$$c_i = c^{\rm s}_i + c^{\rm v}_i \ , \qquad c^{\rm s}_i = -\partial_i c \ , \quad \partial^i c^{\rm v}_i = 0 \ , \tag{2.20}$$

while the traceless 3-tensor $\gamma_{ij}$ can be written in terms of scalar, 3-vector and 3-tensor parts,[5]

$$\gamma_{ij} = \gamma^{\rm s}_{ij} + \gamma^{\rm v}_{ij} + \gamma^{\rm t}_{ij} \ , \tag{2.21}$$

$$\gamma^{\rm s}_{ij} = \left(\partial_i\partial_j - \delta_{ij}\nabla^2/3\right)\gamma \ , \tag{2.22}$$

$$\gamma^{\rm v}_{ij} = -\frac{1}{2}\left(\partial_i\gamma_j + \partial_j\gamma_i\right) \ , \qquad \partial^i\gamma_i = 0 \ , \tag{2.23}$$

$$\gamma^{{\rm t}\,i}{}_{i} = 0 \ , \quad \partial^i\gamma^{\rm t}_{ij} = 0 \ . \tag{2.24}$$

To sum up, for symmetric tensors we have four scalar degrees of freedom $\{c_0, c_{\rm D}, c, \gamma\}$, two 3-vector degrees of freedom $\{c^{\rm v}_i, \gamma_i\}$ with one constraint each, and one 3-tensor degree of freedom $\gamma^{\rm t}_{ij}$ with four constraints in total. As a crosschek, we are left with $4 + 2\times(3-1) + (6-4) = 10$ free variables. Among these only 6 are physical, i.e. non-redundant via coordinate transformations, as we show in appendix A.1. The strange-looking minus and factor-of-two conventions in eq. (2.18) are introduced to simplify the notation in sec. 2.1, and the gauge transformations in appendix A.1.

## 2.1 Flat FLRW metric perturbations

The fluctuations of the spatially flat FLRW metric in conformal coordinates can be computed with eqs. (2.18)–(2.24). Let us introduce the notation

$$g_{\mu\nu} = \bar{g}_{\mu\nu} + \delta g_{\mu\nu} = a^2\left(\eta_{\mu\nu} + h_{\mu\nu}\right) \ , \tag{2.25}$$

where $\eta_{\mu\nu}$ is the Minkowski metric and $h_{\mu\nu}$ its perturbation. The dimensionless scale factor $a$ is normally defined as unperturbed.

Now, the identification of points in the two different space-times $g_{\mu\nu}$ and $\bar{g}_{\mu\nu}$ is gauge-dependent, as discussed in appendix A.1. The quantity $\delta g_{\mu\nu}$ is therefore not a tensor, neither is $h_{\mu\nu}$. To find the inverse $\ell^{\mu\nu} \equiv a^2 g^{\mu\nu} - \eta^{\mu\nu}$ we solve

$$g^{\mu\rho}g_{\rho\nu} \equiv \delta^\mu_\nu \qquad \Rightarrow \quad \eta_{\rho\nu}\ell^{\mu\rho} = -\eta^{\mu\rho}h_{\rho\nu} \quad \Rightarrow \quad \ell^{\mu\sigma} = -\eta^{\mu\rho}\eta^{\sigma\nu}h_{\rho\nu} \equiv -h^{\mu\sigma} \ . \tag{2.26}$$

[5] As many authors only consider scalar perturbations, the convention of e.g. [12] and others is different: $\delta C^{\rm RG}_{ij} = -2\delta_{ij}c^{\rm RG}_{\rm D} + 2\gamma^{\rm RG}_{,ij}$, where $\gamma^{\rm RG}_{,ij}$ is not traceless. However, since the traceless part of $\gamma^{\rm RG}$ agrees with our $\gamma$, we find the relations $\gamma = \gamma^{\rm RG}$ and $c_{\rm D} = c^{\rm RG}_{\rm D} - (\nabla^2\gamma^{\rm RG})/3$ among the two conventions.

Up to linear order, the inverse metric decomposes then as

$$g^{\mu\nu} = \bar{g}^{\mu\nu} + \delta g^{\mu\nu} = a^{-2}(\eta^{\mu\nu} - h^{\mu\nu}) \ . \tag{2.27}$$

To recover the scalar-vector-tensor decomposition, cf. eq. (2.18), we define[6]

$$h_{00} = -2h_0 \ , \tag{2.28}$$
$$h_{0i} = h_{i0} = -h_i \ , \tag{2.29}$$
$$h_{ij} = 2(-\delta_{ij}h_{\rm D} + \vartheta_{ij}) \ . \tag{2.30}$$

In matrix form the metric and its inverse are hence given by

$$g_{\mu\nu} = a^2(\tau)\begin{pmatrix} -1-2h_0 & -h_i \\ -h_i & (1-2h_{\rm D})\delta_{ij} + 2\vartheta_{ij} \end{pmatrix} \ , \tag{2.31}$$
$$g^{\mu\nu} = a^{-2}(\tau)\begin{pmatrix} -1+2h_0 & -h_i \\ -h_i & (1+2h_{\rm D})\delta_{ij} - 2\vartheta_{ij} \end{pmatrix} \ . \tag{2.32}$$

We can now normalize the two vectors defining the slicing and threading of space-time (cf. eq. (2.8)). Recalling that $n^\mu$ is normal to the slices of constant conformal time $\tau$, while $t^\mu$ is tangent to the threads of constant spatial directions $x^i$, we find

$$n^\mu = a^{-1}(-1+h_0, h_i) \ , \qquad n_\mu = a\,(1+h_0, \mathbf{0}) \ , \tag{2.33}$$
$$t^\mu = a^{-1}(1-h_0, \mathbf{0}) \ , \qquad t_\mu = a\,(-1-h_0, -h_i) \ . \tag{2.34}$$

The normal and thread vectors differ by the shift vector $h_i$, while $h_0$ gives the proper time separation between the slices, taken along the thread.

The $0i$ and $ij$-components of the metric can be further decomposed, cf. eqs. (2.20)–(2.24),

$$h_i = -\partial_i h + h_i^{\rm v} \ , \qquad \partial^i h_i^{\rm v} = 0 \ , \tag{2.35}$$
$$\vartheta_{ij} = \vartheta_{ij}^{\rm s} + \vartheta_{ij}^{\rm v} + \vartheta_{ij}^{\rm t} \ , \qquad \vartheta_{ij}^{\rm s} = \left(\partial_i\partial_j - \delta_{ij}\nabla^2/3\right)\vartheta \ , \tag{2.36}$$
$$\vartheta_{ij}^{\rm v} = -\frac{1}{2}\left(\partial_i\vartheta_j + \partial_j\vartheta_i\right) \ , \qquad \partial^i\vartheta_i = 0 \ , \tag{2.37}$$
$$\vartheta^{{\rm t}\,i}_{\ \ i} = 0 \ , \qquad \partial^i\vartheta_{ij}^{\rm t} = 0 \ . \tag{2.38}$$

Under small coordinate transformations $\tilde{x}^\mu = x^\mu + \xi^\mu$ they transform as derived in appendix A.1. The background values can be found by rescaling the zeroth-order components of eq. (2.31): $\bar{C}_{00} = (-a^2)/a^2 = -1$ , $\bar{C} = (a^2)/a^2 = 1$ and $\bar{C}'_{00} = -2a'/a$ , $\bar{C}' = 2a'/a$. We obtain

$$\tilde{h}_0 = h_0 - \xi^{0\prime} - \frac{a'}{a}\xi^0 \ , \tag{2.39}$$
$$\tilde{h}_i = h_i + \xi_i' - \partial_i\xi^0 \qquad \overset{(A.7)}{\Longrightarrow} \qquad \tilde{h} = h + \xi' + \xi^0 \ , \tag{2.40}$$
$$\tilde{h}_i^{\rm v} = h_i^{\rm v} + \xi_i^{{\rm v}\prime} \ , \tag{2.41}$$
$$\tilde{h}_{\rm D} = h_{\rm D} - \frac{1}{3}\nabla^2\xi + \frac{a'}{a}\xi^0 \ , \tag{2.42}$$
$$\tilde{\vartheta}_{ij} = \vartheta_{ij} - \frac{1}{2}(\partial_i\xi_j + \partial_j\xi_i) - \frac{1}{3}\nabla^2\xi \qquad \Longrightarrow \qquad \tilde{\vartheta} = \vartheta + \xi \ , \tag{2.43}$$
$$\tilde{\vartheta}_i = \vartheta_i + \xi_i^{\rm v} \ , \tag{2.44}$$
$$\tilde{\vartheta}_{ij}^{\rm t} = \vartheta_{ij}^{\rm t} \ . \tag{2.45}$$

[6] Another notation frequently used in the literature, see e.g. [18, p.224], is $h_{00} = -2A$, $h_{0i} = h_{i0} = -B_i$ and $h_{ij} = 2(-D\delta_{ij} + E_{ij})$, or variations thereof.

## Newtonian gauge

An intuitive gauge choice is the one where the perturbed metric can be described by an almost diagonal matrix. The conformal Newtonian gauge satisfies this requirement for scalar perturbations, imposing the two gauge conditions

$$\boxed{h^{\mathrm{N}} = \vartheta^{\mathrm{N}} = 0}\,. \tag{2.46}$$

We consider the gauge transformation from an arbitrary gauge to the Newtonian gauge. From eq. (2.40) and eq. (2.43) we get

$$\xi = -\vartheta\ , \qquad \xi^0 = \vartheta' - h\ . \tag{2.47}$$

The remaining scalar quantities transform to

$$\phi \equiv h_0^{\mathrm{N}} = h_0 - (\vartheta' - h)' - \frac{a'}{a}(\vartheta' - h) = h_0 + \frac{1}{a}\left[(h - \vartheta')a\right]'\ , \tag{2.48}$$

$$\psi \equiv h_{\mathrm{D}}^{\mathrm{N}} = h_{\mathrm{D}} + \frac{1}{3}\nabla^2\vartheta + \frac{a'}{a}(\vartheta' - h)\ , \tag{2.49}$$

and define two gauge invariant quantities, known as the Bardeen potentials [16]. Gauge invariance can be proven by using the relation $\tilde{\vartheta}' - \tilde{h} = \vartheta' - h - \xi^0$, yielding

$$\tilde{\phi} = h_0 - \xi^{0\prime} - \frac{a'}{a}\xi^0 + \frac{1}{a}\left[(h + \xi^0 - \vartheta')a\right]' = \phi - \xi^{0\prime} - \frac{a'}{a}\xi^0 + \frac{1}{a}\left(\xi^0 a\right)' = \phi\ , \tag{2.50}$$

$$\tilde{\psi} = h_{\mathrm{D}} - \frac{1}{3}\nabla^2\xi + \frac{a'}{a}\xi^0 + \frac{1}{3}\nabla^2\vartheta + \frac{1}{3}\nabla^2\xi + \frac{a'}{a}(\vartheta' - h - \xi^0) = \psi\ . \tag{2.51}$$

The remaining two gauge conditions can be imposed e.g. as

$$\xi_i^{\mathrm{V}} = -\vartheta_i\ , \quad \partial^i\xi_i^{\mathrm{V}} = -\partial^i\vartheta_i = 0 \quad \Rightarrow \quad \vartheta_i^{\mathrm{N}} = 0\ , \quad h_i^{\mathrm{N}}|_{\mathrm{V}} = h_i^{\mathrm{V}} - \vartheta_i'\ , \tag{2.52}$$

so that in this gauge the scalar, vector and tensor parts of the metric perturbations decouple,

$$h_{\mu\nu}^{\mathrm{N}}|_{\mathrm{S}} = -2\begin{pmatrix}\phi & 0\\ 0 & \psi\delta_{ij}\end{pmatrix}\ , \qquad h_{\mu\nu}^{\mathrm{N}}|_{\mathrm{V}} = \begin{pmatrix}0 & -h_i^{\mathrm{N}}|_{\mathrm{V}}\\ -h_i^{\mathrm{N}}|_{\mathrm{V}} & 0\end{pmatrix}\ , \qquad h_{\mu\nu}^{\mathrm{N}}|_{\mathrm{t}} = 2\begin{pmatrix}0 & 0\\ 0 & \vartheta_{ij}^{\mathrm{t}}\end{pmatrix}\ . \tag{2.53}$$

In the remainder of this section we work in the Newtonian gauge and denote

$$g_{\mu\nu} \equiv g_{\mu\nu}^{\mathrm{N}} = a^2\begin{pmatrix}-(1+2\phi) & -h_i\\ -h_i & (1-2\psi)\delta_{ij} + 2\vartheta_{ij}\end{pmatrix}\ , \qquad \partial^i h_i = 0\ , \quad \vartheta_i{}^i = 0\ , \quad \partial^i\vartheta_{ij} = 0\ . \tag{2.54}$$

In order to evaluate the left-hand side of Einstein's equations, (2.13), we compute the curvature perturbations corresponding to eq. (2.54).

## Space-time curvature perturbations

The results presented in this section are derived in appendix A.2. Here we briefly go through all steps that lead to the Einstein tensor $G^\mu{}_\nu$. The first step is the computation of the Christoffel symbols at zeroth and first order,

$$\Gamma^\rho_{\mu\nu} = \frac{1}{2}g^{\rho\sigma}\left(g_{\sigma\mu,\nu} + g_{\sigma\nu,\mu} - g_{\mu\nu,\sigma}\right)\ . \tag{2.55}$$

The resulting non-zero components of the Ricci tensor,

$$R_{\mu\nu} = R^\alpha_{\mu\alpha\nu} = \Gamma^\alpha_{\mu\nu,\alpha} - \Gamma^\alpha_{\mu\alpha,\nu} + \Gamma^\beta_{\mu\nu}\Gamma^\alpha_{\beta\alpha} - \Gamma^\beta_{\mu\alpha}\Gamma^\alpha_{\beta\nu}\ , \tag{2.56}$$

are to zeroth order

$$\bar{R}_{00} = -3\mathcal{H}' \qquad \Rightarrow \qquad \bar{R}^0_0 = 3a^{-2}\mathcal{H}' \ , \tag{2.57}$$

$$\bar{R}_{ij} = (\mathcal{H}' + 2\mathcal{H}^2)\delta_{ij} \qquad \Rightarrow \qquad \bar{R}^i{}_j = a^{-2}(\mathcal{H}' + 2\mathcal{H}^2)\delta^i{}_j \ . \tag{2.58}$$

For the perturbed Ricci tensor one obtains the components

$$\delta R_{00} = 3\psi'' + \nabla^2\phi + 3\mathcal{H}(\phi' + \psi') \ , \tag{2.59}$$

$$\delta R_{0i} = 2\psi'_{,i} + 2\mathcal{H}\phi_{,i} + \frac{1}{2}\nabla^2 h_i - (\mathcal{H}' + 2\mathcal{H}^2)h_i \ , \tag{2.60}$$

$$\begin{aligned}\delta R_{ij} = {} & \left[\Box\psi - \mathcal{H}(\phi' + 5\psi') - 2(\mathcal{H}' + 2\mathcal{H}^2)(\phi + \psi)\right]\delta_{ij} \\ & + (\psi - \phi)_{,ij} + \frac{1}{2}(h_{i,j} + h_{j,i})' + \mathcal{H}(h_{i,j} + h_{j,i}) \\ & + \vartheta''_{ij} - \nabla^2\vartheta_{ij} + 2\mathcal{H}\vartheta'_{ij} + 2(\mathcal{H}' + 2\mathcal{H}^2)\vartheta_{ij} \ .\end{aligned} \tag{2.61}$$

Raising one index requires the use of the perturbed metric, $\delta R^i{}_j = \bar{g}^{i\mu}\,\delta R_{\mu j} + \delta g^{i\mu}\,\bar{R}_{\mu j}$. The Ricci scalar $R \equiv R^\mu{}_\mu$ is then

$$\bar{R} = 6a^{-2}(\mathcal{H}' + \mathcal{H}^2) = 6\frac{a''}{a^3} \ , \tag{2.62}$$

$$\delta R = 2a^{-2}\left[-3\psi'' + \nabla^2(2\psi - \phi) - 3\mathcal{H}(\phi' + 3\psi') - 6(\mathcal{H}' + \mathcal{H}^2)\phi\right] \ , \tag{2.63}$$

and we can compute the Einstein tensor,

$$G^\mu{}_\nu = R^\mu{}_\nu - \frac{1}{2}\delta^\mu{}_\nu R \ . \tag{2.64}$$

On the left-hand side of the unperturbed Einstein equations we thus have

$$\bar{G}^0{}_0 = -3a^{-2}\mathcal{H}^2 \ , \qquad \bar{G}^i{}_0 = \bar{G}^0{}_i = 0 \ , \qquad \bar{G}^i{}_j = -a^{-2}(2\mathcal{H}' + \mathcal{H}^2)\delta^i{}_j \ , \tag{2.65}$$

while at first order the components of the Einstein tensor are

$$\delta G^0{}_0 = 2a^{-2}\left[-\nabla^2\psi + 3\mathcal{H}(\psi' + \mathcal{H}\phi)\right] \ , \tag{2.66}$$

$$\delta G^i{}_0 = a^{-2}[2(\psi' + \mathcal{H}\phi)^{,i} + \nabla^2 h^i/2 + 2(\mathcal{H}' - \mathcal{H}^2)h^i] \ , \tag{2.67}$$

$$\delta G^0{}_i = -a^{-2}[2(\psi' + \mathcal{H}\phi)_{,i} + \nabla^2 h_i/2] \ , \tag{2.68}$$

$$\begin{aligned}\delta G^i{}_j = {} & a^{-2}\left[2\psi'' - \nabla^2(\psi - \phi) + 2\mathcal{H}(\phi' + 2\psi') + 2(2\mathcal{H}' + \mathcal{H}^2)\phi\right]\delta^i{}_j \\ & + a^{-2}\left[(\psi - \phi)^{,i}_{,j} + \frac{1}{2}(h^i_{,j} + h^{,i}_j)' + \mathcal{H}(h^i_{,j} + h^{,i}_j) - \Box_{\mathcal{H}}\vartheta^i{}_j + 2\mathcal{H}\vartheta^{i\prime}_j\right] \ .\end{aligned} \tag{2.69}$$

We now have all ingredients to evaluate the left-hand side of the Einstein equations and move further to compute the right-hand side.

## 2.2 Energy-momentum tensor perturbations

Let us work again in an arbitrary gauge. Being a symmetric rank-2 tensor, the energy-momentum tensor $T^\mu{}_\nu$ follows eqs. (2.18)–(2.24). Therefore we write

$$T^\mu{}_\nu = \bar{T}^\mu{}_\nu + \delta T^\mu{}_\nu \ , \tag{2.70}$$

and recall that such a tensor has ten degrees of freedom in the perturbations, six of which are physical, while four are gauge degrees of freedom. Before proceeding in their 4 + 4 + 2 scalar-vector-tensor decomposition (2 + 2 + 2 physical), we decompose the energy-momentum tensor in a

perfect-fluid, and a non-perfect-fluid part.[7] The background tensor takes the perfect-fluid form

$$\bar{T}^{\mu\nu} = (\bar{e}+\bar{p})\,\bar{u}^\mu\bar{u}^\nu + \bar{p}\,\bar{g}^{\mu\nu} \ , \qquad \bar{T}^\mu{}_\nu = (\bar{e}+\bar{p})\,\bar{u}^\mu\bar{u}_\nu + \bar{p}\,\delta^\mu{}_\nu \ , \tag{2.71}$$

where $e$ is the energy density and $p$ the pressure of the fluid. Their background values are related to each other by the equation of state

$$\bar{p} = \bar{p}(\bar{e}) \ , \qquad c_s^2 \equiv \frac{\partial\bar{p}}{\partial\bar{e}} \ . \tag{2.72}$$

The 4-velocity of the medium is denoted by $u^\mu$. We assume the fluid to be at rest $\bar{u}^i = 0$, such that the velocity is defined by

$$u^\mu = \bar{u}^\mu + \delta u^\mu \ , \quad \bar{u}^\mu = \left(\frac{d\tau}{dt}, \mathbf{0}\right) = a^{-1}(1,\mathbf{0}) \ , \quad \bar{u}_\mu = a(-1,\mathbf{0}) \ , \tag{2.73}$$

while the physical velocity is $v_i = v^i \equiv au^i = a\delta u^i$ . For the components of the covector $\delta u_\nu$ we find

$$\delta u_0 = \delta g_{0\mu}\bar{u}^\mu + \bar{g}_{0\mu}\delta u^\mu = -2ah_0 - a^2\delta u^0 \ , \tag{2.74}$$

$$\delta u_i = \delta g_{i\mu}\bar{u}^\mu + \bar{g}_{i\mu}\delta u^\mu = -ah_i + a^2\delta_{ij}\delta u^i = a\,(-h_i + v_i) \ . \tag{2.75}$$

The value of $\delta u^0$ is inferred by imposing $u_\mu u^\mu = -1$,

$$u_\mu u^\mu = -1 + a^{-1}(-2ah_0 - a^2\delta u^0) - a\delta u^0 \qquad \Rightarrow \delta u^0 = -a^{-1}h_0 \tag{2.76}$$

$$\Rightarrow \qquad u^\mu = a^{-1}(1-h_0, v^i) \ , \quad u_\mu = a(-1-h_0, v_i - h_i) \ . \tag{2.77}$$

At linear order the perfect fluid (pf) part of the energy-momentum tensor is thus

$$T^\mu{}_\nu|_{\rm pf} = \bar{T}^\mu{}_\nu + (\delta e + \delta p)(-\delta^\mu{}_0\,\delta^0{}_\nu) + (\bar{e}+\bar{p})\left(\frac{1}{a}\delta^\mu{}_0\,\delta u_\nu - a\delta^0{}_\nu\,\delta u^\mu\right) + \delta p\,\delta^\mu{}_\nu \tag{2.78}$$

$$= \begin{pmatrix} -\bar{e} & 0 \\ 0 & \bar{p}\,\delta^i_j \end{pmatrix} + \begin{pmatrix} -\delta e & (\bar{e}+\bar{p})(v_i - h_i) \\ -(\bar{e}+\bar{p})\,v^i & \delta p\,\delta^i_j \end{pmatrix} \ . \tag{2.79}$$

Looking at eq. (2.79), one could be worried about $T^0{}_i \neq T^i{}_0$. However, raising and lowering the indices, we find that the energy-momentum tensor is indeed symmetric, $T^{0i} = T^{i0}$ and $T_{0i} = T_{i0}$ .

The remaining five non-pf degrees of freedom are encoded in the anisotropic stress tensor $\Pi^i_j$,

$$\delta T^i{}_j|_{\rm tot} = \bar{p}\left(\frac{\delta p}{\bar{p}}\delta^i{}_j + \Pi^i{}_j\right) \ . \tag{2.80}$$

Since $\Pi^i{}_j$ is traceless, the separation into $\delta p$ and $\Pi^i{}_j$ is unique. Let us remark that $\delta p$ does not agree with the thermodynamic pressure perturbation, but it rather includes corrections involving velocity gradients as well. We decompose the perturbation $\delta T^\mu_\nu$ in scalar, vector and tensor parts as in eqs. (2.20)–(2.24),

$$v_i = v_i^{\rm s} + v_i^{\rm v} \ , \qquad v_i^{\rm s} = -\partial_i v \ , \qquad \partial^i v_i^{\rm v} = 0 \ , \tag{2.81}$$

$$\Pi_{ij} = \Pi^{\rm s}_{ij} + \Pi^{\rm v}_{ij} + \Pi^{\rm t}_{ij} \ , \qquad \Pi^{\rm s}_{ij} = (\partial_i\partial_j - \delta_{ij}\nabla^2/3)\Pi \ , \tag{2.82}$$

$$\Pi^{\rm v}_{ij} = -\frac{1}{2}(\partial_i\Pi_j + \partial_j\Pi_i) \ , \qquad \partial^i\Pi_i = 0 \ , \tag{2.83}$$

$$\delta^{ij}\Pi^{\rm t}_{ij} = 0 \ , \qquad \partial^i\Pi^{\rm t}_{ij} = 0 \ . \tag{2.84}$$

[7] For a detailed derivation of the energy-momentum tensor of free particles in curved space-time see [12, p. 133].

In order to construct gauge-invariant counterparts for the variables $\delta e$, $\delta p$, $v$ and $\Pi$, in analogy with $\phi$ and $\psi$ for the metric perturbations, we investigate how these transform under gauge transformations. Being $e$ and $p$ four-scalars, they obey eq. (A.3),

$$\delta\tilde{e} = \delta e - \bar{e}'\xi^0 \ , \qquad \delta\tilde{p} = \delta p - \bar{p}'\xi^0 \ . \tag{2.85}$$

Under coordinate transformations, the four-velocity $u^\mu$ behaves as described in eq. (A.5),

$$\delta\tilde{u}^0 = \delta u^0 - \bar{u}^{0\prime}\xi^0 + \xi^{0\prime}\bar{u}^0 = \delta u^0 + \frac{1}{a}(\mathcal{H}\xi^0 + \xi^{0\prime}) \ , \tag{2.86}$$

$$\delta\tilde{u}^i = \delta u^i + \bar{u}^0\xi^{i\prime} = \delta u^i + \frac{1}{a}\xi^{i\prime} \qquad \Rightarrow \quad \tilde{v} \overset{(A.7)}{\underset{(2.81)}{=}} v + \xi' \ . \tag{2.87}$$

Since at zeroth order there is no anisotropic stress $\Pi_{ij}$, the latter transforms trivially. A gauge-invariant formulation could be obtained by fixing these quantities in the Newtonian gauge with $\xi^0 = \vartheta' - h$ and $\xi = -\vartheta$, cf. eq. (2.47).[8] However, the resulting energy-momentum tensor in the Newtonian gauge does not simplify, suggesting the existence a smarter gauge choice for the right-hand side of the Einstein equations. Knowing the relation between the gauges explicitly, we can use them to define new gauge-invariant variables and simplify the Einstein equations.

## Comoving gauge

The *slicing* introduced below eq. (2.7) is said to be *comoving*, if it is orthogonal to the fluid 4-velocity,[9]

$$n^\mu \overset{(2.33)}{=} a^{-1}(1 - h_0, h^i) \overset{!}{=} u^\mu \overset{(2.77)}{=} a^{-1}(1 - h_0, v^i) \ . \tag{2.88}$$

A comoving slicing does therefore not necessarily exist in general. However, for scalar perturbations $v^i_{\rm s} = -v_{,i}$ and $h^i_{\rm s} = -h_{,i}$, it always exists, as one can always impose

$$\text{comoving slicing} \quad \Leftrightarrow \quad v = h \ . \tag{2.89}$$

using the gauge transformations (2.87) and (2.40). Eq. (2.89) is obtained by choosing

$$\xi^0 = v - h \ . \tag{2.90}$$

This does not yet define a (scalar) gauge, as $\xi$ is still arbitrary, i.e. the threading is left unspecified. The *threading* is said to be *comoving*, if the threads are world lines of comoving observers,

$$t^\mu \overset{(2.34)}{=} a^{-1}(1 - h_0, \mathbf{0}) \overset{!}{=} u^\mu \overset{(2.77)}{=} a^{-1}(1 - h_0, v^i) \ . \tag{2.91}$$

For scalar perturbations this means

$$\text{comoving threading} \quad \Leftrightarrow \quad v = 0 \ . \tag{2.92}$$

According to eq. (2.87), we get to comoving threading by the gauge transformation

$$\xi' = -v \ . \tag{2.93}$$

This condition does not fully specify the threading, as one remains free to act with time-independent transformations $\tilde{x}^i = x^i - \xi^{,i}$, cf. eqs. (A.1) and (A.7).

[8] What justifies the expression *gauge invariant* is that we have given expressions for the Newtonian gauge quantities in terms of the corresponding quantities in an arbitrary gauge, and that the Newtonian gauge conditions fix the gauge uniquely. This is not true for all so-called gauges, see e.g. the synchronous gauge condition $h_0 = h = 0$ [19].

[9] Or, when $T^{\mu\nu}$ is not a fluid, if $n_\mu T^{\mu\nu}$ is parallel to $n^\nu$ .

The comoving gauge is defined by requiring both comoving slicing and comoving threading, such that the threading is orthogonal to the slicing,

$$t^\mu = n^\mu = u^\mu \qquad \Leftrightarrow \qquad \boxed{v^{\rm c} = h^{\rm c} = 0} \ . \tag{2.94}$$

In order to transform from arbitrary to comoving gauge, one uses both eqs. (2.90) and (2.93). We relate the comoving and the Newtonian gauges by applying eq. (2.47),

$$\phi = h_0^{\rm c} - \mathcal{H}\vartheta^{\rm c\prime} - \vartheta^{\rm c\prime\prime} \qquad\qquad h_0^{\rm c} = \phi - v^{\rm N\prime} - \mathcal{H}v^{\rm N} \tag{2.95}$$

$$\psi = h_{\rm D}^{\rm c} + \frac{1}{3}\nabla^2\vartheta^{\rm c} + \mathcal{H}\vartheta^{\rm c\prime} \qquad\qquad h_{\rm D}^{\rm c} + \frac{1}{3}\nabla^2\vartheta^{\rm c} = \psi + \mathcal{H}v^{\rm N} \equiv -\mathcal{R} \tag{2.96}$$

$$v^{\rm N} = -\vartheta^{\rm c\prime} \qquad\qquad \vartheta^{\rm c\prime} = -v^{\rm N} \tag{2.97}$$

$$\delta e^{\rm N} = \delta e^{\rm c} - \bar{e}'\vartheta^{\rm c\prime} \qquad\qquad \delta e^{\rm c} = \delta e^{\rm N} - \bar{e}'v^{\rm N} \tag{2.98}$$

$$\delta p^{\rm N} = \delta p^{\rm c} - \bar{p}'\vartheta^{\rm c\prime} \qquad\qquad \delta p^{\rm c} = \delta p^{\rm N} - \bar{p}'v^{\rm N} \ . \tag{2.99}$$

The variable $\mathcal{R}$ introduced in eq. (2.96) gives the trace of the three-dimensional metric in the comoving gauge. It thus describes the curvature of space-like hypersurfaces in this gauge, so that it is often called the *curvature perturbation*. Its form in an arbitrary gauge is

$$\mathcal{R} \equiv -\left[h_{\rm D} + \frac{1}{3}\nabla^2\vartheta + \mathcal{H}(v-h)\right] \ , \qquad \tilde{\mathcal{R}} = \mathcal{R} + \frac{1}{3}\nabla^2\xi - \mathcal{H}\xi^0 - \frac{1}{3}\nabla^2\xi - \mathcal{H}(-\xi^0) = \mathcal{R} \ . \tag{2.100}$$

For later purposes, it is also useful to define a further gauge-invariant variable,

$$\Delta \equiv \frac{\delta e^{\rm c}}{\bar{e}} = \frac{\delta e}{\bar{e}} - \frac{\bar{e}'}{\bar{e}}(v-h) \ , \qquad \tilde{\Delta} = \frac{\delta e}{\bar{e}} - \frac{\bar{e}'}{\bar{e}}\xi^0 - \frac{\bar{e}'}{\bar{e}}(v-h-\xi^0) = \Delta \ . \tag{2.101}$$

### Continuity equations

From the Einstein equations given in eq. (2.13) one can derive the continuity equations

$$T^\mu{}_{\nu;\mu} = T^\mu{}_{\nu,\mu} + \Gamma^\mu_{\alpha\mu}T^\alpha{}_\nu - \Gamma^\alpha_{\nu\mu}T^\mu{}_\alpha = 0 \ , \tag{2.102}$$

for the energy-momentum tensor. Sometimes they suitably replace some of the Einstein equations. For the background, eqs. (2.102), (2.79) and (A.51) yield

$$\bar{T}^\mu{}_{0;\mu} = \bar{T}^0{}_0' + 4\mathcal{H}\,\bar{T}^0{}_0 - \mathcal{H}\,\bar{T}^0{}_0 - \mathcal{H}\delta^i_j\bar{T}^j{}_i = 0 \qquad \Leftrightarrow \qquad \boxed{\bar{e}' = -3\mathcal{H}(\bar{e}+\bar{p})} \ . \tag{2.103}$$

At first order, eq. (2.102) becomes

$$\delta T^\mu{}_{\nu,\mu} + \delta\Gamma^\mu_{\alpha\mu}\,\bar{T}^\alpha{}_\nu + \bar{\Gamma}^\mu_{\alpha\mu}\delta T^\alpha{}_\nu - \delta\Gamma^\alpha_{\nu\mu}\,\bar{T}^\mu{}_\alpha - \bar{\Gamma}^\alpha_{\nu\mu}\delta T^\mu{}_\alpha = 0 \ . \tag{2.104}$$

Restricting to scalar perturbations, we evaluate eq. (2.104) in the Newtonian gauge, in order to make contact with the results of chapter 2.3, obtaining

$$\nu = 0: \qquad \delta e^{\rm N\prime} + 3\mathcal{H}(\delta e^{\rm N} + \delta p^{\rm N}) - (\bar{e}+\bar{p})(\nabla^2 v^{\rm N} + 3\psi') = 0 \ , \tag{2.105}$$

$$\nu = i: \qquad -\delta p^{\rm N} + (\bar{e}+\bar{p})(4\mathcal{H}v^{\rm N} - \phi) + \left[(\bar{e}+\bar{p})v^{\rm N}\right]' - \frac{2}{3}\bar{p}\,\nabla^2\Pi = 0 \ . \tag{2.106}$$

## 2.3 Einstein's equations

In this section we collect together the results of secs. 2.1 and 2.2, to obtain the Einstein equations

$$G^\mu{}_\nu = 8\pi G T^\mu{}_\nu \ , \tag{2.107}$$

in the Newtonian gauge. For an overview, the variety of symbols encountered so far is summed up in table 2.1.

| | $\delta g_{\mu\nu}$ | | | $\delta T^{\mu}{}_{\nu}$ | | |
|---|---|---|---|---|---|---|
| gauge | arbitrary | N | c | arbitrary | c | dof |
| scalar | $h_0, h, h_{\rm D}, \vartheta$ | $\phi, \psi$ | $\mathcal{R}$ | $\delta e, \delta p, v, \Pi$ | $\Delta$ | 2 |
| vector | $h_i^{\rm v}, \vartheta_i$ | $h_i$ | - | $v_i^{\rm v}, \Pi_i$ | - | 2 |
| tensor | $\vartheta_{ij}^{\rm t}$ | $\vartheta_{ij}$ | - | $\Pi_{ij}^{\rm t}$ | - | 2 |

Table 2.1: Overview of metric and energy-momentum perturbations in their different components, and variables in Newtonian (N) or comoving (c) gauges. The number of real degrees of freedom (dof) is listed in the last column. The curvature perturbation $\mathcal{R}$ is listed separately, as it describes scalar metric perturbations using the notion of the fluid velocity $v$.

## Zeroth order

For the homogeneous and isotropic universe, the $0i$ and $i0$-components of

$$\bar{G}^{\mu}{}_{\nu} = 8\pi G\ \bar{T}^{\mu}{}_{\nu} \tag{2.108}$$

vanish, so that we are left with two identities, for the 00 and $ij$-component respectively,

$$3a^{-2}\mathcal{H}^2 = 8\pi G\bar{e}\ , \tag{2.109}$$

$$-a^{-2}(2\mathcal{H}' + \mathcal{H}^2)\delta^i_j = 8\pi G\bar{p}\ \delta^i_j\ . \tag{2.110}$$

Inserting eq. (2.109) in eq. (2.110) we obtain

$$\mathcal{H}^2 = \frac{8\pi G}{3}\bar{e}a^2\ , \tag{2.111}$$

$$\mathcal{H}' = -\frac{4\pi G}{3}(\bar{e} + 3\bar{p})a^2\ . \tag{2.112}$$

Note that eq. (2.112) follows from differentiating eq. (2.111) with respect to conformal time and using the continuity equation (2.103). Therefore, only two of the three equations are independent. To describe the evolution of the background we choose

$$\boxed{\begin{aligned}\mathcal{H}^2 &= \frac{8\pi G}{3}\bar{e}a^2\ , \\ \bar{e}' &= -3\mathcal{H}(\bar{e} + \bar{p})\ .\end{aligned}} \tag{2.113, 2.114}$$

As the energy density $\bar{e}$ and the pressure $\bar{p}$ are related by the equation of state (cf. eq. (2.72)), we are dealing with two equations for two unknown variables: $a$ and $\bar{e}$. From eq. (2.6) we learn that if the expansion of the universe is decelerated, $\ddot{a} < 0$, then $\mathcal{H}' < 0$. By eq. (2.112), the energy density and the pressure must then satisfy $\bar{e} + 3\bar{p} > 0$. On the other hand, an accelerated expansion $\ddot{a} > 0$, as postulated by inflation, implies $\mathcal{H}' > 0$ and therefore $\bar{e} + 3\bar{p} < 0$.

The equation of state takes a simple form in most cosmological applications, so that eqs. (2.113) and (2.114) are immediately solved,

$$\bar{p} = w\bar{e} \quad \Rightarrow \quad \bar{e} \sim a^{-3(1+w)}\ . \tag{2.115}$$

For radiation, non-relativistic matter and vacuum energy one sets respectively $w \in \{1/3, 0, -1\}$.

## First order

We evaluate here the different components of

$$\delta G^{\mu}{}_{\nu} = 8\pi G\delta T^{\mu}{}_{\nu} \tag{2.116}$$

for scalar, vector and tensor perturbations in the Newtonian gauge.

**Scalar perturbations**

The scalar parts of the 00 and $0i$-components of eq. (2.116) yield the coupled equations

$$\nabla^2\psi - 3\mathcal{H}(\psi' + \mathcal{H}\phi) = 4\pi G a^2 \delta e \ , \tag{2.117}$$

$$(\psi' + \mathcal{H}\phi)_{,i} = -4\pi G a^2 (\bar{e} + \bar{p}) v_i \quad \overset{(2.81)}{\Longrightarrow} \quad \boxed{\psi' + \mathcal{H}\phi = 4\pi G a^2 (\bar{e} + \bar{p}) v} \ , \tag{2.118}$$

that combined give the constraint equation

$$\nabla^2\psi = 4\pi G a^2 \underbrace{\left[\delta e + 3\mathcal{H}(\bar{e} + \bar{p}) v\right]}_{=\bar{e}\Delta} \quad \Leftrightarrow \quad \boxed{\nabla^2\psi = 4\pi G a^2 \bar{e}\Delta} \ , \tag{2.119}$$

where we used the continuity equation (2.103) for the background, to identify the gauge invariant quantity $\Delta$, cf. eq. (2.101). An integration constant would in principle enter eq. (2.118). We omit it considering that it would correspond to a background contribution. Remarkably eq. (2.119) reproduces the equation of Newtonian gravity. For the physical interpretation one should however keep in mind that the left-hand side represents the metric perturbation in the Newtonian gauge, while the right-hand side is the density perturbation in the comoving gauge. Moreover the definition of the Newtonian potential is ambiguous, as given by $\phi$ or $\psi$.

The $ij$-components of eq. (2.116) yield a constraint and an evolution equation for the traceless and trace part respectively,

$$\left(\partial_i\partial_j - \frac{1}{3}\delta_{ij}\nabla^2\right)(\psi - \phi) = 8\pi G a^2 \bar{p} \left(\partial_i\partial_j - \frac{1}{3}\delta_{ij}\nabla^2\right)\Pi \ , \tag{2.120}$$

$$\psi'' + \mathcal{H}(2\psi' + \phi') + (2\mathcal{H}' + \mathcal{H}^2)\phi + \frac{1}{3}\nabla^2(\phi - \psi) = 4\pi G a^2 \delta p \ . \tag{2.121}$$

Integrating[10] eq. (2.120) and using eq. (2.110), these can be simplified into

$$\boxed{\begin{aligned} \psi - \phi &= 8\pi G a^2 \bar{p}\ \Pi \ , \\ \psi'' + \mathcal{H}(2\psi' + \phi') &= 4\pi G a^2 \left[2\bar{p}\left(\phi + \frac{1}{3}\nabla^2\Pi\right) + \delta p\right] \ . \end{aligned}} \tag{2.122, 2.123}$$

The continuity equations (2.105) and (2.106) follow from combinations of these four constraint and evolution equations. If there is no anisotropic stress, $\Pi = 0$, the Bardeen potentials coincide, $\phi = \psi$, and the ambiguity of the Newtonian potential is lifted.

There are various ways to turn the coupled system of equations presented above into a single differential equation. Conceptually attractive may be to find a wave equation for a metric perturbation, sourced by energy-momentum perturbations on the right-hand side. Here we briefly demonstrate how this can be done, commenting afterwards on why the result is, however, of limited value in the inflationary context (introduced in chapter 3).

To proceed we eliminate the variable $(\bar{e} + \bar{p})\, v$ by making use of eqs. (2.118) and (2.119). Substituting $8\pi G a^2 \bar{p} = -\mathcal{H}^2 - 2\mathcal{H}'$ in eq. (2.122), one can solve for $\phi$,

$$\phi = \psi + (\mathcal{H}^2 + 2\mathcal{H}')\Pi \tag{2.124}$$

$$\Rightarrow\ \phi' = \psi' + (\mathcal{H}^2 + 2\mathcal{H}')\Pi' + 2(\mathcal{H}\mathcal{H}' + \mathcal{H}'')\Pi \ . \tag{2.125}$$

[10] For this define $D \equiv \psi - \phi - 8\pi G a^2 \bar{p}\ \Pi$. Going over to Fourier space, we find that $(k_i k_j - k^2\delta_{ij}/3) D_{\mathbf{k}} = 0$, implying $D_{\mathbf{k}} = 0$ for all $\boldsymbol{k} \neq 0$.

In the remaining terms, we substitute $4\pi G a^2 = 3\mathcal{H}^2/(2\bar{e})$, whereby the system becomes

$$\nabla^2\psi - 3\mathcal{H}\psi' - 3\mathcal{H}^2\psi = \frac{3\mathcal{H}^2\delta e}{2\bar{e}} + 3\mathcal{H}^2(\mathcal{H}^2 + 2\mathcal{H}')\Pi \,, \tag{2.126}$$

$$\psi'' + 3\mathcal{H}\psi' + (\mathcal{H}^2 + 2\mathcal{H}')\psi = \frac{3\mathcal{H}^2\delta p}{2\bar{e}} - (\mathcal{H}^2 + 2\mathcal{H}')\left(\frac{\nabla^2\Pi}{3} + \mathcal{H}\Pi'\right) - \left[2\mathcal{H}(\mathcal{H}\mathcal{H}' + \mathcal{H}'') + (\mathcal{H}^2 + 2\mathcal{H}')^2\right]\Pi \,. \tag{2.127}$$

Finally we take a linear combination of eqs. (2.126) and (2.127). A particularly illustrative one is obtained by multiplying eq. (2.126) with $-c_s^2$, yielding

$$\left[\partial_\tau^2 - c_s^2\nabla^2 + 3\mathcal{H}(1 + c_s^2)\partial_\tau + 3\mathcal{H}^2\left(c_s^2 - \frac{\bar{p}}{\bar{e}}\right)\right]\psi = \frac{3\mathcal{H}^2}{2}\frac{\delta p - c_s^2\delta e}{\bar{e}} + \frac{\mathcal{H}^2\bar{p}}{\bar{e}}\left[\nabla^2 + 3\mathcal{H}\partial_\tau + 9\mathcal{H}^2\left(\frac{2}{3} - \frac{c_s^2\bar{e}}{\bar{p}} - \frac{\bar{p}}{\bar{e}}\right)\right]\Pi \,, \tag{2.128}$$

where we made use of the background identities

$$\mathcal{H}' = -\frac{\mathcal{H}^2}{2}\left(1 + \frac{3\bar{p}}{\bar{e}}\right) \,, \quad \mathcal{H}'' = \frac{\mathcal{H}^3}{2}\left(1 - \frac{3\bar{p}}{\bar{e}} + 9c_s^2 + \frac{9c_s^2\bar{p}}{\bar{e}}\right) \,. \tag{2.129}$$

A nice feature of eq. (2.128) is that in the absence of anisotropic stress, i.e. for $\Pi = 0$, the right-hand side is simple, and the combination $\delta p - c_s^2\delta e$ is gauge invariant (it is proportional to what is known as the *entropy perturbation*). Furthermore, in the absence of any source, the wave equation (2.128) describes damped oscillations. That said, eq. (2.128) is useful only in the case that $\delta p$, $\delta e$ and $\Pi$ are independent of metric perturbations. The wave equation takes a different form if they are expressed in terms of some microscopic degrees of freedom, like the inflaton field, so that derivatives, and therefore metric perturbations, appear in $\delta T^\mu{}_\nu$, cf. sec. 3.2.

### Vector perturbations

The vector parts of the $0i$ and $i0$ components, cf. eqs. (A.66) and (A.67), yield the (after using eqs. (2.111) and (2.112)) equivalent equations

$$-\frac{1}{2}\nabla^2 h_i = 8\pi G a^2(\bar{e} + \bar{p})(v_i^{\mathrm{v}} - h_i) \,, \qquad \frac{1}{2}\nabla^2 h_i + 2(\mathcal{H}' - \mathcal{H}^2)h_i = -8\pi G a^2(\bar{e} + \bar{p})v_i^{\mathrm{v}} \,. \tag{2.130}$$

The time evolution of vector perturbations is given by the $ij$-components of the Einstein equations, cf. eq. (A.68),

$$\left[a^2(h_{i,j} + h_{j,i})\right]' = -8\pi G a^4\bar{p}\,(\Pi_{i,j} + \Pi_{j,i}) \,. \tag{2.131}$$

If the right-hand side is zero, eq. (2.131) implies a fast decay,

$$\Pi_{i,j} + \Pi_{j,i} = 0 \quad \Rightarrow \quad h_{i,j} + h_{j,i} \sim \frac{1}{a^2} \,, \tag{2.132}$$

i.e., in the absence of anisotropic stress vector perturbations can be neglected.

### Tensor perturbations

The tensor part of the $ij$-components is, cf. eq. (A.68),

$$\vartheta_{ij}'' + 2\mathcal{H}\vartheta_{ij}' - \nabla^2\vartheta_{ij} = 8\pi G a^2\bar{p}\;\Pi_{ij}^{\mathrm{t}} \,. \tag{2.133}$$

The differential operator on the left-hand side is nothing but the wave operator for FLRW coordinates, cf. eq. (2.10). Therefore, if $\Pi_{ij}^{\mathrm{t}} = 0$ eq. (2.133) describes source-less gravitational waves propagating through the expanding universe, $\Box_{\mathcal{H}}\vartheta_{ij} = 0$.

# Chapter 3

# Origin of primordial perturbations from vacuum fluctuations

From the results of chapter 2 we learn that:

* scalar perturbations couple to density perturbations, cf. eq. (2.128),
* vector perturbations decay rapidly in time, cf. eq. (2.131),
* tensor perturbations describe gravitational waves, cf. eq. (2.133).

Primordial scalar perturbations are therefore the seeds of structure in the universe, while tensor perturbations are important messengers from the very early times, as pointed out already in [20]. Gravitational wave detectors capable of measuring a background signal from cosmological sources are now under construction [21]. Until they become operative, the earliest probe of the universe available today comes from the CMB, at $t_{\rm dec}$, where we observe relative scalar perturbations of the order of $\mathcal{O}(\delta T/\bar{T}) \sim 10^{-5}$ [11].

The observation of $\delta T/\bar{T}$ has some important conceptual consequences. In particular, it is not clear where these perturbations originate from, and why they are so small.[11] To elucidate the latter issue, let us recall the discussion about eq. (2.112). If the universe is radiation ($p > 0$) or matter ($p = 0$) dominated, then its expansion is decelerated. Assuming that this is the case already before $t_{\rm dec}$, the size of the visible universe at $t_{\rm dec}$ consists of $\sim 10^3$ causally disconnected regions [12, p.282]. How is it possible that the temperature is so homogeneously distributed over far apart regions, that could have not equilibrated in the past?

The high homogeneity and isotropy observed in the CMB can be explained by an earlier period of accelerated expansion, which is commonly called inflation. At the same time, inflation also offers for an interpretation of primordial perturbations, in terms of quantum fluctuations originated in the past. We sketch this argument with the help of fig. 3.1.

Quantum fluctuations are produced at all scales, but at very early times their physical frequency, $k/a$ on the light-cone, is enhanced by the smallness of the scale factor $a \to 0$. If the universe expands exponentially, the expansion rate, $H$, remains constant, while $k/a$ decreases, meaning that the corresponding wavelengths get stretched rapidly. When the frequency reaches the order of magnitude of the expansion rate, $k/a \sim H$, the evolution of the fluctuations is not determined any more by microscopic quantum interactions, but by classical long-distance effects. We say that *perturbations exit the horizon.*

Inflation is introduced in sec. 3.1, while sec. 3.2 illustrates the generation and evolution of

[11] The standard Big Bang scenario leads also other unnatural observations, see e.g. [25]. Here we discuss only the so-called *horizon problem.*

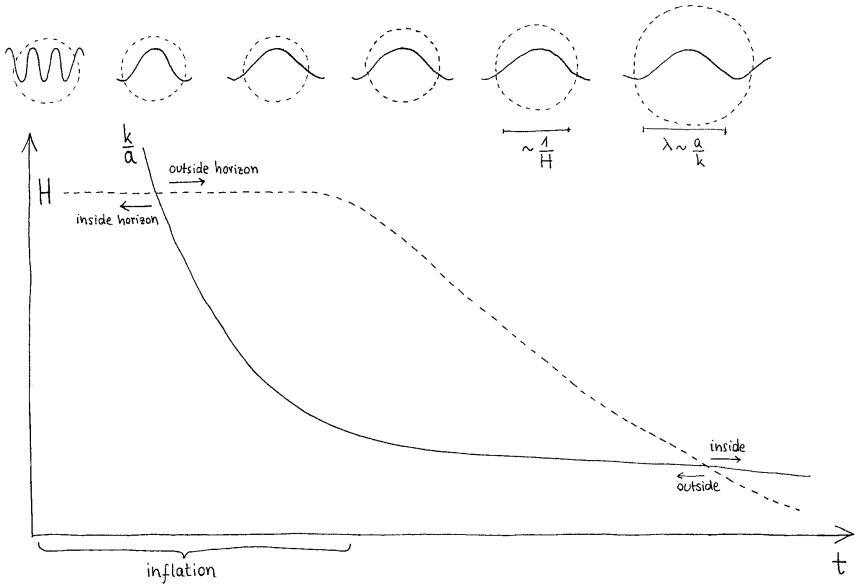


Figure 3.1: Dependence of the physical momentum $k/a$ and the Hubble parameter $H$ on time. During inflation the universe expands fast compared with time scales of physical processes.

vacuum scalar fluctuations during inflation. A similar analysis is performed in sec. 3.3 for tensor fluctuations. Finally, in sec. 3.4 we address the question of how inflationary predictions can be tested experimentally.

## 3.1 Cosmological inflation

The simplest dynamical models of inflation involve a single scalar field $\varphi$ as the order parameter for the evolution of the inflationary energy in time. In the last two decades, a bunch of different inflationary models [22] have been sprouting in the effort of improving on the first idea [23]. The present section should provide a brief summary of the simple *chaotic inflation* example [24].[12]

With the aim of showing that inflation implies a flat ($\kappa \approx 0\mathrm{m}^{-2}$) universe, we use conformal FLRW coordinates $(\tau, r, \theta, \phi)$ with generic curvature $\kappa$ (cf. eq. (2.3)). Some equations are however transformed in standard FLRW coordinates $(t, r, \theta, \phi)$ (cf. eq. (2.1)) to facilitate their discussion. Relations among the standard and conformal frameworks can be found in eqs. (2.6) and (2.7). The unperturbed Einstein tensor for generic $\kappa$ is derived in appendix A.2.

### Essential dynamics

Consider a background (spatially homogenous and isotropic) scalar field $\varphi(\tau, \boldsymbol{x}) = \bar{\varphi}(\tau)$, with self-interaction potential $V(\varphi)$, as the matter source for the universe. The minimally coupled[13] theory of general relativity is described by the action [6]

$$S = \frac{1}{16\pi G} \int \mathrm{d}^4x\sqrt{-g}\, R \; - \; \int \mathrm{d}^4x\sqrt{-g}\Big[\; \frac{1}{2}\varphi_{,\mu}\varphi^{,\mu} + V(\varphi) \;\Big] \; . \tag{3.1}$$

[12] For more details we recommend [25].

[13] Models where the inflaton couples to gravity also via a non-minimal term in the Lagrangian have been considered (see [26] for a literature review). However this is forbidden if the theory is shift-symmetric under $\varphi \to \varphi + c$ with $c \in \mathbb{R}$, cf. chapter 5.

Varying the action by the metric we obtain the unperturbed Einstein equations $\bar{G}^{\mu}_{\nu} = 8\pi G \bar{T}^{\mu}_{\nu}$, while varying it with respect to the field $\varphi$ one gets the scalar field equations

$$(\sqrt{-g}\varphi^{,\mu})_{,\mu} = \sqrt{-g}\, V_{\varphi} \ , \qquad V_{\varphi} \equiv \frac{\partial V}{\partial \varphi} \ . \tag{3.2}$$

For the background FLRW expanding universe spatial derivatives vanish, and with the metric determinant $-\bar{g}(\tau) = [a^2(\tau)]^4$ or $-\bar{g}(t) = [a^2(t)]^3$ one finds

$$\bar{g}^{\tau\tau}\sqrt{-\bar{g}} = -a^2 \frac{r^2 \sin\theta}{\sqrt{1-\kappa r^2}} \qquad \Rightarrow \qquad (\bar{g}^{\tau\tau}\sqrt{-\bar{g}})' = -2a^{-2}\mathcal{H}\sqrt{-\bar{g}} \ , \tag{3.3}$$

$$\bar{g}^{tt}\sqrt{-\bar{g}} = -a^3 \frac{r^2 \sin\theta}{\sqrt{1-\kappa r^2}} \qquad \Rightarrow \qquad (\bar{g}^{tt}\sqrt{-\bar{g}})^{\cdot} = -3H\sqrt{-\bar{g}} \ . \tag{3.4}$$

The evolution equation for $\bar{\varphi}$ that follows from eq. (3.2) is therefore independent of $\kappa$,

$$\bar{\varphi}'' + 2\mathcal{H}\bar{\varphi}' + a^2 V_{\varphi}(\bar{\varphi}) = 0 \qquad \overset{\tau\leftrightarrow t}{\Longleftrightarrow} \qquad \ddot{\bar{\varphi}} + 3H\dot{\bar{\varphi}} + V_{\varphi}(\bar{\varphi}) = 0 \ . \tag{3.5}$$

The energy-momentum tensor,

$$T^{\mu}{}_{\nu} = -\delta^{\mu}{}_{\nu}\left(\frac{1}{2}\varphi_{,\rho}\varphi^{,\rho} + V\right) + \varphi^{,\mu}\varphi_{,\nu} \ , \tag{3.6}$$

is diagonal at zeroth order. Comparing with the unperturbed energy-momentum tensor of a perfect fluid in eq. (2.78), the unperturbed energy density and pressure are

$$\bar{e} = -\bar{T}^{0}{}_{0} \qquad \Rightarrow \qquad \bar{e} = \frac{(\bar{\varphi}')^2}{2a^2} + V(\bar{\varphi}) = \frac{\dot{\bar{\varphi}}^2}{2} + V(\bar{\varphi}) \ , \tag{3.7}$$

$$\bar{p}\,\delta^{i}_{j} = \bar{T}^{i}{}_{j} \qquad \Rightarrow \qquad \bar{p} = \frac{(\bar{\varphi}')^2}{2a^2} - V(\bar{\varphi}) = \frac{\dot{\bar{\varphi}}^2}{2} - V(\bar{\varphi}) \ . \tag{3.8}$$

Inserting eq. (3.7) in the zeroth order $\tau\tau$-component of the Einstein equations[14] one obtains

$$\mathcal{H}^2 + \kappa = \frac{8\pi G}{3}\left[\frac{(\bar{\varphi}')^2}{2} + a^2 V(\bar{\varphi})\right] \qquad \overset{\tau\leftrightarrow t}{\Longleftrightarrow} \qquad H^2 + \frac{\kappa}{a^2} = \frac{8\pi G}{3}\left[\frac{\dot{\bar{\varphi}}^2}{2} + V(\bar{\varphi})\right] \ . \tag{3.9}$$

The continuity condition (2.114) yields precisely the same equation as (3.5). Taking the derivative with respect to $\tau$ or $t$ in (3.9) and using eq. (3.5) yields a $\kappa$-independent evolution equation,

$$\mathcal{H}' = -\frac{8\pi G}{3}\left[(\bar{\varphi}')^2 - a^2 V(\bar{\varphi})\right] \quad \overset{\tau\leftrightarrow t}{\Longleftrightarrow} \quad \dot{H} + H^2 = -\frac{8\pi G}{3}\left[\dot{\bar{\varphi}}^2 - V(\bar{\varphi})\right] \ . \tag{3.10}$$

The latter corresponds to eq. (2.112), from which we recall that an accelerated expansion implies a negative pressure. In this case the potential energy must dominate over the kinetic energy,

$$\frac{\ddot{a}}{a} \overset{(3.10)}{=} -\frac{8\pi G}{3}[\dot{\bar{\varphi}}^2 - V(\bar{\varphi})] > 0 \quad \Rightarrow \quad \dot{\bar{\varphi}}^2 \ll V(\bar{\varphi}) \ . \tag{3.11}$$

The evolution of $\bar{\varphi}$ is then strongly damped by the Hubble expansion term $3H\dot{\bar{\varphi}}$ in eq. (3.5). With eq. (3.11), and omitting $\kappa/a^2$ for a moment, eq. (3.9) approximates to

$$H \equiv \frac{\dot{a}(t)}{a(t)} \approx \sqrt{\frac{8\pi G V}{3}} \approx \text{const} \quad \Rightarrow \quad a(t) = a(0)e^{Ht} \ . \tag{3.12}$$

Therefore, during inflation the radius $a(t)$ of the universe grows exponentially with time. As a consequence, the factor $\kappa/a^2$ in eq. (3.9), whatever value it took before inflation, gets exponentially

[14] For the corresponding Einstein tensor see eq. (A.39).

suppressed. If the inflationary period lasts long enough, eventually its curvature becomes negligible: the universe is stretched out to a flat spatial geometry.

With respect to conformal time we find

$$\frac{\mathrm{d}a}{\mathrm{d}\tau} \approx \mathrm{const} \cdot a^2 \ , \quad \mathrm{const} = H \qquad \Rightarrow \qquad a(\tau) \approx \frac{1}{\frac{1}{a(\tau=0)} - H\tau} \ . \tag{3.13}$$

Choosing $a(\tau = 0)^{-1} = 0$, the conformal time coordinate $\tau$ runs from $-\infty$ to 0, assuring that eq. (3.13) is always positive.

It can be shown [24] that, for any initial value $\bar{\varphi}(0) \neq 0$ far from the minimum of the potential, and for any $\dot{\bar{\varphi}}(0)$, the solution $\bar{\varphi}(t)$ of the eq. (3.9) enters a highly damped *slow-roll* regime,

$$|\ddot{\bar{\varphi}}| \ll |3H\dot{\bar{\varphi}}| \approx |V_\varphi| \ . \tag{3.14}$$

With eq. (3.14) and $H \approx$ const. the non-linear system of equations (3.5) and (3.9) simplifies to a linear one. The slow-roll rate is often parametrized by the slow-roll functions,

$$\epsilon_V \equiv \frac{1}{16\pi G}\left(\frac{V_\varphi}{V}\right)^2 \ll 1 \ , \qquad \eta_V \equiv \frac{1}{8\pi G}\frac{V_{\varphi\varphi}}{V} \ll 1 \ . \tag{3.15}$$

Inflation has thus an attractor property: it erases the memory of the initial conditions. The end of the inflationary period occurs when the slow-roll conditions (3.15) are violated, $\epsilon_V$, $\eta_V \sim 1$, such that the approximation in eq. (3.12) breaks down.

Similarly as for the curvature argument, one can assume a non-homogeneous initial state at the beginning of inflation, such that at $t_{\mathrm{start}}$ different regions are characterized by a different constant value of $\bar{\varphi}$. If inflation lasts long enough, the inflaton field reaches its minimum $\bar{\varphi} = 0$ in every region, and the state at the end of inflation is a homogeneously defined vacuum, with respect to the inflaton field.

The duration of the exponential expansion is parametrized by the number of e-folds

$$\mathrm{d}N(t) \equiv \mathrm{d}\ln\frac{a(t_{\mathrm{end}})}{a(t)} \ , \tag{3.16}$$

that gives the total logarithmic expansion accrued during inflation,

$$N_{\mathrm{tot}} = \int_{t_{\mathrm{start}}}^{t_{\mathrm{end}}} \mathrm{d}t H = \int_{\bar{\varphi}_{\mathrm{start}}}^{\bar{\varphi}_{\mathrm{end}}} \mathrm{d}\bar{\varphi}\frac{H}{\dot{\bar{\varphi}}} \approx -3\int_{\bar{\varphi}_{\mathrm{start}}}^{\bar{\varphi}_{\mathrm{end}}} \mathrm{d}\bar{\varphi}\frac{H^2}{V_\varphi} \approx -\frac{8\pi}{m_{\mathrm{pl}}^2}\int_{\bar{\varphi}_{\mathrm{start}}}^{\bar{\varphi}_{\mathrm{end}}} \mathrm{d}\bar{\varphi}\frac{V}{V_\varphi} \ . \tag{3.17}$$

To guarantee that the modes, which have re-entered the horizon just recently, were causally connected before inflation, it is customary to require that the inflationary period extended for at least $N \gtrsim 60$ *e*-folds [12, p.288].

## The free massive scalar example

We study an example by considering the simple potential $V(\varphi) = \frac{1}{2}m^2\varphi^2$. The slow-roll conditions take the form

$$\epsilon_V = 2\eta_V = \frac{m_{\mathrm{pl}}^2}{6\pi\bar{\varphi}^2} \qquad \Rightarrow \quad \bar{\varphi} \gg \frac{m_{\mathrm{pl}}}{\sqrt{6\pi}} \ . \tag{3.18}$$

For this special choice, the mass $m$ of the inflaton field does not enter eq. (3.18). The fact that $\bar{\varphi}$ is of the order of magnitude of the Planck mass $m_{\mathrm{pl}}$ doesn't involve quantum gravity effects,

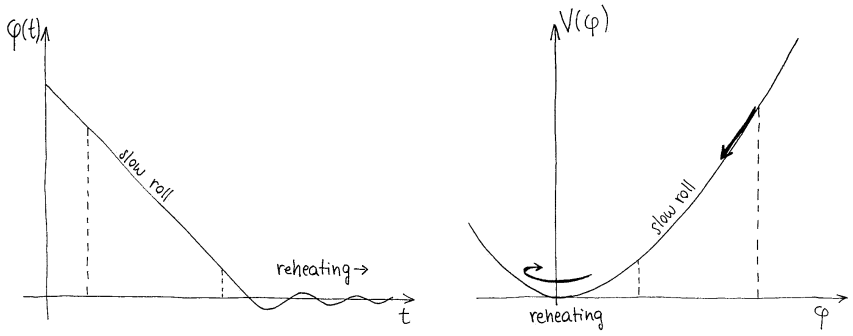


Figure 3.2: Time dependence of the inflaton field (left) and the free massive scalar potential (right).

provided that the physical energy scale satisfies $\sqrt{m\bar{\varphi}} \ll m_{\rm pl}$. The equations (3.9) in the slow-roll approximation become

$$H \approx \sqrt{\frac{4\pi}{3}} \frac{m\bar{\varphi}}{m_{\rm pl}} \ , \tag{3.19}$$

$$3H\dot{\bar{\varphi}} \approx -m^2\bar{\varphi} \ . \tag{3.20}$$

Dividing eq. (3.19) by eq. (3.20), one can solve a simple differential equation for $\bar{\varphi}$,

$$3\dot{\bar{\varphi}} \approx -\sqrt{\frac{3}{4\pi}} m_{\rm pl} m \quad \Rightarrow \quad \bar{\varphi}(t) = \bar{\varphi}_{\rm start} - \frac{m_{\rm pl} m}{\sqrt{12\pi}} t, \quad t_{\rm start} < t < t_{\rm end} \ . \tag{3.21}$$

The time $t_{\rm end}$ is given by $\bar{\varphi}_{\rm end} \sim m_{\rm pl}/\sqrt{6\pi}$. The logarithmic duration of the accelerated expansion,

$$N_{\rm tot} \overset{(3.17)}{\approx} -\frac{4\pi}{m_{\rm pl}^2} \int_{\bar{\varphi}_{\rm start}}^{\bar{\varphi}_{\rm end}} \bar{\varphi} {\rm d}\bar{\varphi} = \frac{2\pi}{m_{\rm pl}^2} \left[ \bar{\varphi}_{\rm start}^2 - \bar{\varphi}_{\rm end}^2 \right] \gtrsim 60 \ , \tag{3.22}$$

can bound the initial field value from below, $\bar{\varphi}_{\rm start} \gtrsim 5 m_{\rm pl}$.

At $\bar{\varphi}$ approaches the minimum of $V$, the kinetic term is no longer suppressed by the potential, and $H$ starts evolving in time. As a result, the dynamics becomes non-linear and the scalar field begins to oscillate around the minimum of the potential, as a damped harmonic oscillator. During the oscillations, $\bar{\varphi}$ is expected to gradually lose its energy to radiation, i.e. Standard Model degrees of freedom. Its pressure, cf. eq. (3.7), averages then to zero, as for non-relativistic matter.

The exact differential equation of motion obtained from eq. (3.9) can be solved numerically. The only unknown parameter is the mass $m$ of the inflaton field. In the present example the value of $m$ does not affect the qualitative behaviour of the solution, shown in figure 3.2, but it is constrained by the observables discussed in section 3.4.

## 3.2 Scalar perturbations

Classically, inflation causes the inflaton field $\varphi$ to become homogeneous inside the horizon. This is a vacuum: no inflaton particles. However, there are quantum fluctuations around this homogeneous value. The fluctuations are generated at all scales, but once a given distance scale exits the causal horizon, the fluctuations at that scale *freeze*: they begin to evolve classically, i.e. they become what we call inhomogeneities, anisotropies, or simply perturbations. At first order we write

$$\varphi(\tau, \boldsymbol{x}) = \bar{\varphi}(\tau) + \delta\varphi(\tau, \boldsymbol{x}) + \mathcal{O}(\delta^2) \ , \tag{3.23}$$

where $\delta\varphi$ is the perturbation originating from the quantum fluctuations. Being a scalar perturbation, under gauge transformations it transforms as described by eq. (A.3),

$$\delta\tilde{\varphi} = \delta\varphi - \bar{\varphi}'\xi^0 \ . \tag{3.24}$$

Let us first work in an arbitrary gauge. The perturbations of the metric are then given in (2.31)–(2.38), and its determinant is

$$-g = a^8(1+2h_0)(1-2h_{\rm D})^3 \qquad \Rightarrow \qquad \sqrt{-g} = a^4(1+h_0-3h_{\rm D}) \ . \tag{3.25}$$

The left and right-hand side of the field equation (3.2) become therefore

$$(3.2)_{\rm L} = -[a^2(1-h_0-3h_{\rm D})\varphi']' + [a^2(-h_i\varphi' + \varphi_{,i})]_{,i} \tag{3.26}$$

$$= -a^2\left[(1-h_0-3h_{\rm D})(\varphi'' + 2\mathcal{H}\varphi') - \nabla^2\varphi - (h_0' + 3h_{\rm D}' - h_{i,i})\varphi'\right] \ , \tag{3.27}$$

$$(3.2)_{\rm R} = a^4(1+h_0-3h_{\rm D})V_\varphi \ . \tag{3.28}$$

We multiply both sides with $(1+h_0+3h_{\rm D})$ and decompose $\varphi = \bar{\varphi} + \delta\varphi$. For scalar perturbations we moreover have $-h_{i,i} = \nabla^2 h$. At first order we obtain so the field equation

$$\delta\varphi'' + 2\mathcal{H}\delta\varphi' - \nabla^2\delta\varphi + a^2V_{\varphi\varphi}\delta\varphi = -a^2 2h_0V_\varphi + (h_0' + 3h_{\rm D}' + \nabla^2 h)\bar{\varphi}' \ . \tag{3.29}$$

In order to evaluate also the Einstein equations at inflation, we need the linear perturbations of the energy-momentum tensor of a minimally coupled scalar source,

$$T^0{}_0 = \frac{1}{2}g^{00}(\varphi')^2 - V(\varphi) + \mathcal{O}(\delta^2) \qquad \overset{(2.32)}{\Rightarrow} \qquad \delta T^0{}_0 = -[a^{-2}\bar{\varphi}'(\delta\varphi' - h_0\bar{\varphi}') + V_\varphi\delta\varphi] \ , \tag{3.30}$$

$$T^0{}_i = g^{00}\varphi'\varphi_{,i} + \mathcal{O}(\delta^2) \qquad \Rightarrow \qquad \delta T^0{}_i = -a^{-2}\bar{\varphi}'\delta\varphi_{,i} \ , \tag{3.31}$$

$$T^i{}_0 = g^{i0}(\varphi')^2 + g^{ij}\varphi_{,j}\varphi' \qquad \Rightarrow \qquad \delta T^i{}_0 = a^{-2}\bar{\varphi}'(\delta\varphi_{,i} + \bar{\varphi}'h_{,i}) \ , \tag{3.32}$$

$$T^i{}_j = \delta^i{}_j\left[-\frac{1}{2}g^{00}(\varphi')^2 - V(\varphi)\right] + \mathcal{O}(\delta^2) \qquad \Rightarrow \qquad \delta T^i{}_j = \delta^i{}_j[a^{-2}\bar{\varphi}'(\delta\varphi' - h_0\bar{\varphi}') - V_\varphi\delta\varphi] \ , \tag{3.33}$$

where $\delta T^0{}_0 = -\delta e$ and $\delta T^i{}_j = \delta p\ \delta^i{}_j$. Note that there is no anisotropic stress at linear order: the energy-momentum tensor has the perfect-fluid form with $T^i{}_j = 0$ for $i \neq j$.[15] Then, as far as $T_{\mu\nu}$ goes, we are left with only one unknown variable $\delta\varphi$ ($\bar{\varphi}$ is given by eq. (3.21)).

Comparing eqs. (3.30)–(3.33) with the scalar perturbations of the energy-momentum tensor in eq. (2.78), and recalling $\bar{e} + \bar{p} = a^{-2}(\bar{\varphi}')^2$ from eqs. (3.7) and (3.8), we find

$$v_i - h_i = -(v-h)_{,i} = -\frac{\delta\varphi_{,i}}{\bar{\varphi}'} \qquad \Rightarrow \qquad v - h = \frac{\delta\varphi}{\bar{\varphi}'} \ . \tag{3.34}$$

According to eq. (2.90), the gauge parameter allowing to transform from arbitrary coordinates to the comoving time slice gauge is precisely $\xi^0 = v - h = \delta\varphi/\bar{\varphi}'$. In particular, this implies that in the comoving gauge

$$\delta\varphi^{\rm c} = \delta\varphi - \bar{\varphi}'\frac{\delta\varphi}{\bar{\varphi}'} = 0 \ , \tag{3.35}$$

so that constant-time hypersurfaces correspond to constant-$\varphi$ hypersurfaces, and the inflaton field $\varphi$ is homogeneous in this gauge.

We use eq. (3.34) to rewrite the curvature perturbation,

$$\mathcal{R} \overset{(2.100)}{=} -\left(h_{\rm D} + \frac{1}{3}\nabla^2\vartheta + \mathcal{H}\frac{\delta\varphi}{\bar{\varphi}'}\right) \underset{(2.49)}{\overset{(2.46)}{=}} -\psi - \mathcal{H}\frac{\delta\varphi^{\rm N}}{\bar{\varphi}'} \ , \tag{3.36}$$

[15] This is no longer true at higher orders in perturbation theory.

and the relative energy density perturbation

$$\bar{e}\Delta \overset{(2.101)}{=} \delta e - \bar{e}'\frac{\delta\varphi}{\bar{\varphi}'} = \frac{\bar{\varphi}'}{a^2}\left(\delta\varphi' - h_0\bar{\varphi}' + \mathcal{H}\delta\varphi - \frac{\bar{\varphi}''}{\bar{\varphi}'}\delta\varphi\right) . \tag{3.37}$$

The first-order Einstein equations (2.118), (2.119), (2.122) and (2.123), are evaluated in the Newtonian gauge. Transforming from an arbitrary gauge to the Newtonian one, we find

$$\delta\varphi^{\mathrm{N}} = \delta\varphi_{\mathrm{N}} \overset{(2.47)}{=} \delta\varphi - \bar{\varphi}'(\vartheta' - h) , \qquad v^{\mathrm{N}} \overset{(2.46)}{=} \frac{\delta\varphi^{\mathrm{N}}}{\bar{\varphi}'} , \tag{3.38}$$

as the gauge parameter in the 0 direction is $\xi^0 = \vartheta' - h$. Starting from eq. (2.122), we find

$$\Pi = 0 \qquad \Rightarrow \qquad \boxed{\psi = \phi} , \tag{3.39}$$

for the diagonal metric perturbations. Therefore, also the left-hand (metric) side of the Einstein equations can be parametrized by one single unknown variable, e.g. $\psi$. However, there are three Einstein equations left to be evaluated, which, together with the field equation for $\delta\varphi_{\mathrm{N}}$, yield a total of four evolution equations, that are no longer independent.

Recalling eqs. (2.46), (2.48) and (2.49), the field equation (3.29) in Newtonian gauge is

$$\delta\varphi_{\mathrm{N}}'' + 2\mathcal{H}\delta\varphi_{\mathrm{N}}' - \nabla^2\delta\varphi_{\mathrm{N}} + a^2 V_{\varphi\varphi}\delta\varphi_{\mathrm{N}} = -2a^2\psi V_\varphi + 4\psi'\bar{\varphi}' . \tag{3.40}$$

Inserting $e$, $p$ and eq. (3.37) in the remaining Einstein equations yields

$$\nabla^2\psi = 4\pi G\left[\bar{\varphi}'\delta\varphi_{\mathrm{N}}' - \psi(\bar{\varphi}')^2 + \mathcal{H}\bar{\varphi}'\delta\varphi_{\mathrm{N}} - \bar{\varphi}''\delta\varphi_{\mathrm{N}}\right] , \tag{3.41}$$

$$\psi'' + 3\mathcal{H}\psi' + (2\mathcal{H}' + \mathcal{H}^2)\psi = 4\pi G\left[\bar{\varphi}'\delta\varphi_{\mathrm{N}}' - \psi(\bar{\varphi}')^2 - a^2 V_\varphi\delta\varphi_{\mathrm{N}}\right] , \tag{3.42}$$

$$\psi' + \mathcal{H}\psi = 4\pi G\bar{\varphi}'\delta\varphi_{\mathrm{N}} . \tag{3.43}$$

The system of equations is solved by transforming to co-moving momentum space. Now, for a scalar field we have just one degree of freedom associated to each Fourier mode. This can be chosen to be the metric perturbation $\psi$, or the field perturbation $\delta\varphi$, as they are related by the Einstein equation (3.43). However, a more natural variable is

$$f \equiv -z\mathcal{R} , \quad z \equiv \frac{\bar{\varphi}'}{\mathcal{H}} \qquad \Rightarrow \quad \delta\varphi_{\mathrm{N}} = f - z\psi . \tag{3.44}$$

defined by the curvature perturbation $\mathcal{R}$. In order to give a physical motivation for $f$, let us rewrite eq. (3.40) for the dimensionless quantity

$$\delta\widehat{\varphi} \equiv a\,\delta\varphi_{\mathrm{N}} . \tag{3.45}$$

Inserting $\delta\widehat{\varphi}' = a'\,\delta\varphi_{\mathrm{N}} + a\,\delta\varphi_{\mathrm{N}}'$ and $\delta\widehat{\varphi}'' = a''\,\delta\varphi_{\mathrm{N}} + 2a'\,\delta\varphi_{\mathrm{N}}' + a\,\delta\varphi_{\mathrm{N}}''$, the equation becomes

$$\delta\widehat{\varphi}'' - \nabla^2\delta\widehat{\varphi} + \left(a^2 V_{\varphi\varphi} - \frac{a''}{a}\right)\delta\widehat{\varphi} = -2a^3\psi V_\varphi + 4a\psi'\bar{\varphi}' . \tag{3.46}$$

The left-hand side has the appearance of an unattenuated wave equation. If we go to early times, $a \to 0$, other terms drop out, and we should be able to make contact with free-particle states. However, in the presence of $a > 0$ the metric perturbations $\psi$ and $\psi'$ on the right-hand side need to be incorporated. This leads to a generalization of $\delta\widehat{\varphi}$, namely $\hat{f} = af$, where $f = \delta\varphi^{\mathrm{f}}$ is the field perturbation in the so-called spatially flat gauge, cf. eq. (3.64).

Appendix A.3 shows how (3.40)–(3.43) boil down to a second order differential equation for $\hat{f}$,

$$\hat{f}'' - \frac{\hat{z}''}{\hat{z}}\hat{f} - \nabla^2\hat{f} = 0 \ , \qquad \hat{f} \equiv af = -az\mathcal{R} \ , \qquad \hat{z} \equiv az \ . \tag{3.47}$$

Therefore, once two initial values are specified on some initial time slice $\tau = \tau_{\rm in}$, the evolution can be solved. Since the coefficients are determined by the background solution, eq. (3.47) still depends implicitly on the shape of the inflaton potential $V(\varphi)$. Going over to Fourier space, the resulting differential equation,

$$\boxed{\hat{f}'' + k^2\hat{f} - \frac{\hat{z}''}{\hat{z}}\hat{f} = 0} \ , \tag{3.48}$$

can be easily solved in the asymptotic limits of short and long wavelengths $\lambda \sim 1/q$, where $q \equiv k/a$ is the physical momentum. Recall that $q$ decreases rapidly in time during inflation, because of the exponential growth of the scale factor $a$. Hence perturbations of different scales $k$ exit the horizon at different times during inflation, and re-enter the horizon later on, after inflation. The smaller is $k$, the earlier they exit the horizon, and the later they re-enter it.

## Short-wavelength perturbations

For large momenta, eq. (3.48) reduces to the equation of motion of a massless scalar field in the static Minkowski space-time,

$$\boxed{k^2 \gg \hat{z}''/\hat{z} \ : \qquad \hat{f}'' + k^2\hat{f} \approx 0} \ . \tag{3.49}$$

This can be immediately solved,

$$\hat{f}_{\mathbf{k}}(\tau) \approx A_{\mathbf{k}}e^{ik\tau} + B_{\mathbf{k}}e^{-ik\tau} \ . \tag{3.50}$$

We quantize the solution $\hat{f}$ to a field operator in the Heisenberg picture [27, p.21],[16]

$$\hat{f}(\tau, \boldsymbol{x}) = \int \frac{\mathrm{d}^3k}{(2\pi)^{3/2}\sqrt{2k}}\left(e^{ik\tau - i\boldsymbol{k}\cdot\boldsymbol{x}}\mathrm{w}_{\mathbf{k}}^\dagger + e^{-ik\tau + i\boldsymbol{k}\cdot\boldsymbol{x}}\mathrm{w}_{\mathbf{k}}\right) \ , \tag{3.51}$$

with frequency $\omega_{\mathbf{k}} = k$. The creation and annihilation operators $\mathrm{w}_{\mathbf{k}}^\dagger$ and $\mathrm{w}_{\mathbf{k}}$ obey the standard commutation relation,

$$\left[\mathrm{w}_{\mathbf{k}'}, \mathrm{w}_{\mathbf{k}}^\dagger\right] = \delta(\boldsymbol{k}' - \boldsymbol{k}) \ . \tag{3.52}$$

To study the validity domain of this solution let us turn to the slow-roll approximation. It is then convenient to abandon conformal time for a moment and write (cf. eqs. (3.44) and (3.47))

$$\hat{z} = \frac{\bar{\varphi}'}{\mathcal{H}}a(\tau) \overset{(2.7)}{=} \frac{\dot{\bar{\varphi}}}{H}a(t) \approx \mathrm{const}\cdot a(t) \ , \tag{3.53}$$

as $\dot{\bar{\varphi}}$ and $H$ evolve slowly during inflation. Therefore, the variable $\hat{z}''/\hat{z} \approx a''/a = a^2(\dot{H} + 2H^2)$ increases exponentially in the slow-roll regime. At a given scale $k$, the short-wavelength regime is thus valid at early times, when $a \to 0$ and therefore physical momenta are large, $k/a \gg H$.

Assuming that this applies at the beginning of inflation, the initial vacuum state for the field $\hat{f}$ is the one annihilated by the operator $\mathrm{w}_{\mathbf{k}}$.

[16] For consistency with the rest of the chapter, here we use different conventions than the ones presented on p. iv. In particular, we quantize in a flat space-time with metric convention $\eta^{00} = -1$.

## Long-wavelength perturbations

For small momenta, i.e. at a late stage of inflation $k \ll Ha$, eq. (3.48) reduces to

$$\boxed{k^2 \ll \hat{z}''/\hat{z} \;:\qquad \hat{f}'' - \frac{\hat{z}''}{\hat{z}}\hat{f} \approx 0} \qquad \Leftrightarrow \qquad \frac{\hat{f}''}{\hat{f}} \approx \frac{\hat{z}''}{\hat{z}} \;. \tag{3.54}$$

As $\hat{z}$ only depends on the background solution and thus on $\tau$, it can be considered as a time variable, and we solve for $\hat{f} = \hat{f}(\hat{z})$. Then a solution is $\hat{f} \approx C_1\hat{z}$, while in general we solve

$$\hat{f}''\hat{z} - \hat{f}\hat{z}'' = 0 \quad \Leftrightarrow \quad \hat{f}''\hat{z} + \hat{f}'\hat{z}' - \hat{f}'\hat{z} - \hat{f}\hat{z}'' = 0 \tag{3.55}$$

$$\Leftrightarrow \quad \hat{f}'\hat{z} - \hat{f}\hat{z}' = \text{const.} \equiv C_2 \tag{3.56}$$

$$\Rightarrow \quad \left(\frac{\hat{f}}{\hat{z}}\right)' = \frac{C_2}{\hat{z}^2} \tag{3.57}$$

$$\Rightarrow \quad \hat{f} = C_2\hat{z}\int\frac{\mathrm{d}\tau}{\hat{z}^2} \;. \tag{3.58}$$

The complete solution in the long-wavelength limit is thus

$$\hat{f}(\tau) \approx C_1\hat{z} + C_2\hat{z}\int\frac{\mathrm{d}\tau}{\hat{z}^2} \;. \tag{3.59}$$

Transforming to physical time $\tau \to t$, in the slow-roll regime we approximate $\hat{z} \approx a$, and find

$$\hat{f}(t) \approx \underbrace{\tilde{C}_1 a}_{\text{growing}} + \underbrace{\tilde{C}_2\, a\int\frac{\mathrm{d}t}{a^3}}_{\text{decreasing}} \;. \tag{3.60}$$

The decreasing part vanishes rapidly as $a$ grows exponentially, and is thus negligible. Comparing eq. (3.59) with the definition $\hat{f} \equiv -\hat{z}\mathcal{R}$ yields

$$\hat{f} \approx \text{const}\cdot\hat{z} = -\mathcal{R}\hat{z} \quad \Rightarrow \quad \mathcal{R} \approx \text{const} \;, \tag{3.61}$$

for long-wavelength modes during the slow-roll regime.

The key result is that we can define a quantity $\mathcal{R}$, related to the perturbation of the spatial curvature, which stays constant while outside the horizon, i.e. $k \ll aH$. At horizon exit, during inflation, $\mathcal{R}$ is related to the inflaton perturbation $\delta\varphi$. This can be seen most easily by transforming to the spatially flat gauge.

## Spatially flat gauge

The spatially flat gauge is defined by vanishing comoving curvature,

$$\boxed{h_{\mathrm{D}}^{\mathrm{f}} + \frac{1}{3}\nabla^2\vartheta^{\mathrm{f}} = 0} \;, \tag{3.62}$$

such that the perturbations of the curvature are only determined by field perturbations,

$$\mathcal{R} \underset{(3.34)}{\overset{(2.100)}{=}} -h_{\mathrm{D}} - \frac{1}{3}\nabla^2\vartheta - \mathcal{H}\frac{\delta\varphi}{\bar{\varphi}'} \overset{(3.62)}{=} -\mathcal{H}\frac{\delta\varphi^{\mathrm{f}}}{\bar{\varphi}'} \;. \tag{3.63}$$

We transform to the spatially flat gauge with the gauge parameter $\xi^0 = -\mathcal{H}^{-1}\left(h_{\mathrm{D}} + \nabla^2\vartheta/3\right)$, cf. eq. (2.42). The other scalar gauge parameter $\xi$ does not need to be specified. In the literature, the inflaton perturbation in this gauge is often called the Sasaki or Mukhanov variable,

$$\delta\varphi^{\mathrm{f}} = \delta\varphi + \frac{\bar{\varphi}'}{\mathcal{H}}\left(h_{\mathrm{D}} + \frac{1}{3}\nabla^2\vartheta\right) \overset{(2.46)}{=} \delta\varphi^{\mathrm{N}} + \frac{\bar{\varphi}'}{\mathcal{H}}\psi \overset{(3.44)}{=} f \;, \tag{3.64}$$

and corresponds precisely to the variable $f \equiv \hat{f}/a$ introduced in eq. (3.44). Since the relation $\delta\varphi^{\rm f} = f = -z\mathcal{R}$ is linear,[17] their power spectra follow a simple relation as well,

$$\mathcal{P}_{\mathcal{R}}(k) = \frac{1}{z^2}\mathcal{P}_f(k) = \left(\frac{\mathcal{H}}{\bar{\varphi}'}\right)^2 \mathcal{P}_f(k) \underset{(2.49)}{\overset{(2.7)}{=}} \left(\frac{H}{\dot{\bar{\varphi}}}\right)^2 \mathcal{P}_f(k) \ . \tag{3.65}$$

## Power spectrum

To find the power spectrum of $f$, we need to interpolate the solutions (3.51) and (3.61) at the time around horizon exit, i.e. when $k \approx aH$. Considering that this happens during inflation, we use eqs. (3.13) and (3.53) to substitute the scale factor $\hat{z} \sim a$ in eq. (3.48) with an explicit expression in $\tau$, and solve

$$\hat{f}'' + \left(-\frac{2}{\tau^2} + k^2\right)\hat{f} = 0 \tag{3.66}$$

$$\Rightarrow \qquad \hat{f}_k^{(\pm)} = \left(1 \pm \frac{i}{k\tau}\right) e^{\pm ik\tau} \ . \tag{3.67}$$

Near horizon exit the quantized solution is

$$\hat{f}(\tau, \boldsymbol{x})_{\{k\}} = \int_{\{k\}} \frac{\mathrm{d}^3 k}{(2\pi)^{3/2}\sqrt{2k}} \left(\hat{f}_k^{(+)}(\tau) e^{-i\boldsymbol{k}\cdot\boldsymbol{x}} \mathrm{w}_{\mathbf{k}}^\dagger + \hat{f}_k^{(-)}(\tau) e^{i\boldsymbol{k}\cdot\boldsymbol{x}} \mathrm{w}_{\mathbf{k}}\right) \ . \tag{3.68}$$

The subscript $\{k\}$ denotes modes of momenta around $k = aH$. We assume that the quantum state is the vacuum state, annihilated by $\mathrm{w}_{\mathbf{k}}$. At early times we recover the flat-space solution, $\hat{f}_k^{(\pm)} \overset{\tau\to-\infty}{\to} e^{\pm ik\tau}$. After horizon exit, $k < aH$, the field becomes

$$\hat{f}(\tau, \boldsymbol{x})_{\{k\}<aH} = \int_{\{k\}<aH} \frac{\mathrm{d}^3 k}{(2\pi)^{3/2}\sqrt{2k}} \left(-\frac{1}{k\tau}\right) \left(e^{-i\boldsymbol{k}\cdot\boldsymbol{x}+i\alpha_k} \mathrm{w}_{\mathbf{k}}^\dagger + e^{i\boldsymbol{k}\cdot\boldsymbol{x}-i\alpha_k} \mathrm{w}_{\mathbf{k}}\right) \ . \tag{3.69}$$

The phases $\alpha_k$ are not specified as they do not enter the power spectrum. Using $f = \hat{f}/a$ and eq. (3.13), the perturbation of the inflaton field $f$, in the spatially flat gauge, and outside the horizon, is

$$f(\tau, \boldsymbol{x})_{\{k\}<aH} = \int_{\{k\}<aH} \frac{\mathrm{d}^3 k}{(2\pi)^{3/2}\sqrt{2k}} \frac{H}{k} \left(e^{-i\boldsymbol{k}\cdot\boldsymbol{x}+i\alpha_k} \mathrm{w}_{\mathbf{k}}^\dagger + e^{i\boldsymbol{k}\cdot\boldsymbol{x}-i\alpha_k} \mathrm{w}_{\mathbf{k}}\right) \ . \tag{3.70}$$

Transforming $\tau \to t$, the mean-square value of vacuum fluctuations is

$$\langle |f_{\mathbf{k}}|^2 \rangle = \left|\frac{H}{(2\pi)^{3/2}\sqrt{2k}k}\right|^2 = \frac{H^2}{2(2\pi)^3}\frac{1}{k^3} \ . \tag{3.71}$$

Eq. (3.71) is evaluated just after horizon exit, denoted by $t_*$, by inserting $H = H_*$. The resulting inflaton power spectrum, defined as in eq. (A.89), does not depend explicitly on the mode $k$,

$$\mathcal{P}_f(k) = 4\pi k^3 \frac{H_*^2}{2(2\pi)^3 k^3} = \left(\frac{H_*}{2\pi}\right)^2 \ . \tag{3.72}$$

From eq. (3.65) we compute the power spectrum of curvature perturbations in the comoving frame,

$$\mathcal{P}_{\mathcal{R}} = \left(\frac{H_*^2}{2\pi\dot{\bar{\varphi}}}\right)^2 \ . \tag{3.73}$$

[17] The interpretation of $f$ as the field perturbation $\delta\varphi$ is gauge-dependent.

## 3.3 Tensor perturbations

From eq. (3.33) we learn that, at first order in perturbation theory, there is no anisotropic stress sourced by inflation. Expanding the tensor perturbations of the metric in a Fourier basis,

$$\vartheta_{ij}(\tau,\boldsymbol{x}) = \int \frac{\mathrm{d}^3k}{(2\pi)^3}\,\vartheta_{ij}(\tau,\boldsymbol{k})\,e^{i\boldsymbol{k}\cdot\boldsymbol{x}}\ , \tag{3.74}$$

the Einstein equations for tensor perturbations, cf. (2.133), reduce to wave equations in vacuum,

$$\Pi^{\mathrm{t}}_{ij} = 0 \quad \Rightarrow \qquad \vartheta''_{ij} + 2\mathcal{H}\vartheta'_{ij} + k^2\vartheta_{ij} = 0\ . \tag{3.75}$$

### Helicity decomposition

Being a symmetric, traceless and transverse $3\times3$ tensor, the number of independent components of $\vartheta_{ij}$ is two. As a consequence, it can be decomposed in a two-dimensional basis of helicity tensors,

$$\vartheta_{ij}(\tau,\boldsymbol{k}) = \sum_{\lambda=+,\times} \epsilon^{\lambda}_{ij}(\boldsymbol{k})\,h_\lambda(\tau,k)\ . \tag{3.76}$$

To construct the latter, let us consider two unit (co)vectors $\boldsymbol{\epsilon}^{(a)}$ and $\boldsymbol{\epsilon}^{(b)}$ orthogonal to each other and to the wave vector $\boldsymbol{k}$, such that together they form a right-handed triple,

$$\left|\boldsymbol{\epsilon}^{(a,b)}\right| = 1\ , \qquad \boldsymbol{\epsilon}^{(a,b)}\cdot\boldsymbol{k} = \boldsymbol{\epsilon}^{(a)}\cdot\boldsymbol{\epsilon}^{(b)} = 0\ , \qquad \boldsymbol{\epsilon}^{(a)}\times\boldsymbol{\epsilon}^{(b)} = \boldsymbol{k}\ , \quad \boldsymbol{\epsilon}^{(a,b)}\times\boldsymbol{k} = \boldsymbol{\epsilon}^{(b,a)}\ . \tag{3.77}$$

Then there are two possible symmetric, traceless and transverse real tensors that can be built,

$$\epsilon^{+}_{ij} = \frac{1}{\sqrt{2}}\big(\epsilon^{(a)}_i\epsilon^{(a)}_j - \epsilon^{(b)}_i\epsilon^{(b)}_j\big)\ , \qquad \epsilon^{\times}_{ij} = \frac{1}{\sqrt{2}}\big(\epsilon^{(a)}_i\epsilon^{(b)}_j + \epsilon^{(b)}_i\epsilon^{(a)}_j\big)\ . \tag{3.78}$$

The (massless) graviton is a spin two particle. The projection (helicity) of its spin along the momentum direction $\boldsymbol{k}$ is thus either plus or minus two. To verify that $\epsilon^{+}_{ij}$ and $\epsilon^{\times}_{ij}$ form an adequate basis, we compute their transformation behaviour under rotations $U\in\mathrm{SO}(2)$ by an angle $\alpha$ around the $\boldsymbol{k}$-axis. Using complex coordinates for the plane normal to $\boldsymbol{k}$,

$$\epsilon^{(\pm1)}_i \equiv \epsilon^{(a)}_i \pm i\,\epsilon^{(b)}_i\ , \qquad \epsilon^{(\pm2)}_{ij} \equiv \epsilon^{+}_{ij} \pm i\,\epsilon^{\times}_{ij} \;=\; \frac{1}{\sqrt{2}}\epsilon^{(\pm1)}_i\epsilon^{(\pm1)}_j\ , \tag{3.79}$$

the symmetry group is $\mathrm{U}(1)$.[18] Under the action of $\mathrm{U}(1)$ we find the transformation behaviours

$$\epsilon^{(\pm1)}_i \;\to\; e^{\pm i\alpha}\,\epsilon^{(\pm1)}_i \qquad \Rightarrow \qquad \epsilon^{(\pm2)}_{ij} \;\to\; e^{\pm2i\alpha}\,\epsilon^{(\pm2)}_{ij}\ . \tag{3.80}$$

A general symmetric, traceless and transverse tensor $\vartheta_{ij}$ is then a linear combination of helicities $\pm2$.

Although transverse polarization modes are defined on the spatial components, it is sometimes useful to work in $D = 3+1$ dimensions (see e.g. sec. 6.2), denoting

$$\epsilon^{(a)}_\mu = (0,\epsilon^{(a)}_i)\ , \quad \epsilon^{+}_{\mu\nu} = \frac{1}{\sqrt{2}}\left(\epsilon^{(a)}_\mu\epsilon^{(a)}_\mu - \epsilon^{(b)}_\mu\epsilon^{(b)}_\nu\right)\ , \quad \epsilon^{\times}_{\mu\nu} = \frac{1}{\sqrt{2}}\left(\epsilon^{(a)}_\mu\epsilon^{(b)}_\mu + \epsilon^{(b)}_\mu\epsilon^{(a)}_\nu\right)\ . \tag{3.81}$$

The polarization vectors satisfy by construction the sum rules

$$\sum_{i,j}\epsilon^{\lambda}_{ij}[\epsilon^{\lambda'}_{ij}]^* = \delta^{\lambda\lambda'}\ , \qquad \sum_{\lambda}\epsilon^{\lambda}_{ij}[\epsilon^{\lambda}_{mn}]^* = \mathbb{L}_{ij;mn}\ , \tag{3.82}$$

[18] The two groups are related by the isomorphism that associates $e^{i\alpha}$ with the matrix $U(\alpha) = \begin{pmatrix}\cos\alpha & \sin\alpha\\ -\sin\alpha & \cos\alpha\end{pmatrix}$.

where $\mathbb{L}$ is the projector onto the traceless components, transverse to the momentum $\mathbf{k}$ of the graviton. In $D = 3 + 1$ dimensions it reads

$$\mathbb{L}_{\alpha\beta;\mu\nu} \equiv \frac{1}{2}\left(\mathbb{K}^{\mathrm{T}}_{\alpha\mu}\mathbb{K}^{\mathrm{T}}_{\beta\nu} + \mathbb{K}^{\mathrm{T}}_{\alpha\nu}\mathbb{K}^{\mathrm{T}}_{\beta\mu} - \mathbb{K}^{\mathrm{T}}_{\alpha\beta}\mathbb{K}^{\mathrm{T}}_{\mu\nu}\right) , \quad \mathbb{K}^{\mathrm{T}}_{\alpha\beta} \equiv \eta_{\alpha i}\eta_{\beta j}\left(\delta_{ij} - \frac{k_i k_j}{k^2}\right) , \tag{3.83}$$

Keeping the sign convention $\eta^{00} = \pm 1$ in the metric unspecified, two useful properties of $\mathbb{K}^{\mathrm{T}}$ are[19]

$$\mathbb{K}^{\mathrm{T}}_{\alpha\mu}\,\mathbb{K}^{\mathrm{T}\mu}_{\beta} = -\eta^{00}\mathbb{K}^{\mathrm{T}}_{\alpha\beta} , \quad \mathbb{K}^{\mathrm{T}\mu}_{\mu} = -2\eta^{00} . \tag{3.84}$$

For the operator $\mathbb{L}_{\alpha\beta;\mu\nu}$ one finds the symmetries

$$\mathbb{L}_{\alpha\beta;\mu\nu} = \mathbb{L}_{\beta\alpha;\mu\nu} = \mathbb{L}_{\alpha\beta;\nu\mu} = \mathbb{L}_{\mu\nu;\alpha\beta} , \tag{3.85}$$

and, from eq. (3.84), the contractions

$$\mathbb{L}_{\alpha\beta;}{}^{\alpha}{}_{\nu} = -\eta^{00}\mathbb{K}^{\mathrm{T}}_{\beta\nu} , \ \dots , \qquad \mathbb{L}_{\alpha}{}^{\alpha}{}_{;\mu\nu} = \mathbb{L}_{\mu\nu;\alpha}{}^{\alpha} = 0 , \qquad \mathbb{L}_{\alpha\beta;}{}^{\alpha\beta} = \mathbb{L}_{\alpha\beta;}{}^{\beta\alpha} = 2 . \tag{3.86}$$

We also find the relations

$$\mathbb{L}_{\alpha\beta;\mu\nu} + \mathbb{L}_{\alpha\nu;\mu\beta} = \mathbb{K}^{\mathrm{T}}_{\alpha\mu}\mathbb{K}^{\mathrm{T}}_{\beta\nu} , \qquad \mathbb{L}_{\alpha\beta;\mu\nu} + \mathbb{L}_{\nu\beta;\mu\alpha} = \mathbb{K}^{\mathrm{T}}_{\alpha\nu}\mathbb{K}^{\mathrm{T}}_{\beta\mu} , \ \dots . \tag{3.87}$$

## Power spectrum

Inserting eq. (3.76), eq. (3.75) boils down to the same scalar equation for each helicity component,

$$h''_\lambda + 2\mathcal{H}h'_\lambda + k^2 h_\lambda = 0 , \qquad \lambda \in \{+, \times\} , \tag{3.88}$$

that describes the propagation of gravity waves with the speed of light. Introducing the variable

$$\hat{h}_\lambda \equiv a\, h_\lambda , \qquad \frac{\hat{h}''_\lambda}{a} = h''_\lambda + 2\mathcal{H}h'_\lambda + \frac{a''}{a}h_\lambda , \tag{3.89}$$

the evolution equation (3.88) for tensor perturbations is

$$\boxed{\hat{h}''_\lambda + k^2\hat{h}_\lambda - \frac{a''}{a}\hat{h}_\lambda = 0} . \tag{3.90}$$

Eq. (3.90) has precisely the same form as the evolution equation (3.48) for scalar perturbations, whose solution we already computed (see eqs. (3.66)–(3.68)).

Summing over the polarizations, the power spectrum of tensor perturbations is

$$\sum_{\lambda,\lambda'}\sum_{i,j}\epsilon^{\lambda}_{ij}\epsilon^{\lambda'}_{ij}\langle h^\lambda h^{\lambda'}\rangle = 2\langle h^\lambda h^\lambda\rangle , \tag{3.91}$$

where $\lambda$ on the right hand-side is one or the other polarization, since they satisfy the same evolution equation.

When quantizing the fields (cf. eq. (3.51)), the normalization is given by the prefactor $1/(32\pi G)$ in the gravity action, and the power spectrum for tensor perturbations is

$$\mathcal{P}_{\mathrm{T}} = 32\pi G\sum_{+,\times}\mathcal{P}_f \overset{(3.72)}{=} \frac{16}{\pi}\left(\frac{H_*}{m_{\mathrm{pl}}}\right)^2 . \tag{3.92}$$

[19] The expressions in (3.84) are used intensively in chapter 6 and appendix C, where we use the *particle physics convention* $\eta^{00} = +1$.

## Stochastic derivation

The *flat* (k-independent) spectrum in eq. (3.92) resembles a *white noise* spectrum. This observation suggests that the same results may be obtained following a stochastic argument (see e.g. [28]), which we briefly present here.

Consider scalar fluctuations $h(\tau,\mathbf{x})$ in position space. For us they represent the Fourier-transform of $h_\lambda(\tau,k)$ for a given polarization $\lambda$ (omitted in the notation from now on). Since the generation of fluctuations is a random process, they are equally distributed among those extending to short and long distances. To study how the evolution of long-distance fluctuations is affected by short-distance ones, we write

$$h(\tau,\mathbf{x}) = \underbrace{h_<}_{\text{short}} + \underbrace{h_>}_{\text{long}} \ , \tag{3.93}$$

and quantize short-distance fluctuations using the same prescriptions as in eq. (3.51),

$$h_<(\tau,\mathbf{x}) \equiv \int \frac{\mathrm{d}^3k}{\sqrt{(2\pi)^3}}\, W(\tau,k)\left[\mathrm{w}_\mathbf{k}\, h_<(\tau,k)\, e^{i\mathbf{k}\cdot\mathbf{x}} + \mathrm{w}^\dagger_\mathbf{k}\, h^*_<(\tau,k)\, e^{-i\mathbf{k}\cdot\mathbf{x}}\right] \ , \tag{3.94}$$

where the coefficients are solutions of eq. (3.88),

$$h_<(\tau,k) = \frac{iH}{\sqrt{2k^3}}(1+ik\tau)\, e^{-ik\tau} \ . \tag{3.95}$$

The window function constrains the momentum integration and can be chosen for example as

$$W(\tau,k) \equiv \theta(k-\epsilon\mathcal{H}) \overset{(3.13)}{=} \theta\left(k-\frac{\epsilon}{\tau}\right) \ , \tag{3.96}$$

where $\epsilon$ is a parameter that drops out when evaluating physical observables. From the evolution equation for $h(\tau,\mathbf{x})$ in position space we obtain a relation among $h_>$ and $h_<$,

$$h'' + 2\mathcal{H}h' - \nabla^2 h = 0 \qquad \overset{(3.13)}{\Leftrightarrow} \qquad h'' - \frac{2}{\tau}h' - \nabla^2 h = 0 \tag{3.97}$$

$$\overset{(3.93)}{\Rightarrow} \qquad h_>'' - \frac{2}{\tau}h_>' - \nabla^2 h_> = \rho_Q \ . \tag{3.98}$$

The dependence on the short-distance fluctuations $h_<$ is encoded in the quantum noise term,

$$\rho_Q \equiv -\left(\partial_\tau^2 - \frac{2}{\tau}\partial_\tau - \nabla^2\right) h_< \ , \tag{3.99}$$

on the right-hand side of eq. (3.98). Inserting eq. (3.94), by construction we have vanishing contributions when the differential operator in $\rho_Q$ acts on $h_<(\tau,k)$. The remaining terms are

$$\rho_Q(\tau,\mathbf{x}) = -\int \frac{\mathrm{d}^3k}{\sqrt{(2\pi)^3}}\left[\mathrm{w}_\mathbf{k}\, \mathcal{F}_k(\tau)\, e^{i\mathbf{k}\cdot\mathbf{x}} + \mathrm{w}^\dagger_\mathbf{k}\, \mathcal{F}^*_k(\tau)\, e^{-i\mathbf{k}\cdot\mathbf{x}}\right] \ , \tag{3.100}$$

$$\mathcal{F}_k(\tau) = \left(W'' - \frac{2}{\tau}W'\right)h_<(\tau,k) + 2W'h_<'(\tau,k) \ . \tag{3.101}$$

The operators $\mathrm{w}_\mathbf{k}$ and $\mathrm{w}^\dagger_\mathbf{k}$ obey the commutation relations introduced in eq. (3.52). For the power spectrum of $h_>$ we need the unequal-time two-point function in spatial momentum space,

$$\langle 0|\, \rho_Q(\tau_1,\mathbf{x}_1)\rho_Q(\tau_2,\mathbf{x}_2)\, |0\rangle = \int \frac{\mathrm{d}^3k}{(2\pi)^3}\, \mathcal{F}_k(\tau_1)\mathcal{F}^*_k(\tau_2)\, e^{i\mathbf{k}\cdot(\mathbf{x}_1-\mathbf{x}_2)} \tag{3.102}$$

$$= \int \frac{\mathrm{d}^3k_1}{(2\pi)^3}\int \frac{\mathrm{d}^3k_2}{(2\pi)^3}\, \langle 0|\, \rho_Q(\tau_1,\mathbf{k}_1)\rho_Q(\tau_2,\mathbf{k}_2)\, |0\rangle\, e^{i(\mathbf{k}_1\cdot\mathbf{x}_1+\mathbf{k}_2\cdot\mathbf{x}_2)}$$

$$\Rightarrow \quad \langle 0|\, \rho_Q(\tau_1,\mathbf{k}_1)\rho_Q(\tau_2,\mathbf{k}_2)\, |0\rangle = (2\pi)^3\delta(\mathbf{k}_1+\mathbf{k}_2)\, \mathcal{F}_k(\tau_1)\mathcal{F}^*_k(\tau_2) \ . \tag{3.103}$$

Back to eq. (3.98), it can be solved using a retarded Green's function $G_{\rm R}$ satisfying

$$\left(\partial_\tau^2 - \frac{2}{\tau}\partial_\tau + k^2\right) G_{\rm R}(\tau,\tau_i,k) = \delta(\tau-\tau_i)\ , \qquad G_{\rm R}(\tau<\tau_i,\tau_i,k)\equiv 0\ . \tag{3.104}$$

For $\tau > \tau_i$ the general solution is the linear combination of two independent solutions,

$$G_{\rm R}(\tau,\tau_i,k) = \theta(\tau-\tau_i)\left[C_k(1+ik\tau)e^{-ik(\tau-\tau_i)} + C_k^*(1-ik\tau)e^{ik(\tau-\tau_i)}\right]\ . \tag{3.105}$$

The coefficients $C_k$ are obtained by integrating eq. (3.104), i.e. from

$$\lim_{\tau\to\tau_i^+} G_{\rm R}(\tau,\tau_i,k) = 0 \qquad\Rightarrow\quad C_k(1+ik\tau_i) = -C_k^*(1-ik\tau_i) \tag{3.106}$$

$$\lim_{\tau\to\tau_i^+} \partial_\tau G_{\rm R}(\tau,\tau_i,k) = 1 \qquad\Rightarrow\quad -2ik^3\tau_i^2 C_k = 1-ik\tau_i\ . \tag{3.107}$$

The resulting Green's function is therefore

$$\begin{aligned} G_{\rm R}(\tau,\tau_i,k) &= \frac{\theta(\tau-\tau_i)}{k^3\tau_i^2}\,{\rm Im}\left[(1+ik\tau_i)(1-ik\tau)e^{ik(\tau-\tau_i)}\right] \\ &= \frac{\theta(\tau-\tau_i)}{k^3\tau_i^2}\left[(1+k^2\tau\tau_i)\,\sin k(\tau-\tau_i) - k(\tau-\tau_i)\,\cos k(\tau-\tau_i)\right]\ , \end{aligned} \tag{3.108}$$

and the solution of eq. (3.98) in spatial momentum space reads

$$h_>(\tau,\mathbf{k}) = \int_{-\infty}^{\tau} {\rm d}\tau_i\, G_{\rm R}(\tau,\tau_i,k)\,\rho_Q(\tau_i,\mathbf{k})\ . \tag{3.109}$$

To obtain the power spectrum for tensor perturbations we compute the equal-time correlator

$$\begin{aligned} \langle\, h_>(\tau,\mathbf{k})\, h_>(\tau,\mathbf{q})\,\rangle \;&=\; \int_{-\infty}^{\tau}{\rm d}\tau_1 \int_{-\infty}^{\tau}{\rm d}\tau_2\, G_{\rm R}(\tau,\tau_1,k)\, G_{\rm R}(\tau,\tau_2,q)\,\langle 0|\,\rho_Q(\tau_1,\mathbf{k}_1)\rho_Q(\tau_2,\mathbf{k}_2)\,|0\rangle \\ &\overset{(3.103)}{=} \delta(\mathbf{k}+\mathbf{q})\,\Big|\underbrace{\int_{-\infty}^{\tau}{\rm d}\tau_i\, G_{\rm R}(\tau,\tau_i,k)\,\mathcal{F}_k(\tau_i)}_{\equiv I}\Big|^2\ . \end{aligned} \tag{3.110}$$

The integral in eq. (3.110) can be carried out by inserting $\mathcal{F}_k$ from eq. (3.101). Choosing the window function as in eq. (3.96) we have $W' = \delta(\tau_i - \tau_{*k})$, where $\tau_{*k} \equiv -\epsilon/k$ denotes the time at which the mode $k$ crosses the horizon. The expression $\mathcal{F}_k$ is therefore made of delta functions and derivatives thereof. To get rid of the latter we use partial integration once, obtaining

$$\begin{aligned} I &\overset{(3.101)}{=} \int_{-\infty}^{\tau}{\rm d}\tau_i\, W'(\tau_i)\left[-(\partial_{\tau_i}G_{\rm R})h_< + G_{\rm R}\left(h_<' - \frac{2}{\tau_i}h_<\right)\right] \\ &\overset{(3.96)}{=} \left\{-\left[\partial_{\tau_i}G_{\rm R}(\tau,\tau_i,k)\right]\,h_<(\tau_i) + G_{\rm R}(\tau,\tau_i,k)\left[h_<'(\tau_i) - \frac{2}{\tau_i}\,h_<(\tau_i)\right]\right\}_{\tau_i=\tau_{*k}}\ . \end{aligned} \tag{3.111}$$

Eqs. (3.95) and (3.108) yield the explicit form of the three terms in $I$. Modulo $A_k(\tau_i) \equiv \frac{iHe^{-ik\tau_i}}{\sqrt{2k^3}\tau_i}$ the latter read

$$\begin{aligned} -\frac{(\partial_{\tau_i}G_{\rm R})\,h_<}{A_k} = (1+ik\tau_i)\Bigg\{ &\sin k(\tau-\tau_i)\left[\cancelto{0}{\delta(\tau-\tau_i)}\,\frac{1+k^2\tau\tau_i}{k^3\tau_i} + \overbrace{\theta(\tau-\tau_i)}^{=1}\left(2\,\frac{1+k^2\tau\tau_i}{k^3\tau_i^2} - \frac{1}{k}\right)\right] \\ &- \cos k(\tau-\tau_i)\left[\underbrace{\delta(\tau-\tau_i)\frac{\tau-\tau_i}{k^2\tau_i}}_{=0} + \underbrace{\theta(\tau-\tau_i)}_{=1}\left(2\,\frac{\tau-\tau_i}{k^2\tau_i^2} - \tau\right)\right]\Bigg\}\ , \end{aligned} \tag{3.112}$$

$$\frac{G_{\rm R}\,h_<'}{A_k} = \underbrace{\theta(\tau-\tau_i)}_{=1}\left[\,\frac{1+k^2\tau\tau_i}{k}\,\sin k(\tau-\tau_i) - (\tau-\tau_i)\,\cos k(\tau-\tau_i)\,\right]\ , \tag{3.113}$$

$$-\frac{2}{\tau_i}\,\frac{G_{\rm R}\,h_<}{A_k} = 2(1+ik\tau_i)\,\underbrace{\theta(\tau-\tau_i)}_{=1}\left[\,\cancel{\frac{\tau-\tau_i}{k^2\tau_i^2}}\,\cos k(\tau-\tau_i) - \cancel{\frac{1+k^2\tau\tau_i}{k^3\tau_i^2}}\,\sin k(\tau-\tau_i)\,\right]\ . \tag{3.114}$$

The sum of the three contributions in eq. (3.111) gives therefore

$$I = \frac{iH}{\sqrt{2k^3}}\, e^{-ik\tau_i}\, \left[\, (1+ik\tau)\, \cos k(\tau-\tau_i) + (-i+k\tau)\, \sin k(\tau-\tau_i)\, \right] = \frac{iH}{\sqrt{2k^3}}\, (1+ik\tau)\, e^{-ik\tau}\ . \quad (3.115)$$

Perturbations of long wavelengths (small momenta) exit the horizon in the earliest stages of the slow-roll regime of inflation and soon satisfy $k \ll \mathcal{H} \approx 1/\tau$. We thus expand at first order in $k\tau$,

$$I \overset{k\tau\ll 1}{\approx} \frac{iH}{\sqrt{2k^3}}\ . \quad (3.116)$$

Inserting the result in eq. (3.110) and multiplying by $2\times 32\pi G\times k^3/(2\pi^2)$ one obtains precisely the power spectrum found in eq. (3.92).

## 3.4 Observational constraints

What is the relation between the power spectra of scalar and tensor fluctuations in eqs. (3.73) and (3.92), and the power spectrum of CMB temperature fluctuations?

Let us follow the evolution of a mode $k$ after inflation. While $k$ is outside the horizon, we expect that inflation ends, the universe gets reheated and becomes then radiation dominated (or even matter dominated for the largest scales, i.e. smallest $k$). During this time the power spectra of the primordial scalar and tensor perturbations remain unchanged. But in the meanwhile the dominant component in the energy density filling the universe changes from the one of the inflaton field, $e_\varphi$, to radiation energy density, $e_r$, that we describe as a fluid satisfying the equation of state $p_r = e_r/3$.

Once the mode has re-entered the horizon, i.e. $k = aH$ has occured again, it propagates through the radiation dominated epoch as described by a more complicated version of Einstein's equations, now coupled with some Boltzmann equations. Then we write the perturbation as a functional of its initial value at $k = aH$. As an example we take the perturbations in the relative energy density at decoupling (but the same applies for tensor modes). In the co-moving gauge we have

$$\Delta(\tau,k) \equiv X(\tau,\tau_*,k)\, \Delta(\tau_*,k)\ , \qquad X(\tau_*,\tau_*,k) \equiv 1\ , \quad \partial_\tau X(\tau,\tau_*,k)|_{\tau=\tau_*} = 0\ , \quad (3.117)$$

cf. eq. (2.101). The initial time $\tau_*$ denotes the moment when $k$ re-enters the horizon, or equivalently when it exits the horizon, if $\Delta$ remains constant in the meanwhile. Therefore the power spectrum observed at $\tau$ is related to the primordial power spectrum at $\tau_*$ by the so-called transfer function,

$$\mathcal{P}_\Delta(\tau,k) = \underbrace{[X(\tau,\tau_*,k)]^2}_{\equiv \mathcal{T}_s(\tau,\tau_*,k)}\, \mathcal{P}_\Delta(\tau_*,k)\ . \quad (3.118)$$

The transfer function $\mathcal{T}_s$ itself contains lots of physics, which has been studied intensively, see e.g. [29–31] and references therein.

Let us relate $\mathcal{P}_\Delta$ to the spectrum of curvature perturbations, $\mathcal{P}_\mathcal{R}$. Transforming eq. (2.119) to comoving gauge, cf. eq. (2.96), and comoving momentum space, yields

$$k^2(\mathcal{R} - \mathcal{H}\cancelto{0}{\vartheta^{\mathrm{c}\prime}}) = 4\pi G a^2 \bar{e}^{\mathrm{c}}\, \frac{\delta e^{\mathrm{c}}}{\bar{e}^{\mathrm{c}}}\ . \quad (3.119)$$

According to eq. (2.97) and eq. (3.38), the second term on the left-hand side corresponds to the velocity $\vartheta^{\mathrm{c}\prime} = -\delta\varphi^{\mathrm{N}}/\bar{\varphi}'$. At the time when the largest scales re-enter the horizon, we assume the latter to be a negligible contribution, while $\mathcal{R}$ remains at the same value since horizon-exit. The right-hand side of eq. (3.119) can be written in terms of $\mathcal{H}^2$ using eq. (2.111), thereby

$$\Delta(\tau,\mathbf{k}) \equiv \frac{\delta e^{\mathrm{c}}}{\bar{e}^{\mathrm{c}}} = \frac{2}{3}\left(\frac{k}{aH}\right)^2 \mathcal{R}(\tau,\mathbf{k})\ . \quad (3.120)$$

When a given mode $k$ crosses the horizon, $k = aH$, we thus have

$$\mathcal{P}_\Delta(\tau_*, k = aH) = \frac{4}{9}\mathcal{P}_\mathcal{R}(\tau_*, k = aH) = \frac{4}{9}\left(\frac{H_*^2}{2\pi\dot{\bar{\varphi}}}\right)^2 , \tag{3.121}$$

which gives the initial conditions for $\mathcal{P}_\Delta(\tau, k)$.

## Cosmic microwave background

In the following it is more convenient to use the physical time coordinate $t$. The observed temperature $T \sim 2.73$ K of the CMB radiation shows (see fig. 3.3, and fig. 3.4 for a broader perspective) relatively small temperature anisotropies of the order of[20] [10, 11]

$$\left(\frac{\delta T}{\bar{T}}\right)_{\rm obs} = \left(\frac{\delta T}{\bar{T}}\right)_{\rm intr} + \left(\frac{\delta T}{\bar{T}}\right)_{\rm jour} \sim 10^{-5} . \tag{3.122}$$

Besides an intrinsic (intr) component already present at recombination, they arise also from different physical processes (jour) occurring during the journey of the photons to the present. Among the latter, the dominant contribution at large scales is known as the *Sachs-Wolfe effect* [32]. This decomposition in an intrinsic and a journey component depends on the gauge chosen, but not their sum, the observed anisotropy.

To relate the perturbations in the energy density at $t_{\rm dec}$ to the temperature perturbations observed in the CMB let us assume the so called adiabatic conditions [33].[21] This means that the composition of the cosmic fluid is everywhere the same, and close to equilibrium the fluctuations in the energy density of each component can be parametrized by temperature fluctuations. Intrinsic temperature perturbations are related to perturbations in the photon energy density by Planck's law for blackbody radiation,[22]

$$e_r \sim T^4 \qquad \Rightarrow \qquad \left(\frac{\delta T}{\bar{T}}\right)_{\rm intr} = \frac{1}{4}\frac{\delta e_r}{\bar{e}_r} . \tag{3.123}$$

The standard deviation in the temperature is thus related to the power spectrum of primordial density fluctuations by

$$\frac{\mathrm{d}\langle[\delta T/\bar{T}]^2(t_{\rm dec})\rangle}{\mathrm{d}\ln k} \overset{(3.121)}{\supset} \frac{1}{36}\mathcal{T}_s(t_{\rm dec}, t_*, k)\,\mathcal{P}_\mathcal{R}(t_*) , \tag{3.124}$$

where $t_*$ denotes horizon exit/entry. Note that this moment is different for all modes $k$. Hence for each mode, $\mathcal{P}_\mathcal{R}(t_*)$ is evaluated at a different moment in time, resulting in a hidden dependence on $k$, which motivates the notation $\mathcal{P}_\mathcal{R}(k) \equiv \mathcal{P}_\mathcal{R}(t_*)$.

Extracting the primordial power spectrum from the observed anisotropy is a complex procedure. Here we sketch how an ansatz for the power spectrum of primordial density perturbations is obtained. First of all, one expands temperature fluctuations in terms of spherical harmonics $Y_{lm}$,[23]

$$\frac{\delta T(\theta, \phi)}{\bar{T}} = \sum_{l,m} a_{lm} Y_{lm}(\theta, \phi) , \tag{3.125}$$

[20] Observations reveal a stronger anisotropy of the order of $\delta T/\bar{T} \sim 10^{-3}$. However, the latter has a clear dipole structure and can be explained by the motion of the Earth relative to the CMB reference frame.

[21] This is a good approximation for most cases, however isocurvature modes may also play a role in general, see e.g. [34]. Moreover, note that the definition of adiabatic modes is gauge-dependent.

[22] At recombination the photon momentum distribution starts deviating from thermal equilibrium. However this effect is negligible for the large scales we are interested in.

[23] Spherical harmonics form an orthonormal basis of square-integrable functions on the sphere (sky). As $l = 1$ corresponds to the contribution discussed in footnote 20, here the sum over $l$ starts from $l = 2$.

where the coefficients $a_{lm}$ are independent complex variables. Averaged over the directional index $m$, their absolute values determine the power spectrum,

$$C_l \equiv \frac{1}{2l+1} \sum_{m=-l}^{l} |a_{lm}|^2 \ . \tag{3.126}$$

We note that the larger is the multipole moment $l$, the smaller is the corresponding angular scale $\theta_l \equiv \pi/l$, and the shorter the wavelength $\lambda \sim k^{-1}$ of the density perturbations producing the temperature fluctuations.[24] The standard deviation of the latter is given by an angular average over the multipoles,

$$\langle [\delta T/\bar{T}]^2 \rangle = \sum_l \sum_{m=-l}^{l} \frac{|a_{lm}|^2}{4\pi} = \sum_l \frac{2l+1}{4\pi} C_l \ , \tag{3.127}$$

and the total power in the multipole $l$ is conventionally defined as [12, p.200]

$$D_l \equiv \frac{l(l+1)}{2\pi} C_l \ . \tag{3.128}$$

The measured $D_l$ (figure 3.3) present an oscillatory behaviour, with a global maximum at $l \sim 200$. The amplitude decreases as $l$ increases, starting from $l \sim 500$, and oscillations are damped after $l \sim 1000$. This shape can be explained by thinking that, in the plasma era just before decoupling, small-wavelength[25] perturbations in the energy density propagate as a sequence of compressions and rarefactions of the medium, like acoustic waves.[26] At wavelength $\lambda_{\rm osc} \sim l^{-1}$ smaller than the photon mean free path $\lambda_{\rm free}$, some photons may escape the compressed regions before colliding with the free electrons and spreading out in the rarefied regions. As a consequence, the wave is smoothened out and the corresponding oscillatory behaviour of $D_l$ is damped at large $l$.[27] For the overall decline of the power spectrum there are many hypotheses considered, e.g. the decrease of the dark matter gravitational potential at high momenta, and the finite thickness of the last scattering surface.

Subtracting all contributions described above, the surviving shape of the power spectrum in terms of $k$ can be parametrized by

$$\mathcal{P}_s(k) = A_s \left(\frac{k}{k_*}\right)^{n_s - 1} \approx \mathcal{P}_{\mathcal{R}}(k) \ , \tag{3.129}$$

with the overall normalization chosen so that this is expected to reproduce the power spectrum of primordial scalar perturbations $\mathcal{P}_{\mathcal{R}}(k)$.

The numerical values of the parameters $A_s$ and $n_s$ from the CMB experiments are [38]

$$A_s^{\rm obs} = (2.0989 \pm 0.0292) \times 10^{-9} \ , \tag{3.130}$$

$$n_s^{\rm obs} = 0.9649 \pm 0.0042 \ . \tag{3.131}$$

Repeating the entire exercise for tensor perturbations [39], one finds the further parameter $r$, given by the ratio of the tensor to the scalar perturbation spectrum, for which only an upper bound is known [38],

$$r^{\rm obs} \equiv \frac{A_t}{A_s} < 0.056 \ . \tag{3.132}$$

[24] An explicit relation among $l$ and $k$ is derived by writing plane waves in terms of spherical harmonics (see e.g. [35, p.12]), with the maximal contribution given by $l \sim k x_{\rm dec}$, where $x_{\rm dec}$ denotes the distance from the observer to the last scattering surface at $t_{\rm dec}$.

[25] This means small compared with the Jeans length $\lambda_J \sim u/\sqrt{e}$, with $u$ the fluid velocity and $e$ the energy density. Larger scales experience gravitational instability, for more details see [12, p.6].

[26] The oscillations in $D_l$ are considered to be a smoking gun of inflation, see however also [36].

[27] This phenomenon is known as *Silk damping* [37]. It affects length scales smaller than those of galaxy clusters, suggesting that the their origin must have a different explanation, e.g. the fragmentation of larger objects.

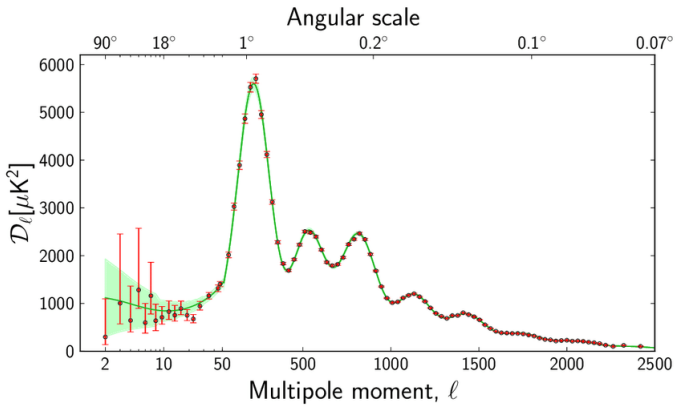


Figure 3.3: The CMB power spectrum as seen by Planck [40]. The red dots with error bars are the data points, the green line is the best fit theoretical model. Theoretical uncertainty (shaded region) arises from averaging over an ensemble of universes (cosmic variance).

With the theoretical predictions of the power spectrum of scalar, eq. (3.73), and tensor, eq. (3.92), perturbations from inflation, the CMB parameters can be computed as

$$A_s \equiv \mathcal{P}_\mathcal{R}(k_*) = \left(\frac{H_*^2}{2\pi\dot\varphi}\right)^2 , \tag{3.133}$$

$$n_s \equiv 1 + \left.\frac{d\ln\mathcal{P}_\mathcal{R}(k)}{d\ln k}\right|_{k_*} = 1 + \frac{2H}{H^2+\dot H}\left(2\frac{\dot H}{H} - \frac{\ddot\varphi}{\dot\varphi}\right) , \tag{3.134}$$

$$r \equiv \left.\frac{\mathcal{P}_\mathrm{T}}{\mathcal{P}_\mathcal{R}}\right|_{k_*} = 4\pi G\left(\frac{4\dot\varphi}{H}\right)^2 . \tag{3.135}$$

These expression can be further simplified by considering that the scales probed experimentally exit the horizon deep in the slow-roll regime of inflation. With eqs. (3.11) and (3.14) we obtain an estimate of eqs. (3.133)–(3.135) in the slow-roll approximation,

$$A_s \approx 16\left.\frac{8\pi G^3}{3}\frac{V^3}{V_\varphi^2}\right|_{t_*} = \left.\frac{8G^2}{3}\frac{V}{\epsilon_V}\right|_{t_*} , \tag{3.136}$$

$$\begin{aligned} n_s &\approx 1 + \left.\frac{\epsilon_V}{V}\frac{\dot\varphi}{H}\partial_\varphi\left(\frac{V}{\epsilon_V}\right)\right|_{t_*} \approx 1 - \left.2\frac{\epsilon_V^2}{V_\varphi}\left[\frac{V_\varphi}{\epsilon_V} - \frac{V_\varphi}{8\pi G\epsilon_V^2}\left(\frac{V_{\varphi\varphi}}{V} - \frac{V_\varphi^2}{V^2}\right)\right]\right|_{t_*} \\ &= 1 - 6\,\epsilon_V(t_*) + 2\,\eta_V(t_*) , \end{aligned} \tag{3.137}$$

$$r \approx 16\cdot 4\pi G\left.\left(\frac{V_\varphi}{8\pi G V}\right)^2\right|_{t_*} = 16\,\epsilon_V(t_*) . \tag{3.138}$$

Hence CMB experiments yield three different constraints on the potential for inflation.

## Gravitational wave background

We have seen in sec. 3.3 that tensor perturbations propagate as gravitational waves during inflation. Analogously to the microwave background signal discussed above, the hope is to detect them as a background signal in future gravitational waves experiments. Other non-resolvable sources will contribute to the background signal as well, impelling theoretical efforts in the search for templates. In particular, in the next decade or so, a new orbiting interferometer, the Laser Interferometer Space Antenna (LISA), should become operative in the frequency range $\sim [10^{-5}, 10]$Hz [41–43].

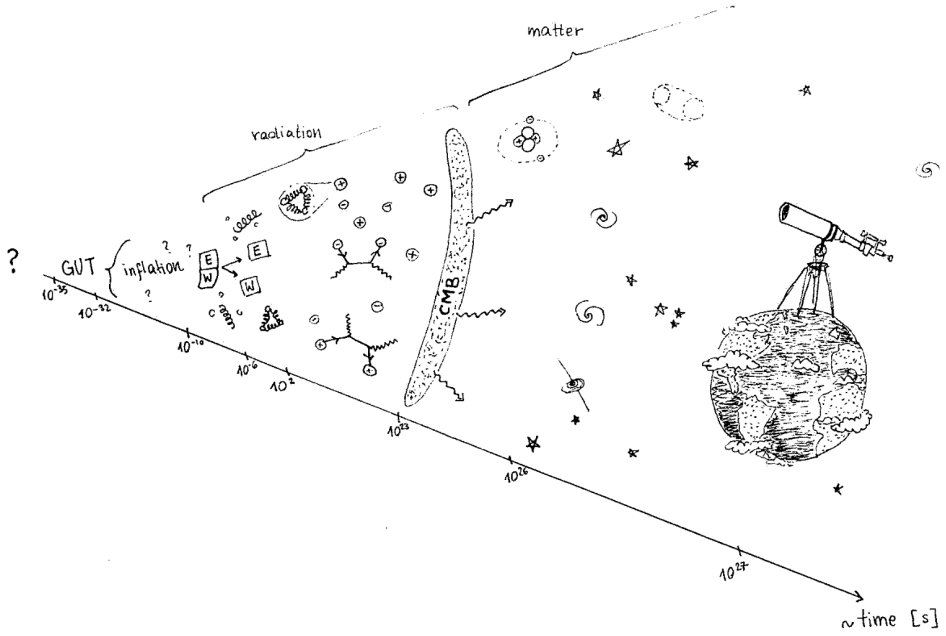


Figure 3.4: An impression of events that distinguish different epochs in the history of our universe.

What LISA may measure *today* ($t_0$) is the fractional energy density carried by gravitational radiation,

$$\Omega_{\rm GW} \equiv \frac{1}{e_c}\frac{\mathrm{d}e_{\rm GW}}{\mathrm{d}\log k}\bigg|_{t_0} , \qquad e_c \equiv e_{\rm rad}(t_0) \overset{(2.113)}{=} \frac{3H_0^2}{8\pi G} , \tag{3.139}$$

where the current value of the Hubble rate is parametrized in terms of the reduced rate, $h$, as $H_0 = 100h\,\mathrm{km\,s^{-1}\,Mpc^{-1}}$. Instead of the wave number $k$, the physical variable for $\Omega_{\rm GW}$ is the frequency $f_0$ of the radiation measured today, which is related to $k$ by

$$k/a_0 = 2\pi f_0 , \qquad f_0|_{\rm LISA} \in [10^{-5}, 10]\,\mathrm{Hz} . \tag{3.140}$$

The lower bound for the LISA sensitivity is [44, fig. 10]

$$h^2\Omega_{\rm GW}^{\rm LISA} \gtrsim 10^{-13} . \tag{3.141}$$

The gravitational wave spectrum observed today can be related to the primordial one as in eq. (3.118), with a different transfer function for tensor modes, which is way simpler than for scalar modes. Here we anticipate the result for a standard inflation scenario, the complete derivation can be found in sec. 6.1,

$$\Omega_{\rm GW}h^2 \sim 10^{-6} \times \frac{16}{\pi}\left(\frac{H_*}{m_{\rm pl}}\right)^2 . \tag{3.142}$$

If observed, $\Omega_{\rm GW}$ would yield a further constraint on the parameters of inflation. In sec. 6 we study further possible contributions to the gravitational wave background, sourced by thermal processes during the inflationary and reheating epoch.

## Effective number of degrees of freedom

The first occurrence of nucleosynthesis of the lightest elements takes place in the radiation dominated epoch, and is known as Big Bang Nucleosynthesis (BBN).[28] Fusion processes of neutrons

[28] Probably one of the oldest references is [45], while a readable review can be found in [46].

and protons into nuclei via weak interactions can only start at energy scales about $T \sim$MeV, corresponding to the first couple of seconds in the early universe. Observed abundances of light elements can therefore impose an upper limit on the expansion rate of the universe via eq. (2.113), which for a radiation dominated universe takes the form

$$H^2 = \frac{8\pi G}{3} e_r \ . \tag{3.143}$$

In this context *radiation* means more broadly light, *relativistic* particles. If we modify $e_r$ by adding more relativistic degrees of freedom, the expansion of the universe is faster, the decoupling happens earlier and the abundances change. Conventionally, the energy density of additional relativistic components is parametrized by an effective number of neutrino species, $N_{\rm eff}$,

$$e_r = e_\gamma + N_{\rm eff} \times e_\nu + \dots \tag{3.144}$$

The Standard Model prediction for $N_{\rm eff}$ after the electron-positron recombination is (see e.g. [47,48])

$$N_{\rm eff}^{\rm SM} = 3.043 \ . \tag{3.145}$$

This value is slightly larger than 3, because neutrinos do not decouple instantaneously, but continue interacting with electrons and positrons for a while [49]. As additional relativistic degree of freedom, the energy density from a primordial gravitational wave background would then contribute as

$$\Delta N_{\rm eff} = N_{\rm eff}^{\rm obs} - N_{\rm eff}^{\rm SM} \supset \frac{e_{\rm GW}}{e_\nu} \ . \tag{3.146}$$

For a specific model of inflation, $e_{\rm GW}$ can be estimated by integrating eq. (3.142) over all modes $k$. From the joint analysis of CMB measurements and BBN light element abundances we have

$$N_{\rm eff}^{\rm obs} = 2.862 \pm 0.306 \tag{3.147}$$

at 95% confidence level [50]. The experimental accuracy is expected to improve, promoting $N_{\rm eff}$ to a precision probe of Beyond Standard Model physics and primordial gravitational waves.

# Chapter 4

# A thermal treatment of the inflationary epoch

The model of inflation predicts that the universe expands exponentially at an early stage of its history. Since the energy density of radiation scales like $a(t)^{-4}$, cf. eq. (2.115), during this period the temperature is expected to decrease rapidly. Thermal effects are therefore usually neglected during inflation, and the mechanism responsible for the transition to a hot universe is known as *reheating* [51, 52].[29] In the same spirit, and keeping in mind that for successful inflation the dominant energy density must be $e_\varphi$, also the interactions of the inflaton field $\varphi$ with other degrees of freedom are normally neglected.

Dreaming of a complete framework, here we want to keep track of the continuous transition from the vacuum dominated (inflation) to the radiation dominated (hot big bang) epoch, assuming that inflation starts in a low temperature regime and in the presence of other fields.[30] The latter enter the Lagrangian via $\mathcal{L}_{\rm bath}$ and an operator $J$ in the interaction term,

$$\mathcal{L} = -\frac{1}{2} g^{\mu\nu} \partial_\mu \varphi \, \partial_\nu \varphi - V_0(\varphi) - \varphi J + \mathcal{L}_{\rm bath} \ . \tag{4.1}$$

Similar efforts with the different goal of enlarging the parameter space for phenomenologically non-viable potentials are classified under the name of *warm inflation* models, see e.g. [53–56]. However, generally speaking the initial conditions for warm inflation are given by a heat bath at a macroscopic temperature, whose interactions with $\varphi$ are on the strong side. Instead, we assume here that the coupling $J$ between $\varphi$ and the heat bath is weak. The evolution of $\varphi$ is characterized by time scales much longer than those of the medium, which equilibrates fast. This setup assures the validity of a decoherent classical evolution equation for $\varphi$ [57, p.188]. Expanding in time derivatives and powers thereof, the background field follows the evolution equation

$$\ddot{\bar{\varphi}} + 3H\dot{\bar{\varphi}} + \partial_\varphi V(\bar{\varphi}) = -\Upsilon \dot{\bar{\varphi}} + \mathcal{O}(\dddot{\bar{\varphi}}, \dot{\bar{\varphi}}^2) \ , \tag{4.2}$$

which is derived in sec. 4.1. As the inflaton interacts with other particles, part of its kinetic energy dissipates to the heat bath, implying that the entropy of the system increases and the medium heats up. This mechanism of energy transfer is encoded in the additional friction coefficient $\Upsilon$. At the same time, the interactions with the medium modify the inflaton potential $V_0(\bar{\varphi}) \to V(\bar{\varphi})$,

[29] The name *reheating* comes from the fact that originally the model of inflation [23] was presented in the format of a phase transition occurring in the hot early universe at the corresponding critical temperature. Therefore after inflation the universe must *heat up again*, to produce the hot and interacting multi-particle environment predicted within the standard *big bang* cosmology. Later on, see e.g. [24], it was realized that, in a simpler manner, an exponential expansion of the universe can be driven by the energy density of a slowly evolving scalar field. Here we follow this second perspective.

[30] Those of GUT or of another generalization of the Standard Model at high energy scales.

often parametrized by a thermal mass $m_{\rm T}$. Although the role of $\Upsilon$ and $m_{\rm T}$ is different, technically they are determined respectively by the imaginary and real part of the retarded correlator of $J$. Their properties depend thus on the characteristics and on the evolution of the heat bath, and eq. (4.2) must be completed with a second equation describing the latter.

If we want to compute concrete predictions we need an input about the nature of $J$. It is a non-trivial task to determine which type of interactions could heat up the universe towards the end of inflation. If the thermal corrections on the potential are large, the slow evolution of $\varphi$ may be spoiled and inflation does not take place. On the other hand, if the interactions are strongly suppressed, it may take forever until a radiation dominated epoch can be reached. Imposing a global symmetry for $\varphi$ solves the problem, as it constrains the modifications to the potential. As an example, in chapter 5 we consider the shift symmetry induced by an axion-like interaction term.

### When is the thermalization assumption self-consistent?

To conclude this introduction, let us address the important question of when the temperature is a useful concept. It is difficult to estimate in general how fast a system equilibrates. A frequent approach used to study the dynamics after inflation is to solve classical field equations of motion [51, 52]. However, classical field dynamics is correct only for large occupation numbers, but not in the diluted regime at large momenta, $p \sim \pi T$, where the occupation is of order unity. Because momenta precisely from the latter domain carry most of the radiation energy density, the issue of thermalization cannot be properly resolved with classical field theory.

Another approach can be found in the heavy-ion context, where thermalization of non-Abelian systems has been studied extensively, relying mostly on effective kinetic theory [58]. In that language we can draw diagrams responsible for thermalization. The gauge plasma equilibration rate is then given by the thermally averaged amplitude squared, $\Gamma_g$. On the other hand, the inflaton equilibration rate is $\sim \Upsilon$. For the example of a non-Abelian gauge plasma, in sec. 5.2 we compare these with the Hubble rate *a posteriori*. The lesson is that $\Gamma_\varphi$ in our setup is suppressed with respect to $\Gamma_g \sim \alpha^2 T$ by several orders of magnitude. Nevertheless, the computations themselves are carried out in the presence of a temperature-like parameter, reminiscently of warm inflation.

## 4.1 Inflaton evolution in the presence of a thermal bath

To derive the evolution equation (4.2), we keep the interaction term $J$ to be a general gauge invariant operator. Considering that multiple plasma interactions occur while $\bar\varphi$ changes only a little, it is useful to recall the equivalence principle, and work with local Minkowskian coordinates. The resulting equation of motion can then be written in a covariant form, and finally evaluated for an expanding FLRW universe.

In a local flat frame, the Euler-Lagrange equation for $\bar\varphi$ resulting from the Lagrangian in eq. (4.1),

$$\ddot{\bar\varphi} + V'(\bar\varphi) = -\langle J(t)\rangle \ , \tag{4.3}$$

is non-trivial because the average value of $J$ depends on the slow evolution of the inflaton $\bar\varphi$. Let us define the time coordinate such that $t = 0$ denotes an arbitrary initial time. The physical picture we are studying is the one of a medium in equilibrium, responding to a small time dependent perturbation, which is induced by the presence of the field $\bar\varphi$. At the same time the interaction term should represent a small correction also during inflation. A linear response argument can thus be applied to determine $\langle J(t)\rangle$.

The Hamiltonian of the system is

$$\hat{H} = \hat{H}_{\rm bath} + \bar{\varphi}\hat{J} \ . \tag{4.4}$$

The equilibrium value for the inflaton is thus $\bar{\varphi} = 0$. Considering that this should also represent the minimum of the potential, $V(0) = 0$, and defining the mass as the curvature of $V$ around the minimum, we expand

$$V(\bar{\varphi}) = \frac{1}{2}m^2\bar{\varphi}^2 + \mathcal{O}(\bar{\varphi}^3) \ . \tag{4.5}$$

Following the time evolution of a physical observable, e.g. the density matrix $\hat{\rho}(t)$ of the heat bath,

$$i\partial_t\hat{\rho}(t) = [\hat{H}(t), \hat{\rho}(t)] \ , \tag{4.6}$$

the average value of $\hat{J}$ can be written as

$$\langle\hat{J}(t)\rangle \equiv {\rm tr}[\hat{\rho}(t)\hat{J}(t)] \ . \tag{4.7}$$

At linear order in $J$ eq. (4.6) is solved by

$$\hat{\rho}(t) - \hat{\rho}(0) = -i\int_0^t {\rm d}t'[\hat{H}(t'), \hat{\rho}(0)] + \mathcal{O}(J^2) = -i\int_0^t {\rm d}t'\bar{\varphi}(t')[\hat{J}(t'), \hat{\rho}(0)] + \mathcal{O}(J^2) \ . \tag{4.8}$$

We insert the result in eq. (4.7) and move to Schrödinger's representation,

$$\hat{J}(t) = e^{-i\hat{H}_{\rm bath}t/\hbar}\hat{J}(0)e^{i\hat{H}_{\rm bath}t/\hbar} \ . \tag{4.9}$$

With the assumption $[\hat{H}_{\rm bath}, \hat{\rho}(0)] = 0$, the contribution from $\hat{\rho}(0)$ is

$$\begin{aligned}{\rm tr}[\hat{\rho}(0)e^{-i\hat{H}_{\rm bath}t/\hbar}\hat{J}(0)e^{i\hat{H}_{\rm bath}t/\hbar}] &= {\rm tr}[e^{i\hat{H}_{\rm bath}t/\hbar}\hat{\rho}(0)e^{-i\hat{H}_{\rm bath}t/\hbar}\hat{J}(0)] \\ &= {\rm tr}[\hat{\rho}(0)\hat{J}(0)] = \langle\hat{J}(0)\rangle_0 \ . \end{aligned} \tag{4.10}$$

Going similarly to the second order in $J$, we get

$$\begin{aligned}\langle\hat{J}(t)\rangle - \langle\hat{J}(0)\rangle_0 &= -\int_0^t {\rm d}t'\bar{\varphi}(t'){\rm tr}\left[i[\hat{J}(t'), \hat{\rho}(0)]\hat{J}(t)\right] + \mathcal{O}(J^3) \\ &= -\int_0^t {\rm d}t'\bar{\varphi}(t'){\rm tr}\left[i\hat{J}(t)[\hat{J}(t'), \hat{\rho}(0)]\right] + \mathcal{O}(J^3) \\ &= -\int_0^t {\rm d}t'\bar{\varphi}(t'){\rm tr}\left[i[\hat{J}(t), \hat{J}(t')]\hat{\rho}(0)\right] + \mathcal{O}(J^3) \\ &= -\int_0^t {\rm d}t'\bar{\varphi}(t')\langle i[\hat{J}(t), \hat{J}(t')]\rangle_0 + \mathcal{O}(J^3) \ . \end{aligned} \tag{4.11}$$

We now define the retarded correlator as

$$G_{\rm R}(t-t') \equiv \theta(t-t')\langle i[\hat{J}(t), \hat{J}(t')]\rangle_0 \ . \tag{4.12}$$

If $\hat{J}$ is odd under discrete symmetry transformations, then $\langle\hat{J}(0)\rangle_0 = 0$, and eq. (4.11) becomes

$$\langle\hat{J}(t)\rangle = -\int_0^\infty {\rm d}t'\bar{\varphi}(t')G_{\rm R}(t-t') + \mathcal{O}(J^3) \ . \tag{4.13}$$

Inserting this back in the equation of motion (4.3), yields

$$\ddot{\bar{\varphi}} + m^2\bar{\varphi}^2 - \int_0^\infty {\rm d}t'\bar{\varphi}(t')G_{\rm R}(t-t') \approx 0 \ . \tag{4.14}$$

To solve the differential equation for $\bar{\varphi}$ we transform into frequency space,

$$\bar{\varphi}(\omega) \equiv \int_0^\infty {\rm d}t\, e^{i\omega t}\bar{\varphi}(t) \ , \qquad \bar{\varphi}(t)\theta(t) = \int_{-\infty}^\infty \frac{{\rm d}\omega}{2\pi}e^{-i\omega t}\bar{\varphi}(\omega) \ , \tag{4.15}$$

$$G_{\rm R}(\omega) = \int_0^\infty {\rm d}t\, e^{i\omega t}G_{\rm R}(t) \ . \tag{4.16}$$

Being agnostic about $G_{\rm R}(t-t')$, one should integrate carefully, as the function may even diverge at short time intervals.[31] Then neither the convolution integral in eq. (4.13), nor its Fourier

[31] This is the case e.g. for a non-renormalizable operator $J$, like the one we consider in chapter 5.

transform are well-defined. Let us assume that, as is usual in quantum field theory, the divergences can be taken care of by introducing some regularization and subsequently cancelling them by local counterterms in eq. (4.14).

A dependence on the initial conditions enters via the transformation of $\ddot{\bar{\varphi}}$,

$$\int_0^\infty \mathrm{d}t\, \ddot{\bar{\varphi}}(t) e^{i\omega t} = -\dot{\bar{\varphi}}(0) + i\omega\bar{\varphi}(0) - \omega^2\bar{\varphi}(\omega) \ . \tag{4.17}$$

Analogously, the counterterms would yield further contributions of the same type. In the following we assume that the counterterms cancel the divergences. Encoding the dependence on $\bar{\varphi}(0)$ and its derivatives in a function $\mathcal{G}$, the solution to eq. (4.14) is

$$\bar{\varphi}(t)\theta(t) = \int_{-\infty}^{\infty} \frac{\mathrm{d}\omega}{2\pi} \frac{e^{-i\omega t}}{\omega^2 - m^2 + G_{\mathrm{R}}(\omega)} \mathcal{G}[\omega, \bar{\varphi}^{(n)}(0)] \ . \tag{4.18}$$

Now, the idea is to consider the dynamics of $\bar{\varphi}$ at some *macroscopic* $t > 0$, far after the regime dictated by the initial conditions. Then it is possible to deform the integration contour in eq. (4.18) into the lower half-plane. The deeper we go, the faster the exponential fall-off of the solution. Hence, the slowest dynamics of $\bar{\varphi}$ can be identified by searching for the singularities closest to the real axis. We note in passing that $\mathcal{G}[\omega, \bar{\varphi}^{(n)}(0)]$ has zeros, however their locations depend on initial conditions, and therefore cannot coincide in general with the roots of the denominator.

Whether a deformation of the integration contour is well defined or not depends on $G_{\mathrm{R}}(\omega)$, which in general is not analytic in the lower half-plane. That said, $G_{\mathrm{R}}$ is still defined in the lower half-plane, but it must have singularities.[32] In the following we assume that the singularity structure of $G_{\mathrm{R}}$ is known and come back to this issue in sec. 5.2 with a concrete example.

For $G_{\mathrm{R}}$ given, let us search for the roots of the denominator. Concretely, we inspect

$$\ddot{\bar{\varphi}} + \Upsilon\dot{\bar{\varphi}} + m_{\mathrm{T}}^2\bar{\varphi} = -\int_{-\infty}^{\infty} \frac{\mathrm{d}\omega}{2\pi} \frac{\omega^2 + \Upsilon i\omega - m_{\mathrm{T}}^2}{\omega^2 - m^2 + G_{\mathrm{R}}(\omega)} e^{-i\omega t} \mathcal{G}[\omega, \bar{\varphi}^{(n)}(0)] \approx 0 \ , \tag{4.19}$$

asking for which parameters $\Upsilon$ and $m_{\mathrm{T}}^2$ the leading singularities at $t > 0$ are lifted.

In general, $\Upsilon$ is a function of the frequency $\omega$ at which the system is probed. Then the full equation of motion does not have a local form, but rather contains a dispersive integral over the medium response. Recalling that the whole setup is consistent only to the extent that $G_{\mathrm{R}}$ is treated as a small correction around the global minimum, we can solve for the roots iteratively. At tree-level, the roots are at $\omega = \pm m$. The symmetries $\mathrm{Re}\, G_{\mathrm{R}}(-m) = \mathrm{Re}\, G_{\mathrm{R}}(m)$ and $\mathrm{Im}\, G_{\mathrm{R}}(-m) = -\mathrm{Im}\, G_{\mathrm{R}}(m)$ imply that the positive root can be chosen as a representative, $\omega \to m$. Denoting

$$G_{\mathrm{R}}(m) = \mathrm{Re}\, G_{\mathrm{R}} + i\, \mathrm{Im}\, G_{\mathrm{R}} \ , \tag{4.20}$$

the desired parameters are given by

$$\Upsilon \approx \frac{\mathrm{Im}\, G_{\mathrm{R}}}{m} \ , \quad m_{\mathrm{T}}^2 \approx m^2 - \mathrm{Re}\, G_{\mathrm{R}} \ . \tag{4.21}$$

Before the system settles to the global minimum, in principle one may rather replace the frequency scale by the curvature of the potential, $\omega \to \sqrt{\max(0, V_{\varphi\varphi})}$.[33] Since the focus of the

[32] A possible way to determine $G_{\mathrm{R}}$ is to solve the Cauchy-Riemann differential equations, taking $G_{\mathrm{R}}(\omega + i0^+)$ as the initial condition. This system can be rephrased as a 2-dimensional Laplace equation. It is known that the solution of the Laplace equation with Cauchy boundary conditions is unstable, reflecting the singularities.

[33] Then, if $V_{\varphi\varphi} \leq 0$, temperature is the only scale at early stages of inflation. But, as shown in sec. 5.4, $T = 0$ is an unstable fixed point in this setup.

current study is the heating-up period, we adopt the replacement $\omega \to m$ throughout, with the understanding that at early stages of inflation this is just a recipe.

The evolution equation in a local Minkowskian frame, eq. (4.19), can be promoted to a general coordinate system,

$$\bar{\varphi}^{;\mu}{}_{;\mu} + \Upsilon u^{\mu}\bar{\varphi}_{;\mu} + m_{\rm T}^2\bar{\varphi} \simeq 0 \,. \tag{4.22}$$

Choosing FLRW coordinates (cf. eq. (2.1)), and returning to the general form of the potential, yields our final equation of motion for the inflaton field,

$$\boxed{\ddot{\bar{\varphi}} + (3H + \Upsilon)\dot{\bar{\varphi}} + \partial_{\varphi}V(\bar{\varphi}) \simeq 0} \,. \tag{4.23}$$

An equation of the same form is used in warm inflation models, see e.g. [59–62]. Our setup is different in the sense that $\Upsilon$ obtained from eq. (4.21) may contain a non-polynomial $T$-dependence, and $m_{\rm T}^2$ may contain a non-trivial correction as well.

The Hubble rate is given by eq. (2.113),

$$\boxed{H^2 = \frac{8\pi}{3m_{\rm pl}^2}e} \,, \tag{4.24}$$

in terms of the total energy density of the system at equilibrium, $e$. Before we turn to study the evolution of the latter (see sec. 4.3), we should complete the discussion about the thermal corrections to the inflaton potential.

## 4.2 Perturbative thermodynamics for a thermalized inflaton

As the system heats up, the inflaton field might equilibrate as well (see however the discussion on p. 37). In that case further temperature dependent corrections affect the potential $V$, contributing to the thermodynamic functions $p_{\varphi}$ and $e_{\varphi}$. Differently from $m^2 \to m_{\rm T}^2$, which only modifies the curvature of the potential around the minimum, now also the shape of $V$ around the minimum may change depending on the temperature. To sum up, the contributions to the potential are

$$V \approx \underbrace{V_0\big|_{m^2}}_{\substack{\text{UV physics}\\ \text{from } J}} + \underbrace{V_0\big|_{m^2\to m_{\rm T}^2-m^2}}_{\substack{\text{thermal mass}\\ \text{from} J}} + \underbrace{V_{\rm eff}^{(1)}}_{\substack{\text{thermalized}\\ \varphi}} \,, \tag{4.25}$$

where $V_{\rm eff}^{(1)}$ denotes the 1-loop expression for a thermal effective potential (independent of $J$).

For thermal corrections that enter the dynamics already during inflation, the interesting interactions are the ones that do not spoil the flatness of the potential. Ideally we would like to satisfy this condition in a trivial way, postulating a symmetry so that the induced corrections vanish at all orders in perturbation theory. On the other hand such operators still have an effect non-perturbatively. At least for the concrete example of an axion-like interaction term (see eq. (5.2)), we show in sec. 5.2 that $m_{\rm T}$ is negligible also non-perturbatively, and mostly temperature independent. In the following we therefore neglect the temperature dependence of $m_{\rm T}$, denoting by $V_0$ the full temperature-independent potential.

Since the hypothetical thermalization of $\varphi$ would happen late after the slow-roll regime of inflation, to study the latter we can consider the inflaton as a weakly coupled massive scalar field, $V_0 \approx m^2\varphi^2/2$. The starting point for the evaluation of $p_{\varphi}$ and $e_{\varphi}$ is then the 1-loop expression for a thermal effective potential, given by the free energy density,

$$V_{\rm eff}^{(1)} = -\lim_{L\to\infty}\frac{T}{L^3}\ln\mathcal{Z}^{(1)} = \int\frac{{\rm d}^3k}{(2\pi)^3}\left[\frac{\epsilon_k}{2} + T\ln\left(1 - e^{-\epsilon_k/T}\right)\right]_{\epsilon_k=\sqrt{k^2+m^2}} \,. \tag{4.26}$$

To obtain eq. (4.26) we have quantized $\varphi$ in a local Minkowski frame, and derived the partition function from the Euclidean action ($t \to -it_{\rm E}$) in the path integral formulation (see e.g. [57, p.15]),

$$\begin{aligned}\mathcal{Z}^{(1)} &= \left(\frac{mT^3}{2\pi}\right)^{\frac{1}{2}} \left(\prod_{n=1}^{\infty} \frac{mT\omega_n^2}{\pi}\right) \int_{\substack{\varphi(0,\mathbf{x}) \\ =\varphi(\beta,\mathbf{x})}} \prod_{\mathbf{x}} [c\mathcal{D}\varphi(t_{\rm E},\mathbf{x})] \, \exp\left[-\frac{T}{2L^3} \sum_{\mathbf{k}} \sum_{l=-\infty}^{\infty} (\omega_l^2 + \epsilon_k^2) \, |\varphi(\omega_l,\mathbf{k})|^2\right] \\ &= \prod_{\mathbf{k}} \frac{T}{\epsilon_k} \prod_{n=1}^{\infty} \frac{\omega_n^2}{\omega_n^2 + \epsilon_k^2} = \prod_{\mathbf{k}} \frac{e^{-\epsilon_k/(2T)}}{1 - e^{-\epsilon_k/T}} \ . \end{aligned} \tag{4.27}$$

The discrete frequency modes $\omega_n \equiv 2\pi nT$ are known as the Matsubara modes.

We absorb the $T$-independent vacuum part of $V_{\rm eff}^{(1)}$ in the definition of $V_0$. Changing integration variables $\mathrm{d}^3k = 4\pi \mathrm{d}k\, k^2 = 4\pi \mathrm{d}\epsilon_k \, \epsilon_k \sqrt{\epsilon_k^2 - m^2}$, the pressure and energy density from eq. (3.7) then obtain the contributions

$$-p_\varphi \supset V \ \supset \ V_0 + \frac{T}{2\pi^2} \int_m^\infty \mathrm{d}\epsilon_k \, \epsilon_k \sqrt{\epsilon_k^2 - m^2} \, \ln\left(1 - e^{-\epsilon_k/T}\right) \ , \tag{4.28}$$

$$e_\varphi \supset V - T\partial_{\rm T} V \ \supset \ V_0 + \frac{1}{2\pi^2} \int_m^\infty \mathrm{d}\epsilon_k \, \epsilon_k^2 \sqrt{\epsilon_k^2 - m^2} \, n_{\rm B}(\epsilon_k) \ , \tag{4.29}$$

where $n_{\rm B}(x) \equiv 1/(e^{x/T} - 1)$ is the Bose distribution. Finally, eqs. (4.39) and (4.41) contain the contribution of $\varphi$ to the heat capacity,

$$-T\partial_{\rm T}\dot{V} \ \supset \ \frac{\dot{T}}{2\pi^2 T^2} \int_m^\infty \mathrm{d}\epsilon_k \, \epsilon_k^3 \sqrt{\epsilon_k^2 - m^2} \, n_{\rm B}(\epsilon_k) \, [1 + n_{\rm B}(\epsilon_k)] \ . \tag{4.30}$$

A numerical evaluation at low or intermediate temperatures may be facilitated by representations in terms of modified Bessel functions. These can be found using geometric series and, for example, via a further substitution to hyperbolic functions $\epsilon_k = m\cosh x$,

$$\begin{aligned} p_\varphi + V_0 &\supset \frac{T}{2\pi^2} \sum_{n=1}^{\infty} \frac{1}{n} \int_m^\infty \mathrm{d}\epsilon_k \, \epsilon_k \sqrt{\epsilon_k^2 - m^2} \, e^{-n\epsilon_k/T} \\ &= \frac{Tm^3}{2\pi^2} \sum_{n=1}^{\infty} \frac{1}{n} \int_0^\infty \mathrm{d}x \, \frac{\sinh(2x)}{2} \, \partial_x \left(-\frac{T}{mn} e^{-\frac{mn}{T}\cosh x}\right) \\ &= \frac{T^2 m^2}{2\pi^2} \sum_{n=1}^{\infty} \frac{1}{n^2} \int_0^\infty \mathrm{d}x \, \cosh(2x) \, e^{-\frac{mn}{T}\cosh x} = \frac{m^2T^2}{2\pi^2} \sum_{n=1}^{\infty} \frac{1}{n^2} K_2\left(\frac{nm}{T}\right) \ . \end{aligned} \tag{4.31}$$

The energy density $e = T\partial_{\rm T} p - p$ and the heat capacity $-T\partial_{\rm T}\dot{V} = \dot{T}\partial_{\rm T} e$ can be obtained from the pressure. Making use of recursive relations for the derivatives of Bessel functions,

$$\partial_x K_\alpha(x) = -K_{\alpha-1}(x) - \frac{\alpha}{x} K_\alpha(x) = \frac{\alpha}{x} K_\alpha(x) - K_{\alpha+1}(x) = -\frac{1}{2}\left[K_{\alpha-1}(x) + K_{\alpha+1}(x)\right] \ , \tag{4.32}$$

eqs. (4.29) and (4.30) become

$$e_\varphi - V_0 \supset \frac{m^2T^2}{2\pi^2} \sum_{n=1}^{\infty} \left\{\frac{1}{n^2} K_2\left(\frac{nm}{T}\right) + \frac{m}{2nT}\left[K_1\left(\frac{nm}{T}\right) + K_3\left(\frac{nm}{T}\right)\right]\right\} \ , \tag{4.33}$$

$$-T\partial_{\rm T}\dot{V} \supset \frac{m^4\dot{T}}{4\pi^2 T} \sum_{n=1}^{\infty} \left\{K_2\left(\frac{nm}{T}\right) + K_4\left(\frac{nm}{T}\right)\right\} \ . \tag{4.34}$$

In the limit of a massless inflaton field, i.e. $m \ll \pi T$, the thermalization of $\varphi$ described in eqs. (4.28)–(4.30) amounts to the addition of one light degree of freedom in the radiation equations of state in eq. (4.42), i.e. $g_* \to g_* + 1$ and $h_* \to h_* + 1$.

## 4.3 Heat bath equation of motion

We now turn to study the energy density entering eq. (4.23) via the Hubble rate in eq. (4.24). To describe the evolution of the system, the equation for $\varphi$ must be completed by a second equation tracking the total energy density in terms of the increasing temperature. The latter can be obtained by imposing either entropy increase or energy conservation.

Let us denote the energy density and pressure of the radiation plasma by $e_r$ and $p_r$, respectively. In equilibrium, the corresponding total variables are

$$e = e_r + e_\varphi \ , \qquad e_\varphi \equiv \frac{\dot{\bar{\varphi}}^2}{2} + V - T\partial_T V \ , \tag{4.35}$$

$$p = p_r + p_\varphi \ , \qquad p_\varphi \equiv \frac{\dot{\bar{\varphi}}^2}{2} - V \ . \tag{4.36}$$

The condition of entropy increase can be imposed as

$$T\partial_t \left[ (s_r - \partial_T V)\, a^3 \right] = a^3 \Upsilon \dot{\bar{\varphi}}^2(t) \ . \tag{4.37}$$

The presence of a thermal potential implies that the free energy density carried by the inflaton field, $V(\bar{\varphi})$, also contributes to the total entropy density. The physical interpretation of the negative sign of $-\partial_T V$ is that, storing free energy in $\bar{\varphi}$, whose value carries definite information, decreases the total entropy.

Making use of

$$e_r = T s_r - p_r \ , \qquad s_r = \partial_T p_r \ , \tag{4.38}$$

eq. (4.37) can equivalently be rewritten as an equation for the energy density,

$$\boxed{\dot{e}_r + 3H\left(e_r + p_r - T\partial_T V\right) - T\partial_T \dot{V} = \Upsilon \dot{\bar{\varphi}}^2(t)} \ . \tag{4.39}$$

We note that, as long as the source given by $\bar{\varphi}$ is active, the sign of $\dot{e}_r$ is determined by many effects. During inflation $e_r$ may fulfil $\dot{e}_r - T\partial_T \dot{V} \simeq 0$, and the corresponding temperature remains around a stationary value. The growth of $T$ becomes significant towards the end of inflation, when $V \sim \dot{\bar{\varphi}}^2$, and the oscillations of $\bar{\varphi}$ inject energy to the plasma for a while. A maximal temperature ($T_{\rm max}$) is reached when the energy dissipated from $\bar{\varphi}$ stops compensating for the Hubble dilution. Denoting $\dot{\bar{\varphi}}^2 = e_\varphi + p_\varphi$, this happens when

$$T_{\rm max}: \qquad 3H(e_r + p_r) - \Upsilon(e_\varphi + p_\varphi) \gtrsim 0 \quad \Leftrightarrow \quad \frac{e_r + p_r}{e_\varphi + p_\varphi} \gtrsim \frac{\Upsilon}{3H} \ . \tag{4.40}$$

In a weakly coupled regime we have $\Upsilon \ll H$ during inflation, implying that $T_{\rm max}$ may be reached already shortly after inflation, when the energy density of the inflaton is still dominating. According to the formal definition, inflation ends when the expansion becomes decelerated, i.e. $e_\varphi \sim \dot{\varphi}^2/2$. Calling *reheating* the subsequent period up to radiation domination, $e_\varphi \lesssim e_r$, we see that generically it starts after $T_{\rm max}$ has been reached, and is characterized by a decreasing temperature.

Coming back to a technical description of eq. (4.39), let us briefly sketch how it is obtained imposing the conservation of the energy-momentum tensor [63]. If we multiply eq. (4.23) by $\dot{\bar{\varphi}}$, the evolution equation for $\bar{\varphi}$ can equivalently be expressed as

$$\dot{e}_\varphi + 3H\dot{\bar{\varphi}}^2 + T\partial_T \dot{V} \ \simeq \ -\Upsilon \dot{\bar{\varphi}}^2 \ . \tag{4.41}$$

Summing together eqs. (4.39) and (4.41) yields the overall energy conservation equation, $\dot{e} + 3H(e + p) = 0$.

If $\Upsilon = 0$, like in standard inflation, there is no source term for the radiation plasma, and any possible initial temperature just redshifts away. It has been realized, however, that the assumption $\Upsilon = 0$ is mathematically troublesome. Even if the $T = 0$ solution represents a fixed point, it can be an unstable one. Just a small perturbation may drive the system to another fixed point, where $T > 0$ and $\Upsilon > 0$ [59, 64]. This thermal fixed point characterizes the almost stationary value of $e_r$ during inflation discussed below eq. (4.39), and is visible in the examples shown in fig. 5.6.

Eqs. (4.23), (4.24) and (4.39) apply for any type of a radiation equation of state. A simple ansatz is given by the conformal form

$$p_r = \frac{g_*\pi^2}{90}T^4 \ , \quad e_r = \frac{g_*\pi^2}{30}T^4 \ , \quad Ts_r = e_r + p_r = \frac{2h_*\pi^2}{45}T^4 \ , \tag{4.42}$$

with $h_* \simeq g_*$ constant. This is a good approximation if the plasma has a weak self-coupling. If this information is not known, one should consider the possibility that plasma interactions can become strong. Then the equation of state eq. (4.42) must be replaced by non-perturbative expressions (see sec. 5.3 for an example).

Motivated by the reasoning above, we consider the possibility that, as the temperature evolves, a critical temperature $T_c$ may be crossed, so that a first-order phase transition takes place in the heat bath. When the system is in a mixed phase, the temperature stays constant at $T = T_c$, so that $\dot{T} = 0$. At the same time, the energy density has a discontinuity, $e_r(T_c^+) - e_r(T_c^-) > 0$, so that $\partial_T e_r|_{T=T_c}$ diverges, and eq. (4.39) needs to be supplemented by another equation.

Although a mixed phase incorporates complicated physics,[34] the overall picture should be well captured by an adiabatic approximation. We re-parametrize $e_r(t)|_{T_c}$ through a volume fraction $u$,

$$e_r(t) \equiv e_r(T_c^+)\, u(t) + e_r(T_c^-)\,[1 - u(t)] \ , \quad 0 \le u \le 1 \tag{4.43}$$

$$\Rightarrow \ \dot{e}_r(t) = \dot{u}(t)\ [\, e_r(T_c^+) - e_r(T_c^-)\,] \ . \tag{4.44}$$

The pressure $p_r$ is continuous at $T = T_c$, since it equals minus the free energy density, and is therefore independent of $u$. Thereby eq. (4.39) gets replaced with

$$\dot{u}\ [\, e_r(T_c^+) - e_r(T_c^-)\,] + 3H\,[e_r(T_c^+)\, u + e_r(T_c^-)\,(1-u) + p_r(T_c)] \ \simeq \ \Upsilon\dot{\bar{\varphi}}^2 \ , \tag{4.45}$$

where $e_r$ depends on $u$ as given in eq. (4.43), and appears also in the Hubble parameter $H$.

The solution of the differential equations needs now to be complemented by a monitoring of $T$ and $u$. If we are solving eq. (4.39), and notice that $T \to T_c^-$ (respectively $T \to T_c^+$), then we need to go over into eq. (4.45), with the initial condition $u = 0$ ($u = 1$). Similarly, if we are solving eq. (4.45), and $u \to 1$ ($u \to 0$), then we need to go over into eq. (4.39), with the initial condition $e_r = e_r(T_c^+)$ ($e_r = e_r(T_c^-)$). It is possible that the system enters and exits the mixed phase from the same side (for instance, if $T_{\rm max} = T_c$), or from different sides (if the transition is passed through on the way towards higher or lower temperatures).

Having suggested a formalism depending on $G_{\rm R}$, the remaining step is to specify its form. Chapter 5 motivates a concrete choice for the interaction term $\bar{\varphi}J$ and constructs a potential for $\bar{\varphi}$.

[34] For example bubble nucleations, sound wave dynamics, turbulence, ... .

# Chapter 5

# Example: axion-like inflation

Let us briefly outline an inevitable (and incomplete) historical overview.

Despite the many advantages of inflation already in its simplest realizations, see sec. 3.1 for an example, the search for the perfect self-coupling potential for the inflaton field $V(\bar{\varphi})$ threatens to turn into a new fine-tuning problem. First models of axion inflation rose originally to construct a potential which is *naturally* flat, a feature that suggests the name *natural inflation*. The earliest examples date back e.g. to [65–67], that appeared shortly after the model of inflation [23].

To understand these early works, one should keep in mind that inflation itself was first presented in the format of a phase transition occurring in the hot early universe. Energy scales were thus compared with a high, decreasing temperature. Denoting by $f_a$ the axion decay constant, first attempts identified the QCD axion with the inflaton at energies $\Lambda_{\rm QCD} \ll e_\varphi \ll f_a$.[35] The parameters of inflation, axion mass and decay constant in this case, are therefore constrained by the high-energy limit of QCD. Precisely the dynamics of QCD instantons is then the origin of a flat inflaton potential at high temperatures (we construct the latter on the next pages).

With the advent of the CMB observations by the Planck satellite and the first constraints on inflation [38, p.19], the QCD axion was ruled out. In its place, an abundance of still undetermined axion-like inflatons started sprouting. Non-thermal models are reviewed in [70], while more recently axion-like interaction terms are widely used in warm inflation models, see e.g. [59–62, 64, 71–76].

Over the past forty years the literature concerning axion-like inflation has grown according to the increasing interest in inflation, with the original idea being modified in a similar manner. To be more precise, in the modern perspective inflation is usually placed foremost in any sketch of the history of the universe, and is described as an exponential expansion driven by the energy density of a slowly evolving scalar field [24]. No notion of the temperature is needed, except if a *warm* inflation scenario is explicitly considered. Hence, generally the UV physics that generates the axion potential is not discussed and the latter is taken as an ansatz.

Strictly speaking, these models do not benefit from a *naturally* flat potential a priori. On the other hand, aiming at a complete framework for inflation that can describe the transition to the radiation dominated epoch, an axion-like potential remains interesting.

We now turn to sketch the original setup of axion-like inflation, coupled to a non-Abelian gauge sector, in order to introduce the framework used in the rest of the present chapter.

[35] Other models identified the QCD axion with a dark spectator during inflation, see [68] for a modern example.

## Basic setup of axion-like inflation

The idea of axion-like inflation is to postulate a symmetry, as in the Peccei-Quinn solution to the strong CP problem,[36] such that the smallness of the coupling constant in the self-interaction of the inflaton $\varphi$ arises dynamically from a ratio of mass scales.

Concretely, considering the Lagrangian in eq. (3.1) for a massless scalar inflaton field, one adds an axion-like interaction term. Required is a Yang-Mills sector with the gauge group $\mathrm{SU}(N_c)$,[37] coupling constant $g^2 = 4\pi\alpha$, field strength tensor $F^a_{\mu\nu}$,

$$\mathcal{L} = -\frac{1}{2} g^{\mu\nu} \partial_\mu\varphi\, \partial_\nu\varphi - \varphi J + \mathcal{L}_{\rm bath} \ , \tag{5.1}$$

$$\varphi J = \frac{\varphi}{f_a} \frac{\alpha}{16\pi} F^a_{\mu\nu} \tilde{F}^{a\,\mu\nu} \ , \qquad F^a_{\mu\nu} = \partial_\mu A^a_v - \partial_\nu A^a_\mu + g f^{abc} A^b_\mu A^c_\nu \ , \quad \tilde{F}^{a\,\mu\nu} \equiv \epsilon^{\mu\nu\rho\sigma} F^a_{\rho\sigma} \ . \tag{5.2}$$

The scale $f_a$ measures the energy at which the axial $U_{\rm A}(1)$ symmetry is explicitly broken by $\varphi J$. It is proportional to the mass scale of further excitations in the broken phase (see footnote 36), and is conventionally called the *axion decay constant*. If the axial $U_{\rm A}(1)$ symmetry is explicitly broken at a high scale $f_a \sim m_{\rm pl}$, then the associated pseudo-Nambu-Goldstone boson $\varphi$ is very weakly coupled to the gauge sector.

The gauge sector itself is characterized by two further scales. Technically, we assume that inflationary physics has an energy scale $\epsilon_\varphi \ll \Lambda_{\rm UV}$, where $\Lambda_{\rm UV}$ is the confinement scale of some unified theory. At the same time, the unbroken $\mathrm{SU}(N_c)$ subgroup also displays a confinement scale $\Lambda_{\rm IR}$. During inflation we mostly assume $\epsilon_\varphi > \Lambda_{\rm IR}$, implying that the gauge sector is weakly coupled $\alpha < 1$ at the energy scale of the inflationary epoch (see however [5] and discussions below).

Because $J$ can be written as a total derivative, it does not contribute to the classical equations of motion of the gauge sector, if $\varphi$ is constant. A non-trivial contribution to the action,

$$\int \mathrm{d}^4x\,\sqrt{-g}\,J = -\frac{Q}{f_a} \ , \qquad Q \equiv \frac{\alpha}{4\pi} \int \mathrm{d}^4x\,\sqrt{-g}\,\partial_\mu \epsilon^{\mu\nu\rho\sigma} \left( A^a_\nu \partial_\rho A^a_\sigma + \frac{g}{3} f^{abc} A^a_\nu A^b_\rho A^c_\sigma \right) \in \mathbb{Z} \ , \tag{5.3}$$

i.e. $Q \neq 0$, arises from non-Abelian gauge fields with pure-gauge boundary conditions $A_\mu \overset{|x|\to\infty}{\longrightarrow} U^{-1}\partial_\mu U$, for $U \in \mathrm{SU}(N_c)$. The topological charge $Q$ represents the winding number of non-trivial field configurations known as instantons ($Q > 0$) and anti-instantons ($Q < 0$).

As a consequence of eq. (5.3), the action corresponding to eq. (5.1) is invariant under the shift symmetry $\varphi \to \varphi + 2\pi f_a$. This is not the case in the presence of a mass term.

Even if $\varphi J$ may not contribute to the classical equations of motion for $A^a_\mu$, it does enter the dynamics of $\bar{\varphi}$ generating a potential and an additional friction term,

$$\ddot{\bar{\varphi}} + 3H\dot{\bar{\varphi}} + \partial_\varphi V(\bar{\varphi}) \simeq -\Upsilon \dot{\bar{\varphi}}^2 \ . \tag{5.4}$$

To derive them it is convenient to use the partition function in the path integral formulation.

In particular, treating $\theta \equiv \varphi/f_a$ as a free parameter, Wick-rotating to the Euclidean action, and integrating over all fields in $J$ and $\mathcal{L}_{\rm bath}$, one can evaluate the potential

$$V(\theta) = -\lim_{L\to\infty} \frac{T}{L^3} \ln\left( \frac{\mathcal{Z}(\theta)}{\mathcal{Z}(0)} \right) \ , \tag{5.5}$$

[36] In the Peccei-Quinn construction [77], the axion $\varphi$ arises from the phase of a complex scalar field $\Phi = \phi e^{i\varphi/f_a}$. The latter is added to the QCD Lagrangian, together with a quark field $Q = (Q_{\rm L}, Q_{\rm R})$, which is a color-triplet, and a singlet under electroweak transformations. The additional fields transform under a postulated global U(1) Peccei-Quinn group, $\phi \to \phi$, $\varphi \to \varphi + c$, $Q_{\rm L,R} \to e^{\mp ic/2}$, and source the anomalous interaction term in the effective Lagrangian at energies $\Lambda_{\rm QCD} \ll e_\varphi \ll f_a$. For a compact review see [78].

[37] The Abelian case has been studied as well, see [79] for an example.

that arises from a non-trivial topological sector,

$$\mathcal{Z}(\theta) = \sum_{Q=-\infty}^{\infty} e^{i\theta Q} \mathcal{Z}_Q \ . \tag{5.6}$$

To further evaluate $V$, it is convenient to assume that for $|Q| > 1$ the dominant contribution to $\mathcal{Z}_Q$ arises from the superposition of $n$ 1-instantons and $\bar{n}$ 1-anti-instantons, such that $Q = n - \bar{n}$. In this semi-classical approximation of a dilute instanton gas, eq. (5.6) can be written as

$$\mathcal{Z}(\theta) \simeq \sum_{n,\bar{n}=0}^{\infty} \frac{[\mathcal{Z}_1 e^{i\theta}]^n}{n!} \frac{[\mathcal{Z}_1 e^{-i\theta}]^{\bar{n}}}{\bar{n}!} = \exp[2\mathcal{Z}_1 \cos\theta] \ . \tag{5.7}$$

Inserting $\Lambda_{\rm UV}^4 \simeq \lim_{L\to\infty} 2T\mathcal{Z}_1/L^3$, the potential for the axion-like inflaton from eq. (5.5) is then

$$V(\varphi) \simeq \Lambda_{\rm UV}^4 \left[1 - \cos\left(\frac{\varphi}{f_a}\right)\right] \ , \qquad V(\varphi + 2\pi f_a) = V(\varphi) \ . \tag{5.8}$$

In the Peccei-Quinn construction, the semi-classical expansion about instantons suffers from an ill-defined integration in $\mathcal{Z}_1$, that diverges in the absence of a physical cut-off scale [80, 81]. The problem arises classically, since then the action of any instanton with $Q = 1$ is $4\pi/\alpha$. However, in the regime of quantum fields at finite temperature one expects confinement to provide a physical scale, which may serve as a cut-off, which we denote here as $\Lambda_{\rm UV}$.

If we define the mass as the curvature of the potential at the minimum, this evaluates to

$$m^2 = \partial_\varphi^2 V(\varphi)\big|_{\varphi=0} = \frac{\Lambda_{\rm UV}^4}{f_a^2} \ , \quad \Rightarrow \quad \Lambda_{\rm UV} \sim \sqrt{m f_a} \ . \tag{5.9}$$

The appearance of the confinement scale means that the amplitude of the potential cannot be addressed via perturbation theory. In terms of a non-perturbative quantity, $m^2$ is related to the topological susceptibility $\chi$,

$$m^2 f_a^2 = \partial_\theta^2 V(\theta)\big|_{\theta=0} = \lim_{L\to\infty} \frac{T}{L^3} \left[ \frac{\sum_{Q=-\infty}^{\infty} Q^2 e^{i\theta Q} \mathcal{Z}_Q}{\mathcal{Z}(0)} - \left( \frac{\sum_{Q=-\infty}^{\infty} Q e^{i\theta Q} \mathcal{Z}_Q}{\mathcal{Z}(0)} \right)^2 \right]_{\theta=0} = \lim_{L\to\infty} \frac{\langle Q^2 \rangle}{\beta L^3} \equiv \chi \ . \tag{5.10}$$

In the QCD context, some exploratory lattice results for $\chi$ were available at the time of the first axion-inflation models [82]. They confirmed that at high temperatures instanton effects are strongly suppressed, and for $T \gg \Lambda_{\rm UV}$ the topological susceptibility decreases rapidly as the temperature increases [83]. The potential is then essentially independent of the axion field, and no value of $\varphi$ is singled out dynamically, but it is randomly distributed between 0 and $2\pi f_a$ ($\mathrm{mod}\, 2\pi f_a$) in causally distinct regions. In those regions where $\varphi \sim \pi f_a$ the inflaton starts inflation by slowly rolling down to the minimum. Because of this stochastic flair, the inflationary setup appears to emerge *naturally*.

For our concrete example we consider $m$ and $f_a$ as free and independent parameters of the model and treat $\Lambda_{\rm UV}$ as a constant. A nice feature of the potential in eq. (5.8) is, that near the minimum $V(\varphi) \approx m^2\varphi^2/2$ reproduces the simple *chaotic* potential, and close to the maximum $\varphi \sim \pi f_a$, $V \sim \mathrm{const} + \mathcal{O}[(\varphi - \pi f_a)^2]$ yields a viable slow-roll regime of inflation. Besides the potential, we keep the interaction term in the Lagrangian, representing the unbroken $\mathrm{SU}(N_c)$ subgroup of the non-Abelian sector. Together the shift-symmetry and the topological nature of $J$ suppress perturbative corrections to the potential and permit for a friction. These are two essential ingredients for a successful inflationary period with a hot final.

To make use of lattice results (cf. e.g. sec. 5.3), as an example we set $N_c = 3$. When lattice results are not available, we adopt a leading-logarithmic running value for the gauge coupling, representative of a Yang-Mills plasma,

$$\alpha \simeq \frac{6\pi}{11N_c} \ln^{-1}\left[\frac{\sqrt{(x\,2\pi\Lambda_{\rm IR})^2 + (2\pi T)^2 + m^2}}{\Lambda_{\rm IR}}\right] . \tag{5.11}$$

The first term in the square root serves as an (arbitrary) infrared (IR) regulator, so that any value of $T$ or $m$ can be inserted; in sec. 5.4 we check the IR sensitivity of the results by varying the parameter $x$ in the range $x \in [0.2, 2.0]$. Nevertheless the expression is guaranteed to be physically meaningful only for $\max\{2\pi T, m\} \gg \Lambda_{\rm IR}$, so that $\alpha \ll 0.3$. Here $\Lambda_{\rm IR}$ represents the confinement scale of the unbroken SU(3) gauge group.

## 5.1 CMB constraints on inflaton mass and decay constant

Scalar perturbations accessible via CMB observations exit the horizon at the beginning of inflation, deep in the slow-roll regime. At this stage, thermal corrections are still negligible, $\Upsilon \approx 0$, but interactions with the gauge sector at high energies enter already via the potential. To compute the CMB observables we therefore solve the simplified evolution,

$$\ddot{\bar\varphi} + 3H\dot{\bar\varphi} + V'(\bar\varphi) \approx 0 , \qquad H^2 \approx \frac{8\pi V}{3m_{\rm pl}^2} , \qquad V(\varphi) \approx m^2 f_a^2\left[1 - \cos\left(\frac{\varphi}{f_a}\right)\right] . \tag{5.12}$$

The free parameters of the model that can be constrained by the CMB are therefore the inflaton mass $m$ and the decay constant $f_a$. Not accessible is the confinement scale $\Lambda_{\rm IR}$ of the Yang-Mills sector. We discuss in sec. 5.4 how the temperature evolution is affected by $\Lambda_{\rm IR}$. In turn, the latter enters the predictions for the gravitational wave background studied in chapter 6.

To solve eq. (5.12) we also need an initial value for the inflaton field, $\bar\varphi_0$. As the slow-roll regime should represent an attractor solution, the expectation about $\bar\varphi_0$ is that its value does not affect the dynamics, as long as the simulation starts far enough away from the minimum of the potential. This means choosing $\bar\varphi_0$ close to one of the maxima, e.g.

$$\bar\varphi_0(f_a) \approx 0.9\,\pi f_a . \tag{5.13}$$

Returning to $m$ and $f_a$, we recall eqs. (3.133)–(3.134) for the CMB observables, which in the slow-roll approximation are replaced by

$$A_s \approx \left.\frac{8G^2}{3}\frac{V}{\epsilon_V}\right|_{t_*} , \tag{5.14}$$

$$n_s \approx 1 - 6\,\epsilon_V(t_*) + 2\,\eta_V(t_*) , \tag{5.15}$$

$$r \approx 16\,\epsilon_V(t_*) . \tag{5.16}$$

The time $t_*$ denotes when vacuum fluctuations exit the causal horizon and become classical perturbations. For the scales probed at the CMB, $t_*$ can be obtained by backtracking $N \simeq 60$ e-folds from the end of inflation $t_{\rm end}$ (cf. eq. (3.17)). A conservative choice of $t_{\rm end}$ is at moment when the exponential expansion ends, i.e. when the parameters (cf. eq. (3.15))

$$\epsilon_V = \frac{1}{16\pi G}\left(\frac{V_\varphi}{V}\right)^2 = \frac{1}{16\pi G f_a^2}\frac{\sin^2\left(\frac{\bar\varphi}{f_a}\right)}{\left[1 - \cos\left(\frac{\bar\varphi}{f_a}\right)\right]^2} , \tag{5.17}$$

$$\eta_V = \frac{1}{8\pi G}\frac{V_{\varphi\varphi}}{V} = \frac{1}{8\pi G f_a^2}\frac{\cos\left(\frac{\bar\varphi}{f_a}\right)}{1 - \cos\left(\frac{\bar\varphi}{f_a}\right)} , \tag{5.18}$$

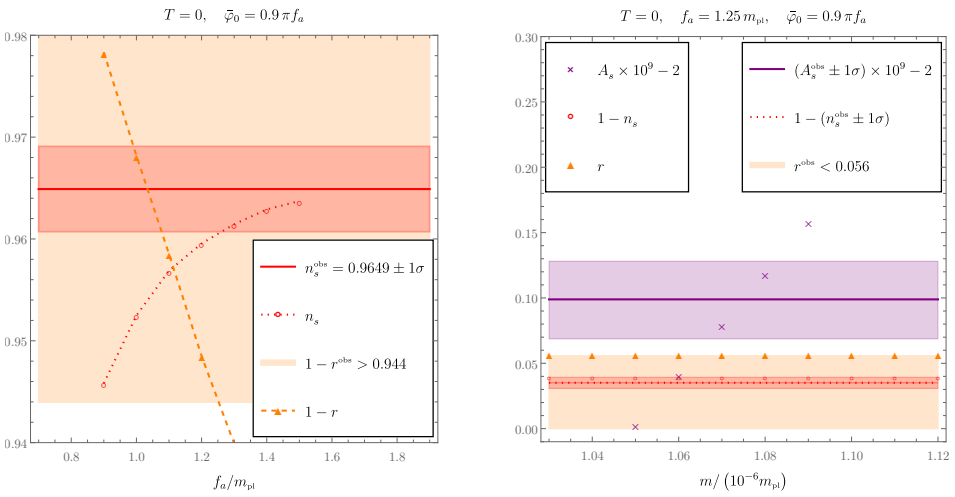


(a) (b)

Figure 5.1: The procedure to establish the values of the parameters $f_a$, in fig. 5.1a, and $m$, in fig. 5.1b. The value of the observables $A_s$, $n_s$ and $r$ is evaluated according to eqs. (3.133)–(3.135). The present figure reproduces the left and middle panels in fig. 2 of [3].

reach order unity. However, considering that the accelerated expansion continues, even if not exponentially, until $V \sim \dot{\bar{\varphi}}^2/2$, and that this could happen later (see the discussion below eq. (4.39)), we choose $t_{\rm end}$ to be the time when the maximal temperature is reached.

Inserting eqs. (5.17) and (5.18) in eqs. (3.136)–(3.137), we learn that $r$ and $n_s$ do not depend directly on the inflaton mass $m$. Considering the experimental constraints [38] (cf. sec. 3.4),

$$r^{\rm obs} < 0.056 \ , \qquad n_s^{\rm obs} = 0.9649 \pm 0.0042 \ , \tag{5.19}$$

we hence first fix the parameter $f_a$, as illustrated in fig. 5.1a ($N > 60$ is satisfied for any value of $f_a$ in the chosen range). More delicate is the matching of $n_s$ and $r$: increasing $f_a/m_{\rm pl}$ increases both $r$ and $n_s$, such that the ideal region for $r$, where $f_a \lesssim 1.25\,m_{\rm pl}$, does not correspond to the one preferable for $n_s$, where $f_a \approx 1.6\,m_{\rm pl}$. We set

$$f_a \approx 1.25\,m_{\rm pl} \ , \tag{5.20}$$

such that both quantities still lie safely within $2\sigma$ distance from the observed value,

$$r(f_a = 1.25\,m_{\rm pl}) \approx 0.055 \ , \qquad n_s(f_a = 1.25\,m_{\rm pl}) \approx 0.9607 \ . \tag{5.21}$$

Once $f_a$ and thus also $\bar{\varphi}_0$ are fixed, we vary $m$ in order to match the observation [38]

$$A_s^{\rm obs} = (2.0989 \pm 0.0292) \times 10^{-9} \ . \tag{5.22}$$

As shown in fig. 5.1b, $A_s$ is highly sensitive to the mass parameter, with the allowed range within the narrow region $m \in [1.05, 1.07) \times 10^{-6} m_{\rm pl}$. Choosing $m = 1.06 \times 10^{-6} m_{\rm pl}$ we obtain the value

$$A_s(f_a = 1.25\,m_{\rm pl}, m = 1.06 \times 10^{-6} m_{\rm pl}) \approx 2.1144 \times 10^{-9} \ . \tag{5.23}$$

Now that we have a first estimate for $m$ and $f_a$, the plan is to solve the full set of equations (4.23), (4.24), (4.39) for different values of the confinement parameter $\Lambda_{\rm IR}$. To proceed towards the numerical solution, in the next sections 5.2 and 5.3 we determine the remaining unknown coefficients entering the equations for the concrete example of an SU(3) Yang-Mills plasma interacting with the inflaton.

## 5.2 Friction coefficient and mass correction

As derived in sec. 4.1, the friction coefficient and the mass correction originating from an interaction term $\mathcal{L} \supset -\varphi J$ are determined respectively by the imaginary and real part of the retarded correlator of $J$, cf. eq. (4.21). For $J$ from eq. (5.2) this takes the form

$$G_{\rm R}(\omega) = \left(\frac{\alpha}{16\pi f_a}\right)^2 \int_0^\infty \mathrm{d}t\, e^{i\omega t} \int \mathrm{d}^3x\, \langle i[F^a_{\mu\nu}\tilde{F}^{a\,\mu\nu}(t,\mathbf{x}), F^b_{\rho\sigma}\tilde{F}^{b\,\rho\sigma}(0,\mathbf{0})]\rangle_0 \ . \tag{5.24}$$

In a weakly coupled thermal system at $T \gg \Lambda_{\rm IR}$, $G_{\rm R}$ contains a lot of structure. At $\omega \gg \pi T$ it is dominated by a vacuum part [84]; at $\omega \sim \pi T$, it develops substantial thermal modifications [85]; at $\omega \sim gT$, features originate from collective plasma excitations and Debye screening [85]. For very small frequencies, $\omega \ll \alpha T$, yet another behaviour takes over, dominated by non-perturbative dynamics [86], so that a reliable determination of $G_{\rm R}$ requires lattice simulations. The real part is related to the topological susceptibility studied in four-dimensional simulations [87, 88], while for the imaginary part only so-called classical real-time simulations [3] can be employed.

An evaluation of the contribution of the scales $\omega \sim gT$ and $\pi T$ [85] suggests that the small-$\omega$ regime is dominated by the contribution from very small $\omega \lesssim \alpha T$ frequencies. Therefore, we adopt a model in which $G_{\rm R}$ only contains a vacuum part, $G_{\rm R}^{\rm UV}$, from $\omega \gg \pi T$ and an infrared part, $G_{\rm R}^{\rm IR}$, from $\omega \lesssim \alpha T$. Furthermore, the *tails* of the two contributions are numerically small outside their domains of validity, so we can establish an interpolation simply by adding the parts together,

$$G_{\rm R}(\omega) \simeq G_{\rm R}^{\rm UV}(\omega) + G_{\rm R}^{\rm IR}(\omega) \ . \tag{5.25}$$

When $T \lesssim \Lambda_{\rm IR}$, the effective-theory type setups used in real-time simulations should be replaced by full four-dimensional lattice simulations. Unfortunately, extracting real-time information from the latter is exponentially hard (see e.g. [89, 90]). To determine $\Upsilon$ and $m_{\rm T}^2$ from the available information in a confined regime we follow two different approaches. However in both cases our estimates contain a systematic error, discussed in the following.

### Friction coefficient

The friction coefficient is defined by (cf. eq. (4.21))

$$\Upsilon \approx \frac{\mathrm{Im}\, G_{\rm R}(m)}{m} \ . \tag{5.26}$$

In [3], classical real-time simulations are used to estimate $\Upsilon$ at very high temperatures, $T \gg \Lambda_{\rm IR}$. The setup for the simulations and perturbative analytical results at leading order in $\alpha$ are illustrated in appendix B.1. Here we report the results originating from the two parts in eq. (5.25),

$$\Upsilon_{\rm IR} = d_{\rm A}\kappa(\alpha N_c)^3 T^3 \left(\frac{\alpha}{f_a}\right)^2 \frac{1 + \frac{m^2}{(c_{\rm IR}\alpha^2 N_c^2 T)^2}}{1 + \frac{m^2}{(c_{\rm m}\alpha N_c T)^2}} \ , \qquad \kappa \approx 1.5 \ , \quad c_{\rm IR} \approx 106 \ , \quad c_{\rm m} \approx 5.1 \ , \tag{5.27}$$

$$\Upsilon_{\rm UV} = d_{\rm A}\left(\frac{\alpha}{16 f_a}\right)^2 \left(\frac{m}{\pi}\right)^3 \left[1 + 2n_{\rm B}\left(\frac{m}{2}\right)\right] \ , \tag{5.28}$$

where $d_{\rm A} \equiv N_c^2 - 1$. $\Upsilon_{\rm UV}$ represents the decay width for the process $\varphi \to gg$.

Little is known about $\Upsilon$ at $T \lesssim \Lambda_{\rm IR}$, even if exploratory studies for determining $\Upsilon_{\rm IR}$ with full four-dimensional lattice simulations have been launched [91,92]. For this reason, we adapt the weak-coupling computation from above to a strongly coupled regime through a modelling of the Yang-Mills coupling $\alpha$. Our estimates contain therefore a systematic error, reflected by the parameter $x$ introduced in eq. (5.11) to test the IR sensitivity of the results.

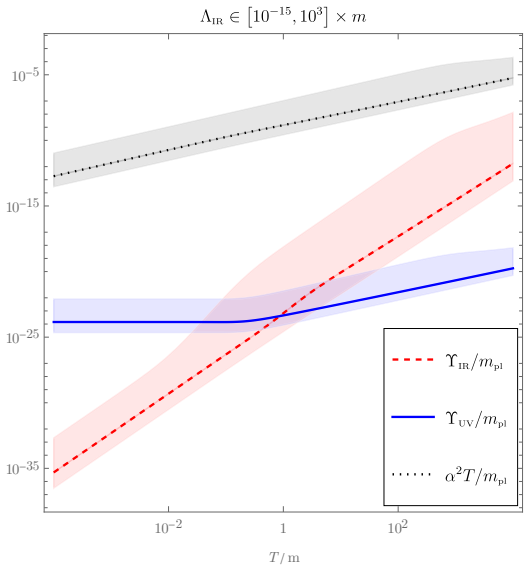


Figure 5.2: Hierarchy of the UV and IR contributions to the friction $\Upsilon$: in the low mass limit $m \ll T$ eq. (5.27) dominates, while at low temperatures $m \gg T$, $\Upsilon \sim \Upsilon_{\rm UV}$ from eq. (5.28). We use the parameter values $m = 1.06 \times 10^{-6} m_{\rm pl}$ and $f_a = 1.25 m_{\rm pl}$ determined in eqs. (5.21) and (5.23). For comparison, we also plot the thermalization rate $\sim \alpha^2 T$ of the heat bath. The error bands originate from varying $\Lambda_{\rm IR}$ in the range $[10^{-15}, 10^{3}] \times m$ (lines are evaluated at $\Lambda_{\rm IR} = 10^{-6} m$).

Figure 5.2 illustrates eqs. (5.27) and (5.28) as functions of $T/m$ and at different $\Lambda_{\rm IR}/m$. The behaviour of $\Upsilon = \Upsilon_{\rm IR} + \Upsilon_{\rm UV}$ changes from vacuum to non-perturbative physics with a gentle cusp when $T \sim m$. Comparing the thermalization rate of the inflaton $\sim \Upsilon_{\rm IR}$ with $\alpha^2 T$, we note that the gauge sector thermalizes more efficiently than the inflaton at both $T \gg m$ and $T \ll m$, with some orders of magnitude difference. When solving the dynamics numerically in sec. 5.4 we therefore omit the thermal corrections to the potential derived in sec. 4.2. Their effects have however been studied in [5], where the interested reader can find more details.

## Mass correction

The effective mass squared is given by (cf. eq. (4.21)),

$$m_{\rm T}^2 \;\approx\; m^2 - \mathrm{Re}\, G_{\rm R}(m)\;. \tag{5.29}$$

### Weakly-coupled Yang-Mills sector

For high temperatures $T \gg \Lambda_{\rm IR}$ we show in appendix B.2 how $\mathrm{Re}\, G_{\rm R}$ can be determined through a perturbative computation in terms of $\alpha$ (or $g^2 = 4\pi\alpha$).

Denoting with $\bar{\mu}^2 \equiv 4\pi\mu^2 e^{-\gamma_{\rm E}}$ the $\overline{\rm MS}$ renormalization scale [93], the result is

$$\mathrm{Re}\, G_{\rm R}(m) = \frac{d_{\rm A} c_\chi^2 g^4 m^2}{\pi^2 f_a^2} \left\{ m^2 \mu^{-2\epsilon} \left( \frac{1}{\epsilon} + \ln \frac{\bar{\mu}^2}{m^2} - 1 \right) + \int_0^\infty \mathrm{d}q\, \mathbb{P} \left[ \frac{16 q^3 n_{\rm B}(q)}{(q - \frac{m}{2})(q + \frac{m}{2})} \right] \right\} + \mathcal{O}(g^6)\;, \tag{5.30}$$

where $\mathbb{P}$ denotes the principal value, and $c_\chi \equiv 1/(64\pi^2)$. Vacuum contributions, i.e. terms without $n_{\rm B}$, are denoted by $\mathrm{Re}\, G_{\rm R}^{\rm UV}$ in the following. The scale parameter appearing in the latter is an auxiliary quantity, and must cancel from physical results. The $1/\epsilon$ divergence and $\ln \bar{\mu}$ in eq. (5.30) can be cancelled by a counterterm, as discussed below eq. (4.16). As a result the combination

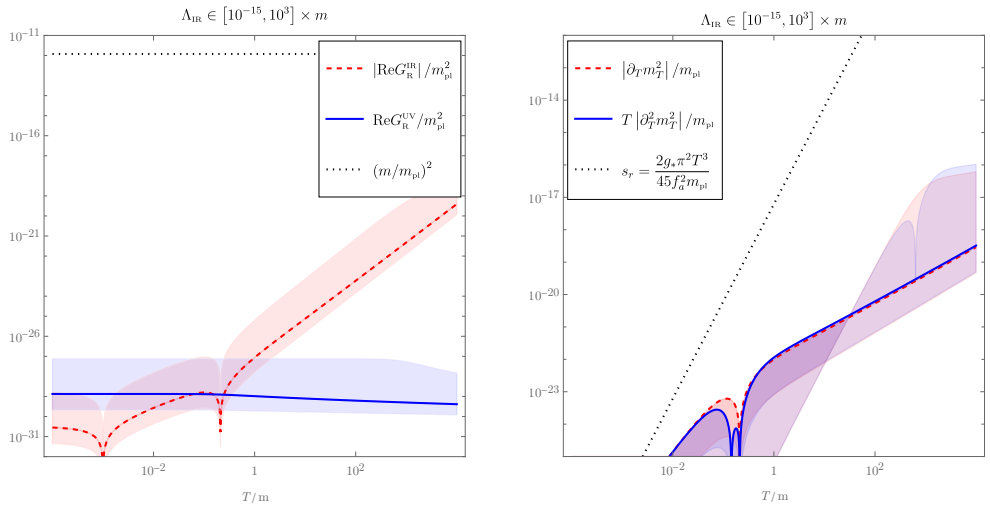


(a) (b)

Figure 5.3: Absolute values of: (a) the UV and IR contributions to the thermal mass $m_{\rm T}^2$ according to eq. (5.31). The cusps at $m \approx 5.2T$ and $m \approx 1023.0\,T$ mark the moments where the IR contributions change sign. (b) the thermal contributions from $m_{\rm T}^2$ to the total entropy density and heat capacity, compared with the entropy density of a radiation plasma in the deconfined phase (normalization factors correspond to eqs. (2.14) and (2.15) of [5]). The cusps are again given by the crossing of zero. We use the parameters $m = 1.06 \times 10^{-6} m_{\rm pl}$ and $f_a = 1.25 m_{\rm pl}$ (cf. eqs. (5.21) and (5.23)). To show how the result would naively extend to a strongly coupled plasma, the shaded ranges indicate the variation of $\Lambda_{\rm IR}$. However, for $m_{\rm T}^2$ we follow a different prescription, as described in eq. (5.33).

$1/\epsilon + \ln\bar{\mu}^2$ gets replaced with a physical logarithm $\ln \Lambda_{\rm UV}^2$, where $\Lambda_{\rm UV}^2 \sim m f_a$ is the UV completion of the theory introduced in eq. (5.8).

An estimate of the thermal part yields the asymptotic behaviour

$$\mathrm{Re}\, G_{\rm R}^{\rm IR}(m) \longrightarrow \begin{cases} -d_{\rm A} c_\chi^2 \frac{64\pi^2}{15} \frac{g^4 T^4}{f_a^2} \,, & T \ll m \\ d_{\rm A} c_\chi^2 \frac{8}{3} \frac{g^4 m^2 T^2}{f_a^2} \,, & T \gg m \end{cases} , \tag{5.31}$$

implying that the thermal mass corrections change sign at $m \approx 5.2T$.

We show in fig. 5.3a that both parts of $\mathrm{Re}\, G_{\rm R}$ are about ten orders of magnitude below the tree level value $m^2$, and in both regimes $T \ll m$ and $T \gg m$ ($T < \Lambda_{\rm UV} \sim 10^{-3} m_{\rm pl} \sim 10^3 m$ is an upper bound in our model). Similarly, the corrections emerging from $\partial_{\rm T} m_{\rm T}^2$ and $\partial_{\rm T}^2 m_{\rm T}^2$ to the thermodynamic functions are generally suppressed, see fig. 5.3b. We therefore omit $m_{\rm T}^2$ and its derivatives in the numerical solutions in sec. 5.4.

### Strongly-coupled Yang-Mills sector

In principle we could carry out a discussion similar to $\Upsilon$ also for $m_{\rm T}^2$, adapting a weak-coupling result at $T \gg \Lambda_{\rm IR}$ to a strongly coupled regime. However, partial non-perturbative lattice information is also available for $\mathrm{Re}\, G_{\rm R}$, so we would like to make use of it, even if it is not exactly what is needed. Let us explain the issues.

The lattice simulations are usually viewed in the context of the QCD axion mass. Since a mass term would break the shift symmetry, it is assumed that the axion has no mass at tree level, so that

all of it is generated by the SU(3) gauge dynamics. Then, the mass correction can be evaluated at $\omega = 0$, in which case it is proportional to the topological susceptibility as described in eq. (5.10). Though the problem is technically challenging, results have become available (cf., e.g., [87,88] and references therein), and we return to them presently (cf. eq. (5.32)).

However, a mass determined at $\omega = 0$ is correct only if there is no *bare mass* from an UV theory. This is a problem, since our inflaton potential $V_0$ already contains a mass; it is envisaged to have been generated by an UV gauge theory, at a scale higher than the IR one on which we focus. In this situation, the contribution to the mass through the SU(3) topological susceptibility is only a correction, and its determination at $\omega = 0$ rather than $\omega \simeq m$ represents an approximation from the physics point of view.

Despite these reservations, we estimate how large the mass correction could be. We denote by $\chi$ the SU(3) topological susceptibility, and by $t_0$ an auxiliary quantity often used for setting the scale in lattice simulations. Then, at $T = 0$, $t_0^2\,\chi = 6.67(7) \times 10^{-4}$ [87], whereas examples of thermal values are $t_0^2\,\chi = 2.25(12) \times 10^{-5}$ at $T\sqrt{8t_0} = 1.081$ and $t_0^2\,\chi = 3.43(27) \times 10^{-6}$ at $T\sqrt{8t_0} = 1.434$ [88]. Inserting a conversion to the critical temperature, $T_c\sqrt{t_0} = 0.2489(14)$ [94], a rough qualitative representation, incorporating an expected functional dependence at higher temperatures, is

$$\chi \simeq \begin{cases} 0.17\,T_c^4 \;, & T \lesssim 0.95 T_c \\ \frac{0.12\,T_c^{11}}{T^7} \;, & T \gtrsim 0.95 T_c \end{cases} \;, \tag{5.32}$$

and the corresponding mass corrections from the IR ($\omega \to 0$) gauge theory evaluate to

$$\delta m_0^2 \overset{T\lesssim 0.95T_c}{\simeq} \frac{0.17\,T_c^4}{f_a^2} \;, \qquad \delta m_{\rm T}^2 \overset{T\gtrsim 0.95T_c}{\simeq} \frac{0.12\,T_c^{11}}{f_a^2 T^7} \;, \qquad \delta m_{\rm T}^2 < \delta m_0^2 \;. \tag{5.33}$$

To connect $\delta m^2$ to the mass parameter appearing in the potential let us recall the discussion about $V_0$ above eq. (4.25). We refer to $V_0$ as the tree-level potential plus those radiative and thermal corrections which do not change the shape of $V_0$ (in contrast, shape-changing structures lead to what we have denoted by $V$). With $m^2$ the value of the tree-level mass, at temperatures below $T_c$ it gets modified to the temperature-independent quantity

$$m^2 \to m_0^2 \equiv m^2 + \delta m_0^2 \;, \tag{5.34}$$

whereas a would-be thermal mass squared at $T > T_c$ reads

$$m^2 \to m_{\rm T}^2 = m^2 + \delta m_{\rm T}^2 = m_0^2 - \delta m_0^2 + \delta m_{\rm T}^2 \;. \tag{5.35}$$

After these order-of-magnitude estimates, let us explain why the mass correction should be unimportant. Inserting the numerical values for $m$ and $f_a$ and estimating the bare mass as $m^2 \sim \Lambda_{\rm UV}^4/f_a^2$ following eq. (5.8), the scale of the UV gauge theory is $\Lambda_{\rm UV} \sim 10^{-3} m_{\rm pl}$. According to sec. 5.4, the solutions fall in two different classes. If the system heats up to $T_{\rm max} \geq T_c$, then $|\delta m_{\rm T}^2 - \delta m_0^2| \sim \Lambda_{\rm IR}^4/f_a^2 \ll \Lambda_{\rm UV}^4/f_a^2 \sim m^2$, i.e. the thermal mass correction is exceedingly small. If $T_{\rm max} < T_c$, the system stays in the confined phase, and there is no thermal mass correction.

## 5.3 Non-perturbative thermodynamics for a radiation bath

As an essential ingredient to eqs. (4.39) and (4.45), we need the thermodynamic energy density and pressure of the radiation plasma, $e_r$ and $p_r$. These are often parametrized through degrees of freedom $g_*$ or $h_*$, according to eq. (4.42). If the plasma is very weakly coupled, $g_*$ is to a

good approximation constant and $h_* \simeq g_*$. However here we want to consider also the case, where interactions can become strong as well.[38] In the latter case, $g_*$ and $h_*$ decrease rapidly at low temperatures, and their complete functional forms are needed.

It turns out to be convenient to parametrize the thermodynamic information through the entropy density, $s_r$. On one hand, this is because we need $s_r$ for eq. (5.49). On the other, $s_r$ can be precisely studied with lattice simulations, cf. [95, 96] and references therein. Denoting by $T_c$ the critical temperature, and setting $N_c = 3$, the results of the deconfined phase of a Yang-Mills plasma can be represented as[39] [96]

$$\left.\frac{s_r}{T^3}\right|_{\text{lattice}} \approx \begin{cases} 6.9829 - \dfrac{1.0348}{\ln(T/T_c)} & , \quad T \geq 3.222 T_c \\ \dfrac{1.7015 + 77.757\ln(T/T_c) + 232.33\ln^2(T/T_c)}{1.0 + 19.033\ln(T/T_c) + 32.200\ln^2(T/T_c)} & , \quad T_c < T < 3.222 T_c \end{cases} . \tag{5.36}$$

For $T/T_c \to \infty$ this agrees within 0.5% with the Stefan-Boltzmann value

$$\left.\frac{s_r}{T^3}\right|_{\text{free}} = \frac{2\pi^2 \times 16}{45} = 7.018 . \tag{5.37}$$

The determination of $s_r/T^3$ is more difficult in the confined phase, as the results soon become exponentially small. Fitting to the tabulated results from [96],[40] *viz.*

| $s_r/T^3$ | $T/T_c$ |
|---|---|
| 0.37(15) | $1.0^-$ |
| 0.31(11) | 0.980 |
| 0.108(23) | 0.904 |
| 0.001(4) | 0.660 |

, (5.38)

which appear to be consistent with [97], we model the low-$T$ region with the ansatz

$$\left.\frac{s_r}{T^3}\right|_{\text{lattice}} \overset{T<T_c}{\simeq} a \left(\frac{T}{T_c}\right)^b \exp\left(-\frac{c\,T_c}{T}\right) , \quad a = 45.8 , \quad b = 6.81 , \quad c = 4.80 . \tag{5.39}$$

The transition is of the first order, so that $s_r/T^3$ displays a discontinuity at $T = T_c$. For the conversion between $T_c$ and $\Lambda_{\text{IR}}$ we estimate $T_c \simeq 1.24\Lambda_{\text{IR}}$ [94].

Given $s_r = \mathrm{d}p_r/\mathrm{d}T$, the other thermodynamic functions can be obtained as

$$p_r(T) - p_r(0) = \int_0^T \mathrm{d}T'\, T'^3 \left(\frac{s_r}{T'^3}\right) , \quad e_r(T) - e_r(0) = T s_r - [p_r(T) - p_r(0)] . \tag{5.40}$$

Furthermore, in order to evaluate $\dot{e}_r = \dot{T} c_r$, we need the heat capacity $c_r = \partial_{\text{T}} e_r = T \partial_{\text{T}} s_r$. At low temperatures eq. (5.39) implies

$$\frac{p_r(T) - p_r(0)}{T^4} \overset{T<T_c}{\simeq} a\, c^b \left(\frac{cT_c}{T}\right)^4 \Gamma\left(-b-4, \frac{cT_c}{T}\right) , \tag{5.41}$$

$$\frac{c_r}{T^3} \overset{T<T_c}{\simeq} a \left[ (b+3)\left(\frac{T}{T_c}\right)^b + c\left(\frac{T}{T_c}\right)^{b-1} \right] \exp\left(-\frac{c\,T_c}{T}\right) , \tag{5.42}$$

[38] In this section we make use of non-perturbative information, so that the coupling can be arbitrarily strong.

[39] [96] gives $T = 3.433 T_c$ as the transition point between the two functional forms; we have replaced this with the value at which the curves cross each other, with the approximate coefficients at our disposal.

[40] The first number can be found in the text, not the table. The last number appears to contain a typo in the table of [96]; we have reconstructed the correct value from the $e_r$ and $p_r$ given on the same line.

where $\Gamma(s,x) = \int_x^\infty \mathrm{d}t\, t^{s-1}\, e^{-t}$ is an incomplete gamma function.

Restricting to the SU(3) plasma is a special case, however this is the system for which the most reliable non-perturbative information is available. In addition, it entails a weak first-order transition, which is typical of many other thermal systems.

## 5.4 Numerical results and parameter scan

Having established all the coefficients appearing in the evolution equations (4.23), (4.39) and (4.45), we now want to solve them. From the results of secs. 5.1–5.3 we learn that the thermalization of the inflaton field is a slow process compared with the thermalization of the gauge plasma,[41] and that interactions among the two yield negligible thermal corrections to the inflaton mass and to the shape of the potential. It is therefore a fair approximation to simplify the potential by setting $\partial_{\mathrm{T}} V \approx \partial_{\mathrm{T}} \dot{V} \approx 0$.[42] We hence finally solve

$$\ddot{\bar{\varphi}} + (3H + \Upsilon)\dot{\bar{\varphi}} + V'(\bar{\varphi}) \simeq 0 \tag{5.43}$$

$$\Upsilon\, \dot{\bar{\varphi}}^2 \simeq \begin{cases} \dot{e}_r + 3H\,(e_r + p_r) \ , & T \neq T_c \\ \dot{u}\,[\, e_r(T_c^+) - e_r(T_c^-)\,] + 3H\,[e_r(T_c^+)\,u + e_r(T_c^-)\,(1-u) + p_r(T_c)] \ , & T = T_c \end{cases} \tag{5.44}$$

numerically for the functions $\{\varphi(t),\ T(t),\ u(t)\}$. With the simplifications discussed above, the Hubble rate and the potential read

$$H^2 \simeq \frac{8\pi}{3m_{\mathrm{pl}}^2}\left(e_r + \frac{\dot{\bar{\varphi}}^2}{2} + V\right) \ , \qquad V(\bar{\varphi}) \simeq m^2 f_a^2\left[1 - \cos\left(\frac{\bar{\varphi}}{f_a}\right)\right] \ . \tag{5.45}$$

The form of the friction $\Upsilon = \Upsilon_{\mathrm{IR}} + \Upsilon_{\mathrm{UV}}$ as a function of $m$, $T$, $f_a$ and $\alpha$ is given in eqs. (5.27) and (5.28), where the coupling $\alpha$ in eq. (5.11) is parametrized by $m$, $T$ and $\Lambda_{\mathrm{IR}}$. Conveniently the time parameter is normalized by a reference *Hubble time*

$$t_{\mathrm{ref}} \equiv \sqrt{\frac{3m_{\mathrm{pl}}^2}{8\pi V[\bar{\varphi}_0]}} \approx \frac{1}{H(t_{\mathrm{ref}})} \ . \tag{5.46}$$

With the values

$$m \approx 1.06 \times 10^{-6} m_{\mathrm{pl}} \ , \qquad f_a \approx 1.25\, m_{\mathrm{pl}} \ , \tag{5.47}$$

fixed by the CMB constraints (see sec. 5.1), the only free parameter left is $\Lambda_{\mathrm{IR}}$. We thus scan the solutions in terms of $\Lambda_{\mathrm{IR}}$, discovering a rich dynamics, that determines the value of the maximal temperature reached after inflation.

To determine the convenient initial conditions for eqs. (5.43)–(5.45), we study the emergence of a stationary temperature, $T_{\mathrm{stat}}$, analytically.

### Stationary temperature

The existence of a stationary temperature at intermediate stages of warm natural inflation follows from the argumentation in [59, 64]. Physically, this corresponds to a situation in which the energy released from the inflaton to radiation through friction, precisely balances against the energy diluted by the Hubble expansion. After a while, $T$ starts to increase above $T_{\mathrm{stat}}$, obtaining a maximal value, $T_{\mathrm{max}}$. While estimating $T_{\mathrm{max}}$ requires the solution of the coupled set of differential equations, for $T_{\mathrm{stat}}$ we can employ slow-roll approximations to find algebraic equations.

[41] This is not the only argument. In fig. 5.6(right) we show that it appears unlikely that the inflaton thermalizes, because its would-be thermalization rate $\sim \Upsilon_{\mathrm{IR}}$ is much below the Hubble rate, for any choice of $\Lambda_{\mathrm{IR}}$.

[42] In [5] we illustrate solutions in the three qualitatively different cases of a Yang-Mills plasma and: (i) a non-thermal inflaton, (ii) a thermalized inflaton, (iii) a thermalized inflaton + one extra degree of freedom.

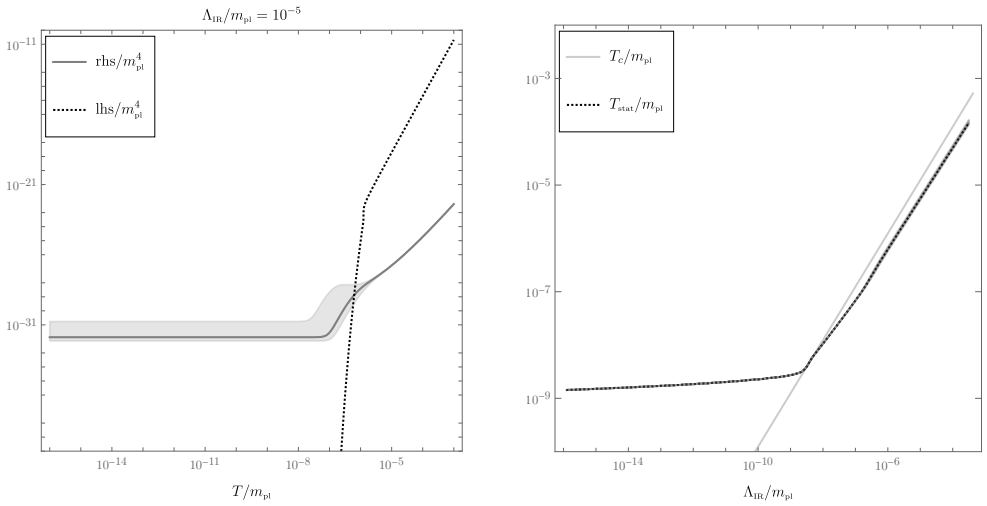


(a) (b)

Figure 5.4: (a) Example of left hand-side (lhs) and right hand-side (rhs) of eq. (5.49) at $\Lambda_{\rm IR} = 10^{-5} m_{\rm pl}$. The band correspond to the variation of $x \in (0.2, 2.0)$ in the parametrization of $\alpha$, eq. (5.11). (b) Solution $T_{\rm stat}$ of eq. (5.49) at different values of $\Lambda_{\rm IR}$. $T_c$ denotes the critical temperature. The present figure reproduces partially fig. 3 of [5].

Let us start with the slow-roll approximation of eq. (5.43),

$$\dot{\bar{\varphi}} \simeq -\frac{V_\varphi}{3H + \Upsilon} , \tag{5.48}$$

while in eq. (5.44), we search for a stationary solution, with $\dot{e}_r \simeq 0$. Recalling the thermodynamic relation $e + p = Ts$, where $s$ is the entropy density, yields the master relation

$$3T_{\rm stat} s \simeq \frac{\Upsilon}{H} \frac{V_\varphi^2}{(3H + \Upsilon)^2} . \tag{5.49}$$

As further simplifications, the Hubble rate can be approximated as $H \simeq \sqrt{8\pi V/(3m_{\rm pl}^2)}$ during the slow-roll period, and we may furthermore set $\bar{\varphi} \to \bar{\varphi}_0$ in $V$ and $V_\varphi$.

The left and right-hand sides (lhs, rhs) of eq. (5.49) are illustrated in fig. 5.4a. The resulting values of $T_{\rm stat}/m_{\rm pl}$, from the crossings of the respective curves, are plotted in fig. 5.4b. It can be observed from fig. 5.4b that there is a specific domain of $\Lambda_{\rm IR}$ at which the behaviour of the system changes. To determine the smallest value $\Lambda_{\rm min}$ for which the system reaches $T_c$, we ask for which $\Lambda_{\rm IR}$ the stationary temperature satisfies $T_{\rm stat} = T_c$. This corresponds to

$$3T_c s = \left. \frac{\Upsilon}{H} \frac{V_\varphi^2}{(3H + \Upsilon)^2} \right|_{\Lambda_{\rm IR} \to \Lambda_{\rm min}} \quad \Rightarrow \quad \Lambda_{\rm min} \simeq 3 \times 10^{-9}\, m_{\rm pl} . \tag{5.50}$$

In fig. 5.4a the cusp in the rhs curve is where the behaviour of $\Upsilon$ changes, from $\Upsilon_{\rm UV}$ at low temperatures to $\Upsilon_{\rm IR}$ at high temperatures. When $\Lambda_{\rm IR} = \Lambda_{\rm min}$ the lines cross in a domain where $\Upsilon \approx \Upsilon_{\rm UV}$. Therefore, $\Lambda_{\rm min}$ is independent of the non-perturbative physics of $\Upsilon_{\rm IR}$.

## Maximal temperature

We now move on to a full solution of eqs. (5.43) and (5.44). As initial conditions, we take

$$T(t_{\rm ref}) \simeq 0.2 T_{\rm stat} , \quad \bar{\varphi}(t_{\rm ref}) = 0.9\pi f_a , \quad \dot{\bar{\varphi}}(t_{\rm ref}) \simeq -V_\varphi/(3H) \tag{5.51}$$

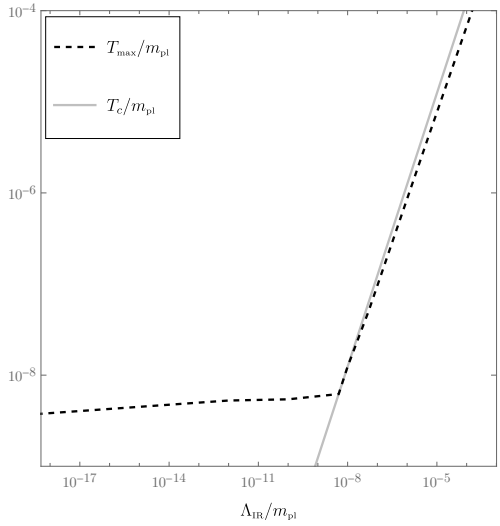


Figure 5.5: Scan of $T_{\max}$ as a function of $\Lambda_{\rm IR}/m_{\rm pl}$ from the solution of eqs. (5.43) and (5.44). Our setup is self-consistent only for $\Lambda_{\rm IR} < \Lambda_{\rm UV} \sim 10^{-3} m_{\rm pl}$. $T_c$ denotes the critical temperature. The present figure reproduces partially fig. 5 of [5].

from sec. 5.1. However, the solution is an attractor, and therefore soon independent of the initial conditions. For the given parameters, the confinement scale at which the system heats up exactly to $T_c$ is found to be in the vicinity of $\Lambda_{\max} \sim 2 \times 10^{-8} m_{\rm pl}$.

Examples of solutions are shown in fig. 5.6, and a scan of $T_{\max}$ in fig. 5.5. We conclude that

* if $\Lambda_{\rm IR} < \Lambda_{\max}$, $T_{\max} > T_c$ and a phase transition occurs as the system cools down (cf. fig. 5.6a).
* for $\Lambda_{\min} < \Lambda_{\rm IR} < \Lambda_{\max}$, the system undergoes two phase transitions, one as it heats up to $T_{\max}$, one as it cools down. Yet in this domain $\alpha^2 T \ll T \ll H$, so it is questionable whether the temperature has a literal meaning during the first transition. The maximal temperature has the numerical value $T_{\max} \lesssim \Lambda_{\max} \sim 2 \times 10^{-8} m_{\rm pl}$ (cf. fig. 5.6c).
* if $\Lambda_{\rm IR} \sim \Lambda_{\max}$, then the system heats up to $T_{\max} \sim T_c$. This happens just between the examples in figs. 5.6c and 5.6e.
* if $\Lambda_{\rm IR} > \Lambda_{\max}$, $T_{\max} < T_c$ and the system undergoes no phase transition. Nevertheless it heats up to a high temperature, $T_{\max} \sim \Lambda_{\rm IR}$ (cf. fig. 5.6g).

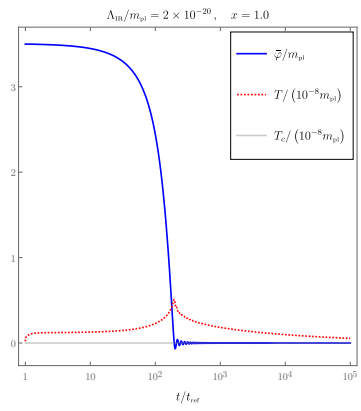


(a)

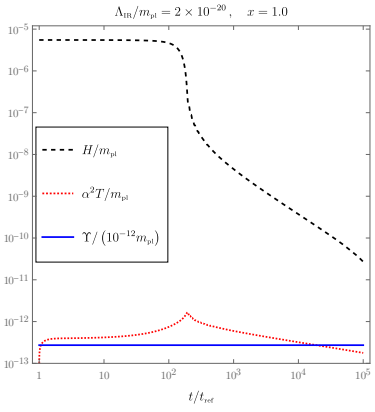


(b)

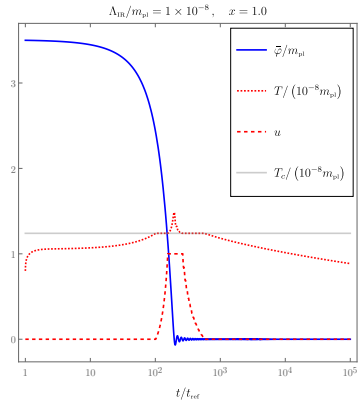


(c)

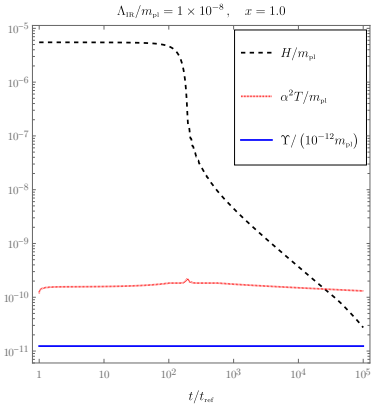


(d)

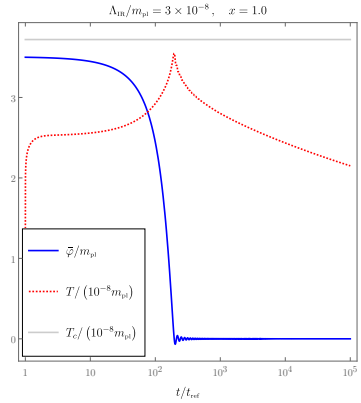


(e)

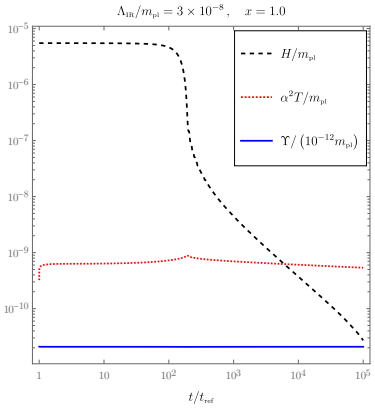


(f)

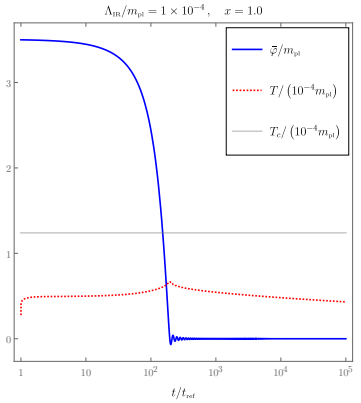


(g)

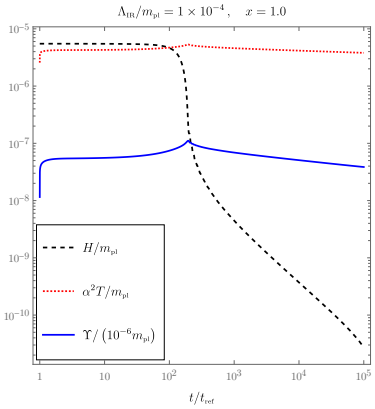


(h)

Figure 5.6: For explanations see the text below eq. (5.51).

# Chapter 6

# Gravitational waves from thermal processes

We are interested in estimating the contribution to the gravitational wave background, that can be associated with a thermal axion-like inflation scenario, as described in chapter 5.[43] Our starting point is thus the interaction Lagrangian

$$\mathcal{L} \supset -\varphi J + \hat{h}^{\mu\nu} T_{\mu\nu} \ , \qquad J \equiv \frac{\alpha}{16\pi f_a} \epsilon^{\mu\nu\rho\sigma} F^c_{\mu\nu} F^c_{\rho\sigma} \ , \tag{6.1}$$

where $\hat{h}^{\mu\nu}$ represents the propagating part of a graviton field (suitably rescaled). The parameter $f_a$ denotes the decay constant of the scalar field into the gauge bosons that populate the thermal bath. Interactions in the latter are described by the Yang-Mills coupling constant $g^2 = 4\pi\alpha$, the Yang-Mills field strength $F^c_{\mu\nu}$, and $c \in \{1, \ ..., N_c^2 - 1\}$, for $N_c$ the number of colours.

During inflation, scalar perturbations (cf. sec. 3.2) are sourced quantum mechanically, from the vacuum fluctuations of the inflaton field. Tensor perturbations (cf. sec. 3.3) are geometrical vacuum fluctuations, and grow according to the exponential expansion, until they exit the horizon. For scalar perturbations produced during warm inflation [110–113], thermal corrections are negligible in the regime $\Upsilon \ll H$ where the thermal friction is small compared to the Hubble friction.

We show in sec. 6.1 that the story is different for tensor perturbations, which get directly sourced by thermal fluctuations of physical momenta $k/a \lesssim \alpha^2 T$. Since the Hubble friction still dominates for a long period after the slow-roll regime, in general we have $\alpha^2 T \ll H$. This means that physical modes exit the horizon at the very beginning of inflation, and remain outside for its whole duration. Gravitational waves are sourced by thermal fluctuations continuously in time, not only at horizon crossing. For the primordial gravitational wave spectrum we derive an interpolating formula that incorporates both vacuum and thermal production during inflation. The resulting signal has a model-independent frequency shape $f_0^3$ in the LISA window [41], whose coefficient allows to measure the maximal shear viscosity predicted by the model. Our methods and results [4] are to a certain extent comparable to those of [107, 108], respectively.[44]

The vacuum and thermal perturbations produced during inflation are outside the horizon in the reheating period. However, new fluctuations are produced at different scales by the interactions between the oscillating inflaton field and the heat bath at equilibrium. These modes are therefore inside the horizon and the Minkowski metric offers suitable local coordinates to describe the

[43] Gravitational waves for non-thermal axion-like inflation have been studied e.g. in [98, 99], or [100–106], where contributions from efficient non-thermal *particle production* mechanisms are considered during or after the inflationary epoch. Thermal contributions are usually taken into account in the context of warm inflation, e.g. [107–109].

[44] However, [107] applies the same methods to scalar instead of tensor perturbations during warm inflation, while [108] computes the thermal contributions to tensor perturbations during the slow-roll regime (without interpolation with the vacuum contribution, nor transfer function), and assumes $\Upsilon \sim T^n$ for the friction coefficient.

interactions. In sec. 6.2 we compute the gravitational energy contribution from the momentum regime $H \ll k/a \lesssim \alpha^2 T$, and report the results for larger momenta, $k/a \sim \pi T$, derived in appendix C. Gravitational waves at reheating are found to peak at high (GHz) frequencies [2].

Having shown in sec. 5.2 that thermal corrections to the inflaton mass are irrelevant, we neglect them throughout the entire chapter, and denote by $m$ the tree-level mass.

## 6.1 During inflation

Thermal corrections affect tensor perturbations in different ways. The most obvious contributions enter via the non-vanishing fluid anisotropies $\Pi^{\rm t}_{ij} \neq 0$ produced by thermal fluctuations, which directly source gravitational waves through Einstein's equations (2.133). On top of them, tensor perturbations may also get damped by an additional thermal friction in this scenario. However, the corresponding damping coefficient for tensor perturbations is suppressed by $m_{\rm pl}^2$, $\Upsilon_{\rm t} \sim \eta/m_{\rm pl}^2$, where $\eta$ is the shear viscosity of the plasma, and thus negligible compared with the damping caused by the expansion of the universe $H \sim T^2/m_{\rm pl}$. Finally, the tensor perturbations produced at inflation propagate through the thermal era before we can observe them today. The way their signal gets modified during this journey is encoded in the transfer function. In the present section we study the first and third contributions mentioned above, and draw some conclusions on the observability of the gravitational wave signal.

### Tensor perturbations from thermal fluctuations

We start from the evolution equations (2.133) for tensor perturbations. Going over to co-moving momentum space and helicity basis, the dynamics of a given $\lambda$-helicity mode reads

$$(\partial_\tau^2 + 2\mathcal{H}\partial_\tau + k^2)\vartheta_\lambda(\tau,\mathbf{k}) = 8\pi G a^2 \bar{p} \sum_{ij} \epsilon^\lambda_{ij} \Pi^{\rm t}_{ij}(\tau,\mathbf{k}) \equiv \rho(\tau,\mathbf{k}) \ . \tag{6.2}$$

Independently of the source $\rho$, eq. (6.2) can be solved using a retarded Green's function. At $\tau > \tau_i$, we are thus solving the same equation already encountered for the vacuum solution of tensor perturbations, cf. eq. (3.98) and eq. (3.109). Considering that small momenta exit the horizon in the earliest stage of inflation, and soon satisfy $k \ll \mathcal{H}$, to find the super-horizon Green's function we solve the equations,

$$\left[a^2 G'_{\rm R}(\tau,\tau_i)\right]' \approx \delta(\tau-\tau_i) \ , \quad G_{\rm R}(\tau<\tau_i,\tau_i) \equiv 0 \ , \quad \lim_{\tau\to\tau_i^+} G'_{\rm R}(\tau,\tau_i) \equiv 1 \ , \tag{6.3}$$

$$\Rightarrow \quad G_{\rm R}(\tau,\tau_i) \overset{k\ll\mathcal{H}}{\approx} a^2(\tau_i) \int_{\tau_i}^{\tau} \frac{{\rm d}\tilde{\tau}}{a^2(\tilde{\tau})} \ , \tag{6.4}$$

which does not depend on $k$. In principle, during the slow-roll regime of inflation one could use the relation $a(\tau) \approx -1/(H\tau)$. However, thermal fluctuations contribute mostly at high temperatures, i.e. when the thermal bath warms up to its maximal temperature towards the end of inflation. In this regime the de Sitter approximation is no longer valid and we should rather solve eq. (6.3) as we are solving the inflation dynamics numerically.

The solution of eq. (6.2) is then the convolution integral, such that its correlator can be written in terms of the one of the source. In order to make use of this property, we need the correlator of the thermal perturbations in the energy-momentum tensor, which at large wavelengths are known as hydrodynamic fluctuations [114, §88].

The macroscopic variables that describe the fluid are the local temperature $T$, and the local fluid velocity $v^i$. At first order, the energy-momentum tensor is then expressed as a gradient expansion,

$$T^{\rm hydro}_{\mu\nu} = \bar{T}^{\rm hydro}_{\mu\nu} + \delta T^{\rm hydro}_{\mu\nu} + S_{\mu\nu} + \mathcal{O}(\delta^2) \ , \tag{6.5}$$

where the zeroth order $\bar{T}^{\rm hydro}_{\mu\nu}$ contains no gradients and depends therefore on the averaged variables $\bar{T}$ and $\bar{v}^i = 0$.[45] At linear order in small perturbations, there are contributions from the first order expansion in $\delta T$ and $v^i \equiv \delta v^i$, which we denote by $\delta T^{\rm hydro}_{\mu\nu}$. There, the dependence on $T$ is parametrized by the shear viscosity $\eta$, and the bulk viscosity $\zeta$ [115, p.44]. Since viscosities transfer part of the kinetic energy of the fluid to thermal energy, at the same order an extra thermal noise term $S_{\mu\nu}$ must be included [114, §88,89]. The latter is characterized by the autocorrelator [116][46]

$$\langle S_{ij}(\tau_1,\mathbf{x}_1)\, S_{mn}(\tau_2,\mathbf{x}_2)\rangle = 2T \overbrace{\left[\eta(\delta_{im}\delta_{jn}) + \left(\zeta - \frac{2\eta}{3}\right)\delta_{ij}\delta_{mn}\right]}^{\mathcal{S}_{ij;mn}(\eta,\zeta)} \frac{\delta(\mathbf{x}_1-\mathbf{x}_2)\,\delta(\tau_1-\tau_2)}{\sqrt{-{\rm det} g_{\mu\nu}}} \tag{6.6}$$

$$\Rightarrow \quad \langle S_{ij}(\tau_1,\mathbf{k}_1)\, S^*_{mn}(\tau_2,\mathbf{k}_2)\rangle = \frac{2T}{a^4}\mathcal{S}_{ij;mn}(\eta,\zeta)\,\delta(\tau_1-\tau_2)\,(2\pi)^3\delta(\mathbf{k}_1+\mathbf{k}_2) \ . \tag{6.7}$$

In a decomposition according to eqs. (2.21)–(2.24), $\delta T^{\mu\nu}_{\rm hydro}$ has only scalar and vector modes, and no contribution to tensor modes. These get thus sourced only by the shear viscosity,

$$\begin{aligned}
\bar{p}^2 \sum_\lambda \epsilon^\lambda_{ij}(\mathbf{k}_1)\,[\epsilon^\lambda_{mn}(\mathbf{k}_2)]^*\,\langle \Pi^t_{ij}(\tau_1,\mathbf{k}_1)\,[\Pi^t_{mn}(\tau_2,\mathbf{k}_2)]^*\rangle & \\
= \quad \sum_\lambda \epsilon^\lambda_{ij}(\mathbf{k}_1)\,[\epsilon^\lambda_{mn}(\mathbf{k}_2)]^*\,\langle S_{ij}(\tau_1,\mathbf{k}_1)\,S^*_{mn}(\tau_2,\mathbf{k}_2)\rangle & \qquad (6.8)\\
\overset{(6.7)}{=}_{(3.82)} \ \frac{2T}{a^4}\mathbb{L}_{ij;mn}(\mathbf{k}_1)\mathcal{S}_{ij;mn}(\eta,\zeta)\,\delta(\tau_1-\tau_2)\,(2\pi)^3\delta(\mathbf{k}_1+\mathbf{k}_2) & \qquad (6.9)\\
\overset{(6.6)}{=} \ \frac{8T\eta}{a^4}\delta(\tau_1-\tau_2)\,(2\pi)^3\delta(\mathbf{k}_1+\mathbf{k}_2) \ . & \qquad (6.10)
\end{aligned}$$

In a system with a thermalized inflaton coupled to a heat bath through a damping coefficient $\Upsilon$, the shear viscosity gets two contributions: $\eta_J$ from the interactions between the inflaton and the plasma, and $\eta_g$ from reactions characteristic of a pure gauge plasma.

In general, the form of $\eta$ is derived in a local rest frame of the fluid. For physical modes inside the horizon, $H \ll k/a \lesssim \alpha^2 T$, interactions are fast compared to the expansion of the universe, and we can use local Minkowskian coordinates. The same assumption is not accurate for modes outside the horizon, and in principle an out-of-equilibrium shear viscosity should be derived in an expanding frame. However, the modes were within the horizon a short time earlier, and for a first estimate we retain the thermal value.

The scalar field contribution to $\eta$ is studied in detail in sec. 6.2, and here we only report the result for low temperatures,

$$T\eta_J = \lim_{\omega,k\to 0}\frac{T\,{\rm Im}\,G^{\rm R}_{xy;xy}(\omega,k)}{\omega} \overset{T\ll m}{\approx} \frac{T^5}{\Upsilon(T)}\left(\frac{2\pi m}{T}\right)^{\frac{3}{2}} e^{-m/T} \ . \tag{6.11}$$

The gauge plasma contribution dates back to [117],

$$T\eta_g \overset{\substack{N_{\rm c}=3\\ N_{\rm f}=0}}{\simeq} \frac{27.126\,T^4}{g^4\ln\left(\frac{2.765\,T}{m_{\rm D}}\right)} \ , \qquad m_{\rm D} \equiv \frac{g^2T^2}{3} \ . \tag{6.12}$$

[45] This corresponds to the perfect-fluid energy-momentum tensor introduced in eq. (2.71).

[46] Only the spatial part yields a non-vanishing contribution at this order.

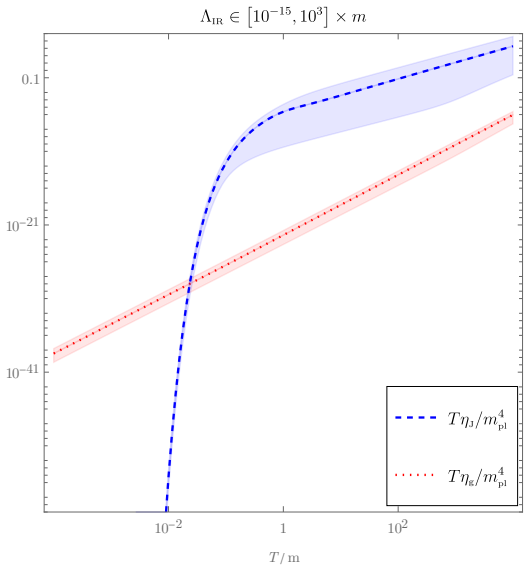


Figure 6.1: Contributions to the shear viscosity of the thermal plasma by interactions with the inflaton field $T\eta_J$, and by pure gauge plasma reactions $T\eta_g$. The error bands originate from varying $\Lambda_{\rm IR}$ in the range $[10^{-15}, 10^{3}] \times m$ (lines are evaluated at $\Lambda_{\rm IR} = 10^{-6}m$).

The inflaton contribution eq. (6.11) is exponentially suppressed at, relatively speaking, low temperatures $T \ll m$, i.e. most of the time during the inflationary epoch. The two contributions are shown in fig. 6.1 beyond the low-$T$ expansion. Through $g$, which appears also in the definition of $\Upsilon$, cf. eqs. (5.27) and (5.28), and through the non-linear dynamics that gives $T$, they depend non-trivially on the confinement scale $\Lambda_{\rm IR}$ of the dark sector.

It is worth remarking that we find no momentum dependence, neither in the Green's function, nor in the correlator of the source, such that the resulting power spectrum scales like $\sim k^3$. However, before evaluating the power spectrum for thermal fluctuations, for a more accurate prediction we want to incorporate also tensor perturbations that originate from vacuum fluctuations.

## Combining vacuum and thermal fluctuations

We start again from eq. (6.2), with the thermal source term on the right-hand side, and write $\vartheta_\lambda(\tau, \mathbf{k})$ as the sum of short $\vartheta_<$, and large $\vartheta_>$ distance fluctuations, as in the stochastic approach in sec. 3.3. The evolution of the slowly varying large-distance fluctuations is then described by

$$(\partial_\tau^2 + 2\mathcal{H}\partial_\tau + k^2)\vartheta_>(\tau, \mathbf{k}) = (\rho_{\rm T} + \rho_{\rm Q})(\tau, \mathbf{k}) \ , \tag{6.13}$$

where $\rho_{\rm Q}$ is defined in eq. (3.99). Taking already into account canonical normalization (see discussion above eq. (3.92)), its autocorrelator is given by

$$\langle \rho_{\rm Q}(\tau_1, \mathbf{k}_1)\, \rho_{\rm Q}(\tau_2, \mathbf{k}_2)\rangle \overset{(3.103)}{=} 32\pi G \delta(\mathbf{k}_1 + \mathbf{k}_2)\, \mathcal{F}_k(\tau_1)\mathcal{F}_k^*(\tau_2) \ , \tag{6.14}$$

where $\mathcal{F}_k$ can be taken from eq. (3.101), since vacuum fluctuations freeze out once they exit the horizon, and this happens deep in the slow-roll regime of inflation. Therefore eq. (6.14) is evaluated at $\tau_{1,2} \in \{-\infty, \tau_{1,2}^*\}$, where $\tau_{1,2}^*$ denotes the moment just after horizon exit.

Since the mixed noise correlator is suppressed by higher powers of $G$, with the result for the thermal autocorrelator

$$\langle \rho_{\rm T}(\tau_1, \mathbf{k}_1)\, \rho_{\rm T}(\tau_2, \mathbf{k}_2)\rangle \underset{(6.10)}{\overset{(6.2)}{=}} (16\pi G)^2 2T\eta\, \delta(\tau_1 - \tau_2)\delta(\mathbf{k}_1 + \mathbf{k}_2) \ , \tag{6.15}$$

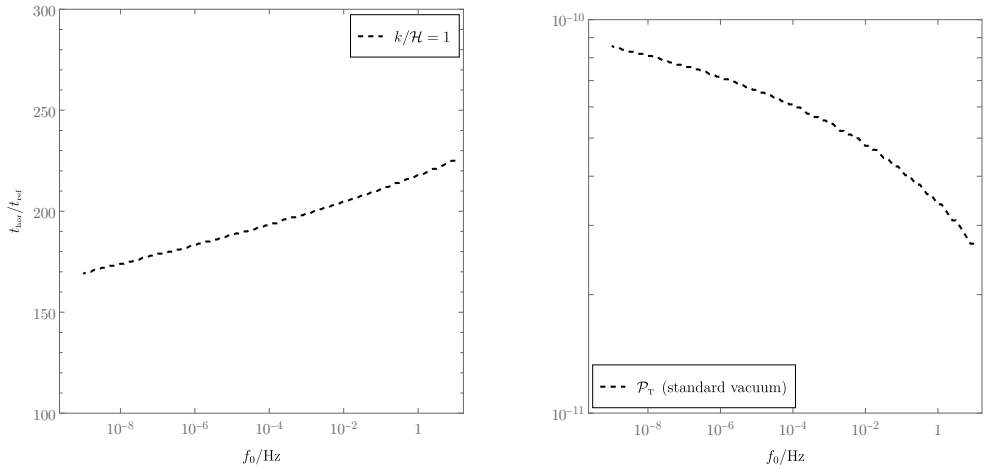


(a) (b)

Figure 6.2: Vacuum contribution to the primordial power spectrum of tensor perturbations from inflation, cf. the first term in eq. (6.16): (a) time of horizon exit, (b) corresponding value of eq. (3.92). The present figure reproduces fig. 4 of [4].

we can write the result for the power spectrum of tensor perturbations from inflation,

$$\mathcal{P}_{\rm T}(k) = \frac{64\pi G k^3}{2\pi^2}\left\{\left|\int_{-\infty}^{\tau_e} \mathrm{d}\tau_i\, G_{\rm R}(\tau_e,\tau_i,k)\,\mathcal{F}_k(\tau_i)\right|^2 + 32\pi G\int_{-\infty}^{\tau_e}\mathrm{d}\tau_i\, G_{\rm R}^2(\tau_e,\tau_i,k)\,T(\tau_i)\eta(\tau_i)\right\}\,. \quad (6.16)$$

While for each mode $k$ the first term gets integrated only up to the specific moment of horizon exit $\tau_{*k}$, the source in the second term never switches off, such that thermal fluctuations at all scales continue contributing until the end of the inflationary period $\tau_e$, compensating partially for the additional $1/m_{\rm pl}^2$ suppression. We choose $\tau_e$ as a moment when all momenta affecting cosmological predictions are safely outside the horizon (see discussion below eq. (6.29)).

As discussed around eq. (3.116), the integrand for the vacuum contribution can be simplified in the slow-roll regime, obtaining again eq. (3.92). This is not the case for the thermal contribution, since $T\eta$ is a complicated function of time, and in particular it peaks at a late time, long after the breakdown of the slow-roll regime. Examples of the two contributions to eq. (6.16) are shown in figs. 6.2 and 6.3, respectively.

## From the primordial power spectrum to today's energy density

In coordinate space, the energy density carried by gravitational waves today ($\tau_0$) is [118]

$$e_{\rm GW}(\tau_0) = \frac{\langle h'_{ij}(\tau_0,\mathbf{x})h'_{ij}(\tau_0,\mathbf{x})\rangle}{32\pi G\,a^2(t)}\,. \quad (6.17)$$

The average brackets on the right-hand side denote here simultaneously an average over vacuum and thermal states. Transforming to co-moving Fourier frame in the spatial direction, and again to a helicity basis (see sec. 3.3), the power spectrum is

$$\frac{\mathrm{d}e_{\rm GW}(\tau_0)}{\mathrm{d}\log k} = 2\frac{k^3}{2\pi^2}\frac{\langle\vartheta'_\lambda(\tau_0,k)\vartheta'_\lambda(\tau_0,k)\rangle}{32\pi G\,a^2(\tau_0)}\,. \quad (6.18)$$

Tensor perturbations today can be written as functionals of their initial values, taken to be at

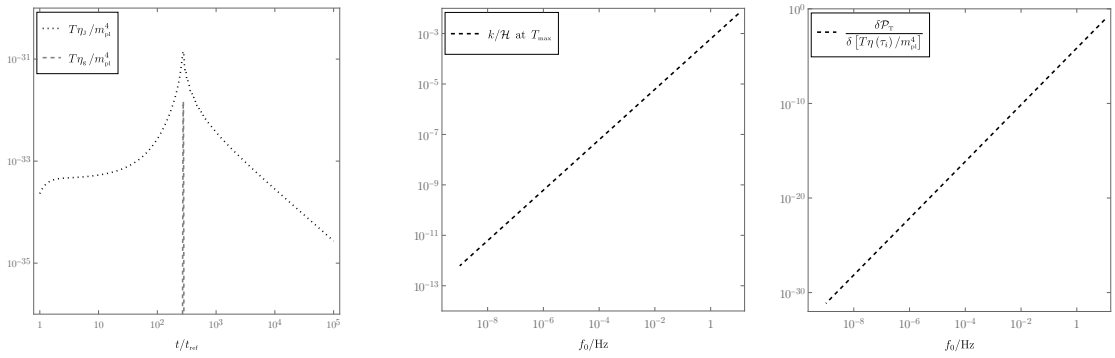


(a) (b) (c)

Figure 6.3: Thermal contribution to the primordial power spectrum of tensor perturbations from inflation for $\Lambda_{\rm IR} = 0.2\,\text{GeV}$: (a) evolution of the shear viscosities in time, (b) all modes in the considered frequency range are outside the horizon when $T\eta$ peaks, (c) the Green's function entering the second term in eq. (6.16). The present figure reproduces fig. 5 of [4].

the end of inflation (see discussion below eq. (6.16)),

$$\vartheta_\lambda(\tau_0,k) \equiv X(\tau_0,\tau_e,k)\,\vartheta_\lambda(\tau_e,k)\ , \qquad X(\tau_e,\tau_e,k) \equiv 1\ , \quad \partial_{\tau_0} X(\tau_0,\tau_e,k)|_{\tau_e=\tau_0} = 0\ . \tag{6.19}$$

The evolution equation (6.2) at $\tau > \tau_e$ is therefore in terms of $X$,[47]

$$(\partial_\tau^2 + 2\mathcal{H}\partial_\tau + k^2) X(\tau,\tau_e,k) = 0\ , \tag{6.20}$$

and the time derivative in eq. (6.18) acts only on $X$. The observable $\Omega_{\rm GW}$ can so be expressed in terms of the primordial power spectrum of tensor perturbations from inflation (cf. eq. (6.16)),

$$\Omega_{\rm GW}(k) \equiv \underbrace{\frac{[\partial_{\tau_0} X(\tau_0,\tau_e,k)]^2}{12\mathcal{H}_0^2}}_{\equiv \mathcal{T}_{\rm T}(k)} \mathcal{P}_{\rm T}(k)\ , \tag{6.21}$$

where $\mathcal{H}$ is defined in accordance to $H_0$ given in eq. (3.139). The transfer function $\mathcal{T}_{\rm T}(k)$ encodes the evolution of tensor perturbations from the end of inflation until today.

To solve eq. (6.20), it is convenient to change variables and reason in terms of the ratio $k/\mathcal{H}$ [121],

$$\partial_u^2 X + \frac{2\partial_u X}{k/\mathcal{H}} + X = 0\ , \qquad u \equiv k\tau > u_e\ . \tag{6.22}$$

Outside the horizon, $k \ll \mathcal{H}$, the perturbations remain close to the initial value at $u_e$,

$$\partial_u X \overset{k\ll\mathcal{H}}{\approx} 0 \quad \Rightarrow \quad X \approx 1\ . \tag{6.23}$$

After inflation the expansion of the universe starts decelerating, $\mathcal{H}' < 0$ (cf. eq. (2.112)), and at some point $k \sim \mathcal{H}$ again. Modes that correspond to frequencies in the LISA window re-enter the horizon deep in the radiation-dominated epoch. Therefore, from now on, we denote by $\tau_e$ the end of the inflationary epoch, i.e. the moment where the dominant component of the energy density is given by radiation. Then the heat bath is already represented by the full Standard Model, and described by the thermodynamic equation of state,

$$c_s^2 \equiv \frac{\mathrm{d}p_r}{\mathrm{d}e_r} = \frac{\partial_T p_r}{\partial_T e_r} = \frac{s_r}{c_r}\ , \tag{6.24}$$

[47] In principle, in the radiation-dominated era tensor modes are damped by freely streaming neutrinos [119]. However, this effect is visible only at frequencies $f_0 \lesssim 10^{-9}$Hz below the LISA window [120].

where the energy density, pressure, entropy density and heat capacity satisfy the standard relations

$$e_r + p_r = T s_r \ , \quad s_r = \partial_T p_r \ , \quad c_r \equiv \partial_T e_r = T \partial_T s_r \ . \tag{6.25}$$

Once $k \gtrsim \mathcal{H}$, we solve the full equation (6.22) for $X$. Using the identities in eq. (6.25) and going back to the time coordinate for a moment, the background evolution equation (2.114) for a heat bath composed only of radiation can be written as the conservation of entropy,

$$e_r' = -3\mathcal{H}(e_r + p_r) \quad \Leftrightarrow \quad s_r' + 3\mathcal{H} s_r = 0 \quad \Leftrightarrow \quad (s_r\, a^3)' = 0 \ . \tag{6.26}$$

Denoting $a_e \equiv a[T(\tau_e)]$ and $s_e \equiv s_r[T(\tau_e)]$, the Hubble rate in eq. (6.20) is more naturally given as a function of the temperature,

$$a(T) = a_e \left(\frac{s_e}{s_r(T)}\right)^{\frac{1}{3}} \quad \Rightarrow \quad \mathcal{H}(T) = \sqrt{\frac{8\pi e_r(T)}{3m_{\rm pl}^2}}\, a_e \left(\frac{s_e}{s_r(T)}\right)^{\frac{1}{3}} \ . \tag{6.27}$$

To track the evolution of $X$ in the radiation-dominated epoch it is therefore helpful to change integration variable from $\tau$, or $u$, to

$$z \equiv \log\left(\frac{T_e}{T}\right) \ , \tag{6.28}$$

such that we solve the system of coupled equations that follows from eqs. (6.22) and (6.26),

$$\begin{cases} \partial_u^2 X + \frac{2\partial_u X}{k/\mathcal{H}} + X = 0 \ , \\ \partial_u z = -\frac{\partial_u T}{T} \overset{(6.26)}{=} \frac{3c_s^2}{k/\mathcal{H}} \ , \end{cases} \tag{6.29}$$

with the initial conditions $X|_{T_e} = 1$ and $\partial_z X|_{T_e} = 0$. To track the evolution of $k/\mathcal{H}$ in terms of $f_0$ and $T$, we can use eqs. (3.140) and (6.27),

$$\frac{k}{\mathcal{H}} = 2\pi f_0 \sqrt{\frac{3m_{\rm pl}^2}{8\pi e_r}} \frac{a_0}{a_e} \left(\frac{s_r}{s_e}\right)^{\frac{1}{3}} = f_0 m_{\rm pl} \sqrt{\frac{3\pi}{2e_r}} \left(\frac{s_r}{s_0}\right)^{\frac{1}{3}} = \underbrace{\sqrt{\frac{3\pi}{2}} \frac{1}{sT_0}}_{=6.0837\times 10^{-12}} \frac{f_0}{\rm Hz} \frac{m_{\rm pl}/T}{\sqrt{e_r/T^4}} \left(\frac{s_r/T^3}{s_0/T_0^3}\right)^{\frac{1}{3}} \ . \tag{6.30}$$

To compute the prefactor we have restored physical units $(T_0 s)^{-1} = \frac{(\hbar/{\rm eVs})}{(T_0/{\rm K})(k_{\rm B}\,{\rm K/eV})}$. The temperature evolution of $s_r/T^3$, $e_r/T^4$ and $c_s^2$ has been studied in [122], and is available online at [123].

Using eq. (6.30) we can now follow how a mode $f_0$ starts outside the horizon at $T_e$, re-enters at some point, and finally goes over into a highly oscillatory regime, once $k \gg \mathcal{H}$, so that the last term in eq. (6.22) dominates. This asymptotic solution for modes deep inside the horizon can be found analytically,

$$\partial_u^2 X + X \overset{k\gg\mathcal{H}}{\approx} 0 \quad \Rightarrow \quad X \approx C\, \frac{a_m}{a} \sin(u - u_m + \gamma) \ , \tag{6.31}$$

where $C$ and $\gamma$ are integration constants,

$$\gamma = \arctan\left[\left(\frac{\mathcal{H}}{k} + \frac{\partial_u X}{X}\right)^{-1}\right]_{u=u_m} \ , \qquad C = \frac{X(u_m)}{\sin\gamma} \ , \tag{6.32}$$

and $u_m$ denotes the moment where the solutions of eqs. (6.29) and (6.31) match. Concretely, we choose $u_m$ such that $k/\mathcal{H} = 30$, resulting in $30/(2\pi) \sim 5$ oscillations.

To find the transfer function in eq. (6.21), $X$ is evaluated at $u_0 \equiv k\tau_0$, when all modes satisfy $k \gg \mathcal{H}$. We can thus insert the asymptotic solution (6.31),

$$\mathcal{T}_{\rm T} \approx \frac{C^2}{12} \left(\frac{k}{a_0 H_0}\right)^2 \left(\frac{s_0}{s_m}\right)^{\frac{2}{3}} \cos^2(u_0 - u_m + \gamma) \ , \tag{6.33}$$

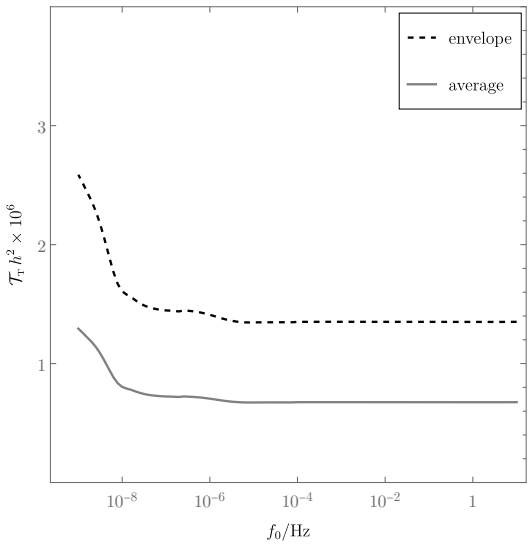


Figure 6.4: Average (solid line) and envelope (dashed line) of the transfer function from eq. (6.34). The present figure reproduces fig. 1 of [4].

but we need to solve the whole dynamics anyway to fix $C$ and $\gamma$.[48] Restoring again physical units,

$$\mathcal{T}_{\rm T} h^2 \approx \frac{C^2}{12}\left(\frac{f_0}{\rm Hz}\right)^2 \underbrace{\left[\frac{2\pi(hc/{\rm m}/H_0)(T_0/{\rm K})(k_{\rm B}{\rm K/eV})}{10^9(c{\rm s/m})}\right]^2}_{[4.5535\times10^5]^2} \left(\frac{\rm GeV}{T_m}\right)^2 \left(\frac{s_0/T_0^3}{s_m/T_m^3}\right)^{\frac{2}{3}} \cos^2(u_0 - u_m + \gamma) \ . \tag{6.34}$$

The envelope and average over the rapid oscillations in eq. (6.34) are shown in fig. 6.4 for frequencies around the LISA window. The general shape can be understood with [122] and [124]: small frequency modes, $f_0 \sim 10^{-8}\,$Hz, re-enter the horizon later, at temperatures $T \lesssim T_{\rm QCD} \sim 160\,$MeV. They are therefore sensitive to the QCD crossover, which affects the thermodynamics of the Standard Model heat bath [124]. In particular, in that $T$ range, $3c_s^2 \neq 1$ enters eq. (6.29), and $s_r/T^3$ and $e_r/T^4$ enter eq. (6.30), modifying the dynamics in a non-trivial way and contributing to the enhancement of the amplitude $C$, visible in fig. 6.4. In a similar way, the crossing of the mass thresholds at some higher temperatures [124], results in the smooth features at $f_0 \sim 10^{-6}\,$Hz.

To estimate an upper bound for the resulting gravitational wave signal $\Omega_{\rm GW}h^2$, we multiply $\mathcal{T}_{\rm T}h^2 \sim 10^{-6}$ from fig. 6.4 with the result of fig. 6.2 for vacuum fluctuations, and with the results of figs. 6.3a and 6.3c for thermal fluctuations. Inserting first only the numerical values of model-independent quantities we obtain

$$\Omega_{\rm GW}h^2 \sim 10^{-6} \times \Bigg[ \underbrace{\frac{16}{\pi}\left(\frac{H_*}{m_{\rm pl}}\right)^2}_{\rm vacuum} + \underbrace{\left(\frac{f_0}{10{\rm Hz}}\right)^3 \times \left(\frac{T\eta}{m_{\rm pl}^4}\right)_{\rm max}}_{\rm thermal} \Bigg] \ . \tag{6.35}$$

For the potential and the parameters $m$ and $f_a$ chosen here,[49] the amplitude of the vacuum contribution is roughly $\Omega_{\rm GW}h^2|_{\rm vac} \sim 10^{-6} \times 16(H_*/m_{\rm pl})^2/\pi \sim 10^{-16}$, which amounts to a signal that

[48] Note that, even if $C$, $u_m$ and $s_m$ depend on the matching point, this is not the case for final results, as long as $u_m$ is chosen after $k/\mathcal{H} \gtrsim 20$.

[49] These parameters are fixed by the CMB constraints, see sec. 5.1. The parameter $\Lambda_{\rm IR}$ does not affect the Hubble rate in this regime, since the vacuum energy of the inflaton field is the dominant contribution.

will not be seen by LISA: $\Omega_{\rm GW}h^2|_{\rm vac} < \Omega_{\rm GW}^{\rm LISA}h^2 \sim 10^{-13}$. For the thermal contributions, we note that the maximal value of $T\eta$ depends on the confinement scale $\Lambda_{\rm IR}$ of the heat bath.

The example shown in fig. 6.3a for $\Lambda_{\rm IR} = 0.2\,\text{GeV} \sim 10^{-20} m_{\rm pl}$ yields $T\eta/m_{\rm pl}^4 \sim 10^{-31}$, i.e. an amplitude far below the LISA sensitivity [44]. Moving $\Lambda_{\rm IR}$ to larger values increases the maximal temperature considerably [5], however, the result for the shear viscosity presented here should then be revisited. Increasing the coefficient of $f_0^3$ it may happen that the peak amplitude of the gravitational wave spectrum breaks the upper bound given by $N_{\rm eff}$ (cf. p. 35). However, this occurs only at $T_{\rm max} \approx 2\times 10^{17}$ GeV [125, 126]. With a larger coefficient the power spectrum could move close to the observation threshold of the LISA or Einstein Telescope (ET) window, particularly if the peak in $T\eta$ is broad.

## 6.2 During reheating

At some point after the end of inflation, when the expansion of the universe turns to decelerated, plasma reactions become fast compared with the dilution caused by the expansion, $\alpha^2 T > H$. In this regime, computations can be carried out in a local Minkowskian frame. As we therefore move from general relativity to particle physics, to facilitate the comparison with the literature we also change the convention for the signature of the Minkowski metric into

$$\eta = \text{diag}(+,-,-,-)\ . \tag{6.36}$$

To distinguish 4-vectors in the local frame we introduce curly capital letters $\mathcal{X} \equiv (t, \mathbf{x})$.

In a local Minkowskian frame, the production rate of the energy density carried by gravitational radiation can be expressed as [125, 126]

$$\frac{\mathrm{d}e_{\rm GW}}{\mathrm{d}t\,\mathrm{d}\ln k} \;=\; \frac{k^4 \dot{f}_{\rm GW}}{\pi^2}\ , \tag{6.37}$$

where $f_{\rm GW}$ is the polarization-averaged phase-space density of gravitons, and the dot stands for a time derivative. On general grounds [127], the evolution equation for $f_{\rm GW}$ takes the form

$$\dot{f}_{\rm GW} \;=\; \Gamma(k)\,\left[n_{\rm B}(k) - f_{\rm GW}\right] + \mathcal{O}(m_{\rm pl}^{-4})\ , \tag{6.38}$$

where $n_{\rm B}(k) \equiv 1/(e^{k/T}-1)$ is the Bose distribution, and $m_{\rm pl} \approx 1.221\times 10^{19}$ GeV is the Planck mass. In practice, $f_{\rm GW} \ll n_{\rm B}(k)$, so the right-hand side can be approximated as $\Gamma(k)\,n_{\rm B}(k)$.

The dynamical information about the processes taking place is encoded in the interaction rate $\Gamma(k)$, which in turn can be expressed as [126]

$$\Gamma(k) = \frac{4\pi \mathbb{L}^{\alpha\beta;\mu\nu}\,\mathrm{Im}\,G^{\rm R}_{\alpha\beta;\mu\nu}(k,k)}{k\,m_{\rm pl}^2}\ , \tag{6.39}$$

where $G^{\rm R}_{\alpha\beta;\mu\nu}(\omega,k)$ is the retarded correlator related to the energy-momentum tensor $T_{\mu\nu}$,

$$G^{\rm R}_{\alpha\beta;\mu\nu}(\omega,k) \;\equiv\; i\int_{\mathcal{X}} e^{i\mathcal{K}\cdot\mathcal{X}}\theta(t)\left\langle\left[T_{\alpha\beta}(\mathcal{X})\,,\,T_{\mu\nu}(0)\right]\right\rangle_{\rm T}\ ,\quad \mathcal{K}\cdot\mathcal{X} \equiv \omega t - \mathbf{k}\cdot\mathbf{x}\ , \tag{6.40}$$

and $\langle ...\rangle_{\rm T}$ denotes a thermal average. In practice, it is sometimes convenient to choose the special frame in which $\mathbf{k} = k\,\mathbf{e}_z$, whereby rotational symmetry implies that[50]

$$\mathbb{L}^{\alpha\beta;\mu\nu}G^{\rm R}_{\alpha\beta;\mu\nu} \;\overset{D=4}{=}\; 4\,G^{\rm R}_{xy;xy}\big|_{\mathbf{k}=k\,\mathbf{e}_z}\ . \tag{6.41}$$

[50] Physically, there are two transverse-traceless polarizations, and if we choose the one in non-diagonal components as a representative, *viz.* $(T_{xy}+T_{yx})/\sqrt{2}$, then the equality $T_{xy} = T_{yx}$ leads to the additional factor $(\sqrt{2})^2 = 2$.

The method to compute $\mathrm{Im}\, G^{\mathrm{R}}_{xy;xy}$ depends on the momentum range considered. For very small momenta, we find ourselves in the so-called hydrodynamic domain. Then $\mathrm{Im}\, G^{\mathrm{R}}_{xy;xy}$ evaluates to $\eta\omega$, where $\eta$ is the shear viscosity [125]. On the other hand, for typical thermal momenta, $k \sim \pi T$, elementary gauge bosons and axions can be resolved as quasi-particles. Then we are faced with a Boltzmann type of a computation, which is outlined here and performed in appendix C.

## Hydrodynamic regime

At low frequencies, elementary particles cannot be resolved, and the relevant degrees of freedom for the gauge plasma are hydrodynamic fluctuations. In the hydrodynamic domain, the traceless part of the energy-momentum tensor is then given by

$$T_{\mu\nu} \supset \partial_\mu\varphi\,\partial_\nu\varphi + T^{\mathrm{r}}_{\mu\nu} \;, \tag{6.42}$$

where $T^{\mathrm{r}}_{\mu\nu}$ is the contribution of radiation. The interaction Lagrangian is therefore

$$\mathcal{L} \supset -\frac{\varphi}{f_a}\chi + \hat{h}^{\mu\nu}(\partial_\mu\varphi\,\partial_\nu\varphi + T^{\mathrm{r}}_{\mu\nu}) \;. \tag{6.43}$$

In order to compute the contribution of $\varphi$ to eq. (6.41), we make use of the real-time formalism of thermal field theory. In the so-called Keldysh $(r/a)$ basis (cf. e.g. [57, p.131]) the propagator of $\varphi$ becomes a matrix,

$$\begin{pmatrix} G_{rr} & G_{ra} \\ G_{ar} & G_{aa} \end{pmatrix} = \begin{pmatrix} \Delta & -i\Pi^{\mathrm{R}} \\ -i\Pi^{\mathrm{A}} & 0 \end{pmatrix} . \tag{6.44}$$

All components are determined by the retarded propagator that follows from eq. (4.22),

$$\Pi^{\mathrm{R}}(\omega,\mathbf{p}) = \frac{1}{-\omega^2+\epsilon_p^2 - i\omega\Upsilon} \;, \quad \epsilon_p^2 \equiv p^2+m^2 \;, \tag{6.45}$$

with $m$ the inflaton mass, using the relations

$$\Delta = [1+2n_{\mathrm{B}}(\omega)]\rho \;, \quad \rho = \mathrm{Im}\,\Pi^{\mathrm{R}} = \frac{\omega\Upsilon}{(\omega^2-\epsilon_p^2)^2+\omega^2\Upsilon^2} \;, \quad \Pi^{\mathrm{A}} = (\Pi^{\mathrm{R}})^* \;. \tag{6.46}$$

The vertices are obtained by substituting $\varphi_1 = \varphi_r + \varphi_a/2$ and $\varphi_2 = \varphi_r - \varphi_a/2$ in the Lagrangian $\mathcal{L}(\varphi_1) - \mathcal{L}(\varphi_2)$,

$$h_1T_1 - h_2T_2 = \left(h_r+\frac{h_a}{2}\right)\left(T_r+\frac{T_a}{2}\right) - \left(h_r-\frac{h_a}{2}\right)\left(T_r-\frac{T_a}{2}\right) = h_aT_r + h_rT_a \;, \tag{6.47}$$

where in our chosen frame

$$T_r = \varphi_{r,x}\varphi_{r,y} + \frac{\varphi_{a,x}\varphi_{a,y}}{4} \;, \quad T_a = \varphi_{a,x}\varphi_{r,y} + \varphi_{r,x}\varphi_{a,y} \;. \tag{6.48}$$

We can now compute the retarded correlator needed in eq. (6.39). Given that the propagator $G_{aa}$ vanishes (cf. eq. (6.44)), the contribution of $\varphi$ originates from

$$-i\, G^{\mathrm{R}}_{xy;xy}\big|_{\mathbf{k}=k\,\mathbf{e}_z} = \langle T_rT_a\rangle = \langle(\varphi_{r,x}\varphi_{r,y})(\varphi_{a,x}\varphi_{r,y}+\varphi_{r,x}\varphi_{a,y})\rangle \;. \tag{6.49}$$

Wick-contracting and going over to momentum space with eqs. (6.45) and (6.46) yields

$$\langle(\varphi_{r,x}\varphi_{r,y})(\varphi_{a,x}\varphi_{r,y}+\varphi_{r,x}\varphi_{a,y})\rangle \overset{\mathbf{x}\to\mathbf{k}}{\longrightarrow} \Delta_{,xx}\Pi^{\mathrm{R}}_{,yy} + 2\Delta_{,xy}\Pi^{\mathrm{R}}_{,xy} + \Delta_{,yy}\Pi^{\mathrm{R}}_{,xx} \;, \tag{6.50}$$

such that, taking the imaginary part and symmetrizing in $\mathcal{P}_1 \leftrightarrow \mathcal{P}_2$, eq. (6.49) becomes

$$\begin{aligned}\mathrm{Im}\, G^{\mathrm{R}}_{xy;xy}(\omega,k)\big|_{\mathbf{k}=k\,\mathbf{e}_z} \;=\; & \int_{\mathcal{P}_1,\mathcal{P}_2} \delta(\mathcal{K}-\mathcal{P}_1-\mathcal{P}_2)\,[1+n_{\mathrm{B}}(\omega_1)+n_{\mathrm{B}}(\omega_2)] \\ & \times\{\rho_{,x,x}(\mathcal{P}_1)\rho_{,y,y}(\mathcal{P}_2)+\rho_{,y,y}(\mathcal{P}_1)\rho_{,x,x}(\mathcal{P}_2)+2\rho_{,x,y}(\mathcal{P}_1)\rho_{,y,x}(\mathcal{P}_2)\}\;,\end{aligned} \tag{6.51}$$

where $\int_{\mathcal{P}}\delta(\mathcal{P})\equiv 1$ and $\mathcal{P}_a\equiv(\omega_a,\mathbf{p}_a)$. The Bose distributions can be factorized,

$$1+n_{\mathrm{B}}(\omega_1)+n_{\mathrm{B}}(\omega_2) = n_{\mathrm{B}}^{-1}(\omega)n_{\mathrm{B}}(\omega_1)n_{\mathrm{B}}(\omega_2)\;. \tag{6.52}$$

We use the $\delta$-distribution to integrate over $\mathcal{P}_2$, and the identity $\rho(\mathcal{P})_{,x} = ip_x\rho(\mathcal{P})$, obtaining

$$\begin{aligned}(6.51) &= n_{\mathrm{B}}^{-1}(\omega)\int_{\mathcal{P}_1} n_{\mathrm{B}}(\omega_1)n_{\mathrm{B}}(\omega-\omega_1)\;4p_x^2p_y^2\;\rho(\mathcal{P}_1)\;\rho(\mathcal{K}-\mathcal{P}_1) \\ &= n_{\mathrm{B}}^{-1}(\omega)\int\frac{\mathrm{d}^3p}{(2\pi)^3}\,4p_x^2p_y^2\int_{-\infty}^{\infty}\frac{d\omega_1}{2\pi}\;n_{\mathrm{B}}(\omega_1)n_{\mathrm{B}}(\omega-\omega_1) \\ &\qquad\times\frac{\omega_1\Upsilon}{(\omega_1^2-\epsilon_p^2)^2+\omega_1^2\Upsilon^2}\;\frac{(\omega-\omega_1)\Upsilon}{[(\omega-\omega_1)^2-\epsilon_{pk}^2]^2+(\omega-\omega_1)^2\Upsilon^2}\;,\end{aligned} \tag{6.53}$$

where $\mathbf{p}\equiv\mathbf{p}_1$ and $\epsilon_{pk}\equiv(\mathbf{p}-\mathbf{k})^2+m^2$. The $\omega_1$-dependence in the spectral functions can be partial-fractioned, as

$$\frac{4\tilde\epsilon_p\times\omega_1\Upsilon}{(\omega_1^2-\epsilon_p^2)^2+\omega_1^2\Upsilon^2} = \frac{\Upsilon}{(\omega_1-\tilde\epsilon_p)^2+\frac{\Upsilon^2}{4}}-\frac{\Upsilon}{(\omega_1+\tilde\epsilon_p)^2+\frac{\Upsilon^2}{4}}\;, \tag{6.54}$$

$$\frac{4\tilde\epsilon_{pk}\times(\omega-\omega_1)\Upsilon}{[(\omega-\omega_1)^2-\epsilon_{pk}^2]^2+(\omega-\omega_1)^2\Upsilon^2} = \frac{\Upsilon}{(\omega-\omega_1-\tilde\epsilon_{pk})^2+\frac{\Upsilon^2}{4}}-\frac{\Upsilon}{(\omega-\omega_1+\tilde\epsilon_{pk})^2+\frac{\Upsilon^2}{4}}\;, \tag{6.55}$$

having introduced the variables $\tilde\epsilon_p^2\equiv\epsilon_p^2-\Upsilon^2/4$ and $\tilde\epsilon_{pk}$ (defined analogously).

As a next step, we integrate over $\omega_1$ with the residue theorem. The poles are given by

- the poles of the Bose distribution $n_{\mathrm{B}}(\omega_1)$ at $\omega_1 = i\omega_n\equiv i2\pi nT$, $n\in\mathbb{Z}$. The poles at $\omega_1=0$ and $\omega-\omega_1=0$ (the latter from $n_{\mathrm{B}}(\omega-\omega_1)$) are however lifted by the spectral function contributions.
- the poles of the spectral functions $\rho$, respectively $\omega_1=\pm\omega_\pm(p)$ and $\omega_1=\omega\pm\omega_\pm(pk)$, with $\omega_\pm(p)\equiv\pm\tilde\epsilon_p+i\Upsilon/2$.

Choosing to close the contour in the upper half-plane, the poles contributing to the integral are $\omega_1\in\{i\omega_n,\;\omega+i\omega_n,\;\omega_\pm(p),\;\omega+\omega_\pm(pk)\}$, with $n\geq 1$. We therefore write

$$(6.53) = n_{\mathrm{B}}^{-1}(\omega)\int\frac{\mathrm{d}^3p}{(2\pi)^3}\,\frac{p_x^2p_y^2}{4\tilde\epsilon_p\tilde\epsilon_{pk}}\;i\sum_{\substack{n\geq1\\ \sigma=\pm}}\Big[I_{n_{\mathrm{B}}}|_{i\omega_n}+I_{n_{\mathrm{B}}}|_{\omega+i\omega_n}+I_\rho|_{\omega_\sigma(p)}+I_\rho|_{\omega+\omega_\sigma(pk)}\Big]\;, \tag{6.56}$$

and evaluate the single contributions separately. From $n_{\mathrm{B}}(\omega_1)$ we obtain

$$\begin{aligned}I_{n_{\mathrm{B}}}|_{i\omega_n} = 2in_{\mathrm{B}}(\omega)\Upsilon^2T\;\mathrm{Im}&\left[(\tilde\epsilon_p+i\omega_n)^2+\frac{\Upsilon^2}{4}\right]^{-1} \\ &\times\left[\frac{1}{(\tilde\epsilon_{pk}-\omega+i\omega_n)^2+\frac{\Upsilon^2}{4}}-\frac{1}{(\tilde\epsilon_{pk}+\omega-i\omega_n)^2+\frac{\Upsilon^2}{4}}\right]\;,\end{aligned} \tag{6.57}$$

while $n_{\mathrm{B}}(\omega-\omega_1)$ yields

$$\begin{aligned}I_{n_{\mathrm{B}}}|_{\omega+i\omega_n} = 2in_{\mathrm{B}}(\omega)\Upsilon^2T\;\mathrm{Im}&\left[(\tilde\epsilon_{pk}+i\omega_n)^2+\frac{\Upsilon^2}{4}\right]^{-1} \\ &\times\left[\frac{1}{(\tilde\epsilon_p-\omega-i\omega_n)^2+\frac{\Upsilon^2}{4}}-\frac{1}{(\tilde\epsilon_p+\omega+i\omega_n)^2+\frac{\Upsilon^2}{4}}\right]\;.\end{aligned} \tag{6.58}$$

The contributions from the spectral functions are given by

$$I_\rho|_{\omega_+(p)} = i\; n_{\rm B}(\tilde\epsilon_p + i\Upsilon/2)\,[\;1 + n_{\rm B}(\tilde\epsilon_p - \omega + i\Upsilon/2)\;]\;\Upsilon \times\left[\frac{1}{\left(\omega - \tilde\epsilon_p - \tilde\epsilon_{pk} - i\frac{\Upsilon}{2}\right)^2 + \frac{\Upsilon^2}{4}} - \frac{1}{\left(\omega - \tilde\epsilon_p + \tilde\epsilon_{pk} - i\frac{\Upsilon}{2}\right)^2 + \frac{\Upsilon^2}{4}}\right], \tag{6.59}$$

$$I_\rho|_{\omega_-(p)} = -i\; n_{\rm B}(\tilde\epsilon_p + \omega - i\Upsilon/2)\,[\;1 + n_{\rm B}(\tilde\epsilon_p - i\Upsilon/2)\;]\;\Upsilon \times\left[\frac{1}{\left(\omega + \tilde\epsilon_p - \tilde\epsilon_{pk} - i\frac{\Upsilon}{2}\right)^2 + \frac{\Upsilon^2}{4}} - \frac{1}{\left(\omega + \tilde\epsilon_p + \tilde\epsilon_{pk} - i\frac{\Upsilon}{2}\right)^2 + \frac{\Upsilon^2}{4}}\right], \tag{6.60}$$

$$I_\rho|_{\omega+\omega_+(pk)} = -i\; n_{\rm B}(\tilde\epsilon_{pk} + \omega + i\Upsilon/2)\,[\;1 + n_{\rm B}(\tilde\epsilon_{pk} + i\Upsilon/2)\;]\;\Upsilon \times\left[\frac{1}{\left(\omega - \tilde\epsilon_p + \tilde\epsilon_{pk} + i\frac{\Upsilon}{2}\right)^2 + \frac{\Upsilon^2}{4}} - \frac{1}{\left(\omega + \tilde\epsilon_p + \tilde\epsilon_{pk} + i\frac{\Upsilon}{2}\right)^2 + \frac{\Upsilon^2}{4}}\right], \tag{6.61}$$

$$I_\rho|_{\omega+\omega_-(pk)} = i\; n_{\rm B}(\tilde\epsilon_{pk} - i\Upsilon/2)\,[\;1 + n_{\rm B}(\tilde\epsilon_{pk} - \omega - i\Upsilon/2)\;]\;\Upsilon \times\left[\frac{1}{\left(\omega - \tilde\epsilon_p - \tilde\epsilon_{pk} + i\frac{\Upsilon}{2}\right)^2 + \frac{\Upsilon^2}{4}} - \frac{1}{\left(\omega + \tilde\epsilon_p - \tilde\epsilon_{pk} + i\frac{\Upsilon}{2}\right)^2 + \frac{\Upsilon^2}{4}}\right]. \tag{6.62}$$

Even if the result can be integrated numerically, it is helpful to put it in a more transparent form, by considering

$$\omega, k, \Upsilon \ll \epsilon_p \sim \pi T\ . \tag{6.63}$$

The residues $I_{n_{\rm B}}$ in eqs. (6.57) and (6.58) are parametrically suppressed by the prefactor. The remaining contributions (6.59)–(6.62) can be simplified by approximating

$$\tilde\epsilon_p \approx \epsilon_p\ , \qquad \tilde\epsilon_{pk} \approx \epsilon_p - v_z k\ , \qquad v_z \equiv \frac{p_z}{\epsilon_p}\ , \tag{6.64}$$

such that all Bose-distributions evaluate to $\sim n_{\rm B}(\epsilon_p)$. The sum of the residues in the integrand of eq. (6.56) yields

$$\sum_{\substack{n\geq 1\\ \sigma=\pm}} \Big[ I_{n_{\rm B}}|_{i\omega_n} + I_{n_{\rm B}}|_{\omega+i\omega_n} + I_\rho|_{\omega_\sigma(p)} + I_\rho|_{\omega+\omega_\sigma(pk)}\Big] \tag{6.65}$$

$$\overset{\omega,k,\Upsilon\ll\pi T}{\approx}\ -i\; n_{\rm B}(\epsilon_p)[1 + n_{\rm B}(\epsilon_p)]\;\Upsilon\; 2\,{\rm Re}\left[\frac{1}{\left(v_z k - \omega + i\frac{\Upsilon}{2}\right)^2 + \frac{\Upsilon^2}{4}} + \frac{1}{\left(v_z k + \omega + i\frac{\Upsilon}{2}\right)^2 + \frac{\Upsilon^2}{4}}\right].$$

Inserting into eq. (6.56) and substituting $p_z \to -p_z$ in the second term yields

$$\begin{aligned}{\rm Im}\, G^{\rm R}_{xy;xy}(\omega,k) &\approx n_{\rm B}^{-1}(\omega)\Upsilon \int \frac{{\rm d}^3p}{(2\pi)^3}\frac{p_x^2p_y^2}{\epsilon_p^2}\; n_{\rm B}(\epsilon_p)[1+n_{\rm B}(\epsilon_p)]\;{\rm Re}\left[\left(kv_z - \omega + i\frac{\Upsilon}{2}\right)^2 + \frac{\Upsilon^2}{4}\right]^{-1}\\ &= n_{\rm B}^{-1}(\omega)\Upsilon \int \frac{{\rm d}^3p}{(2\pi)^3}\frac{p_x^2p_y^2}{\epsilon_p^2}\;\frac{n_{\rm B}(\epsilon_p)[1+n_{\rm B}(\epsilon_p)]}{(kv_z-\omega)^2 + \Upsilon^2}\ .\end{aligned} \tag{6.66}$$

The result in eq. (6.66) is either directly or inversely proportional to the coupling $\Upsilon$, depending on whether we are in the regime $\omega, k \gg \Upsilon$ or $\omega, k \ll \Upsilon$, respectively. The latter regime ($\sim 1/\Upsilon$) of very low frequencies describes the hydrodynamic fluctuations originating from the most weakly interacting particle species.

Going over to spherical coordinates, using

$$\int_0^{2\pi} d\phi \cos^2\phi\;\sin^2\phi = \frac{\pi}{4}\ , \tag{6.67}$$

and denoting $z = \cos\theta$, the remaining angular integration becomes

$$\mathcal{F}(\omega, vk, \Upsilon) \equiv \int_{-1}^{+1} \mathrm{d}z \, \frac{(1-z^2)^2}{(vkz+\omega)^2 + \Upsilon^2} \,, \qquad v \equiv \frac{p}{\epsilon_p} \,. \tag{6.68}$$

At light-cone $\omega = k$ and for the largest wavelengths $k \ll \Upsilon$, eq. (6.68) simplifies to

$$\mathcal{F}(k, vk, \Upsilon) \overset{k\ll\Upsilon}{\approx} \int_{-1}^{+1} \mathrm{d}z \, \frac{(1-z^2)^2}{\Upsilon^2} = \frac{16}{15\Upsilon^2} \,. \tag{6.69}$$

Otherwise, the integral in eq. (6.68) can be solved analytically by partial-fractioning the integrand. The full expression on the light-cone reads

$$\begin{aligned} \mathcal{F}(k, vk, \Upsilon) = {} & \frac{2}{3}\frac{k^2(9-5v^2) - 3\Upsilon^2}{(vk)^4} - 2k\frac{k^2(1-v^2) - \Upsilon^2}{(vk)^5} \ln\frac{k^2(1+v)+\Upsilon^2}{k^2(1-v)+\Upsilon^2} \\ & + \frac{[k^2(1-v^2) - \Upsilon^2]^2 - 4k^2\Upsilon^2}{(vk)^5\Upsilon} \left[\arctan\frac{k(1+v)}{\Upsilon} - \arctan\frac{k(1-v)}{\Upsilon}\right] \,, \end{aligned} \tag{6.70}$$

from which we can extract an estimate also for the small wavelengths $k \gg \Upsilon$:

$$\mathcal{F}(k, vk, \Upsilon) \approx \begin{cases} \frac{16}{15\Upsilon^2} & k \ll \Upsilon \\ \frac{2}{3v^5k^2}\left[v(9-5v^2) - 6(1-v^2)\ln\frac{1+v}{1-v}\right] \overset{v\approx 1}{\approx} \frac{8}{3k^2} & k \gg \Upsilon \end{cases} \,. \tag{6.71}$$

The gravitational wave production rate can now be expressed as

$$\frac{\mathrm{d}e_{\mathrm{GW}}}{\mathrm{d}t\,\mathrm{d}\ln k} \overset{\omega,k,\Upsilon\ll\pi T}{\approx} \frac{k^3\Upsilon}{2\pi^3 m_{\mathrm{pl}}^2} \int_0^\infty \mathrm{d}p \, \frac{p^6}{\epsilon_p^2} \, n_{\mathrm{B}}(\epsilon_p)[1+n_{\mathrm{B}}(\epsilon_p)] \, \mathcal{F}\left(k, \frac{p}{\epsilon_p}k, \Upsilon\right) \,. \tag{6.72}$$

This grows fast, $\sim k^3$, for $k \ll \Upsilon$ and more moderately, $\sim k$, for $k \gg \Upsilon$, suggesting that most of the energy density carried by gravitational waves lies at larger momenta.

In both limits of large and small wavelengths, the dependence on the momentum $p$ in $\mathcal{F}(k, \frac{p}{\epsilon_p}k, \Upsilon)$ cancels out, such that we are left with the integral

$$\mathcal{J}(m,T) \equiv \int_0^\infty \mathrm{d}p \, \frac{p^6}{\epsilon_p^2} n_{\mathrm{B}}(\epsilon_p)[1+n_{\mathrm{B}}(\epsilon_p)] \,. \tag{6.73}$$

For a numerical evaluation we change integration variable and express eq. (6.73) in terms of the dimensionless quantity

$$\frac{\mathcal{J}}{m^5} = \int_1^\infty \mathrm{d}x \, \frac{(x^2-1)^{\frac{5}{2}}}{x} \frac{e^{\frac{m}{T}x}}{(e^{\frac{m}{T}x}-1)^2} \,. \tag{6.74}$$

At small values of $\Lambda_{\mathrm{IR}} \ll m$, the maximal temperature reached in the reheating period in the considered set-up is generally speaking $\mathcal{O}(T/m) \sim 10^{-3}$. In this regime, using partial integration and the geometric series $\sum_{n=0}^\infty x^n = (1-x)^{-1}$ for $|x| < 1$, eq. (6.73) evaluates to

$$\begin{aligned} \mathcal{J} &= -T\sum_{n=1}^\infty \int_m^\infty \mathrm{d}\epsilon_p \, \frac{(\epsilon_p^2 - m^2)^{\frac{5}{2}}}{\epsilon_p} \partial_{\epsilon_p} e^{-n\epsilon_p/T} \\ &\overset{m\gg T}{\approx} -T\int_m^\infty \mathrm{d}\epsilon_p \, \frac{(\epsilon_p^2-m^2)^{\frac{5}{2}}}{\epsilon_p} \partial_{\epsilon_p} e^{-\epsilon_p/T} = Tm^4 \int_1^\infty \mathrm{d}x \, (x^2-1)^{\frac{3}{2}} \Big[\, 5 - \cancel{\frac{x^2-1}{x^2}}^{\mathcal{O}(T/m)} \,\Big] e^{-\frac{m}{T}x} \\ &\overset{m\gg T}{\approx} 5Tm^4\left(-\frac{T}{m}\right)\int_0^\infty \mathrm{d}y \, \sinh^3 y \, \partial_y e^{-\frac{m}{T}\cosh y} \\ &= \frac{15}{2}T^2m^3\left(-\frac{T}{m}\right)\int_0^\infty \mathrm{d}y \, \sinh(2y) \, \partial_y e^{-\frac{m}{T}\cosh y} = 15T^5\left(\frac{m}{T}\right)^2 K_2\left(\frac{m}{T}\right) \\ &\overset{m\gg T}{\approx} 15T^5\sqrt{\frac{\pi}{2}}\left(\frac{m}{T}\right)^{\frac{3}{2}} e^{-m/T} \,. \end{aligned} \tag{6.75}$$

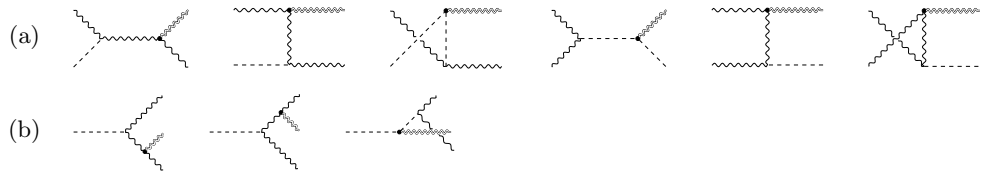


Figure 6.5: Kinematically allowed (a) $2 \to 2$ and (b) $1 \to 3$ processes contributing to the production of gravitational waves at large momenta, $k \sim \pi T$. Dashed lines denote the inflaton $\varphi$; wiggly lines gauge fields; doubled lines gravitons; blobs the insertions of the energy-momentum tensor.

Here $K_\alpha(x) \overset{x\to\infty}{\longrightarrow} \sqrt{\pi/(2x)}e^{-x}$ is a modified Bessel function of the second kind.

Increasing $\Lambda_{\rm IR}$, the ratio $T/m$ could reach order unity at some point in the reheating period. The integration over $p$ can then be carried out approximating $\epsilon_p \approx p$,

$$\mathcal{J} \overset{m\ll T}{\approx} \int_0^\infty \mathrm{d}p\, p^4\; n_{\rm B}(p)[1+n_{\rm B}(p)] \tag{6.76}$$

$$= \int_0^\infty \mathrm{d}p\, \frac{p^4\, e^{\frac{p}{T}}}{(e^{\frac{p}{T}}-1)^2} = \int_0^\infty \mathrm{d}p\, p^4\; \partial_p\left(\frac{-T}{e^{\frac{p}{T}}-1}\right)$$

$$= 4T\int_0^\infty \mathrm{d}p\, \frac{p^3}{e^{\frac{p}{T}}-1} = 4T\sum_{n=1}^\infty \int_0^\infty \mathrm{d}p\, p^3\; e^{-\frac{np}{T}}$$

$$= 24\; T^4 \sum_{n=1}^\infty n^{-3} \int_0^\infty \mathrm{d}p\, e^{-\frac{np}{T}} = 24\; T^5\; \underbrace{\zeta(4)}_{\frac{\pi^4}{90}} = \frac{4\pi^4}{15}T^5\ . \tag{6.77}$$

Inserting $\mathcal{J}(m,T)$ back in eq. (6.72) yields[51]

$$\frac{\mathrm{d}e_{\rm GW}}{\mathrm{d}t\,\mathrm{d}\ln k} \overset{k\ll\Upsilon}{\approx} \begin{cases} 2\pi\left(\frac{4}{15}\right)^2 \frac{k^3}{m_{\rm pl}^2}\frac{T^5}{\Upsilon_{\rm IR}} & m \ll T \\ \frac{16}{\pi}\frac{k^3}{m_{\rm pl}^2}\frac{T^5}{\Upsilon_{\rm UV}}\left(\frac{m}{2\pi T}\right)^{\frac{3}{2}} e^{-m/T} & m \gg T \end{cases} . \tag{6.78}$$

The result in the regime $m \ll T$ is illustrated numerically in figure 6.8a.

## Boltzmann regime

Larger momenta, $k \sim \pi T$, allow for elementary particle excitations to be resolved. The energy-momentum tensor for the fields in eq. (6.1) is

$$T_{\mu\nu} \supset \partial_\mu\varphi\,\partial_\nu\varphi - F^c_{\mu\alpha}F^{\alpha c}_\nu\ . \tag{6.79}$$

Trace parts are omitted, since they drop out when projected with eq. (3.83). The production rate of gravitational waves from processes whose vertex structure is included in the Standard Model Lagrangian has been computed in [126]. Here we study the additional production of gravitons involving one appearance of the vertex in eq. (6.1). This contribution is represented as

$$\mathbb{L}^{\alpha\beta;\mu\nu}\,\mathrm{Im}\,G^{\rm R}_{\alpha\beta;\mu\nu}(k,k) = \bigoplus \mathrm{scat}_{n\to m}(g_1,\varphi,g_2)\,\Theta_{n\to m}(\mathcal{P}_{g_1},\mathcal{P}_\varphi,\mathcal{P}_{g_2})\ , \tag{6.80}$$

where $\mathrm{scat}_{n\to m}$ is a phase-space average, and $g_1$, $g_3$ label two (identical) gauge bosons (cf. fig. 6.5a). The function $\Theta$ in eq. (6.80) contains the dynamical information concerning the production process and it may be referred to as the *matrix element squared*.

[51] The friction $\Upsilon$ can be parametrized by $\Upsilon_{\rm IR}$ (cf. eq. (5.27)) in the low-mass limit $m \ll T$, and by $\Upsilon_{\rm UV}$ (cf. eq. (5.28)) in the low-temperature limit $m \gg T$.

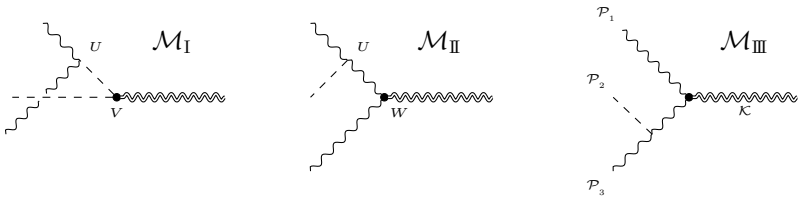


Figure 6.6: Kinematically not allowed $3 \to 1$ amplitudes used for deriving eq. (6.80).

To evaluate the rates of these reactions, we adopt the method presented in [128]. The computations are sketched in appendix C, while here we briefly present the methods and the result.

We start by considering the processes in fig. 6.6, which are not kinematically allowed, but have a simple structure, as non-equilibrium and plasma particles are on different sides of the reaction. The allowed $2 \to 2$ and $1 \to 3$ processes can then be obtained by permuting one or two legs respectively to be final states. We therefore simplify the notation to

$$\Theta \equiv \Theta_{3\to1}(\mathcal{P}_{g_1}, \mathcal{P}_\varphi, \mathcal{P}_{g_2}) \ . \tag{6.81}$$

In order to estimate $\Theta$, we first determine the Feynman rules. We define the propagators for

- **scalars** with momentum $\mathcal{P}$ and mass $m$: $\Delta^\varphi(\mathcal{P})$ (virtual),
- **gauge bosons** with momentum $\mathcal{P}$, helicity $s$ and SU($N_c$) index $a$: $\Delta^{g,ab}_{\alpha\beta}(\mathcal{P})$ (virtual), and $\hat{g}_\mu(\mathcal{P}, s)$ (external),
- **graviton** with momentum $\mathcal{K}$ and helicity $\lambda$: $\hat{h}_{\alpha\beta}(\mathcal{K}, \lambda)$ (external).

Vertices can be written as

$$\varphi \to gg: \quad U_{\alpha\beta}(\mathcal{P}^a_{g_1}, \mathcal{P}^b_{g_2}) = -8i\frac{c_\chi g^2}{f_a}\delta^{ab}\epsilon_{\alpha\beta\gamma\delta}\mathcal{P}^\gamma_{g_1}\mathcal{P}^\delta_{g_2} \ , \tag{6.82}$$

$$h \to \varphi\varphi: \quad V^{\alpha\beta}(\mathcal{P}_{\varphi_1}, \mathcal{P}_{\varphi_2}) = 2i\mathcal{P}^\alpha_{\varphi_1}\mathcal{P}^\beta_{\varphi_2} \ , \tag{6.83}$$

$$h \to gg: \quad W^{\alpha\beta\gamma\delta}(\mathcal{P}^c_{g_1}, \mathcal{P}^d_{g_2}) = -2i\delta^{cd}\left[\mathcal{P}^\alpha_{g_1}\mathcal{P}^\beta_{g_2}\eta^{\gamma\delta} + (\mathcal{P}_{g_1}\cdot\mathcal{P}_{g_2})\eta^{\gamma\alpha}\eta^{\delta\beta} - \eta^{\alpha\gamma}\mathcal{P}^\beta_{g_2}\mathcal{P}^\delta_{g_1} - \eta^{\alpha\delta}\mathcal{P}^\beta_{g_1}\mathcal{P}^\gamma_{g_2}\right] \ , \tag{6.84}$$

where $c_\chi \equiv 1/(64\pi^2)$. With the definitions above, and denoting $\mathcal{P}_{1,3} \equiv \mathcal{P}_{g_{1,2}}$, $\mathcal{P}_2 \equiv \mathcal{P}_\varphi$ and $\mathcal{Q}_i \equiv \mathcal{K} - \mathcal{P}_i$ for $i = 1, 2, 3$, the amplitudes in fig. 6.6 can be written as

$$\mathcal{M}^{cd}_{\rm I} \equiv \hat{h}^{\alpha\beta}(\mathcal{K}, \lambda)V_{\alpha\beta}(\mathcal{Q}_2, \mathcal{P}_2)\,\frac{i}{s_{13} - m^2}\,U^{\gamma\delta}(\mathcal{P}^c_1, \mathcal{P}^d_3)\,\hat{g}_\gamma(\mathcal{P}_1, s_1)\hat{g}_\delta(\mathcal{P}_3, s_3) \ , \tag{6.85}$$

$$\mathcal{M}^{cd}_{\rm II} \equiv \hat{h}^{\alpha\beta}(\mathcal{K}, \lambda)W^{\zeta\delta}_{\alpha\beta}(\mathcal{Q}^b_3, \mathcal{P}^d_3)\,\Delta^{g,ba}_{\zeta\kappa}(\mathcal{Q}_3)\,U^{\kappa\gamma}(\mathcal{Q}^a_3, \mathcal{P}^c_1)\,\hat{g}_\gamma(\mathcal{P}_1, s_1)\hat{g}_\delta(\mathcal{P}_3, s_3) \ , \tag{6.86}$$

$$\mathcal{M}^{cd}_{\rm III} \equiv \mathcal{M}^{cd}_{\rm II}\,|_{1\leftrightarrow3} \ . \tag{6.87}$$

The squared amplitudes can be represented as the self-energy diagrams illustrated in fig. 6.7,

$$\Theta = \frac{\Theta_{\rm I,I}}{2} + \frac{\Theta_{\rm II,II}}{2} + \frac{\Theta_{\rm III,III}}{2} + \Theta_{\rm I,II} + \Theta_{\rm I,III} + \Theta_{\rm II,III} \ , \tag{6.88}$$

$$\Theta_{A,B} = \sum_\lambda \sum_{s_1,s_3} \left(\mathcal{M}_A\mathcal{M}^\dagger_B + \mathcal{M}_B\mathcal{M}^\dagger_A\right) \ , \qquad A, B \in \{\rm I, II, III\} \ . \tag{6.89}$$

For $s_{13} \equiv (\mathcal{K} - \mathcal{P}_2)^2 = (\mathcal{P}_1 + \mathcal{P}_3)^2$, the result derived in appendix C is

$$\Theta(\mathcal{P}_{g_1}, \mathcal{P}_\varphi, \mathcal{P}_{g_3}) \ = \ \frac{16g^4 d_A c^2_\chi}{f_a^2}\frac{s^4_{13} + m^8}{(s_{13} - m^2)^2} \ \overset{m^2 \ll s_{13}}{\longrightarrow} \ \frac{16g^4 d_A c^2_\chi}{f_a^2}s^2_{13} \ . \tag{6.90}$$

Figure 6.7: Self-energy diagrams as matrix elements squared entering eq. (6.88).

The matrix element squared is free from poles if the mass scale is negligible, $m \ll T$. Let us point out that the analysis exposed in the present chapter has been carried out with the idea of dealing with a high temperature regime. After a careful parameter scan in [5] this expectation turned out to be in general not satisfied. The results presented here should then be extended for $m \gg T$ for a complete picture.

In the regime of high temperatures $m \ll T$, the contribution to the production of gravitational waves is only from $2 \to 2$ scattering processes (see fig. 6.5a). Going over to the channels $2 \to 2$ means inverting one of the initial state momenta to a final state momentum. There are thus two possibilities to invert a gluon momentum and one possibility to invert the inflaton momentum,

$$\begin{aligned} 2 \leftrightarrow 2: \qquad & \Theta(-\mathcal{P}_{g_1}; \mathcal{P}_\varphi, \mathcal{P}_{g_3}) = \Theta(-\mathcal{P}_{g_3}; \mathcal{P}_{g_1}, \mathcal{P}_\varphi) \propto t^2 \ , \\ & \Theta(-\mathcal{P}_\varphi; \mathcal{P}_{g_1}, \mathcal{P}_{g_3}) \propto s^2 \ , \end{aligned} \tag{6.91}$$

corresponding to the $t$ and $s$-channel in terms of the Mandelstam variables. Note that the function $\Theta(\mathcal{P}_{g_1}, \mathcal{P}_\varphi, \mathcal{P}_{g_3})$ of the $s$-channel is identical to eq. (6.90), as there is no dependence on $\mathcal{P}_\varphi$. Inserting the results in eq. (6.37) the dependence of the production rate on $f_a$, $T$ and $m_{\rm pl}^2$ is parametrized by the dimensionless combination

$$\frac{f_a^2\, m_{\rm pl}^2}{T^9} \frac{\mathrm{d}e_{\rm GW}}{\mathrm{d}t\, \mathrm{d}\ln k} \overset{k\sim\pi T}{\approx} d_A \frac{k^3 n_{\rm B}(k)}{\pi\, T^9} \left(\frac{\alpha}{2\pi}\right)^2 \left[\ \mathrm{scat}_{2\to2}(s^2) + \mathrm{scat}_{2\to2}(2t^2)\ \right] . \tag{6.92}$$

In order to evaluate eq. (6.92), the integrations in $\mathrm{scat}_{2\to2}$ can be performed numerically modifying the algorithm provided in [128].

## Numerical results

The infrared (IR), cf. eq. (6.78), and ultraviolet (UV), cf. eq. (6.92), contributions to the production rate show a parametrically different behaviour. At high temperatures $m \ll T$ we find

$$\text{IR:} \qquad \frac{\mathrm{d}e_{\rm GW}}{\mathrm{d}t\, \mathrm{d}\ln k} \approx C_{\rm IR}\left(\frac{k}{T}\right) \frac{f_a^2\, T^5}{m_{\rm pl}^2} \ , \tag{6.93}$$

$$\text{UV:} \qquad \frac{\mathrm{d}e_{\rm GW}}{\mathrm{d}t\, \mathrm{d}\ln k} \approx C_{\rm UV}\left(\frac{k}{T}\right) \frac{T^9}{f_a^2\, m_{\rm pl}^2} \ , \tag{6.94}$$

inserting $\Upsilon_{\rm IR}$ from eq. (5.27). The numerical solution for the dimensionless coefficients $C_{\rm IR}$ and $C_{\rm UV}$ is illustrated in fig. 6.8. In the limit $m \ll T$, the mass parameter $m$ is neglected, although in principle it still enters the evaluation of $C_{\rm IR}$ and $C_{\rm UV}$ via the parametrization of $\alpha$ in (5.11).

In order to establish an upper bound for the production rate in the regime $m \ll T$, in [2] we adopted $\Lambda_{\rm IR} \sim 0.2\,\mathrm{GeV}$, and $T \sim T_{\rm max} \sim (10^{-5}, 10^{-2}) m_{\rm pl}$. In the later work [4] we realized that, with the values of $m$ and $f_a$ dictated by the CMB constraints (see sec. 5.1), for such a low confinement scale the system only heats up to $T_{\rm max} \sim 10^{-9} m_{\rm pl} \ll m \sim 10^{-6} m_{\rm pl}$, as shown in fig. 5.6a. A valid $T \gg m$ regime is rather obtained at $\Lambda_{\rm IR} \sim 10^{-4} m_{\rm pl}$ (see fig. 5.6g), where the interactions within the thermal plasma are strong. However, our computations for the gravitational wave production rate both in the UV and IR regime were carried out with the assumption $\alpha \ll 1$. We hope to come back to this issue in the future and generalize our results to a strongly coupled gauge sector.

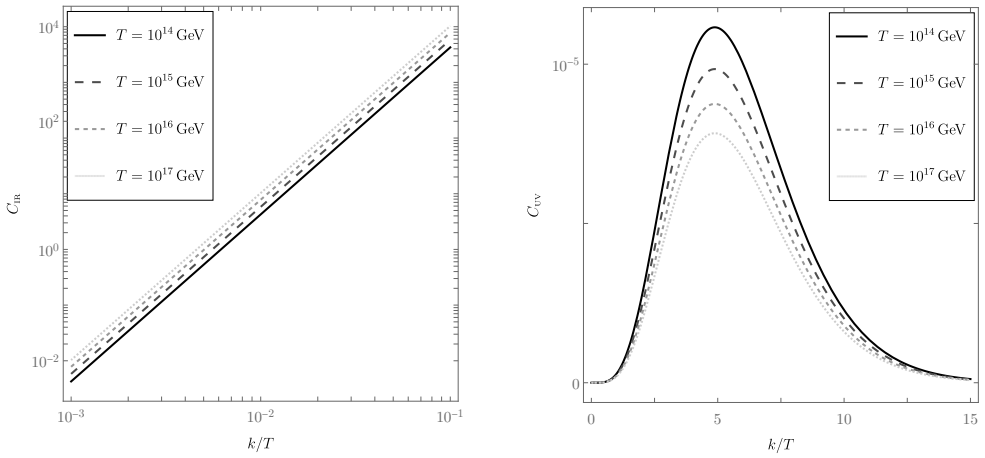


(a) (b)

Figure 6.8: Coefficients of the (a) infrared (IR) and (b) ultraviolet (UV) part of the axion contribution to the production rate of gravitational radiation during reheating, see eqs. (6.93) and (6.94). The present figure reproduces the middle and right panels in fig. 3 of [2].

The Standard Model contribution to the production rate computed in [126] has a similar shape as the UV axion contribution shown in fig. 6.8b. To compare with the latter, let us set $k \sim \pi T$, where the UV production rate peaks. We redefine the coefficient $C_{\rm UV} \to \tilde{C}_{\rm UV}$ to track the dependence on $\alpha$. Then, the parametric behaviours are

$$\begin{aligned} \text{axion-like inflation:} \qquad & \frac{\mathrm{d}e_{\rm GW}}{\mathrm{d}t\,\mathrm{d}\ln k} \approx \tilde{C}_{\rm UV}\left(\frac{k}{T}\right)\frac{\alpha^2 T^9}{m_{\rm pl}^2 f_a^2}\,, \\ \text{Standard Model:} \qquad & \frac{\mathrm{d}e_{\rm GW}}{\mathrm{d}t\,\mathrm{d}\ln k} \approx C_{\rm SM}\left(\frac{k}{T}\right)\frac{\alpha T^7}{m_{\rm pl}^2}\,, \end{aligned} \tag{6.95}$$

and the proportion of the corresponding numerical coefficients is $\tilde{C}_{\rm UV}/C_{\rm SM} \sim \mathcal{O}(10^{-4})$ [125]. In order for the axion contribution to exceed the Standard Model one, the maximal temperature reached during the reheating period should then satisfy $10^{-4} \times \alpha T^2 \gtrsim f_a^2 \sim m_{\rm pl}^2$. Assuming $T < m_{\rm pl}$ in general, the conclusion is that, around its maximum, the production rate of gravitational waves during the reheating period is dominated by the Standard Model contribution.

# Chapter 7

# Conclusions

## 7.1 Overview

The model of inflation explains how primordial perturbations originate from the vacuum fluctuations of a postulated scalar field, which, in a quasi-static initial regime, drives an exponential expansion of the early universe. Since the radiation-dominated epoch is the earliest epoch probed experimentally today, to consolidate inflationary predictions, a reasonable mechanism for the transition to a radiation dominated universe is needed. New experimental constraints on these epochs are expected from the detection of a gravitational wave background by future interferometers.

### Towards a realistic friction coefficient

*Warm inflation* models incorporate the inflationary mechanism into a thermal bath via a strong coupling and high temperature. Early attempts at modelling this complex thermal system using a simple friction coefficient yielded discouraging results [53, 54]. Recently, there has been a renewed interest in warm axion inflation models, noting that a more realistic thermal friction coefficient changes the nature of the solution, possibly rendering a phenomenologically viable scenario [59–62]. However, these studies acknowledge that the new friction coefficient is still not entirely realistic, but specific to a certain frequency domain, which may or may not be realized by the actual solution.

The purpose of [1] has been to present a theoretical framework which permits to eliminate this approximation. In particular, we focus on the heating-up process following a standard inflation scenario. Therefore we assume that the inflaton field is coupled weakly to a thermal plasma, and that the latter thermalizes efficiently. The evolution equations for such a system with generic interaction term are derived in chapter 4.

To compute concrete predictions, in chapter 5 we come back to the example of axion inflation. Regarding the friction coefficient, we confirm the existence of scenarios proposed in [59–62] on a qualitative level. However, we find a strong dependence on the vacuum contribution in (5.28), which was not considered in those works. In particular, the friction $\Upsilon \sim T^n$ used in [59–62] is not effective at the beginning of inflation, when the thermalization rate of the plasma is small compared with the mass scale of the inflaton field, $\alpha^2 T \ll m$. Our results for $\Upsilon$ are supported by a quantitative study of the retarded pseudo-scalar correlator using real-time lattice simulations [3].

### Neat example

The allowed values of the inflaton field's mass $m$ and decay constant $f_a$ are strongly constrained by the CMB Planck data [38]. Having constructed the interaction term around a non-Abelian Yang-Mills sector, we treat the confinement scale $\Lambda_{\rm IR}$ describing the self-interactions of the latter as a free parameter. A closer look at the dynamics emerging for a strongly coupled gauge sector is taken in [5], asking whether a transition between the deconfined and the confined phase may occur in the plasma as the system cools down (or heats up).

Numerical benchmark results in fig. 5.6 show that this system would preserve the powerful predictions of standard inflation and at the same time heat up efficiently afterwards.

For the largest confinement scales, $\Lambda_{\rm IR} \sim (10^{-8}\text{–}10^{-3}) m_{\rm pl}$, we observe relatively high temperatures in the solution. This can be explained by the fact that in the confined phase of a Yang-Mills sector, thermodynamic functions such as entropy density and heat capacity are exponentially small. Therefore, a small release of energy density from the inflaton field can lead to a significant increase in temperature. As a result the system heats up efficiently, even if it remains just slightly below $T_c$ (see fig. 5.6g). This scenario is treated most reliably by our methods, as the gauge field thermalization rate clearly exceeds the Hubble rate. Thus, there is no doubt about the validity of temperature as a physical notion (see fig. 5.6h).

Lowering the confinement scale, $\Lambda_{\rm IR} < 10^{-8} m_{\rm pl}$, the system heats up above the critical temperature, confirming the possibility of a first-order phase transition in the gauge plasma [129]. Whether the maximal temperature is above $T_c$ or not has implications also for dark matter production, but the details are very model-dependent (see e.g. [130–132]).

### Physical implications for gravitational waves

Non-Abelian gauge fields are believed to thermalize rapidly [58]. In view of this fact, in [4] we have considered the contribution of thermal fluctuations to the gravitational wave background that originates during inflation, concentrating specifically on the LISA frequency window. We have derived a model-independent interpolating formula, eq. (6.35), that incorporates both vacuum and thermal contributions. Moreover, its validity is not restricted to de Sitter spacetime, which becomes an inadequate approximation towards the end of inflation.

Our key finding is that, in stark contrast to the approximately constant vacuum contribution, the thermal contribution scales as $f_0^3$ in terms of the current-day gravitational wave frequency. Since the tensor-to-scalar ratio, $r$, originates from very small frequencies, $f_0 \ll 10^{-15}$ Hz, such a growth implies that CMB constraints can be respected, yet the signal could in principle be observable in the LISA or Einstein Telescope window, $f_0 \sim (10^{-5} - 10^{2})$ Hz. The growth is cut off only at very large frequencies, $f_0 \sim 10^{11}$ Hz, where most of the gravitational energy density lies [125] (the overall shape of the spectrum is illustrated in fig. 7.1).

Whether the thermal part could be observable depends on the coefficient of the $f_0^3$ growth. This coefficient is proportional to the maximal shear viscosity $\eta$ of the inflaton plus radiation system. For the particular model where an SU(3) plasma is weakly coupled to an axion-like inflaton, we have found that $T\eta \sim T^4$, whereby the dominant contributions emerge from $T_{\rm max}$. A *hot* scenario is thus particularly interesting.

The production rate of gravitational waves during the reheating period after inflation depends on the magnitude of $T_{\rm max}$ as well. This was studied in [2], in the limit $m \ll \pi T_{\rm max}$ (prior to parameter scanning in [4], we expected this regime to be realized towards the end of inflation). Parametrically, the contribution from interactions involving an axion-like inflaton exceeds the one

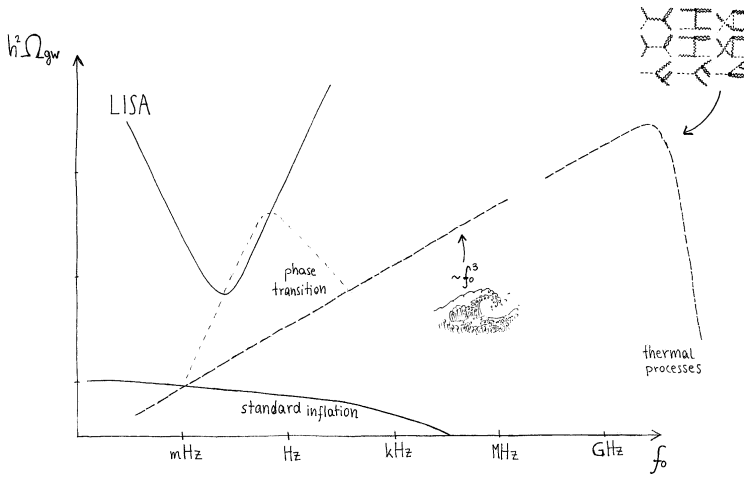


Figure 7.1: Possible shapes of the gravitational wave spectrum from the inflationary epoch. The $f_0^3$ growth originates from hydrodynamical fluctuations (sec. 6.1), while the turnover at $f_0 \sim$ GHz from elementary scatterings (sec. 6.2).

from Standard-Model interactions [125] if $10^{-4} \times \alpha T_{\rm max}^2 > f_a^2 \sim m_{\rm pl}^2$, which is unlikely. If this is not the case, the signal is not strongly constrained by $N_{\rm eff}$, given that for $T_{\rm max} \sim 10^{17}$ GeV the Standard Model contribution yields only $\Delta N_{\rm eff} \ll 10^{-3}$ [126].

However, after [4] and [5], we know that a valid $T \gg m$ regime is obtained at $\Lambda_{\rm IR} \sim 10^{-4} m_{\rm pl}$ (see fig. 5.6g), where the interactions within the thermal plasma are strong. The problem then is that our computations for the gravitational wave production rate both in the UV and IR regime were carried out with the assumption $\alpha \ll 1$.

Axion-like inflation has been used as a motivation for the LISA physics program, asserting that an observable signal could be obtained in certain Abelian cases [41], where an efficient tachyonic instability may convert a significant fraction of energy density to gravitational waves. Our study demonstrates that this statement depends on model details, and is unlikely to apply to generic non-Abelian constructions. One of the reasons why the non-Abelian case differs so notably from the Abelian one is that if the system thermalizes, tensor modes are excited only through interactions, whereby their production is suppressed by $\alpha$.

## 7.2 Outlook

There are multiple directions in which our work could be expanded. One concerns the retarded pseudoscalar correlator $G_{\rm R}$, which determines the value of the vacuum or thermal friction coefficient. Hoping that exploratory low-temperature investigations of the friction coefficient [91, 92] turn ultimately into a semi-quantitative tool, we could improve our results beyond the perturbative expansion in the gauge coupling constant. Similarly, a reliable derivation of the shear viscosity of a strongly coupled gauge sector would allow for more robust conclusions about the $f_0^3$-part of the gravitational wave background.

Furthermore, it would be intriguing to investigate how the visible sector present in the radiation-dominated epoch is populated within our scenario. Finally, the non-equilibrium physics of a system possessing two adjacent transitions (see fig. 5.6c) might reveal interesting gravitational wave signatures and thus merit further investigation.

# Appendix A

# Cosmological perturbation theory

This chapter collects together derivations of the properties and relations within the perturbative approach to cosmological inhomogeneities. It thus complements the general overview presented in chapters 2 and 3, and illustrated in table A.1. The first three sections follow mostly [13], while sec. A.4 is the result of multiple discussions with C. Caprini, A. Midiri and A. Roper Pol, and is based on unpublished notes by M. Laine.

| | background | perturbed universe |
|---|---|---|
| | 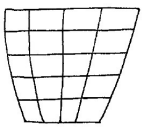 | 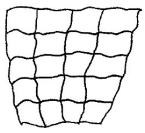 |
| metric | $\bar{g}_{\mu\nu}$ | $g_{\mu\nu} = \bar{g}_{\mu\nu} + \delta g_{\mu\nu}$ |
| Einstein tensor | $\bar{G}^{\mu}{}_{\nu}$ | $G^{\mu}{}_{\nu} = \bar{G}^{\mu}{}_{\nu} + \delta G^{\mu}{}_{\nu}$ |
| energy-momentum tensor | $\bar{T}^{\mu}{}_{\nu}$ | $T^{\mu}{}_{\nu} = \bar{T}^{\mu}{}_{\nu} + \delta T^{\mu}{}_{\nu}$ |
| Einstein equations | $\bar{G}^{\mu}{}_{\nu} = 8\pi G \bar{T}^{\mu}{}_{\nu}$ | $G^{\mu}{}_{\nu} = 8\pi G T^{\mu}{}_{\nu}$ |

Table A.1: Comparison of the homogeneous and isotropic background and the perturbed theory (sketches in $D = 1 + 1$ dimensions). Unperturbed background quantities are denoted by a bar, perturbations up to linear order are indicated by a $\delta$.

## A.1 Coordinate transformations

An intrinsic property of general relativity is the absence of a preferred choice of coordinates. In the perturbative picture, any set of coordinates describing the inhomogeneous and anisotropic universe assigns a space-time point $p$ in the unperturbed background $\mathcal{U}_0$, to a space-time point $q$ in the perturbed universe $\mathcal{U}_\delta$. The points $p$ and $q$ are thus labelled with the same coordinates $x^\alpha$. Let us define this point identification map as $f_\delta : \mathcal{U}_0 \to \mathcal{U}_\delta$. However, the space-time slicing in the perturbed universe $\mathcal{U}_\delta$, and thus the choice of $q$, is not unique. A small coordinate transformation[52]

[52]Comparing literature, one should be careful with the existence of two non-equivalent definitions of *small transformations*. On one hand, *active* transformations are defined as acting only on the physical quantities. These are thus evaluated at the same coordinate point. On the other hand, in the context of diffeomorphisms, one may also consider *passive* transformations. These are transformations of the coordinates and act therefore on all quantities as a relabelling. In the framework of cosmological perturbation theory, both points of view are valid. Active transformations of the fluctuations correspond to coordinate transformations on the unperturbed $\mathcal{U}_0$, while passive

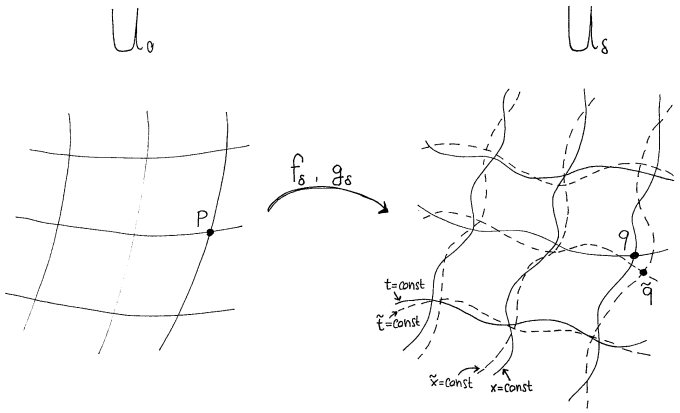


Figure A.1: Sketch in $D = 1 + 1$ dimensions of the identification of a point $q$ in the perturbed universe $\mathcal{U}_\delta$ with one $p$ in the unperturbed universe $\mathcal{U}_0$. Another choice of coordinates in $\mathcal{U}_\delta$ would lead to another point identification map, between $p$ and $\tilde{q}$.

on the perturbed universe $\mathcal{U}_\delta$,

$$\tilde{x}^\alpha(q) \approx x^\alpha(q) + \xi^\alpha(q) \ , \qquad \Xi^{\tilde{\mu}}_{\rho} \equiv \frac{\partial \tilde{x}^\mu}{\partial x^\rho} \approx \delta^\mu_\rho + \xi^\mu_{,\rho} \ , \quad \Xi^{\mu}_{\tilde{\rho}} \equiv \frac{\partial x^\mu}{\partial \tilde{x}^\rho} \approx \delta^\mu_\rho - \xi^\mu_{,\rho} \ , \tag{A.1}$$

such that $q$ becomes $\tilde{q}$ in the new coordinates,

$$\tilde{x}^\alpha(\tilde{q}) = x^\alpha(q) \qquad \Rightarrow \quad x^\alpha(\tilde{q}) \approx x^\alpha(q) - \xi^\alpha(q) \ , \tag{A.2}$$

leads to another mapping $g_\delta : \mathcal{U}_0 \to \mathcal{U}_\delta$ among the unperturbed and the perturbed universe. In particular, $\xi^0$ changes the slicing, while $\xi^i$ the threading of the perturbed universe. The non-uniqueness of the mapping automatically leads to redundancies in the physical description, interpretable as gauge freedom. This can be used as a powerful tool to simplify the computations, as done in sections 2.1 and 2.2, where we introduce the Newtonian and the comoving gauge, and in section 3.2, where we mention the spatially flat gauge. It is thus useful to derive the transformation behaviours of the quantities of interest.

In this section we denote a general function by $\tilde{Q} \equiv \tilde{Q}(\tilde{q})$, and compute how the fluctuations of arbitrary scalar, vector or tensor quantities behave under gauge transformations defined as in eq. (A.1). Since scalars do not transform, and the background only depends on time, we find

$$\tilde{A} = \bar{\tilde{A}} + \delta\tilde{A} \overset{(A.2)}{=} \bar{A} - (\partial_\alpha \bar{A})\xi^\alpha + \delta A + \mathcal{O}(\delta\xi) \qquad \Rightarrow \quad \boxed{\delta\tilde{A} \approx \delta A - \bar{A}'\xi^0} \ . \tag{A.3}$$

Perturbations in scalars thus only depend on the slicing of the space-time. Vector perturbations can be calculated as

$$\tilde{B}^\mu = \Xi^{\tilde{\mu}}_{\rho}\left[\bar{B}^\rho - (\partial_\alpha \bar{B}^\rho)\xi^\alpha + \delta B^\rho + \mathcal{O}(\delta\xi)\right] \approx \bar{B}^\mu - (\partial_\alpha \bar{B}^\mu)\xi^\alpha + \bar{B}^\alpha \xi^\mu_{,\alpha} + \delta B^\mu \tag{A.4}$$

$$\Rightarrow \quad \boxed{\delta\tilde{B}^\mu \approx \delta B^\mu - \bar{B}^{\mu\prime}\xi^0 + \bar{B}^0\xi^{\mu\prime}} \ . \tag{A.5}$$

For the zeroth component it follows that

$$\tilde{b}^0 = b^0 - \bar{B}^{0\prime}\xi^0 + \bar{B}^0\xi^{0\prime} \ . \tag{A.6}$$

transformations of the fluctuations are induced by coordinate transformations in the perturbed universe $\mathcal{U}_\delta$. Here we follow the passive picture, as described in figure A.1. For a mathematically detailed discussion of both approaches see [133], the active picture is partially followed e.g. in [134].

By decomposing the spatial gauge parameter into its scalar[53] and vector parts,

$$\xi^i = -\partial^i \xi + \xi^i_{\rm v} \ , \qquad \partial_i \xi^i_{\rm v} = 0 \ , \tag{A.7}$$

one finds the transformation behaviour of the scalar and vector components of $\delta B^i$, *cf.* eq. (2.16),

$$\tilde{b}^i_{\rm s} = -\partial^i \left( b + \bar{B}^0 \xi' \right) \quad \Rightarrow \quad \tilde{b} = b + \bar{B}^0 \xi' \ , \tag{A.8}$$

$$\tilde{b}^i_{\rm v} = b^i_{\rm v} + \bar{B}^0 \xi^{i\prime}_{\rm v} \ . \tag{A.9}$$

The behaviour of tensorial perturbations under small coordinate transformations is

$$\tilde{C}_{\mu\nu} = \Xi^\rho_{\tilde{\mu}} \, \Xi^\sigma_{\tilde{\nu}} \left[ \bar{C}_{\rho\sigma} - (\partial_\alpha \bar{C}_{\rho\sigma}) \xi^\alpha + \delta C_{\rho\sigma} + \mathcal{O}(\delta\xi) \right] \tag{A.10}$$

$$\approx \bar{C}_{\mu\nu} - \xi^\rho_{,\mu} \bar{C}_{\rho\nu} - \xi^\rho_{,\nu} \bar{C}_{\mu\rho} - (\partial_\alpha \bar{C}_{\mu\nu}) \xi^\alpha + \delta C_{\mu\nu} \tag{A.11}$$

$$\Rightarrow \quad \boxed{\delta\tilde{C}_{\mu\nu} \approx \delta C_{\mu\nu} - \xi^\rho_{,\mu} \bar{C}_{\rho\nu} - \xi^\rho_{,\nu} \bar{C}_{\mu\rho} - \bar{C}'_{\mu\nu} \xi^0} \ . \tag{A.12}$$

Using eqs. (2.18)–(2.24) we find how the single components transform. The 00-component of eq. (A.12) yields

$$\tilde{c}_0 = c_0 + \bar{C}_{00} \xi^{0\prime} + \frac{1}{2} \bar{C}'_{00} \xi^0 \ . \tag{A.13}$$

For the $0i$-components we apply eq. (A.7) and eq. (2.19) and obtain for the quantities in eq. (2.20)

$$\tilde{c}_i = c_i + \bar{C} \xi'_i + \bar{C}_{00} \xi^0_{,i} \qquad \Rightarrow \quad \tilde{c} = c + \bar{C} \xi' - \bar{C}_{00} \xi^0 \ , \tag{A.14}$$

$$\tilde{c}^{\rm v}_i = c^{\rm v}_i + \bar{C} \xi^{\rm v}_i \ . \tag{A.15}$$

Analogously, one finds the transformation behaviour of the $ij$-components

$$\delta\tilde{C}_{ij} = \delta C_{ij} - \bar{C} \underbrace{\left( \xi_{j,i} + \xi_{i,j} - \frac{2}{3} \delta_{ij} \xi^k_{,k} \right)}_{\rm tr=0} - \frac{2}{3} \bar{C} \delta_{ij} \xi^k_{,k} - \bar{C}' \delta_{ij} \xi^0 \tag{A.16}$$

$$\Rightarrow \quad \tilde{c}_{\rm D} = c_{\rm D} - \frac{1}{3} \bar{C} \nabla^2 \xi + \frac{1}{2} \bar{C}' \xi^0 \ , \tag{A.17}$$

$$\tilde{\gamma}_{ij} = \gamma_{ij} - \frac{1}{2} \bar{C} \left( \xi_{j,i} + \xi_{i,j} \right) - \frac{1}{3} \bar{C} \delta_{ij} \nabla^2 \xi \tag{A.18}$$

$$\Rightarrow \ \tilde{\gamma} = \gamma + \bar{C} \xi \ , \ \ \tilde{\gamma}_i = \gamma_i + \bar{C} \xi^{\rm v}_i \ , \ \ \tilde{\gamma}^{\rm t}_{ij} = \gamma^{\rm t}_{ij} \ . \tag{A.19}$$

Let us sum up the total gauge degrees of freedom. In addition to two scalar gauge parameters $\xi^0$ and $\xi$, there are also the 3-vector degrees of freedom of $\xi^i_{\rm v}$. Imposing the divergence-free constraint from eq. (A.7), they reduce to two more degrees of freedom. Useful gauges and gauge invariant quantities are introduced in chapters 2 and 3. For the moment we only list them:

- **Newtonian gauge:** introduced in section 2.1 to derive the Einstein equations.
- **Comoving gauge:** introduced in section 2.2 to define curvature perturbations $\mathcal{R}$.
- **Spatially flat gauge:** introduced in section 3.2 to compute the power spectrum of scalar (and tensor) perturbations.

## A.2 Computing the Einstein tensor for a FLRW metric

In this section we derive the results presented in sec. 2.1.

[53] For some reasons in [7], and in the following literature, the scalar part of the gauge parameter is defined with the opposite sign: $\xi^i_{\rm s} = \partial^i \xi$. However, here we want to keep the traditional minus sign for a scalar potential. Final results agree with [7].

## Zeroth order Einstein tensor for curved FLRW universe

As a warm-up for the derivation of the perturbed Einstein tensor, we first show the computations of the unperturbed Einstein tensor for a background universe described by the FLRW metric with generic spatial curvature $\kappa$ (*cf.* eqs. (2.1) and (2.3)). Using conformal and reduced-circumference polar coordinates $(\tau, r, \theta, \phi)$, the latter is given by

$$\bar{g}_{\mu\nu} = a^2 \,\mathrm{diag}(-1,\ (1-\kappa r^2)^{-1},\ r^2,\ r^2\sin^2\theta)\ . \tag{A.20}$$

The Christoffel symbols at zeroth order are given by

$$\bar{\Gamma}^{\rho}_{\mu\nu} = \frac{1}{2}\bar{g}^{\rho\sigma}(\bar{g}_{\sigma\mu,\nu} + \bar{g}_{\sigma\nu,\mu} - \bar{g}_{\mu\nu,\sigma})\ . \tag{A.21}$$

The non-vanishing ones are

$$\bar{\Gamma}^{\tau}_{\tau\tau} = \bar{\Gamma}^{r}_{\tau r} = \bar{\Gamma}^{\theta}_{\tau\theta} = \bar{\Gamma}^{\phi}_{\tau\phi} = \frac{1}{2}a^{-2}(a^2)' = \mathcal{H}\ , \tag{A.22}$$

$$\bar{\Gamma}^{\tau}_{rr} = \frac{1}{2}(-a^{-2})\left(-\frac{a^2}{1-\kappa r^2}\right)' = \frac{\mathcal{H}}{1-\kappa r^2}\ , \tag{A.23}$$

$$\bar{\Gamma}^{\tau}_{\theta\theta} = \frac{1}{2}(-a^{-2})(-a^2r^2)' = r^2\mathcal{H}\ , \tag{A.24}$$

$$\bar{\Gamma}^{\tau}_{\phi\phi} = \frac{1}{2}(-a^{-2})(-a^2r^2\sin^2\theta)' = r^2\sin^2\theta\,\mathcal{H}\ , \tag{A.25}$$

$$\bar{\Gamma}^{r}_{rr} = \frac{1}{2}a^{-2}(1-\kappa r^2)\partial_r\left(\frac{a^2}{1-\kappa r^2}\right) = \frac{\kappa r}{1-\kappa r^2}\ , \tag{A.26}$$

$$\bar{\Gamma}^{\theta}_{r\theta} = \bar{\Gamma}^{\phi}_{r\phi} = \frac{1}{2}r^{-2}\partial_r(r^2) = r^{-1}\ , \tag{A.27}$$

$$\bar{\Gamma}^{r}_{\theta\theta} = \frac{1}{2}a^{-2}(1-\kappa r^2)\partial_r(-a^2r^2) = -r(1-\kappa r^2)\ , \tag{A.28}$$

$$\bar{\Gamma}^{r}_{\phi\phi} = \frac{1}{2}a^{-2}(1-\kappa r^2)\partial_r(-a^2r^2\sin^2\theta) = -r\sin^2\theta\,(1-\kappa r^2)\ , \tag{A.29}$$

$$\bar{\Gamma}^{\phi}_{\theta\phi} = \frac{1}{2}a^{-2}r^{-2}\sin^{-2}\theta\,\partial_\theta(a^2r^2\sin^2\theta) = \frac{\cos\theta}{\sin\theta}\ , \tag{A.30}$$

$$\bar{\Gamma}^{\theta}_{\phi\phi} = \frac{1}{2}a^{-2}r^{-2}\partial_\theta(-a^2r^2\sin^2\theta) = -\sin\theta\cos\theta\ . \tag{A.31}$$

The Ricci tensor

$$\bar{R}_{\mu\nu} = \bar{R}^{\alpha}_{\mu\alpha\nu} = \bar{\Gamma}^{\alpha}_{\mu\nu,\alpha} - \bar{\Gamma}^{\alpha}_{\mu\alpha,\nu} + \bar{\Gamma}^{\beta}_{\mu\nu}\bar{\Gamma}^{\alpha}_{\beta\alpha} - \bar{\Gamma}^{\beta}_{\mu\alpha}\bar{\Gamma}^{\alpha}_{\beta\nu}\ , \tag{A.32}$$

resulting from eqs. (A.22)–(A.31) is diagonal, with the components

$$\bar{R}_{\tau\tau} = \mathcal{H}' - 4\mathcal{H}' + \mathcal{H}(4\mathcal{H}) - 4\mathcal{H}^2 = -3\mathcal{H}'\ , \tag{A.33}$$

$$\begin{aligned}\bar{R}_{rr} &= \cancel{-2\partial_r r^{-1}} + \frac{\kappa r}{1-\kappa r^2}\left(2r^{-1} + \cancel{\frac{\kappa r}{1-\kappa r^2}}\right) - \cancel{\left(\frac{\kappa r}{1-\kappa r^2}\right)^2} - \cancel{2r^{-2}} \\ &\quad + \frac{\mathcal{H}'}{1-\kappa r^2} + \frac{4\mathcal{H}^2}{1-\kappa r^2} - \frac{2\mathcal{H}^2}{1-\kappa r^2} \\ &= \frac{1}{1-\kappa r^2}(\mathcal{H}' + 2\mathcal{H}^2 + 2\kappa)\ ,\end{aligned} \tag{A.34}$$

$$\begin{aligned}\bar{R}_{\theta\theta} &= \mathcal{H}'r^2 - 1 + 3\kappa r^2 - \partial_\theta\left(\frac{\cos\theta}{\sin\theta}\right) + 4\mathcal{H}(r^2\mathcal{H}) - r(1-\kappa r^2)\left(\frac{\kappa r}{1-\kappa r^2} + 2r^{-1}\right) \\ &\quad - 2\left[r^2\mathcal{H}^2 - (1-\kappa r^2)\right] - \left(\frac{\cos\theta}{\sin\theta}\right)^2 \\ &= r^2(\mathcal{H}' + 2\mathcal{H}^2 + 2\kappa)\ ,\end{aligned} \tag{A.35}$$

$$\begin{aligned}\bar{R}_{\phi\phi} &= r^2\sin^2\theta\ \mathcal{H}' - \partial_\theta(\sin\theta\cos\theta) - \partial_r[r\sin^2\theta\,(1-\kappa r^2)] - \cos^2\theta \\ &\quad - r\sin^2\theta(1-\kappa r^2)\left(\cancel{2r^{-1}} + \frac{\kappa r}{1-\kappa r^2}\right) + r^2\sin^2\theta\ \mathcal{H}(4\mathcal{H}) - 2r^2\sin^2\theta\ \mathcal{H}^2 \\ &\quad + \cancel{2\sin^2\theta\,(1-\kappa r^2)} + 2\cos^2\theta \\ &= r^2\sin^2\theta(\mathcal{H}' + 2\mathcal{H}^2 + 2\kappa)\ . \end{aligned} \tag{A.36}$$

Raising one index, the components of the Ricci tensor simplify to

$$\bar{R}^\tau{}_\tau = 3a^{-2}\mathcal{H}'\ , \quad \bar{R}^r{}_r = a^{-2}(\mathcal{H}' + 2\mathcal{H}^2 + 2\kappa)\ , \quad \bar{R}^\theta{}_\theta = \bar{R}^\phi{}_\phi = a^{-2}(\mathcal{H}' + 2\mathcal{H}^2 + 2\kappa)\ . \tag{A.37}$$

The Ricci scalar is therefore

$$\bar{R} = \bar{R}^\mu{}_\mu = 6a^{-2}(\mathcal{H}' + \mathcal{H}^2 + \kappa)\ , \tag{A.38}$$

yielding the Einstein tensor $\bar{G}^\mu{}_\nu = \bar{R}^\mu{}_\nu - \delta^\mu{}_\nu\bar{R}/2$,

$$\bar{G}^\tau{}_\tau = -3a^{-2}(\mathcal{H}^2 + \kappa)\ , \tag{A.39}$$

$$\bar{G}^r{}_r = \bar{G}^\theta{}_\theta = \bar{G}^\phi{}_\phi = -a^{-2}(2\mathcal{H}' + \mathcal{H}^2 + \kappa)\ , \tag{A.40}$$

which is also diagonal.

## First order Einstein tensor for flat FLRW universe

Setting now $\kappa = 0$, we recall the unperturbed flat FRLW metric in conformal coordinates,

$$\bar{g}_{\mu\nu} = a^2\begin{pmatrix}-1 & \\ & \delta_{ij}\end{pmatrix}\ , \qquad \bar{g}^{\mu\nu} = a^{-2}\begin{pmatrix}-1 & \\ & \delta_{ij}\end{pmatrix}\ . \tag{A.41}$$

All computations are performed in the Newtonian gauge, where metric perturbations are

$$\delta g_{\mu\nu} = a^2\begin{pmatrix}-2\phi & -h_i \\ -h_i & -2\psi\delta_{ij} + 2\vartheta_{ij}\end{pmatrix}\ , \qquad \delta g^{\mu\nu} = a^{-2}\begin{pmatrix}2\phi & -h_i \\ -h_i & 2\psi\delta_{ij} - 2\vartheta_{ij}\end{pmatrix}\ , \tag{A.42}$$

with the constraints

$$\partial^i h_i = 0\ , \qquad \partial^i\vartheta_{ij} = 0\ , \quad \vartheta^i_i = 0\ . \tag{A.43}$$

The scale factor $a = a(\tau)$ depends only on time, such that $\partial_i a = \partial_i\mathcal{H} = 0$ for $i = 1,2,3$. Indices of linear perturbations are moved up or down with the background metric, such that we are free to choose spatial indices to be always down.

### Christoffel symbols

To compute the perturbed Christoffel symbols we first write

$$\delta\Gamma^\rho_{\mu\nu} = \frac{1}{2}\delta g^{\rho\sigma}(\bar{g}_{\sigma\mu,\nu} + \bar{g}_{\sigma\nu,\mu} - \bar{g}_{\mu\nu,\sigma}) + \frac{1}{2}\bar{g}^{\rho\sigma}(\delta g_{\sigma\mu,\nu} + \delta g_{\sigma\nu,\mu} - \delta g_{\mu\nu,\sigma})\ , \tag{A.44}$$

and evaluate it for the different components, yielding

$$\delta\Gamma^0_{00} = \frac{a^{-2}}{2}\left\{-(-2a^2\phi)' + 2\phi[2(-a^2)' - (-a^2)']\right\} = \cancel{2\mathcal{H}\phi} + \phi' - \cancel{2\mathcal{H}\phi} = \phi' \ , \tag{A.45}$$

$$\delta\Gamma^0_{0i} = \frac{a^{-2}}{2}\left[-(-2a^2\phi)_{,i} - h_i(a^2)'\right] = \phi_{,i} - \mathcal{H}h_i \ , \tag{A.46}$$

$$\begin{aligned}\delta\Gamma^i_{00} &= \frac{a^{-2}}{2}\left\{[2(-a^2h_i)' - (-2a^2\phi)_{,i}] - h_i(-a^2)'\right\} = -2\mathcal{H}h_i - h_i' + \phi_{,i} + \mathcal{H}h_i \\ &= \phi_{,i} - \mathcal{H}h_i - h_i' \ ,\end{aligned} \tag{A.47}$$

$$\begin{aligned}\delta\Gamma^0_{ij} &= \frac{a^{-2}}{2}\left\{-[(-a^2h_i)_{,j} + (-a^2h_j)_{,i} - (-2a^2\psi\delta_{ij} + 2a^2\vartheta_{ij})'] + 2\phi[-(a^2)']\right\} \\ &= \frac{1}{2}(h_{i,j} + h_{j,i}) - \delta_{ij}[\psi' + 2\mathcal{H}(\psi + \phi)] + \vartheta'_{ij} + 2\mathcal{H}\vartheta_{ij} \ ,\end{aligned} \tag{A.48}$$

$$\begin{aligned}\delta\Gamma^i_{0j} &= \frac{a^{-2}}{2}\left\{[(-a^2h_i)_{,j} + (-2a^2\psi\delta_{ij} + 2a^2\vartheta_{ij})' - (-a^2h_j)_{,i}] + 2(\psi\delta_{ik} - \vartheta_{ik})(a^2\delta_{kj})'\right\} \\ &= \frac{1}{2}(h_{j,i} - h_{i,j}) + \delta_{ij}(-\psi' - \cancel{2\mathcal{H}\psi} + \cancel{2\mathcal{H}\psi}) + \vartheta'_{ij} + \cancel{2\mathcal{H}\vartheta_{ij}} - \cancel{2\mathcal{H}\vartheta_{ij}} \\ &= \frac{1}{2}(h_{j,i} - h_{i,j}) - \delta_{ij}\psi' + \vartheta'_{ij} \ ,\end{aligned} \tag{A.49}$$

$$\begin{aligned}\delta\Gamma^i_{jk} &= [(-\psi\delta_{ij} + \vartheta_{ij})_{,k} + (-\psi\delta_{ik} + \vartheta_{ik})_{,j} - (-\psi\delta_{jk} + \vartheta_{jk})_{,i}] - \frac{a^{-2}}{2}h_i[-(a^2\delta_{jk})'] \\ &= -\delta_{ij}\psi_{,k} - \delta_{ik}\psi_{,j} + \delta_{jk}\psi_{,i} + \vartheta_{ij,k} + \vartheta_{ik,j} - \vartheta_{jk,i} + \mathcal{H}h_i\delta_{jk} \ .\end{aligned} \tag{A.50}$$

The unperturbed Christoffel symbols follow from eq. (2.55) straightforwardly,

$$\bar\Gamma^0_{0i} = \bar\Gamma^i_{00} = \bar\Gamma^i_{jk} = 0 \ , \qquad \bar\Gamma^0_{00} = \mathcal{H} \ , \quad \bar\Gamma^0_{ij} = \mathcal{H}\delta_{ij} \ , \quad \bar\Gamma^i_{0j} = \mathcal{H}\delta^i_j \ . \tag{A.51}$$

**Ricci tensor**

From the Christoffel symbols we calculate the components of the perturbed Ricci tensor,

$$\delta R_{\mu\nu} = \delta R^\alpha_{\mu\alpha\nu} = \delta\Gamma^\alpha_{\mu\nu,\alpha} - \delta\Gamma^\alpha_{\mu\alpha,\nu} + \bar\Gamma^\beta_{\mu\nu}\delta\Gamma^\alpha_{\beta\alpha} + \bar\Gamma^\alpha_{\beta\alpha}\delta\Gamma^\beta_{\mu\nu} - \bar\Gamma^\beta_{\mu\alpha}\delta\Gamma^\alpha_{\beta\nu} - \bar\Gamma^\alpha_{\beta\nu}\delta\Gamma^\beta_{\mu\alpha} \ . \tag{A.52}$$

The results are summarized in eqs. (2.59)–(2.61), with the intermediate steps amounting to

$$\begin{aligned}\delta R_{00} = \delta R^\alpha_{0\alpha0} &= \delta\Gamma^\alpha_{00,\alpha} - \delta\Gamma^\alpha_{0\alpha,0} + \bar\Gamma^\beta_{00}\delta\Gamma^\alpha_{\beta\alpha} + \bar\Gamma^\alpha_{\beta\alpha}\delta\Gamma^\beta_{00} - \bar\Gamma^\beta_{0\alpha}\delta\Gamma^\alpha_{\beta0} - \bar\Gamma^\alpha_{\beta0}\delta\Gamma^\beta_{0\alpha} \\ &= \cancel{\phi''} + \nabla^2\phi - \cancel{\phi''} + 3\psi'' + \mathcal{H}\delta\Gamma^\alpha_{0\alpha} + 4\mathcal{H}\delta\Gamma^0_{00} - 2\mathcal{H}\delta\Gamma^0_{00} - 2\mathcal{H}\delta\Gamma^i_{0i} \\ &= 3\psi'' + \nabla^2\phi + 3\mathcal{H}(\psi + \phi)' \ ,\end{aligned} \tag{A.53}$$

$$\begin{aligned}\delta R_{0i} = \delta R^\alpha_{0\alpha i} &= \delta\Gamma^\alpha_{0i,\alpha} - \delta\Gamma^\alpha_{0\alpha,i} + \bar\Gamma^\beta_{0i}\delta\Gamma^\alpha_{\beta\alpha} + \bar\Gamma^\alpha_{\beta\alpha}\delta\Gamma^\beta_{0i} - \bar\Gamma^\beta_{0\alpha}\delta\Gamma^\alpha_{\beta i} - \bar\Gamma^\alpha_{\beta i}\delta\Gamma^\beta_{0\alpha} \\ &= -\mathcal{H}'h_i - \mathcal{H}h_i' + \cancel{\phi'_{,i}} + \frac{1}{2}\nabla^2h_i - \psi'_{,i} - \cancel{\phi'_{,i}} + 3\psi'_{,i} + \mathcal{H}\delta\Gamma^\alpha_{i\alpha} + 4\mathcal{H}\delta\Gamma^0_{0i} \\ &\quad - 2\mathcal{H}\delta\Gamma^0_{0i} - \mathcal{H}\delta\Gamma^j_{ij} - \mathcal{H}\delta_{ij}\delta\Gamma^j_{00} \\ &= -\mathcal{H}'h_i - \cancel{\mathcal{H}h_i'} + \frac{1}{2}\nabla^2h_i + 2\psi'_{,i} + 3\mathcal{H}(-\mathcal{H}h_i + \phi_{,i}) - \mathcal{H}(-\mathcal{H}h_i - \cancel{h_i'} + \phi_{,i}) \\ &= 2(\psi' + \mathcal{H}\phi)_{,i} + \frac{1}{2}\nabla^2h_i - (\mathcal{H}' + 2\mathcal{H}^2)h_i \ ,\end{aligned} \tag{A.54}$$

$$\begin{aligned}\delta R_{ij} = \delta R^\alpha_{i\alpha j} &= \delta\Gamma^\alpha_{ij,\alpha} - \delta\Gamma^\alpha_{i\alpha,j} + \bar\Gamma^\beta_{ij}\delta\Gamma^\alpha_{\beta\alpha} + \bar\Gamma^\alpha_{\beta\alpha}\delta\Gamma^\beta_{ij} - \bar\Gamma^\beta_{i\alpha}\delta\Gamma^\alpha_{\beta j} - \bar\Gamma^\alpha_{\beta j}\delta\Gamma^\beta_{i\alpha} \\ &= \frac{1}{2}(h_{i,j} + h_{j,i})' - \delta_{ij}\psi'' + \vartheta''_{ij} - 2\mathcal{H}'[(\phi + \psi)\delta_{ij} - \vartheta_{ij}] - 2\mathcal{H}[(\phi + \psi)\delta_{ij} - \vartheta_{ij}]'\end{aligned}$$

$$
\begin{aligned}
&- 2\psi_{,ij} + \delta_{ij}\nabla^2\psi - \nabla^2\vartheta_{ij} + \cancel{\mathcal{H}h_{i,j}} - \phi_{,ij} - \cancel{\mathcal{H}h_{i,j}} + 3\psi_{,ij} + \mathcal{H}\delta_{ij}\delta\Gamma^{\alpha}_{0\alpha} \\
&+ 4\mathcal{H}\delta\Gamma^0_{ij} - \mathcal{H}(2\delta\Gamma^0_{ij} + \delta\Gamma^i_{0j} + \delta\Gamma^j_{0i}) \\
&= \frac{1}{2}(h_{i,j} + h_{j,i})' - \delta_{ij}\psi'' + \vartheta''_{ij} - 2\mathcal{H}'[(\phi+\psi)\delta_{ij} - \vartheta_{ij}] - 2\mathcal{H}[(\phi+\psi)\delta_{ij} - \vartheta_{ij}]' \\
&+ \psi_{,ij} + \delta_{ij}\nabla^2\psi - \nabla^2\vartheta_{ij} - \phi_{,ij} + \mathcal{H}\delta_{ij}(\phi - 3\psi)' + \mathcal{H}(h_{i,j} + h_{j,i}) \\
&- \cancel{2\mathcal{H}(\delta_{ij}\psi - \vartheta_{ij})'} - 4\mathcal{H}^2[(\phi+\psi)\delta_{ij} - \vartheta_{ij}] - \cancel{\frac{\mathcal{H}}{2}(h_{j,i} - h_{i,j})} \\
&+ \cancel{2\mathcal{H}(\delta_{ij}\psi - \vartheta_{ij})'} + \cancel{\frac{\mathcal{H}}{2}(h_{j,i} - h_{i,j})} \\
&= -\delta_{ij}\left[\psi'' + \mathcal{H}(\phi + 5\psi)' + 2(\mathcal{H}' + 2\mathcal{H}^2)(\phi+\psi) - \nabla^2\psi\right] + (\psi - \phi)_{,ij} \\
&+ \frac{1}{2}(h_{i,j} + h_{j,i})' + \mathcal{H}(h_{i,j} + h_{j,i}) + \vartheta''_{ij} + 2\mathcal{H}\vartheta'_{ij} - \nabla^2\vartheta_{ij} + 2(\mathcal{H}' + 2\mathcal{H}^2)\vartheta_{ij} \ . \qquad \text{(A.55)}
\end{aligned}
$$

The components of the unperturbed Ricci tensor follow directly from eq. (2.56) and eq. (A.51),

$$
\bar{R}_{00} = -3\mathcal{H}' \ , \quad \bar{R}_{0i} = 0 \ , \quad \bar{R}_{ij} = (\mathcal{H}' + 2\mathcal{H}^2)\delta_{ij} \ . \qquad \text{(A.56)}
$$

Let us now raise one index of the perturbed Ricci tensor. With

$$
\delta R^{\mu}_{\nu} = \bar{g}^{\mu\rho}\delta R_{\rho\nu} + \delta g^{\mu\rho}\bar{R}_{\rho\nu} \qquad \text{(A.57)}
$$

we obtain

$$
\begin{aligned}
\delta R^0_0 &= -a^{-2}\left[3\psi'' + \nabla^2\phi + 3\mathcal{H}(\phi' + \psi') + 6\mathcal{H}'\phi\right] \ , \qquad \text{(A.58)} \\
\delta R^0_i &= -a^{-2}\left[2\psi'_{,i} + 2\mathcal{H}\phi_{,i} + \frac{1}{2}\nabla^2 h_i - \cancel{(\mathcal{H}' + 2\mathcal{H}^2)h_i} + \cancel{(\mathcal{H}' + 2\mathcal{H}^2)h_i}\right] \\
&= -a^{-2}\left[2(\psi' + \mathcal{H}\phi)_{,i} + \frac{1}{2}\nabla^2 h_i\right] \ , \qquad \text{(A.59)} \\
\delta R^i_0 &= a^{-2}\left[2\psi'_{,i} + 2\mathcal{H}\phi_{,i} + \frac{1}{2}\nabla^2 h_i - (\mathcal{H}' + 2\mathcal{H}^2)h_i + 3\mathcal{H}'h_i\right] \\
&= a^{-2}\left[2(\psi' + \mathcal{H}\phi)_{,i} + \frac{1}{2}\nabla^2 h_i + 2(\mathcal{H}' - \mathcal{H}^2)h_i\right] \ , \qquad \text{(A.60)} \\
\delta R^i_j &= a^{-2}\left[\delta R_{ij} + 2(\mathcal{H}' + 2\mathcal{H}^2)(\psi\delta_{ij} - \vartheta_{ij})\right] \\
&= -a^{-2}\left[\psi'' + \mathcal{H}(\phi' + 5\psi') + 2(\mathcal{H}' + 2\mathcal{H}^2)\phi - \nabla^2\psi\right]\delta_{ij} \\
&\quad + a^{-2}\left[(\psi - \phi)_{,ij} + \frac{1}{2}(h_{i,j} + h_{j,i})' + \mathcal{H}(h_{i,j} + h_{j,i}) + \vartheta''_{ij} + 2\mathcal{H}\vartheta'_{ij} - \nabla^2\vartheta_{ij}\right] \ . \qquad \text{(A.61)}
\end{aligned}
$$

Computing the unperturbed trace $\bar{R}^{\mu}_{\mu}$ with eq. (A.56), we obtain the Ricci scalar at zeroth order,

$$
\frac{1}{2}\bar{R} = 3a^{-2}(\mathcal{H}' + \mathcal{H}^2) \ . \qquad \text{(A.62)}
$$

The perturbed Ricci scalar follows from eq. (A.58) and eq. (A.61),

$$
\begin{aligned}
\frac{1}{2}\delta R = \frac{1}{2}\delta R^{\mu}_{\mu} &= \frac{1}{2}(\delta R^0_0 + \delta R^i_i) \\
&= \frac{a^{-2}}{2}\left[-3\psi'' - \nabla^2\phi - 3\mathcal{H}(\phi' + \psi') - 6\mathcal{H}'\phi\right. \\
&\qquad \left. -3\psi'' - 3\mathcal{H}(\phi' + 5\psi') - 6(\mathcal{H}' + 2\mathcal{H}^2)\phi + 3\nabla^2\psi + \nabla^2(\psi - \phi)\right] \\
&= -a^{-2}\left[3\psi'' + \nabla^2(\phi - 2\psi) + 3\mathcal{H}(\phi' + 3\psi') + 6(\mathcal{H}' + \mathcal{H}^2)\phi\right] \ . \qquad \text{(A.63)}
\end{aligned}
$$

**Einstein tensor**

We have now all ingredients to compute the perturbed Einstein tensor

$$\delta G^\mu_\nu = \delta R^\mu_\nu - \frac{1}{2}\delta R \delta^\mu_\nu \ . \tag{A.64}$$

We evaluate its components and distinguish the parts involving scalar (s), vector (v) or tensor (t) metric perturbations,

$$\begin{aligned}
\delta G^0_0 &= a^{-2}\Big[ \cancel{-3\psi''} - \cancel{\nabla^2\phi} - 3\mathcal{H}(\cancel{\phi'} + \psi') - \cancel{6\mathcal{H}'\phi} \\
&\qquad \cancel{+3\psi''} + \cancel{\nabla^2\phi} - 2\nabla^2\psi + 3\mathcal{H}(\cancel{\phi'} + 3\psi') + 6(\cancel{\mathcal{H}'} + \mathcal{H}^2)\phi \Big] \\
&= 2a^{-2} \underbrace{\Big[ 3\mathcal{H}(\psi' + \mathcal{H}\phi) - \nabla^2\psi \Big]}_{\text{s}} \ ,
\end{aligned} \tag{A.65}$$

$$\delta G^0_i = \delta R^0_i = -a^{-2}[\ \underbrace{2(\psi' + \mathcal{H}\phi)_{,i}}_{\text{s}} + \underbrace{\nabla^2 h_i/2}_{\text{v}}\ ] \ , \tag{A.66}$$

$$\delta G^i_0 = \delta R^i_0 = a^{-2}[\ \underbrace{2(\psi' + \mathcal{H}\phi)_{,i}}_{\text{s}} + \underbrace{\nabla^2 h_i/2 + 2(\mathcal{H}' - \mathcal{H}^2)h_i}_{\text{v}}\ ] \ , \tag{A.67}$$

$$\begin{aligned}
\delta G^i_j &= -a^{-2}\Big[ \psi'' + \mathcal{H}(\phi' + 5\psi') + 2(\mathcal{H}' + 2\mathcal{H}^2)\phi - \nabla^2\psi \\
&\qquad -3\psi'' - \nabla^2(\phi - 2\psi) - 3\mathcal{H}(\phi' + 3\psi') - 6(\mathcal{H}' + \mathcal{H}^2)\phi \Big]\delta_{ij} \\
&\quad + a^{-2}\left[ (\psi - \phi)_{,ij} + \frac{1}{2}(h_{i,j} + h_{j,i})' + \mathcal{H}(h_{i,j} + h_{j,i}) + \vartheta''_{ij} + 2\mathcal{H}\vartheta'_{ij} - \nabla^2\vartheta_{ij} \right] \\
&= 2a^{-2} \underbrace{\Big[ \psi'' + \mathcal{H}(2\psi' + \phi' + \mathcal{H}\phi) + 2\mathcal{H}'\phi + \nabla^2(\phi - \psi)/3 \Big]}_{\text{s}}\delta_{ij} + \underbrace{a^{-2}[\ \circledast\ ]}_{\text{tr=0}} \ ,
\end{aligned} \tag{A.68}$$

$$\circledast = \underbrace{\left(\partial_i\partial_j - \delta_{ij}\nabla^2/3\right)(\psi - \phi)}_{\text{s}} + \underbrace{\left(\partial_0/2 + \mathcal{H}\right)(h_{i,j} + h_{j,i})}_{\text{v}} + \underbrace{\vartheta''_{ij} + 2\mathcal{H}\vartheta'_{ij} - \nabla^2\vartheta_{ij}}_{\text{t}} \ .$$

These results are summed up in eqs. (2.66)–(2.69).

## A.3 Simplifying Einstein's equations for scalar perturbations at inflation

In this section we reduce the evolution equations for the metric and inflaton perturbations during inflation, *cf.* eqs. (3.40)–(3.43). As only two of the four equations are independent, we choose two of the Einstein equations, *viz.*

$$\nabla^2\psi = 4\pi G\left[ \bar\varphi'\delta\varphi'_{\text{N}} - \psi(\bar\varphi')^2 + \mathcal{H}\bar\varphi'\delta\varphi_{\text{N}} - \bar\varphi''\delta\varphi_{\text{N}} \right] \ , \tag{A.69}$$

$$\psi' + \mathcal{H}\psi = 4\pi G\bar\varphi'\delta\varphi_{\text{N}} \ . \tag{A.70}$$

The following identity, obtained by adding eqs. (3.9) and (3.10), turns out to be useful,

$$\mathcal{H}^2 - \mathcal{H}' = 4\pi G(\bar\varphi')^2 \ . \tag{A.71}$$

The results of this section are used in section 3.2 to compute the early universe observables predicted by the theory of inflation.

Let us start by rewriting the given system of equations in terms of the curvature perturbation,

$$\mathcal{R} \overset{(3.36)}{=} -\psi - \frac{\mathcal{H}}{\bar{\varphi}'}\delta\varphi_{\mathrm{N}} \ . \tag{A.72}$$

We use eq. (A.71) and eq. (A.70) to manipulate the right-hand side of eq. (A.69),

$$\begin{aligned}
(\text{A.69})_{\mathrm{R}} \ &= \ 4\pi G\frac{(\bar{\varphi}')^2}{\mathcal{H}}\left[-\psi\mathcal{H} + \frac{\mathcal{H}^2}{\bar{\varphi}'}\delta\varphi_{\mathrm{N}} + \frac{\mathcal{H}}{\bar{\varphi}'}\delta\varphi_{\mathrm{N}}' - \mathcal{H}\frac{\bar{\varphi}''}{(\bar{\varphi}')^2}\delta\varphi_{\mathrm{N}}\right] \\
&\overset{(\text{A.71})}{\underset{(\text{A.70})}{=}} \ 4\pi G\frac{(\bar{\varphi}')^2}{\mathcal{H}}\left[\psi' - \cancel{4\pi G\bar{\varphi}'\delta\varphi_{\mathrm{N}}} + \frac{\mathcal{H}'}{\bar{\varphi}'}\delta\varphi_{\mathrm{N}} + \cancel{4\pi G\bar{\varphi}'\delta\varphi_{\mathrm{N}}} + \frac{\mathcal{H}}{\bar{\varphi}'}\delta\varphi_{\mathrm{N}}' - \mathcal{H}\frac{\bar{\varphi}''}{(\bar{\varphi}')^2}\delta\varphi_{\mathrm{N}}\right] \\
&= \ 4\pi G\frac{(\bar{\varphi}')^2}{\mathcal{H}}\left(\psi + \mathcal{H}\frac{\delta\varphi_{\mathrm{N}}}{\bar{\varphi}'}\right)' \overset{(\text{A.72})}{=} -4\pi G\frac{(\bar{\varphi}')^2}{\mathcal{H}}\mathcal{R}' \ .
\end{aligned} \tag{A.73}$$

With the left-hand side of eq. (A.69) this yields

$$\nabla^2\psi = -4\pi G\frac{(\bar{\varphi}')^2}{\mathcal{H}}\mathcal{R}' \ . \tag{A.74}$$

We thus guess new variables

$$f \equiv -z\mathcal{R} \ , \quad z \equiv \frac{\bar{\varphi}'}{\mathcal{H}} \qquad \overset{(\text{A.72})}{\Longrightarrow} \qquad \delta\varphi_{\mathrm{N}} = f - z\psi \ . \tag{A.75}$$

In terms of $f$ and $z$ eq. (A.74) becomes

$$\nabla^2\psi = 4\pi G\mathcal{H}z^2\left(\frac{f}{z}\right)' \ . \tag{A.76}$$

We rewrite also eq. (A.70) substituting $\delta\varphi_{\mathrm{N}}$ with $f$, $z$ and $\psi$,

$$\begin{aligned}
(\text{A.70}) \quad &\Longleftrightarrow \quad \psi' + \mathcal{H}\psi = 4\pi G\bar{\varphi}'(f - z\psi) \\
&\overset{(\text{A.75})}{\Longleftrightarrow} \quad \psi' + \left(\mathcal{H} + 4\pi G\frac{(\bar{\varphi}')^2}{\mathcal{H}}\right)\psi = 4\pi G\bar{\varphi}' f \\
&\overset{(\text{A.71})}{\Longleftrightarrow} \quad \psi' + \left(2\mathcal{H} - \frac{\mathcal{H}'}{\mathcal{H}}\right)\psi = 4\pi G\bar{\varphi}' f \\
&\Longleftrightarrow \quad \left(\frac{a^2}{\mathcal{H}}\psi\right)' = 4\pi G\hat{z}\hat{f} \ , \qquad \hat{z} \equiv az \ , \quad \hat{f} \equiv af = -\hat{z}\mathcal{R} \ .
\end{aligned} \tag{A.77}$$

Applying the operator $\nabla^2$ to eq. (A.77) and using eq. (A.76) one then gets

$$\begin{aligned}
\nabla^2(\text{A.77}) \quad &\Leftrightarrow \quad \left[\frac{\cancel{a^2}}{\cancel{\mathcal{H}}}\cancel{4\pi G}\frac{\cancel{\mathcal{H}}}{\cancel{a^2}}\hat{z}^2\left(\frac{\hat{f}}{\hat{z}}\right)'\right]' = \cancel{4\pi G}\hat{z}\nabla^2\hat{f} \\
&\Leftrightarrow \quad (\hat{z}\hat{f}' - \hat{z}'\hat{f})' = \hat{z}\nabla^2\hat{f} \\
&\Leftrightarrow \quad \boxed{\hat{f}'' - \frac{\hat{z}''}{\hat{z}}\hat{f} - \nabla^2\hat{f} = 0} \ .
\end{aligned} \tag{A.78}$$

This is a second order differential equation for the variable $\hat{f} = af$. In section 3.2 we see how the variable $f$ turns out to match the inflaton field perturbations in the spatially flat gauge.

## A.4 Statistical properties of small perturbations

In this section we explore the implications of assuming randomly generated small perturbations, and derive useful properties for the computation of ensemble averages in stochastic correlators. For

cosmological perturbations, randomness and Gaussianity are assumed in the space-like directions, while the time evolution is often given deterministically by some evolution equations. In the following we work in co-moving conformal coordinates and denote $x = (\tau, \mathbf{x})$.

Consider a discrete Fourier transformation over space-like directions, in a box of co-moving size $L$ (and physical size $aL$). By construction, each Fourier component $\delta Q_{\mathbf{k}}$ evolves independently and the set $\{\delta Q_{\mathbf{k}}\}$ is the result of a random process, such that we cannot predict the individual values $\delta Q_{\mathbf{k}}$. However, by the central limit theorem, random fluctuations can to a good approximation be described by a Gaussian distribution. A pedagogical and rigorous treatment can be found in [12, p. 433]. Let us discuss a generic scalar Gaussian perturbation (for vector and tensor perturbations all results follow analogously)

$$\delta A(\tau, \mathbf{x}) = \frac{1}{L^3} \sum_{\mathbf{k}} \delta A_{\mathbf{k}}(\tau)\, e^{i\mathbf{k}\cdot\mathbf{x}} \ , \tag{A.79}$$

where the set $\{\delta A_{\mathbf{k}}\}$ is the result of a random process, and each mode $\delta A_{\mathbf{k}}$ evolves according to some given equations. From now on we let the argument $\tau$ implicit for all Fourier coefficients.

If $\delta A(x)$ is assumed to be real, then for the Fourier components $\delta A_{-\mathbf{k}} = \delta A^*_{\mathbf{k}}$, so that one finds even and odd symmetries

$$R_{\mathbf{k}} \equiv \mathrm{Re}(\delta A_{\mathbf{k}}) = R_{-\mathbf{k}} \ , \qquad I_{\mathbf{k}} \equiv \mathrm{Im}(\delta A_{\mathbf{k}}) = -I_{-\mathbf{k}} \tag{A.80}$$

of the real and imaginary part respectively. This means that only half of the momenta $\mathbf{k}$ are independent. Dealing with a Gaussian random process implies that the real quantities $R_{\mathbf{k}}$ and $I_{\mathbf{k}}$ are picked from Gaussian distributions

$$p(R_{\mathbf{k}}) = \frac{1}{\sqrt{2\pi}\sigma_{\mathbf{k}}} \exp\left(-\frac{1}{2}\frac{R^2_{\mathbf{k}}}{\sigma^2_{\mathbf{k}}}\right) \ , \qquad p(I_{\mathbf{k}}) = \frac{1}{\sqrt{2\pi}\sigma_{\mathbf{k}}} \exp\left(-\frac{1}{2}\frac{I^2_{\mathbf{k}}}{\sigma^2_{\mathbf{k}}}\right) \ , \tag{A.81}$$

meaning that the probability of $R_{\mathbf{k}}$ to be in the interval $\mathrm{d}R_{\mathbf{k}}$ is $p(R_{\mathbf{k}})\mathrm{d}R_{\mathbf{k}}$ (similarly for $I_{\mathbf{k}}$). The width of the distribution is described by the dispersion $\sigma_{\mathbf{k}}$, while $\sigma^2_{\mathbf{k}}$ is the variance $(\Delta R_{\mathbf{k}})^2 = \langle R^2_{\mathbf{k}}\rangle - \langle R_{\mathbf{k}}\rangle^2$ from the expectation values $\langle R_{\mathbf{k}}\rangle = 0$ and $\langle I_{\mathbf{k}}\rangle = 0$, as

$$\langle R^2_{\mathbf{k}}\rangle \equiv \int_{-\infty}^{\infty} \mathrm{d}R_{\mathbf{k}}\, R^2_{\mathbf{k}}\ p(R_{\mathbf{k}}) = \sigma^2_{\mathbf{k}} = \langle I^2_{\mathbf{k}}\rangle \qquad \Rightarrow \quad \langle|\delta A_{\mathbf{k}}|^2\rangle = \langle R^2_{\mathbf{k}}\rangle + \langle I^2_{\mathbf{k}}\rangle = 2\sigma^2_{\mathbf{k}} \ . \tag{A.82}$$

Note that, if we restrict to the corresponding domain of $\mathbf{k}$-space, the variables $\{R_{\mathbf{k}}, I_{\mathbf{k}}\}$ are all independent, $\langle R_{\mathbf{k}}, I_{\mathbf{k}}\rangle = 0$ and $\langle R_{\mathbf{k}} R_{\mathbf{k}'}\rangle = \langle I_{\mathbf{k}} I_{\mathbf{k}'}\rangle = 0$ for $\mathbf{k}' \neq \mathbf{k}$, but $R_{\mathbf{k}}$ and $I_{\mathbf{k}}$ have the same variance $\sigma^2_{\mathbf{k}}$. Except for the reality condition, the different $\delta A_{\mathbf{k}}$ are therefore independent random variables obeying

$$\langle \delta A^*_{\mathbf{k}} \delta A_{\mathbf{k}'}\rangle = 2\delta_{\mathbf{k}\mathbf{k}'}\sigma^2_{\mathbf{k}} = \delta_{\mathbf{k}\mathbf{k}'}\langle|\delta A_{\mathbf{k}}|^2\rangle \ . \tag{A.83}$$

In particular, this relation holds also for $\mathbf{k}' = -\mathbf{k}$ as $\langle \delta A_{-\mathbf{k}}\delta A_{-\mathbf{k}}\rangle = \langle R^2_{-\mathbf{k}} + 2iR_{-\mathbf{k}}I_{-\mathbf{k}} - I^2_{-\mathbf{k}}\rangle = 0$.

We assume here that fluctuations are produced democratically in all directions, such that the variance $\sigma^2_{\mathbf{k}} = \sigma^2_k$ is independent of the direction of $\mathbf{k}$, where $k = |\mathbf{k}|$. Since $\delta A(x)$ is a perturbation, it satisfies $\langle \delta A(x)\rangle = 0$, while the magnitude of the perturbation is given by the positive quantity

$$\langle \delta A(x)^2\rangle = \frac{1}{L^6}\sum_{\mathbf{k},\mathbf{k}'}\langle \delta A^*_{\mathbf{k}}\delta A_{\mathbf{k}'}\rangle e^{i(\mathbf{k}'-\mathbf{k})\cdot\mathbf{x}} = \frac{1}{L^6}\sum_{k}\langle|\delta A_k|^2\rangle = \frac{2}{L^6}\sum_k \sigma^2_k \ . \tag{A.84}$$

## Power spectrum

The dependence of the variance of $\delta A_{\mathbf{k}}$ on the wave number $k$ is called the power spectrum of $A$,[54]

$$\mathcal{P}_A(\tau, k) \equiv \left(\frac{1}{2\pi L}\right)^3 4\pi k^3 \langle|\delta A_k|^2\rangle \ , \tag{A.85}$$

[54]Often used is also the spectral density $P_A(\tau,k) \equiv \frac{1}{L^3}\langle|\delta A_k|^2\rangle = \frac{2\pi^2}{k^3}\mathcal{P}_A(\tau,k)$.

which is commonly used to parametrize the variance of $\delta A(x)$,

$$\sigma_A^2(x) \equiv \langle \delta A(x)^2 \rangle = \frac{1}{L^6} \sum_k \langle |\delta A_k|^2 \rangle = \left(\frac{2\pi}{L}\right)^3 \sum_k \frac{1}{4\pi k^3} \mathcal{P}_A(\tau, k) \ . \tag{A.86}$$

At this point we take the limit of large box size $L \to \infty$, replacing series with integrals,

$$\delta A(\tau, \mathbf{x}) = \int \frac{\mathrm{d}^3 k}{(2\pi)^3} \, \delta A(\tau, \mathbf{k}) \, e^{i\mathbf{k}\cdot\mathbf{x}} \ , \qquad \delta A(\tau, \mathbf{k}) = \int \mathrm{d}^3 x \, \delta A(\tau, \mathbf{x}) \, e^{-i\mathbf{k}\cdot\mathbf{x}} \ , \tag{A.87}$$

such that we have the correspondences

$$\frac{1}{L^3} \sum_{\mathbf{k}} \ \to \ \int \frac{\mathrm{d}^3 k}{(2\pi)^3} \, , \qquad \delta A_{\mathbf{k}} \ \to \ \delta A(\tau, \mathbf{k}) \ . \tag{A.88}$$

In the infinite volume limit, eq. (A.86) becomes

$$\sigma_A^2(x) = \frac{1}{4\pi} \int \frac{\mathrm{d}^3 k}{k^3} \, \mathcal{P}_A(\tau, k) = \int_0^\infty \frac{\mathrm{d}k}{k} \, \mathcal{P}_A(\tau, k) = \int_{-\infty}^\infty \mathrm{d} \ln k \, \mathcal{P}_A(\tau, k) \ . \tag{A.89}$$

The power spectrum $\mathcal{P}_A(\tau, k)$ describes the contribution to the variance per logarithmic interval. Since $\mathcal{P}_A(\tau, k)$ represents the meeting point among theoretical predictions, simulations and observations, it is important to understand how it is evaluated from different sides.

## Translation invariance in space and momentum conservation

The equivalence among the different prescriptions follows form translation invariance and stochasticity. These two properties allow us to express statistical averages as spatial averages, and eventually evaluate them over the initial conditions. In an expanding homogeneous and isotropic universe, we can use translation invariance in space-like directions, but generically not in time.[55] In our applications, small stochastic fluctuations $\delta A(\tau, \mathbf{x})$ satisfy some differential equation

$$\mathcal{D} \, \delta A(\tau, \mathbf{x}) = \rho(\tau, \mathbf{x}) \ , \tag{A.90}$$

$$\Rightarrow \ \delta A(\tau, \mathbf{x}) = \int_0^\tau \mathrm{d}\tau_1 \int \mathrm{d}^3 y \, G_{\mathrm{R}}(\tau, \tau_1, \mathbf{x} - \mathbf{y}) \, \rho(\tau_1, \mathbf{y}) \ , \tag{A.91}$$

where the coefficients of the differential operator $\mathcal{D}$ do not depend on $\mathbf{x}$. Then $\mathcal{D}$ and thus also the Green's function $G_{\mathrm{R}} \equiv \mathcal{D}^{-1}$ are translationally (and rotationally) invariant and we can assume $G_{\mathrm{R}}(\tau, \tau_1, \mathbf{x} - \mathbf{y}) = G_{\mathrm{R}}(\tau, \tau_1, |\mathbf{x} - \mathbf{y}|)$.

If the observable $\mathcal{O}[A] \equiv A^2$ is quadratic in $A$ and we want to evaluate its average over the observed final state over different realizations, then we are considering the equal-time correlator. Translational invariance implies that the equal-time correlator evaluated at two different space locations $\mathbf{x}_{1,2}$ is a function of the distance,

$$\langle \delta A(\tau, \mathbf{x}_1) \, \delta A(\tau, \mathbf{x}_2) \rangle = \langle \delta A(\tau, \mathbf{x}_1 - \mathbf{x}_2) \, \delta A(\tau, \mathbf{0}) \rangle \ . \tag{A.92}$$

[55] Time translation invariance is a property of Minkowskian space-time, that allows similar manipulations of the correlators when the nature of the source is not stochastic, but the background is static. Some results may thus appear in a similar form.

Fourier-transforming to co-moving momentum yields

$$\begin{aligned}\langle \delta A(\tau,\mathbf{k}_1)\,\delta A^*(\tau,\mathbf{k}_2)\rangle &= \int \mathrm{d}^3x_1 \int \mathrm{d}^3x_2\, e^{-i(\mathbf{x}_1\cdot\mathbf{k}_1-\mathbf{x}_2\cdot\mathbf{k}_2)}\langle \delta A(\tau,\mathbf{x}_1)\,\delta A(\tau,\mathbf{x}_2)\rangle \\ &= \int \mathrm{d}^3x_1 \int \mathrm{d}^3x_2\, e^{-i(\mathbf{x}_1\cdot\mathbf{k}_1-\mathbf{x}_2\cdot\mathbf{k}_2)}\langle \delta A(\tau,\mathbf{x}_1-\mathbf{x}_2)\,\delta A(\tau,\mathbf{0})\rangle \\ &\overset{\mathbf{x}_1\to\mathbf{x}_1+\mathbf{x}_2}{=} \int \mathrm{d}^3x_1 \int \mathrm{d}^3x_2\, e^{-i\mathbf{x}_2\cdot(\mathbf{k}_1-\mathbf{k}_2)}e^{-i\mathbf{x}_1\cdot\mathbf{k}_1}\langle \delta A(\tau,\mathbf{x}_1)\,\delta A(\tau,\mathbf{0})\rangle \\ &= (2\pi)^3\delta^{(3)}(\mathbf{k}_1-\mathbf{k}_2)\underbrace{\int \mathrm{d}^3x_1\, e^{-i\mathbf{x}_1\cdot\mathbf{k}_1}\langle \delta A(\tau,\mathbf{x}_1)\,\delta A(\tau,\mathbf{0})\rangle}_{\equiv P_A(\tau,\mathbf{k}_1)}\,, \end{aligned} \tag{A.93}$$

which can be interpreted as momentum conservation (Noether's theorem). Therefore, when we compute the equal-time correlator of an operator taken twice at the same location, in co-moving momentum space this amounts to

$$\begin{aligned}\langle \delta A(\tau,\mathbf{x})\,\delta A(\tau,\mathbf{x})\rangle &= \int \frac{\mathrm{d}^3k_1}{(2\pi)^3}\int \frac{\mathrm{d}^3k_2}{(2\pi)^3}\, e^{i\mathbf{x}\cdot(\mathbf{k}_1-\mathbf{k}_2)}(2\pi)^3\delta^{(3)}(\mathbf{k}_1-\mathbf{k}_2)P_A(\tau,\mathbf{k}_1) \\ &= \int \frac{\mathrm{d}^3k_1}{(2\pi)^3}P_A(\tau,\mathbf{k}_1) = \int_0^\infty \mathrm{d}k_1\, k_1^2 \int \frac{\mathrm{d}\Omega_{\mathbf{k}_1}}{(2\pi L)^3}\,\langle \delta A(\tau,\mathbf{k}_1)\,\delta A^*(\tau,\mathbf{k}_1)\rangle\,, \end{aligned} \tag{A.94}$$

where $\mathrm{d}\Omega_{\mathbf{k}} \equiv \mathrm{d}\phi\,\mathrm{d}\theta\sin\theta$ is the infinitesimal solid angle of $\mathbf{k} = k(\sin\theta\cos\phi, \sin\theta\sin\phi, \cos\theta)$ in spherical coordinates. For simplicity we omit the limit $\lim_{L\to\infty}$ in the infinite spatial volume $L^3$ that arises from $(2\pi)^3\delta^{(3)}(\mathbf{0}) = \int_{\mathbf{x}} = \lim_{L\to\infty} L^3$ in eq. (A.93).

Looking at the result in eq. (A.94), we observe that indeed the right-hand side does not depend on $\mathbf{x}$ any more. We identify the power spectrum $\mathcal{P}_A(\tau,k)$ as the angular average of the equal-time and equal-momentum statistical correlator of $A$, on a logarithmic scale $\mathrm{d}\ln k = \mathrm{d}k/k$,

$$\mathcal{P}_A(\tau,k) \equiv \frac{k^3}{(2\pi L)^3}\int \mathrm{d}\Omega_{\mathbf{k}}\,\langle \delta A(\tau,\mathbf{k})\,\delta A^*(\tau,\mathbf{k})\rangle\,. \tag{A.95}$$

If the fluctuations $\delta A$ are produced randomly at all scales and in all directions, such that the spectral density $P_A$ only depends on $k \equiv |\mathbf{k}|$, then the average over the direction of $\mathbf{k}$ is trivial,

$$\langle \delta A(\tau,\mathbf{x})\,\delta A(\tau,\mathbf{x})\rangle = \int_0^\infty \mathrm{d}k\, k^2 \frac{4\pi}{(2\pi)^3}P_A(\tau,k) = \int_{-\infty}^\infty \mathrm{d}\ln k\, \underbrace{\frac{k^3}{2\pi^2}P_A(\tau,k)}_{=\mathcal{P}_A(\tau,k)}\,. \tag{A.96}$$

## Statistical vs. spatial averages

A statistical average, like the one in eqs. (A.92)–(A.94), is generically defined as the weighted sum over all possible configurations,

$$\langle \mathcal{O}[A]\rangle \equiv \sum_i p_i\,\mathcal{O}[A^{(i)}]\,, \tag{A.97}$$

with $p_i$ the probability to realize the $i$-th configuration. If the interactions underlying $A$ are random, and many different configurations are possible, then far away regions are uncorrelated, and for the generic 2-point function[56] at unequal times we have

$$\langle \mathcal{O}(\tau_1,\mathbf{x})\,\mathcal{O}(\tau_2,\mathbf{y})\rangle \overset{|\mathbf{x}-\mathbf{y}|\to\infty}{\longrightarrow} \langle \mathcal{O}(\tau_1,\mathbf{x})\rangle\langle \mathcal{O}(\tau_2,\mathbf{y})\rangle\,. \tag{A.98}$$

In most systems, the approach to this limit is exponentially fast, such that we can write

$$\langle \mathcal{O}(\tau_1,\mathbf{x})\,\mathcal{O}(\tau_2,\mathbf{y})\rangle = \langle \mathcal{O}(\tau_1,\mathbf{x})\rangle\langle \mathcal{O}(\tau_2,\mathbf{y})\rangle + f(\tau_1,\tau_2,\mathbf{x}-\mathbf{y})e^{-|\mathbf{x}-\mathbf{y}|/\xi}\,, \tag{A.99}$$

[56] That corresponds to a 4-point function in $A$, if $\mathcal{O}$ is quadratic in $A$.

where $\xi$ is the characteristic correlation length of the system. Therefore, if we observe and measure $\mathcal{O}[A]$ in domains separated by a distance which is large compared with $\xi$, we do not obtain information about the non-trivial quadrupole moment $f$ of $A$, but instead we are probing distinct representations of the ensemble, with their respective probabilities.

We can therefore replace the statistical average in eq. (A.97) by a volume average over a volume that is large compared with the correlation length of the ensemble. Transforming to co-moving momentum we find,

$$\langle \mathcal{O}[A](\tau,\mathbf{x})\rangle = \frac{1}{L^3}\int \mathrm{d}^3x\, \delta A(\tau,\mathbf{x})\delta A(\tau,\mathbf{x}) \tag{A.100}$$

$$= \frac{1}{L^3}\int \mathrm{d}^3x \int \frac{\mathrm{d}^3k_1}{(2\pi)^3}\int \frac{\mathrm{d}^3k_2}{(2\pi)^3}\, e^{i\mathbf{x}\cdot(\mathbf{k}_1-\mathbf{k}_2)}\delta A(\tau,\mathbf{k}_1)\delta A^*(\tau,\mathbf{k}_2) \tag{A.101}$$

$$= \int \frac{\mathrm{d}^3k}{(2\pi L)^3}\,\delta A(\tau,\mathbf{k})\delta A^*(\tau,\mathbf{k})\ . \tag{A.102}$$

To summarize, we have found that, as a consequence of space-translational invariance, and for random interactions, the statistical average of the quadratic observable $\mathcal{O}(\tau,\mathbf{x})$ can be written as the average of its counterpart in momentum space $\tilde{\mathcal{O}}(\tau,\mathbf{k})$, over all momenta $\mathbf{k}$,

$$\langle \mathcal{O}[A](\tau,\mathbf{x})\rangle = \int_{-\infty}^{\infty}\mathrm{d}\ln k\,\frac{k^3}{(2\pi L)^3}\int \mathrm{d}\Omega_{\mathbf{k}}\,\tilde{\mathcal{O}}[A](\tau,\mathbf{k})\ ,\quad \tilde{\mathcal{O}}(\tau,\mathbf{k})\equiv \delta A(\tau,\mathbf{k})\,\delta A^*(\tau,\mathbf{k})\ . \tag{A.103}$$

For the power spectrum $\mathcal{P}_A(\tau,k)$, this means it is entirely determined by the average over the direction of $\mathbf{k}$,

$$\boxed{\mathcal{P}_A(\tau,k) = \frac{k^3}{(2\pi L)^3}\int \mathrm{d}\Omega_{\mathbf{k}}\,\delta A(\tau,\mathbf{k})\delta A^*(\tau,\mathbf{k})\ ,} \tag{A.104}$$

provided that $A$ is the result of a random process and the physics is invariant under translations in space. Analogous results can be found applying time-translation invariance in Minkowski space.

## Average over initial vs. final ensemble

If we now go back to eq. (A.91) and transform this to co-moving momentum space,

$$\begin{aligned} A(\tau,\mathbf{k}) &= \int \mathrm{d}^3x\int_0^\tau \mathrm{d}\tau_1\int \mathrm{d}^3y\, G_{\mathrm{R}}(\tau,\tau_1,|\mathbf{x}-\mathbf{y}|)\,\rho(\tau_1,\mathbf{y})\,e^{-i\mathbf{k}\cdot\mathbf{x}} \\ &= \int_0^\tau \mathrm{d}\tau_1\int \mathrm{d}^3y\,\rho(\tau_1,\mathbf{y})e^{-i\mathbf{k}\cdot\mathbf{y}}\int \mathrm{d}^3x\, G_{\mathrm{R}}(\tau,\tau_1,|\mathbf{x}-\mathbf{y}|)e^{-i\mathbf{k}\cdot(\mathbf{x}-\mathbf{y})} \\ &= \int_0^\tau \mathrm{d}\tau_1\,\rho(\tau_1,\mathbf{k})\,G_{\mathrm{R}}(\tau,\tau_1,k)\ , \end{aligned} \tag{A.105}$$

then the power spectrum in eq. (A.104) can be written as

$$\boxed{\mathcal{P}_A(\tau,k) = \frac{k^3}{(2\pi L)^3}\int \mathrm{d}\Omega_{\mathbf{k}}\left|\int_0^\tau \mathrm{d}\tau_1\,\rho(\tau_1,\mathbf{k})\,G_{\mathrm{R}}(\tau,\tau_1,k)\right|^2\ .} \tag{A.106}$$

Yet another representation is obtained by noting that, since the statistical properties of $A$ are determined by the properties of the source $\rho$,[57] then the statistical average in eq. (A.96) can be transported to the initial state. Assuming the latter to be invariant under space translations as

[57] The contribution of the Green's function $G$ is deterministic as dictated by the evolution equation (A.90).

| | $\mathcal{P}_A(\tau,k)$ | $\mathcal{P}_\rho(\tau_1,\tau_2,k)$ |
|---|---|---|
| **experiments** | spatial average over measured $\delta A$: eq. (A.104) | - |
| **theory** | from $\mathcal{P}_\rho(\tau_1,\tau_2,k)$: eq. (A.107) | ensemble average |
| **simulations** | spatial average over randomly generated $\rho$: eq. (A.106) | - |

Table A.2: Comparison of experimental, theoretical and computational methods to obtain the power spectrum $\mathcal{P}_A$ of the perturbations of a physical quantity, sourced by a stochastic source $\rho$.

well, we find

$$
\begin{aligned}
\langle \delta A(\tau,\mathbf{x})\delta A(\tau,\mathbf{x})\rangle &= \int_0^\tau \mathrm{d}\tau_1 \int_0^\tau \mathrm{d}\tau_2 \int \mathrm{d}^3y_1 \int \mathrm{d}^3y_2\, G_{\mathrm{R}}(\tau,\tau_1,|\mathbf{y}_1-\mathbf{x}|)G_{\mathrm{R}}(\tau,\tau_2,|\mathbf{y}_2-\mathbf{x}|) \\
&\qquad \times \langle \rho(\tau_1,\mathbf{y}_1)\rho^*(\tau_2,\mathbf{y}_2)\rangle \\
&= \int_0^\tau \mathrm{d}\tau_1 \int_0^\tau \mathrm{d}\tau_2 \int \mathrm{d}^3y_1 \int \mathrm{d}^3y_2 \int \frac{\mathrm{d}^3k_1}{(2\pi)^3}\int \frac{\mathrm{d}^3k_2}{(2\pi)^3} e^{i\mathbf{x}\cdot(\mathbf{k}_1+\mathbf{k}_2)} e^{-i\mathbf{y}_1\cdot\mathbf{k}_1} e^{-i\mathbf{y}_2\cdot\mathbf{k}_2} \\
&\qquad \times G_{\mathrm{R}}(\tau,\tau_1,k_1)G_{\mathrm{R}}(\tau,\tau_2,k_2)\,\langle \rho(\tau_1,\mathbf{y}_1)\rho^*(\tau_2,\mathbf{y}_2)\rangle \\
&\overset{\mathbf{k}_2\to-\mathbf{k}_2}{=} \int_0^\tau \mathrm{d}\tau_1 \int_0^\tau \mathrm{d}\tau_2 \int \mathrm{d}^3y_1 \int \mathrm{d}^3y_2 \int \frac{\mathrm{d}^3k_1}{(2\pi)^3}\int \frac{\mathrm{d}^3k_2}{(2\pi)^3} e^{i\mathbf{x}\cdot(\mathbf{k}_1-\mathbf{k}_2)} e^{-i\mathbf{y}_1\cdot\mathbf{k}_1} e^{i\mathbf{y}_2\cdot\mathbf{k}_2} \\
&\qquad \times G_{\mathrm{R}}(\tau,\tau_1,k_1)G_{\mathrm{R}}(\tau,\tau_2,k_2)\,\langle \rho(\tau_1,\mathbf{y}_1)\rho^*(\tau_2,\mathbf{y}_2)\rangle \\
&= \int_0^\tau \mathrm{d}\tau_1 \int_0^\tau \mathrm{d}\tau_2 \int \frac{\mathrm{d}^3k_1}{(2\pi)^3}\int \frac{\mathrm{d}^3k_2}{(2\pi)^3} e^{i\mathbf{x}\cdot(\mathbf{k}_1-\mathbf{k}_2)} G_{\mathrm{R}}(\tau,\tau_1,k_1)G_{\mathrm{R}}(\tau,\tau_2,k_2) \\
&\qquad \times \langle \rho(\tau_1,\mathbf{k}_1)\rho^*(\tau_2,\mathbf{k}_2)\rangle \\
&= \int_0^\tau \mathrm{d}\tau_1 \int_0^\tau \mathrm{d}\tau_2 \int \frac{\mathrm{d}^3k_1}{(2\pi)^3}\int \frac{\mathrm{d}^3k_2}{(2\pi)^3} e^{i\mathbf{x}\cdot(\mathbf{k}_1-\mathbf{k}_2)} G_{\mathrm{R}}(\tau,\tau_1,k_1)G_{\mathrm{R}}(\tau,\tau_2,k_2) \\
&\qquad \times (2\pi)^3\delta(\mathbf{k}_1-\mathbf{k}_2)P_\rho(\tau_1,\tau_2,\mathbf{k}_1) \\
&= \boxed{\int_{-\infty}^{\infty}\mathrm{d}\ln k \underbrace{\int_0^\tau \mathrm{d}\tau_1 \int_0^\tau \mathrm{d}\tau_2\, G_{\mathrm{R}}(\tau,\tau_1,k)G_{\mathrm{R}}(\tau,\tau_2,k)\mathcal{P}_\rho(\tau_1,\tau_2,\mathbf{k})}_{\mathcal{P}_A(\tau,k)}} \,. \qquad \text{(A.107)}
\end{aligned}
$$

Comparing eqs. (A.106) and (A.107) for the unequal-time power spectrum of the source $\rho$ we conclude

$$
\mathcal{P}_\rho(\tau_1,\tau_2,k) = \frac{k^3}{(2\pi L)^3}\int \mathrm{d}\Omega_{\mathbf{k}}\,\rho(\tau_1,\mathbf{k})\rho^*(\tau_2,\mathbf{k}) = \frac{k^3}{2\pi^2}P_\rho(\tau_1,\tau_2,k)\,. \qquad \text{(A.108)}
$$

The very same conclusion would follow from applying the reasoning in eq. (A.104) for $\rho$. This means that assuming space-translation invariance and randomness for the final state is equivalent to the same assumptions for the initial state.

Having shown their equivalence, different methods to compute the power spectrum from the experimental, theoretical and computational point of view are summarized in table A.2.

# Appendix B

# The retarded pseudoscalar correlator

The goal of the present appendix is to elaborate on the estimation of the friction coefficient, $\Upsilon$, and the mass correction, $m_{\rm T}$, introduced in chapter 4, for the axion-like-inflaton example of chapter 5. The two quantities are determined respectively by the imaginary and real part of the retarded correlator (cf. eq. (5.24)),

$$G_{\rm R}(\omega) = \int_0^\infty \mathrm{d}t\, e^{i\omega t} \int_{\mathbf{x}} \langle i[J(t,\mathbf{x}), J(0,\mathbf{0})]\rangle_0 \ , \qquad \int_{\mathbf{x}} \equiv \int \mathrm{d}^3x \ , \tag{B.1}$$

of the topological charge density operator

$$f_a J \equiv c_\chi g^2 \epsilon^{\mu\nu\rho\sigma} F^a_{\mu\nu} F^a_{\rho\sigma} \ , \qquad a \in \{1, \ldots, N_c^2 - 1\} \ , \qquad c_\chi \equiv 1/(64\pi^2) \ . \tag{B.2}$$

Here $F^a_{\mu\nu}$ denotes the Yang-Mills field strength defined by

$$T^a F^a_{\mu\nu} \equiv \frac{i}{g}[D_\mu, D_\nu] \ , \qquad D_\mu \equiv \partial_\mu - igT^b A^b_\mu \ , \tag{B.3}$$

where $g^2 \equiv 4\pi\alpha$ is the Yang-Mills coupling and $T^a$ are Hermitean generators of SU($N_c$), normalized as $\mathrm{tr}[T^a, T^b] = \delta^{ab}/2$.

The friction coefficient, cf. eqs. (5.27) and (5.28), is determined using three-dimensional lattice measurements [3]. To compare with the latter, in sec. B.1 we compute the imaginary part of $G_{\rm R}$ in the classical limit. For the mass correction, cf. eq. (5.30), in sec. B.2 we evaluate the real part of $G_{\rm R}$ in the quantum theory for $g^2 \ll 1$.

## B.1 Imaginary part: Chern-Simons diffusion rate

The way how thermal rates can be extracted from equilibrium 2-point correlation functions is described by the so-called Green-Kubo relations. In our case the relation for the inflaton decay rate, cf. eq. (4.21), is

$$\Upsilon = \left.\frac{\mathrm{Im}\, G_{\rm R}(\omega)}{\omega}\right|_{\omega\to m} \ . \tag{B.4}$$

Physical observables on the lattice are however more directly related to a *statistical*, i.e. time-symmetric, correlator,

$$G_{\rm S}(\omega) \equiv \int_{-\infty}^\infty \mathrm{d}t\, e^{i\omega t} G_{\rm S}(t) \ , \qquad G_{\rm S}(t) \equiv f_a^2 \int_{\mathbf{x}} \left\langle \frac{1}{2}\{J(t,\mathbf{x}), J(0,\mathbf{0})\} \right\rangle \ . \tag{B.5}$$

The imaginary part of the retarded correlator can be obtained from eq. (B.5) via

$$G_{\rm S}(\omega) = f_a^2 [1 + 2n_{\rm B}(\omega)]\, \mathrm{Im}\, G_{\rm R}(\omega + i0^+) \ , \tag{B.6}$$

where $n_{\rm B}(\omega) \equiv 1/(e^{\beta\omega}-1)$ is the Bose distribution.

In order to provide a calibration for a lattice study, we want to compute the classical limit,

$$G_{\rm S}^{(\rm cl)}(\omega) \equiv \lim_{\hbar\to 0} G_{\rm S}(\omega) \;, \tag{B.7}$$

perturbatively at $g^2T \ll \omega$. We consider a theory discretized in the spatial directions, with lattice spacing $a$,[58] such that $\omega \sim a^{-1}$, and we quantize it in the gauge $A_0^b = 0$. For this, we transform the time coordinate $t$ to an imaginary-time coordinate $t_{\rm E} \in (0,\beta)$, $\beta \equiv 1/T$, and denote $X \equiv (t_{\rm E}, \mathbf{x})$. Within this framework we obtain the imaginary-time correlator

$$G_{\rm E}(t_{\rm E}) \equiv f_a^2 \int_{\mathbf{x}} \langle J(t_{\rm E},\mathbf{x}), J(0,\mathbf{0})\rangle \;, \qquad 0 < t_{\rm E} < \beta \;, \tag{B.8}$$

$$G_{\rm E}(\omega_n) \equiv \int_0^\beta {\rm d}t_{\rm E}\, e^{i\omega_n t_{\rm E}} G_{\rm E}(t_{\rm E}) \;, \qquad \omega_n = 2\pi n T \;. \tag{B.9}$$

Transforming to frequency space, we obtain the statistical correlator by

$$G_{\rm S}(\omega) = [1 + 2n_{\rm B}(\omega)]\, {\rm Im}\, G_{\rm E}[\omega_n \to -i(\omega + i0^+)] \;. \tag{B.10}$$

For the classical limit we should keep $\hbar$ explicit, so that energies appear as $\hbar\omega$. However, to simplify the computations we suppress $\hbar$ from the notation till the end and finally recall

$$n_{\rm B}(\hbar\omega) \;\stackrel{\hbar\to 0}{\longrightarrow}\; \frac{T}{\hbar\omega} \;. \tag{B.11}$$

## Imaginary-time correlator

The continuum operator in eq. (B.2) can be written as

$$f_a J = 4c_\chi \epsilon_{ijk} g^2 F^b_{0i} F^b_{jk} \;. \tag{B.12}$$

To define the analogue of the continuum field strength on the lattice, we introduce the link matrices

$$U_i(X) = e^{iagT^b A_i^b(X)} = 1 + iagT^b A_i^b(X) + \mathcal{O}(g^2) \;, \quad U_{-i}(X) \equiv U_i^\dagger(X - a\mathbf{i}) \;, \tag{B.13}$$

using the notation $X + \mathbf{y} \equiv X + (0,\mathbf{y})$. The canonical momentum is denoted as $\mathcal{E}_i(X)$, and conveniently averaged for numerical purposes,

$$\bar{\mathcal{E}}_i(X) \equiv \frac{1}{2}\left[\mathcal{E}_i(X) + U_i^\dagger(X - a\mathbf{i})\mathcal{E}_i(X - a\mathbf{i})U_i(X - a\mathbf{i})\right] . \tag{B.14}$$

In the canonical real-time formalism, the Gauss law constraints must be satisfied at any time $t$ and location $\mathbf{x}$ [57, p.63],

$$\mathcal{G}(t,\mathbf{x}) = \mathcal{E}_i(t,\mathbf{x}) - U_i^\dagger(t,\mathbf{x} - a\mathbf{i})\mathcal{E}_i(t,\mathbf{x} - a\mathbf{i})U_i(t,\mathbf{x} - a\mathbf{i}) = 0 \;. \tag{B.15}$$

In the imaginary-time path integral representation of the partition function $\mathcal{Z}$, eq. (B.15) means that we are only interested in the contribution to $\mathcal{Z}$ from the states annihilated by the operator $\mathcal{G}$. The relevant contribution to the partition function can thus be written as a trace over all states, with the insertion of a Kronecker delta function, $\mathcal{Z}_{\rm phys} = {\rm tr}\left[\delta_{\mathcal{G}}\, e^{\beta\hat{H}}\right]$. We may represent the latter with the help of an auxiliary function $\tilde{A}_0^b$,

$$\delta_{\mathcal{G}} \equiv \int \frac{{\rm d}\tilde{A}_0^b}{2\pi}\, e^{i\tilde{A}_0^b \mathcal{G}} \;. \tag{B.16}$$

[58] Note that, throughout the rest of this document, $a$ denotes the cosmological scale factor.

A plaquette is defined as

$$P_{ij}(X) = U_i(X)U_j(X + a\mathbf{i})U_i^\dagger(X + a\mathbf{j})U_j^\dagger(X) \ . \tag{B.17}$$

We rewrite eq. (B.17) by expanding the link matrices as in eq. (B.13). The Fourier transform

$$A_i^b(X) = \sum\!\!\!\!\!\!\int_P A_i^b(P)\, e^{iP\cdot(X+a\mathbf{i}/2)} \tag{B.18}$$

of the gauge field, refers to the notation $\sum\!\!\!\!\!\!\int_P \equiv T\sum_{p_n}\int_{\mathbf{p}}$, and $P = (p_n, \mathbf{p})$, where $p_n = 2n\pi T$ are the Matsubara modes. The spatial integral $\int_{\mathbf{p}} = \int_{-\pi/a}^{\pi/a} d^3p/(2\pi)^3$ is restricted to a Brillouin zone. Up to linear order, the plaquette (B.17) is

$$\begin{aligned}
P_{ij}^b(X) &= 1 + iag\left\{\left[A_i^b(X) - A_i^b(X + a\mathbf{j})\right] - \left[A_j^b(X) - A_j^b(X + a\mathbf{i})\right]\right\} + \mathcal{O}(g^2) \\
&= 1 + iag\sum\!\!\!\!\!\!\int_P e^{iP\cdot X}\left\{A_i^b(P)e^{ia\mathbf{p}\cdot\mathbf{i}/2}e^{ia\mathbf{p}\cdot\mathbf{j}/2}\left[e^{-ia\mathbf{p}\cdot\mathbf{j}/2} - e^{ia\mathbf{p}\cdot\mathbf{j}/2}\right]\right. \\
&\qquad \left. - A_j^b(P)e^{ia\mathbf{p}\cdot\mathbf{j}/2}e^{ia\mathbf{p}\cdot\mathbf{i}/2}\left[e^{-ia\mathbf{p}\cdot\mathbf{i}/2} - e^{ia\mathbf{p}\cdot\mathbf{i}/2}\right]\right\} + \mathcal{O}(g^2) \\
&= 1 + a^2g\sum\!\!\!\!\!\!\int_P e^{iP\cdot X}\left\{A_i^b(P)\tilde{p}_j - A_j^b(P)\tilde{p}_i\right\}e^{ia(p_i+p_j)/2} + \mathcal{O}(g^2) \ ,
\end{aligned} \tag{B.19}$$

where to simplify the expressions we have adopted the notation

$$\tilde{p}_j \equiv \frac{2}{a}\sin\left(\frac{ap_j}{2}\right) \ , \qquad \underset{\sim}{p}_j \equiv \cos\left(\frac{ap_j}{2}\right) \ , \qquad \mathring{p}_j \equiv \frac{1}{a}\sin\left(ap_j\right) = \tilde{p}_j\underset{\sim}{p}_j \ . \tag{B.20}$$

Inverting spatial directions with the definition of $U_{-i}$ in eq. (B.13), the plaquettes become

$$\begin{aligned}
P_{-ij}^b(X) &= 1 + iag\left\{-\left[A_i^b(X - a\mathbf{i}) - A_i^b(X + a\mathbf{j} - a\mathbf{i})\right] - \left[A_j^b(X) - A_j^b(X - a\mathbf{i})\right]\right\} + \mathcal{O}(g^2) \\
&= 1 + iag\sum\!\!\!\!\!\!\int_P e^{iP\cdot X}\left\{-A_i^b(P)e^{-ia\mathbf{p}\cdot\mathbf{i}/2}e^{ia\mathbf{p}\cdot\mathbf{j}/2}\left[e^{-ia\mathbf{p}\cdot\mathbf{j}/2} - e^{ia\mathbf{p}\cdot\mathbf{j}/2}\right]\right. \\
&\qquad \left. -A_j^b(P)e^{ia\mathbf{p}\cdot\mathbf{j}/2}e^{-ia\mathbf{p}\cdot\mathbf{i}/2}\left[e^{ia\mathbf{p}\cdot\mathbf{i}/2} - e^{-ia\mathbf{p}\cdot\mathbf{i}/2}\right]\right\} + \mathcal{O}(g^2)
\end{aligned} \tag{B.21}$$

$$= 1 - a^2g\sum\!\!\!\!\!\!\int_P e^{iP\cdot X}\left\{A_i^b(P)\tilde{p}_j - A_j^b(P)\tilde{p}_i\right\}e^{-ia(p_i-p_j)/2} + \mathcal{O}(g^2)\,, \tag{B.22}$$

$$P_{i-j}^b(X) = 1 - a^2g\sum\!\!\!\!\!\!\int_P e^{iP\cdot X}\left\{A_i^b(P)\tilde{p}_j - A_j^b(P)\tilde{p}_i\right\}e^{ia(p_i-p_j)/2} + \mathcal{O}(g^2)\,, \tag{B.23}$$

$$P_{-i-j}^b(X) = 1 + a^2g\sum\!\!\!\!\!\!\int_P e^{iP\cdot X}\left\{A_i^b(P)\tilde{p}_j - A_j^b(P)\tilde{p}_i\right\}e^{-ia(p_i+p_j)/2} + \mathcal{O}(g^2)\,. \tag{B.24}$$

The *magnetic* part of the field strength tensor $F_{jk}^b(x)$ is given by

$$F_{jk}^b(X) \equiv \frac{-i}{8a^2g}\left[Q_{jk}^b(X) - Q_{kj}^b(X)\right] \ , \tag{B.25}$$

where we have defined

$$\begin{aligned}
Q_{jk}^b(X) &\equiv P_{jk}^b(X) + P_{k-j}^b(X) + P_{-j-k}^b(X) + P_{-kj}^b(X) \\
&= 4 + a^2g\sum\!\!\!\!\!\!\int_P e^{iP\cdot X}\left[A_j^b(P)\tilde{p}_k - A_k^b(P)\tilde{p}_j\right] + \mathcal{O}(g^2) \\
&\qquad \times\left[e^{ia(p_j+p_k)/2} + e^{-ia(p_j-p_k)/2} + e^{-ia(p_j+p_k)/2} + e^{ia(p_j-p_k)/2}\right] + \mathcal{O}(g^2) \\
&= 4 + 2a^2g\sum\!\!\!\!\!\!\int_P e^{iP\cdot X}\left[A_j^b(P)\tilde{p}_k - A_k^b(P)\tilde{p}_j\right]\left[\cos\left(a\frac{p_j+p_k}{2}\right) + \cos\left(a\frac{p_j-p_k}{2}\right)\right] + \mathcal{O}(g^2) \\
&= 4 + 4a^2g\sum\!\!\!\!\!\!\int_P e^{iP\cdot X}\left[A_j^b(P)\tilde{p}_k - A_k^b(P)\tilde{p}_j\right]\cos\left(\frac{ap_j}{2}\right)\cos\left(\frac{ap_k}{2}\right) + \mathcal{O}(g^2) \\
&= 4 + 4a^2g\sum\!\!\!\!\!\!\int_P e^{iP\cdot X}\left[A_j^b(P)\underset{\sim}{p}_j\mathring{p}_k - A_k^b(P)\underset{\sim}{p}_k\mathring{p}_j\right] + \mathcal{O}(g^2) \ .
\end{aligned} \tag{B.26}$$

(B.27)

Then the field in eq. (B.25) can be expressed at zeroth order in $g$ as

$$F^b_{jk}(X) = i \sum\!\!\!\!\!\!\int_P e^{iP\cdot X}\left[\mathring{p}_j \underset{\sim}{p}_k A^b_k(P) - \mathring{p}_k \underset{\sim}{p}_j A^b_j(P)\right] + \mathcal{O}(g) \ . \tag{B.28}$$

A discretized Euclidean *electric* field strength $F^b_{0i}$ can be defined using the auxiliary field $\tilde{A}^b_0$ introduced in eq. (B.16),

$$\tilde{F}_{0i}(X) \equiv \frac{1}{iag}[\partial_{t_\mathrm{E}} U_i(X)]U_i^\dagger(X) + \frac{1}{a}[\tilde{A}_0(X) - U_i(X)\tilde{A}_0(X+a\mathbf{i})U_i^\dagger(X)] \, . \tag{B.29}$$

Similarly to the averaged operator in eq. (B.14), we define

$$\tilde{F}^b_{0i}(X)\big|_{\mathrm{av}} \equiv \frac{1}{2}\left[\tilde{F}^b_{0i}(X) + U_i^\dagger(X-a\mathbf{i})\tilde{F}^b_{0i}(X-a\mathbf{i})U_i(X-a\mathbf{i})\right] \ . \tag{B.30}$$

Expanding $\tilde{A}_0(X)$ in a Fourier representation, like in eq. (B.18), at zeroth order in $g$ we find

$$\begin{aligned}
\tilde{F}^b_{0i}(X) &= \partial_{t_\mathrm{E}} A^b_i(X) + \frac{1}{a}[\tilde{A}^b_0(X) - \tilde{A}^b_0(X+a\mathbf{i})] + \mathcal{O}(g) \\
&= i \sum\!\!\!\!\!\!\int_P p_n A^b_i(P) e^{iP\cdot(X+a\mathbf{i}/2)} + \frac{1}{a}\sum\!\!\!\!\!\!\int_P \tilde{A}^b_0(P) e^{iP\cdot X}\left(1 - e^{i\mathbf{p}\cdot a\mathbf{i}}\right) + \mathcal{O}(g) \\
&= i \sum\!\!\!\!\!\!\int_P e^{iP\cdot(X+a\mathbf{i}/2)}\left[p_n A^b_i(P) - \tilde{p}_i \tilde{A}^b_0(P)\right] + \mathcal{O}(g) \ ,
\end{aligned} \tag{B.31}$$

and the corresponding averaged operator from eq. (B.30) at order $g$ is

$$\tilde{F}^b_{0i}(X)\big|_{\mathrm{av}} = \frac{1}{2}\left[\tilde{F}^b_{0i}(X) + \tilde{F}^b_{0i}(X-a\mathbf{i})\right] + \mathcal{O}(g) = i \sum\!\!\!\!\!\!\int_P e^{iP\cdot X} \underset{\sim}{p}_i \left[p_n A^b_i(P) - \tilde{p}_i \tilde{A}^b_0(P)\right] + \mathcal{O}(g) \ . \tag{B.32}$$

With the results from eqs. (B.28) and (B.32), the topological charge density at order $g^2$ becomes

$$f_a J(X)\big|_{\mathrm{av}} = 8ic_\chi g^2 \epsilon_{ijk} \sum\!\!\!\!\!\!\int_{P,Q} e^{i(P+Q)\cdot X} \underset{\sim}{p}_i (\delta_{\mu i}\, p_n - \delta_{\mu 0}\, \tilde{p}_i) \underset{\sim}{q}_j \mathring{q}_k A^b_\mu(P) A^b_j(Q) + \mathcal{O}(g^4) \ , \tag{B.33}$$

using the notation $\mu \in \{0,1,2,3\}$ and $i,j,k \in \{1,2,3\}$, and summing over repeated Greek indices. To compute the Wick contractions for $G_\mathrm{E}$ (cf. eq. (B.8)), we write

$$f_a J(0)\big|_{\mathrm{av}} = 8ic_\chi g^2 \epsilon_{suv} \sum\!\!\!\!\!\!\int_{P',Q'} \underset{\sim}{p}'_s (\delta_{\alpha s}\, p'_n - \delta_{\alpha 0}\, \tilde{p}'_s) \underset{\sim}{q}'_u \mathring{q}'_v A^b_\alpha(P') A^b_u(Q') + \mathcal{O}(g^4) \ . \tag{B.34}$$

For $G_\mathrm{E}$ we need the two-point correlation function of the gauge fields,

$$\langle A^a_\alpha(P) A^b_\beta(Q)\rangle = \delta^{ab}\, \delta\!\!\!^{-}(P+Q) \Delta_{\alpha\beta}(P) \ , \tag{B.35}$$

where $\Delta_{\alpha\beta}$ denotes the gauge field propagator, and the $\delta$-distribution is defined as

$$\delta\!\!\!^{-}(P+Q) \equiv \beta \delta_{p_n+q_n,0} (2\pi)^3 \delta^{(3)}(\mathbf{p}+\mathbf{q}) = \int_0^\beta \mathrm{d}t_\mathrm{E}\, e^{i(p_n+q_n)t_\mathrm{E}} \int_{\mathbf{x}} e^{i(\mathbf{p}+\mathbf{q})\cdot\mathbf{x}} \ . \tag{B.36}$$

Carrying out the integrals with $\delta$-functions, eliminating the sums with the Dirac-$\delta$'s, and defining $d_\mathrm{A} \equiv \delta^{bc}\delta^{bc} = N_c^2 - 1$, the imaginary-time correlator becomes

$$\begin{aligned}
G_\mathrm{E}(t_\mathrm{E})\big|_{\mathrm{av}} = -64 c_\chi^2 g^4 d_\mathrm{A} T^2 (2\pi)^6 \sum\!\!\!\!\!\!\int_{P,Q} \sum\!\!\!\!\!\!\int_{P',Q'} \int_{\mathbf{x}} \epsilon_{ijk}\epsilon_{suv}\, e^{i(P+Q)\cdot X} \underset{\sim}{p}_i \underset{\sim}{p}'_s \\
\times \underset{\sim}{q}_j \mathring{q}_k \underset{\sim}{q}'_u \mathring{q}'_v (\delta_{\mu i}\, p_n - \delta_{\mu 0}\, \tilde{p}_i)(\delta_{\alpha s}\, p'_n - \delta_{\alpha 0}\, \tilde{p}'_s) \\
\times \big[\delta_{-p_n,p'_n}\delta_{-q_n,q'_n}\delta^{(3)}(\mathbf{p}+\mathbf{p}')\delta^{(3)}(\mathbf{q}+\mathbf{q}')\Delta_{\mu\alpha}(P)\Delta_{ju}(Q) \\
+\delta_{-p_n,q'_n}\delta_{-q_n,p'_n}\delta^{(3)}(\mathbf{p}+\mathbf{q}')\delta^{(3)}(\mathbf{q}+\mathbf{p}')\Delta_{\mu u}(P)\Delta_{j\alpha}(Q)\big] + \mathcal{O}(g^6)
\end{aligned}$$

$$
\begin{aligned}
&= -64c_\chi^2 g^4 d_{\rm A} T^2 \sum_{p_n,q_n} e^{i(p_n+q_n)t_{\rm E}} \int_{\mathbf{p},\mathbf{q}} (2\pi)^3\delta^{(3)}(\mathbf{p}+\mathbf{q})\,\epsilon_{ijk}\epsilon_{suv}\,\underset{\sim}{p}_i \underset{\sim}{q}_j \mathring{q}_k (\delta_{\mu i}\,p_n - \delta_{\mu 0}\,\tilde{p}_i) \\
&\qquad \times \big[\Delta_{\mu\alpha}(P)\Delta_{ju}(Q)\underset{\sim}{p}_s \underset{\sim}{q}_u (-\mathring{q}_v)(-1)(\delta_{\alpha s}\,p_n - \delta_{\alpha 0}\,\tilde{p}_s) \\
&\qquad\quad + \Delta_{\mu u}(P)\Delta_{j\alpha}(Q)\underset{\sim}{q}_s \underset{\sim}{p}_u (-\mathring{p}_v)(-1)(\delta_{\alpha s}\,q_n - \delta_{\alpha 0}\,\tilde{q}_s)\big] + \mathcal{O}(g^6) \\
&= -64c_\chi^2 g^4 d_{\rm A} T^2 \sum_{p_n,q_n} e^{i(p_n+q_n)t_{\rm E}} \int_{\mathbf{p}} \epsilon_{ijk}\epsilon_{suv}\,\underset{\sim}{p}_i \underset{\sim}{p}_j (-\mathring{p}_k)\underset{\sim}{p}_s \underset{\sim}{p}_u \mathring{p}_v (\delta_{\mu i}\,p_n - \delta_{\mu 0}\,\tilde{p}_i) \\
&\qquad \times \big[-\Delta_{\mu\alpha}(p_n,\mathbf{p})\Delta_{ju}(q_n,-\mathbf{p})(\delta_{\alpha s}\,p_n - \delta_{\alpha 0}\,\tilde{p}_s) \\
&\qquad\quad + \Delta_{\mu u}(p_n,\mathbf{p})\Delta_{j\alpha}(q_n,-\mathbf{p})(\delta_{\alpha s}\,q_n + \delta_{\alpha 0}\,\tilde{p}_s)\big] + \mathcal{O}(g^6)\ . \qquad \text{(B.37)}
\end{aligned}
$$

Its Fourier transform is

$$
\begin{aligned}
G_{\rm E}(\omega_n)\big|_{\rm av} &= -64c_\chi^2 g^4 d_{\rm A} T \sum_{p_n,q_n} \delta_{\omega_n+p_n+q_n,0} \int_{\mathbf{p}} \epsilon_{ijk}\epsilon_{suv}\,\underset{\sim}{p}_i \underset{\sim}{p}_j \mathring{p}_k \underset{\sim}{p}_s \underset{\sim}{p}_u \mathring{p}_v (\delta_{\mu i}\,p_n - \delta_{\mu 0}\,\tilde{p}_i) \\
&\qquad \times \big[\Delta_{\mu\alpha}(p_n,\mathbf{p})\Delta_{ju}(q_n,-\mathbf{p})(\delta_{\alpha s}\,p_n - \delta_{\alpha 0}\,\tilde{p}_s) \\
&\qquad\quad - \Delta_{\mu u}(p_n,\mathbf{p})\Delta_{j\alpha}(q_n,-\mathbf{p})(\delta_{\alpha s}\,q_n + \delta_{\alpha 0}\,\tilde{p}_s)\big] + \mathcal{O}(g^6)\ . \qquad \text{(B.38)}
\end{aligned}
$$

Defining $\tilde{p}_0 \equiv p_n$, the longitudinal $\Delta^{\parallel}_{\alpha\beta} \sim \tilde{p}_\alpha \tilde{p}_\beta$ contribution from the propagator vanishes,

$$\Delta^{\parallel}_{\mu\alpha}(p_n,\mathbf{p})(\delta_{\alpha s}\,p_n - \delta_{\alpha 0}\,\tilde{p}_s) \sim \tilde{p}_\mu(\tilde{p}_s p_n - p_n \tilde{p}_s) = 0\ , \qquad \text{(B.39)}$$

$$\Delta^{\parallel}_{j\alpha}(q_n,-\mathbf{p})(\delta_{\alpha s}\,q_n + \delta_{\alpha 0}\,\tilde{p}_s) \sim \tilde{q}_j(-\tilde{p}_s q_n + q_n \tilde{p}_s) = 0\ , \qquad \text{(B.40)}$$

$$\Delta^{\parallel}_{\mu u}(p_n,\mathbf{p})(\delta_{\mu i}\,p_n - \delta_{\mu 0}\,\tilde{p}_i) \sim \tilde{p}_u(\tilde{p}_i p_n - p_n \tilde{p}_i) = 0\ , \qquad \text{(B.41)}$$

$$\Delta^{\parallel}_{ju}(q_n,-\mathbf{p})\epsilon_{ijk}\epsilon_{suv}\,\underset{\sim}{p}_j \underset{\sim}{p}_u \mathring{p}_k \mathring{p}_v \sim \epsilon_{ijk}\epsilon_{suv}\,\mathring{p}_j \mathring{p}_u \mathring{p}_k \mathring{p}_v = -\epsilon_{ijk}\epsilon_{suv}\,\mathring{p}_j \mathring{p}_v \mathring{p}_k \mathring{p}_u = 0\ , \qquad \text{(B.42)}$$

as expected. Therefore, propagators can be replaced by their Feynman parts,

$$\Delta_{\alpha\beta}(P) \longrightarrow \frac{\delta_{\alpha\beta}}{p_n^2 + \tilde{p}^2}\ , \qquad \tilde{p}^{2n} \equiv \sum_{j=1}^{3} \tilde{p}_j^{2n}\ , \quad n = 1, 2, \dots\ , \qquad \text{(B.43)}$$

and eq. (B.38) reduces to

$$G_{\rm E}(\omega_n)\big|_{\rm av} = -64c_\chi^2 g^4 d_{\rm A} T \sum_{p_n,q_n} \int_{\mathbf{p}} \frac{\delta_{\omega_n+p_n+q_n,0}\ \Phi(\mathbf{p})\big|_{\rm av}}{(p_n^2 + \tilde{p}^2)(q_n^2 + \tilde{p}^2)} + \mathcal{O}(g^6)\ . \qquad \text{(B.44)}$$

Writing the index summations explicitly, the function $\Phi(\mathbf{p})\big|_{\rm av}$ in the integrand of eq. (B.44) is

$$
\begin{aligned}
\Phi(\mathbf{p})\big|_{\rm av} &= \sum_{\alpha,\mu}\sum_{i,j,k}\sum_{s,u,v} \epsilon_{ijk}\epsilon_{suv}\,\underset{\sim}{p}_i \underset{\sim}{p}_j \mathring{p}_k \underset{\sim}{p}_s \underset{\sim}{p}_u \mathring{p}_v\,(\delta_{\mu i}\,p_n - \delta_{\mu 0}\,\tilde{p}_i) \\
&\qquad \times \big[\delta_{\mu\alpha}\delta_{ju}(\delta_{\alpha s}\,p_n - \delta_{\alpha 0}\,\tilde{p}_s) - \delta_{\mu u}\delta_{j\alpha}(\delta_{\alpha s}\,q_n + \delta_{\alpha 0}\,\tilde{p}_s)\big] \\
&= \sum_{i,j,k}\sum_{s,u,v} \epsilon_{ijk}\epsilon_{suv}\,\underset{\sim}{p}_i \underset{\sim}{p}_j \mathring{p}_k \underset{\sim}{p}_s \underset{\sim}{p}_u \mathring{p}_v \big[(\delta_{is}\,p_n^2 + \tilde{p}_i\tilde{p}_s)\delta_{ju} - \delta_{iu}\delta_{js}\,p_n q_n\big] \\
&= \sum_{i\neq j\neq k} (p_n^2 + p_n q_n)\,\underset{\sim}{p}_i^2 \underset{\sim}{p}_j^2 \mathring{p}_k^2 \equiv (p_n^2 + p_n q_n)\phi(\mathbf{p})\ . \qquad \text{(B.45)}
\end{aligned}
$$

Using trigonometric relations,

$$\underset{\sim}{p}_i^2 = 1 - \frac{a^2}{4}\tilde{p}_i^2\ , \qquad \mathring{p}_i^2 = \tilde{p}_i^2 - \frac{a^2}{4}\tilde{p}_i^2\ , \qquad \text{(B.46)}$$

the function $\phi$ in eq. (B.45) becomes

$$\phi(\mathbf{p}) \equiv \sum_{i\neq j\neq k} \left(1 - \frac{a^2}{4}\tilde{p}_i^2\right)\left(1 - \frac{a^2}{4}\tilde{p}_j^2\right)\left(\tilde{p}_k^2 - \frac{a^2}{4}\tilde{p}_k^4\right)\ . \qquad \text{(B.47)}$$

The two Matsubara sums in eq. (B.44) can be carried out using the Dirac-$\delta$'s,

$$\delta_{0,\omega_n+p_n+q_n} = T\int_0^\beta \mathrm{d}t_\mathrm{E}\, e^{i(\omega_n+p_n+q_n)t_\mathrm{E}} \ . \tag{B.48}$$

Moreover, we take advantage of the $p_n \leftrightarrow q_n$ symmetry to replace the expression $p_n^2 + p_n q_n$ in eq. (B.45) with its symmetrized version,

$$p_n^2 + p_n q_n \quad \longrightarrow \quad \frac{1}{2}(p_n+q_n)^2 \quad \xrightarrow{\delta_{0,\omega_n+p_n+q_n}} \quad \frac{\omega_n^2}{2} \ . \tag{B.49}$$

Denoting $\tilde{p} \equiv \sqrt{\tilde{p}^2}$ from eq. (B.43) and using the relations derived in [57, p.133], both contributions from $p_n$ and $q_n$ are of the form

$$T\sum_{p_n} \frac{e^{ip_n t_\mathrm{E}}}{p_n^2+\tilde{p}^2} = \frac{n_\mathrm{B}(\tilde{p})}{2\tilde{p}}\left[e^{\tilde{p}t_\mathrm{E}} + e^{\tilde{p}(\beta-t_\mathrm{E})}\right] \ , \tag{B.50}$$

yielding the result

$$\begin{aligned}
G_\mathrm{E}(\omega_n)\big|_\mathrm{av} &= -64c_\chi^2 g^4 d_\mathrm{A}\frac{\omega_n^2}{2}\int_0^\beta \mathrm{d}t_\mathrm{E}\, e^{i\omega_n t_\mathrm{E}}\int_\mathbf{p}\frac{n_\mathrm{B}(\tilde{p})^2}{4\tilde{p}^2}[e^{\tilde{p}t_\mathrm{E}}+e^{\tilde{p}(\beta-t_\mathrm{E})}]^2\phi(\mathbf{p}) + \mathcal{O}(g^6) \\
&= -64c_\chi^2 g^4 d_\mathrm{A}\frac{\omega_n^2}{2}\int_\mathbf{p}\frac{n_\mathrm{B}(\tilde{p})^2}{4\tilde{p}^2}\left[2e^{\tilde{p}\beta}\cancelto{0}{\delta_{\omega_n,0}} + \frac{e^{2\tilde{p}\beta}-1}{i\omega_n+2\tilde{p}} + \frac{1-e^{2\tilde{p}\beta}}{i\omega_n-2\tilde{p}}\right]\phi(\mathbf{p}) + \mathcal{O}(g^6) \\
&= -64c_\chi^2 g^4 d_\mathrm{A}\frac{\omega_n^2}{2}\int_\mathbf{p}\frac{n_\mathrm{B}(\tilde{p})^2}{4\tilde{p}^2}(e^{2\tilde{p}\beta}-1)\left[\frac{1}{i\omega_n+2\tilde{p}} - \frac{1}{i\omega_n-2\tilde{p}}\right]\phi(\mathbf{p}) + \mathcal{O}(g^6) \\
&= -64c_\chi^2 g^4 d_\mathrm{A}\frac{\omega_n^2}{2}\int_\mathbf{p}\frac{1+2n_\mathrm{B}(\tilde{p})}{4\tilde{p}^2}\left[\frac{1}{i\omega_n+2\tilde{p}} - \frac{1}{i\omega_n-2\tilde{p}}\right]\phi(\mathbf{p}) + \mathcal{O}(g^6) \ .
\end{aligned} \tag{B.51}$$

To arrive at eq. (B.51), in the last step we have used the identity

$$e^{2\tilde{p}\beta} - 1 = n_\mathrm{B}(\tilde{p})^{-2} + 2n_\mathrm{B}(\tilde{p})^{-1} \ . \tag{B.52}$$

## Statistical correlator

Substituting $\omega_n \to -i(\omega + i0^+)$ and taking the imaginary part in eq. (B.51) yields the cut

$$\mathrm{Im}\left[\frac{1}{\omega-2\tilde{p}+i0^+}\right] = -\pi\delta(\omega-2\tilde{p}) = -\frac{\pi}{2}\delta\left(\tilde{p}-\frac{\omega}{2}\right) \ . \tag{B.53}$$

All in all, the averaged statistical correlator is

$$\begin{aligned}
G_\mathrm{S}(\omega) &= [1+2n_\mathrm{B}(\omega)]\left(-\frac{\omega^2}{2}\right)(-64c_\chi^2 g^4 d_\mathrm{A})\left(-\frac{\pi}{2}\right)\int\frac{\mathrm{d}^3p}{(2\pi)^3}\,\frac{1+2n_\mathrm{B}(\tilde{p})}{4\tilde{p}^2}]\left[\cancelto{0}{\delta\left(\tilde{p}+\frac{\omega}{2}\right)} - \delta\left(\tilde{p}-\frac{\omega}{2}\right)\right]\phi(\mathbf{p}) \\
&= 16\pi c_\chi^2 g^4 d_\mathrm{A}\omega^2[1+2n_\mathrm{B}(\omega)]\int\frac{\mathrm{d}^3p}{(2\pi)^3}\,\frac{1+2n_\mathrm{B}(\tilde{p})}{4\tilde{p}^2}\delta\left(\tilde{p}-\frac{\omega}{2}\right)\phi(\mathbf{p}) \ .
\end{aligned} \tag{B.54}$$

In the continuum limit $a \to 0$ we have $\tilde{p} \to p$ and $\phi(\mathbf{p}) \to 2p^2$, and eq. (B.54) becomes

$$\begin{aligned}
G_\mathrm{S}(\omega) &\overset{a\to 0}{\to} 16c_\chi^2 g^4 d_\mathrm{A}\omega^2[1+2n_\mathrm{B}(\omega)]\frac{4\pi^2}{8\pi^3}\int_0^\infty \mathrm{d}p\,\frac{1+2n_\mathrm{B}(p)}{4}\,2p^2\,\delta\left(p-\frac{\omega}{2}\right) \\
&= \frac{16}{\pi}c_\chi^2 g^4 d_\mathrm{A}\omega^2[1+2n_\mathrm{B}(\omega)]\left[1+2n_\mathrm{B}\left(\frac{\omega}{2}\right)\right]\frac{1}{4}\left(\frac{\omega}{2}\right)^2 \\
&= \frac{c_\chi^2 g^4 d_\mathrm{A}\omega^4}{\pi}[1+2n_\mathrm{B}(\omega)]\left[1+2n_\mathrm{B}\left(\frac{\omega}{2}\right)\right] \ .
\end{aligned} \tag{B.55}$$

In order to have an illustrative limiting value in the domain $ag^2T \ll a\omega \ll 1$, we take the classical limit of eq. (B.55). Restoring $\hbar$ in the Bose distributions yields

$$\lim_{\hbar\to 0}\left[1+2n_{\mathrm{B}}(\omega)\right]\left[1+2n_{\mathrm{B}}\left(\frac{\omega}{2}\right)\right] = \frac{2T}{\hbar\omega}\frac{4T}{\hbar\omega} \ . \tag{B.56}$$

With the normalization introduced in [86] and setting again $\hbar = 1$ we find

$$\frac{G_{\mathrm{S}}^{(\mathrm{cl})}(\omega)}{(\alpha T)^4} \overset{ag^2T\ll a\omega\ll 1}{\approx} \frac{16^2\cancel{\pi^4}}{g^8}\frac{g^4 d_A}{16^3\cancel{\pi^4}}\frac{8}{\pi}\frac{\omega^2}{T^2} = \frac{d_A}{2\pi}\left(\frac{\omega}{g^2T}\right)^2 \ . \tag{B.57}$$

We now proceed to a full (i.e. at $a \neq 0$) evaluation of eq. (B.54) in the classical limit. Using the $\delta$-function we can still take the factor $[1+2n_{\mathrm{B}}(\omega/2)]$ out of the integral and apply eq. (B.56). Moreover, we introduce the rescaled integration variables

$$q_i \equiv a p_i \qquad \Rightarrow \qquad \tilde{q}_i \equiv a\tilde{p}_i \ , \tag{B.58}$$

such that eq. (B.54) becomes

$$G_{\mathrm{S}}^{(\mathrm{cl})}(\omega) = 16\pi c_\chi^2 g^4 d_{\mathrm{A}}\frac{8T^2}{\omega^2}\frac{2}{a^3}\int_0^\pi\frac{\mathrm{d}q_1}{\pi}\int_0^{q_1}\frac{\mathrm{d}q_2}{\pi}\int_0^\pi\frac{\mathrm{d}q_3}{\pi}\delta\left(\frac{\tilde{q}}{a}-\frac{\omega}{2}\right)\phi\left(\frac{\mathbf{q}}{a}\right) \ . \tag{B.59}$$

The upper boundary of the integration over $q_2$ becomes $q_1$ by taking into account the symmetry in $q_1$, $q_2$ and $q_3$ of the integrand and choosing $q_3$ to evaluate the $\delta$-function. This yields the factor of two in front of the integration. Evaluating the $\delta$-function for the variable $q_3$ instead of $\tilde{q}$ yields the Jacobian

$$\left|\frac{\mathrm{d}(\tilde{q}/a)}{\mathrm{d}q_3}\right|^{-1} = \frac{a\tilde{q}}{\left|\sin\left(\frac{q_3}{2}\right)\cos\left(\frac{q_3}{2}\right)\right|} \quad \xrightarrow{\delta} \quad \frac{a^2\omega}{|\sin q_3(q_1,q_2,a\omega)|} \ . \tag{B.60}$$

Using the notation introduced in eq. (B.43) and eq. (B.20) and performing the integration over $q_3$ using the $\delta$-function, the integrand $\phi$ from eq. (B.47) becomes

$$\begin{aligned}\phi\left(\frac{\mathbf{q}}{a}\right) &= \frac{\tilde{q}^2}{64a^2}(4-\tilde{q}_1^2)(4-\tilde{q}_2^2)(4-\tilde{q}_3^2)\\ &\xrightarrow{\delta} \quad \frac{\omega^2}{(16)^2}(4-\tilde{q}_1^2)(4-\tilde{q}_2^2)[4-\tilde{q}_3^2(q_1,q_2,a\omega)]\\ &\overset{(\mathrm{B.20})}{=} \quad \frac{2\omega^2}{16}\cos^2\left(\frac{q_1}{2}\right)\cos^2\left(\frac{q_2}{2}\right)\left[4-\frac{(a\omega)^2}{8}-\cos q_1-\cos q_2\right] \ .\end{aligned} \tag{B.61}$$

We now drop all the prefactors and define the full integrand after the integration over $q_3$ to be

$$\begin{aligned}\bar{\phi}(q_1,q_2,a\omega) \equiv \frac{a\omega}{|\sin q_3(q_1,q_2,a\omega)|}\cos^2\left(\frac{q_1}{2}\right)\cos^2\left(\frac{q_2}{2}\right)\left[4-\frac{(a\omega)^2}{8}-\cos q_1-\cos q_2\right] \\ \times\,\theta\left[\frac{(a\omega)^2}{16}-\sin^2\left(\frac{q_1}{2}\right)-\sin^2\left(\frac{q_2}{2}\right)\right]\theta\left[1-\frac{(a\omega)^2}{16}+\sin^2\left(\frac{q_1}{2}\right)+\sin^2\left(\frac{q_2}{2}\right)\right] \ ,\end{aligned} \tag{B.62}$$

where the step functions $\theta$ take care of the integration range for $q_3$. Normalizing as in eq. (B.57),

$$\frac{G_{\mathrm{S}}^{(\mathrm{cl})}(\omega)}{(\alpha T)^4} = \frac{a^4 G_{\mathrm{S}}^{(\mathrm{cl})}(\omega)}{16\,c_\chi^2(ag^2T)^4} \ , \tag{B.63}$$

we are left with the expression

$$\begin{aligned}\frac{G_{\mathrm{S}}^{(\mathrm{cl})}(\omega)}{(\alpha T)^4} &= \frac{a^4}{\cancel{16}c_\chi^{\cancel{2}}(ag^2T)^4}\frac{\cancel{16^2}c_\chi^{\cancel{2}}d_{\mathrm{A}}g^4T^2}{\pi^2a^3\cancel{\omega^2}}\frac{2a\cancel{\omega^2}}{\cancel{16}}\int_0^\pi\mathrm{d}q_1\int_0^{q_1}\mathrm{d}q_2\,\bar{\phi}(q_1,q_2,a\omega)\\ &= \frac{2d_{\mathrm{A}}}{\pi^2(ag^2T)^2}\int_0^\pi\mathrm{d}q_1\int_0^{q_1}\mathrm{d}q_2\,\bar{\phi}(q_1,q_2,a\omega) \ ,\end{aligned} \tag{B.64}$$

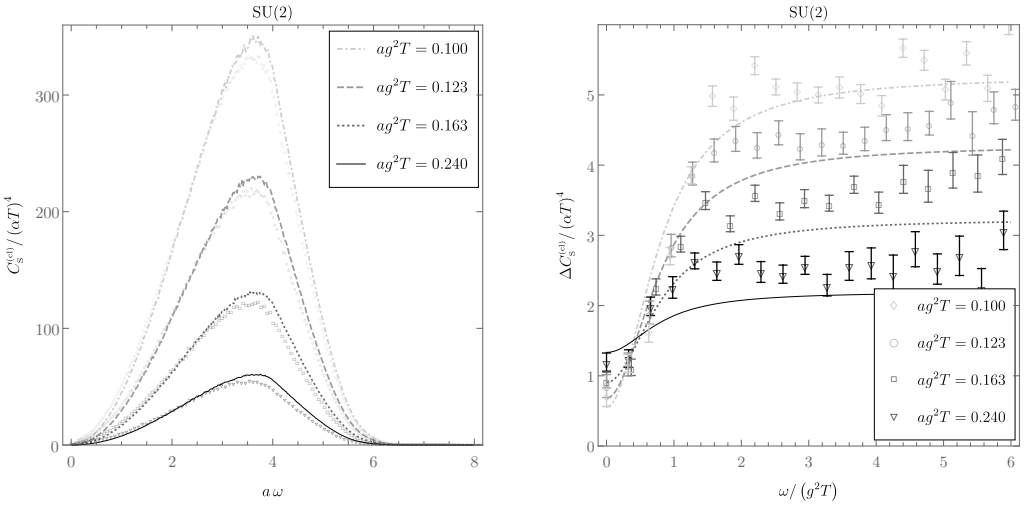


(a) (b)

Figure B.1: (a) Open symbols illustrate the lattice data for $G_{\rm S}^{(\rm cl)}(\omega)/(\alpha T)^4$ in the SU(2) example [3]. Lines represent perturbative results, i.e. the numerical integration of eq. (B.64). (b) Lattice data for $G_{\rm S}^{(\rm cl)}(\omega)/(\alpha T)^4$ in the SU(2) example [3], after the subtraction of the perturbative contribution (cf. fig. B.1a), and a relabelling of the $x$-axis. The lines indicate a qualitative interpolation (cf. eq. (5.27)). The present figure reproduces the left panels in figs. 4 and 5 of [3].

that can be integrated numerically as a function of $a\omega$. Benchmark solutions for $N_c = 2$, $ag^2T = 0.244$, $ag^2T = 0.163$, $ag^2T = 0.123$ and $ag^2T = 0.100$ are shown in figure B.1a.

For a better resolution, in fig. B.1b we show the non-perturbative remainder, after subtracting eq. (B.64) from the lattice data. The fits illustrated by the curves correspond to eq. (5.27), and are discussed in detail in [3] (also for $N_c = 3$).

## B.2 Real part: thermal mass correction

In the weak coupling limit $\alpha \ll 1$, the thermal mass correction,

$$m_{\rm T}^2 \;\approx\; m^2 - \mathrm{Re}\, G_{\rm R}(m)\;, \tag{B.65}$$

can be evaluated perturbatively in the full quantum theory by evaluating the real part of the 2-point correlator of the operator $J$, cf. eq. (5.24). For this we start from eq. (3.2) of [135],[59]

$$G_{\rm R}(\omega + i0^+) = \frac{8d_{\rm A}c_\chi^2}{f_a^2}(D-3)(D-2)g^4 \underbrace{\sum\!\!\!\!\!\!\int_Q \left\{\frac{K^4}{Q^2(Q-K)^2} - \frac{2K^2}{Q^2}\right\}_{K\to(-i[\omega+i0^+],\mathbf{0})}}_{I(\omega+i0^+)} + \mathcal{O}(g^6)\;, \tag{B.66}$$

where $D = 4-2\epsilon$, and the overall sign has been inverted to conform with the Minkowskian convention. Our task here is to carry out the integral $I(\omega + i0^+)$, which we write explicitly as

$$I(\omega + i0^+) = T\sum_{q_n}\int_{\mathbf{q}} \left\{\frac{\omega_n^4}{[q_n^2+q^2][(q_n-\omega_n)^2+q^2]} - \frac{2\omega_n^2}{q_n^2+q^2}\right\}_{\omega_n\to -i[\omega+i0^+]}\;, \tag{B.67}$$

[59] Eq. (B.66) can be derived using the machinery introduced in appendix C (the propagator and the vertex are defined in eqs. (C.6) and (C.12) respectively), using the imaginary-time formalism.

using the notation $q \equiv |\mathbf{q}|$. The expectation is to obtain precisely the continuum version of eq. (B.51), after the substitution $\omega_n \to -i[\omega + i0^+]$.

We evaluate eq. (B.67) by carrying out the Matsubara sums first. Using the formula eq. (B.50) for $t_{\mathrm{E}} = 0$, the second term gives the simple contribution

$$-2\omega_n^2 T \sum_{q_n} \frac{1}{q_n^2 + q^2} = \frac{-2\omega_n^2}{2q}[1 + 2n_{\mathrm{B}}(q)] \;\longrightarrow\; \frac{\omega^2}{q}[1 + 2n_{\mathrm{B}}(q)] \,. \tag{B.68}$$

To evaluate the contribution from the first term in eq. (B.67) we make also use of the Dirac-$\delta$ and its integral expression in eq. (B.48),

$$\begin{aligned}
T \sum_{q_n} \frac{\omega_n^4}{[q_n^2 + q^2][(q_n - \omega_n)^2 + q^2]} &= \omega_n^4 T \sum_{q_n} T \sum_{r_n} \beta \delta_{0, r_n + q_n - \omega_n} \frac{1}{q_n^2 + q^2} \frac{1}{r_n^2 + q^2} \\
&\overset{(B.48)}{=} \omega_n^4 \int_0^\beta \mathrm{d}t_{\mathrm{E}}\, e^{-i\omega_n t_{\mathrm{E}}} \left[ T \sum_{q_n} \frac{e^{iq_n t_{\mathrm{E}}}}{q_n^2 + q^2} \right] \left[ T \sum_{r_n} \frac{e^{ir_n t_{\mathrm{E}}}}{r_n^2 + q^2} \right] \\
&\overset{(B.51)}{=} \omega_n^4 \int_0^\beta \mathrm{d}t_{\mathrm{E}}\, e^{-i\omega_n t_{\mathrm{E}}} \left\{ \frac{n_{\mathrm{B}}(q)}{2q} [e^{qt_{\mathrm{E}}} + e^{q(\beta - t_{\mathrm{E}})}] \right\}^2 \\
&\overset{(B.52)}{=} [1 + 2n_{\mathrm{B}}(q)] \frac{\omega_n^4}{4q^2} \left[ \frac{1}{i\omega_n + 2q} - \frac{1}{i\omega_n - 2q} \right] \\
&\longrightarrow\; [1 + 2n_{\mathrm{B}}(q)] \frac{\omega^4}{4q^2} \left[ \frac{1}{2q + \omega + i0^+} + \frac{1}{2q - \omega - i0^+} \right] .
\end{aligned} \tag{B.69}$$

As expected, we recover here the continuum limit of eq. (B.51). With eqs. (B.68) and (B.69) the real part of the correlator in eq. (B.66) is therefore given by

$$\begin{aligned}
\mathrm{Re}\, G_{\mathrm{R}}(\omega + i0^+) &= \frac{8 d_{\mathrm{A}} c_\chi^2}{f_a^2} (D-3)(D-2) g^4 \omega^2 \int_{\mathbf{q}} \frac{1 + 2n_{\mathrm{B}}(q)}{q} \left[ \frac{\omega^2}{(2q + \omega)(2q - \omega)} + 1 \right] \\
&= \frac{8 d_{\mathrm{A}} c_\chi^2}{f_a^2} (D-3)(D-2) g^4 \omega^2 \underbrace{\int_{\mathbf{q}} [1 + 2n_{\mathrm{B}}(q)] \frac{q}{\left(q + \frac{\omega}{2}\right)\left(q - \frac{\omega}{2}\right)}}_{\mathcal{I}(\omega, \dots)} \,.
\end{aligned} \tag{B.70}$$

## Renormalization of UV divergences

The term without the Bose distribution $n_{\mathrm{B}}$ in the integral $\mathcal{I}$ is a vacuum contribution $\mathcal{I}_0$. Its evaluation can be carried out analytically, but it requires the renormalization of UV divergences. For this we first write $\int_{\mathbf{q}}$ in $d$-dimensional spherical coordinates and carry out angular integrations,

$$\frac{\mathrm{d}^d q}{(2\pi)^d} \;\to\; \frac{2}{(4\pi)^{d/2} \Gamma(d/2)}\, q^{d-1} dq \,. \tag{B.71}$$

Subsequently we perform the substitutions $q^2 = \omega^2 t/4$ and $t = 1 - 1/s$,

$$\begin{aligned}
\mathcal{I}_0(\omega, \dots) &= \frac{2}{(4\pi)^{d/2}\Gamma(d/2)} \int_0^\infty \mathrm{d}q\, \frac{q^d}{q^2 - \frac{\omega^2}{4}} \\
&= \frac{-1}{(4\pi)^{d/2}\Gamma(d/2)} \left(\frac{\omega}{2}\right)^{d-1} \int_0^\infty \mathrm{d}t\, t^{\frac{d-1}{2}} (1 - t)^{-1} \\
&= \frac{-1}{(4\pi)^{d/2}\Gamma(d/2)} \left(\frac{\omega}{2}\right)^{d-1} \underbrace{\int_0^1 \mathrm{d}s\, s^{-\frac{d+1}{2}} (1 - s)^{\frac{d-1}{2}}}_{\beta\left(\frac{1-d}{2}, \frac{1+d}{2}\right)} \,.
\end{aligned} \tag{B.72}$$

We recall the relation among the $\beta$ and the $\Gamma$ functions,

$$\begin{aligned}\Gamma(x)\Gamma(y) \;&\equiv\; \int_0^\infty \mathrm{d}t\, t^{x-1}e^{-t}\int_0^\infty \mathrm{d}s\, s^{y-1}e^{-s} = \int_0^\infty \mathrm{d}t\int_t^\infty \mathrm{d}u\, t^{x-1}(u-t)^{y-1}e^{-u} \\ &\overset{t\to zu}{=} \underbrace{\int_0^1 \mathrm{d}z\, z^{x-1}(1-z)^{y-1}}_{\equiv\beta(x,y)}\underbrace{\int_0^\infty \mathrm{d}u\, u^{x+y-1}e^{-u}}_{\equiv\Gamma(x+y)}\end{aligned} \tag{B.73}$$

$$\Rightarrow \beta\left(\frac{1-d}{2},\frac{1+d}{2}\right) = \frac{\Gamma\left(\frac{1-d}{2}\right)\Gamma\left(\frac{1+d}{2}\right)}{\Gamma(1)}\ . \tag{B.74}$$

The next step is to insert eq. (B.74) in eq. (B.72) and substitute $d = 3-2\epsilon$ and $D = 4-2\epsilon$, recovering also the prefactor $(D-3)(D-2)$ from eq. (B.70),

$$(D-3)(D-2)\mathcal{I}_0(\omega,\dots) = -2\frac{(1-\epsilon)(1-2\epsilon)}{(4\pi)^{\frac{3}{2}-\epsilon}}\left(\frac{\omega^2}{4}\right)^{1-\epsilon}\frac{\Gamma(\epsilon-1)\Gamma(2-\epsilon)}{\Gamma\left(\frac{3}{2}-\epsilon\right)}\ . \tag{B.75}$$

The result (B.75) can be expanded up to zeroth order in $\epsilon$ using the properties of the $\Gamma$ function,

$$\left.\begin{aligned}&\Gamma(\epsilon-1) = \tfrac{1}{(\epsilon-1)\epsilon}\Gamma(1+\epsilon)\\ &\Gamma(2-\epsilon) = (1-\epsilon)\Gamma(1-\epsilon)\end{aligned}\right\} \quad\Rightarrow\quad \Gamma(\epsilon-1)\Gamma(2-\epsilon) = -\frac{1}{\epsilon}+\mathcal{O}(\epsilon)\ , \tag{B.76}$$

$$\begin{aligned}&\Gamma\left(\frac{3}{2}-\epsilon\right) = \left(\frac{1}{2}-\epsilon\right)\Gamma\left(\frac{1}{2}-\epsilon\right) \approx \sqrt{\pi}\left(\frac{1}{2}-\epsilon\right)[1+\epsilon(\gamma_{\mathrm{E}}+\ln 4)] \\ &\qquad\Rightarrow\quad \Gamma\left(\frac{3}{2}-\epsilon\right)^{-1} = \frac{2}{\sqrt{\pi}}[1+\epsilon(2-\gamma_{\mathrm{E}}-\ln 4)]+\mathcal{O}(\epsilon^2)\ ,\end{aligned} \tag{B.77}$$

and its derivatives as [136]

$$\Gamma'\left(\frac{1}{2}\right) = -\sqrt{\pi}(\gamma_{\mathrm{E}}+2\ln 2)\ , \qquad \Gamma'(1)\equiv\gamma_{\mathrm{E}}\ . \tag{B.78}$$

The remaining terms to be expanded are

$$\left(\frac{\omega^2}{4}\right)^{1-\epsilon} = \frac{\omega^2}{4}\mu^{-2\epsilon}\left(1+\epsilon\ln\frac{4\mu^2}{\omega^2}\right)+\mathcal{O}(\epsilon^2)\ , \tag{B.79}$$

$$(4\pi)^{\epsilon-\frac{3}{2}} = (4\pi)^{-\frac{3}{2}}(1+\epsilon\ln 4\pi)+\mathcal{O}(\epsilon^2)\ , \tag{B.80}$$

where $\mu^{-2\epsilon}\mu^{2\epsilon}=1$ is a scale introduced in the logarithm for dimensional reasons. Denoting $\bar{\mu}^2 = 4\pi\mu^2 e^{-\gamma_{\mathrm{E}}}$ the $\overline{\mathrm{MS}}$ renormalization scale [93, p.137], eq. (B.75) becomes

$$\begin{aligned}(D-3)(D-2)\,\mathcal{I}_0(\omega,\mu,\epsilon) &\approx \frac{2\omega^2}{(4\pi)^2}\frac{\mu^{-2\epsilon}}{\epsilon}(1-3\epsilon)[1+\epsilon(2-\gamma_{\mathrm{E}}-\ln 4)]\left(1+\epsilon\ln\frac{4\mu^2}{\omega^2}\right)(1+\epsilon\ln 4\pi) \\ &= \frac{\omega^2\mu^{-2\epsilon}}{8\pi^2}\left(\frac{1}{\epsilon}+\ln\frac{\bar{\mu}^2}{\omega^2}-1\right)+\mathcal{O}(\epsilon)\ .\end{aligned} \tag{B.81}$$

## Numerical estimate of IR contributions

Going back to eq. (B.70), the term with the Bose distribution leads to finite contributions, but it needs to be estimated numerically via a principal value integral $\mathbb{P}$. Transforming to spherical coordinates and carrying out the angular integrations, one finds

$$(D-3)(D-2)\,\mathcal{I}_{\mathrm{T}}(\omega) = \frac{2}{\pi^2}\int_0^\infty \mathrm{d}q\,\mathbb{P}\left[\frac{q^3\,n_{\mathrm{B}}(q)}{\left(q-\frac{\omega}{2}\right)\left(q+\frac{\omega}{2}\right)}\right]\ . \tag{B.82}$$

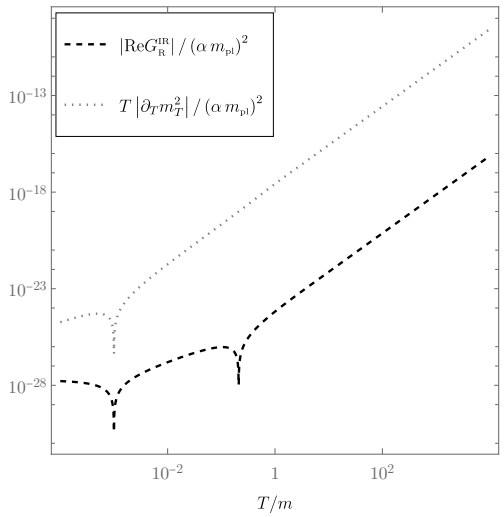


Figure B.2: Absolute value (in units of $(\alpha m_{\mathrm{pl}})^2$) of the temperature-dependent contribution to the thermal mass (second term in eq. (B.86)), and the corresponding correction to the entropy density, (B.88) and eq. (2.14) of [4], integrated numerically. The cusps indicate where the thermal corrections change sign. For the parameters we have set $m = 1.06 \times 10^{-6} m_{\mathrm{pl}}$ and $f_a = 1.25 m_{\mathrm{pl}}$ determined in eqs. (5.21) and (5.23). The full results taking into account the running of the coupling $\alpha^2$ are shown in fig. 5.3.

Before proceeding with the numerical integration, we can estimate limiting values for $\omega \ll T$ and $\omega \gg T$, considering that in both regimes, the dominant momentum contribution to $\mathcal{I}_{\mathrm{T}}$ arises from $q \sim T$. Therefore, in the limit of high and small temperatures we have

$$\mathcal{I}_{\mathrm{T}} \overset{\omega \ll T}{\longrightarrow} \frac{1}{\pi^2}\int_0^\infty \mathrm{d}q\, \frac{q}{e^{q/T}-1} = \frac{1}{\pi^2}\sum_{n=1}^{\infty}\int_0^\infty \mathrm{d}q\, q e^{-\frac{nq}{T}} = \frac{T^2}{\pi^2}\underbrace{\sum_{n=1}^{\infty}\frac{1}{n^2}}_{\zeta(2)} = \frac{T^2}{6}\ , \tag{B.83}$$

$$\mathcal{I}_{\mathrm{T}} \overset{\omega \gg T}{\longrightarrow} -\frac{4}{\pi^2\omega^2}\int_0^\infty \mathrm{d}q\, \frac{q^3}{e^{q/T}-1} = -\frac{4}{\pi^2\omega^2}\sum_{n=1}^{\infty}\int_0^\infty \mathrm{d}q\, q^3 e^{-\frac{nq}{T}} = -\frac{24T^4}{\pi^2\omega^2}\underbrace{\sum_{n=1}^{\infty}\frac{1}{n^4}}_{\zeta(4)} = -\frac{4\pi^2 T^4}{15\,\omega^2}\ , \tag{B.84}$$

$$\Rightarrow \quad (D-3)(D-2)\,\mathcal{I}_{\mathrm{T}}(\omega) \longrightarrow \begin{cases} \frac{T^2}{3}\ , & \omega \ll T \\ -\frac{8\pi^2 T^4}{15\,\omega^2}\ , & \omega \gg T \end{cases}\ . \tag{B.85}$$

For the numerics we divide eq. (B.82) by $\omega^2$, in order to obtain a function of $\omega/T$. The result is illustrated in figure B.2 (with $\omega \to m$).

All in all, the real part of the retarded correlator can be expressed as

$$\mathrm{Re}\, G_{\mathrm{R}}(\omega) = \frac{d_{\mathrm{A}} c_\chi g^4 \omega^2}{\pi^2 f_a^2}\left\{\omega^2\mu^{-2\epsilon}\left(\frac{1}{\epsilon}+\ln\frac{\bar{\mu}^2}{\omega^2}-1\right)+\int_0^\infty \mathrm{d}q\, \mathbb{P}\left[\frac{16q^3\, n_{\mathrm{B}}(q)}{\left(q-\frac{\omega}{2}\right)\left(q+\frac{\omega}{2}\right)}\right]\right\}\ . \tag{B.86}$$

Inserting eq. (B.86) in eq. (B.65), we should require the thermal mass $m_{\mathrm{T}}^2$ to be positive, with $\mathrm{Re}\, G_{\mathrm{R}}$ representing a small correction, such that $\mathrm{Re}\, G_{\mathrm{R}}(m) \ll m^2$. Considering the limiting values in eq. (B.85), this is not obvious in the regime $T \gg m$, where $\mathrm{Re}\, G_{\mathrm{R}}(m) > 0$. However, the constraint $\mathrm{Re}\, G_{\mathrm{R}}(m) \ll m^2$ is satisfied for $\alpha^2 T^2 \ll f_a^2$, which is the condition for the validity of the effective theory description (see discussion in section 5).

Thermal corrections enter the dynamics not only via the thermal mass $m_{\mathrm{T}}$, but also through its derivatives by the temperature, cf. eq. (4.39). These can be computed using eq. (B.86) and

$$\partial_{\mathrm{T}} n_{\mathrm{B}}(q) = \frac{q}{T^2} n_{\mathrm{B}}(q)[1 + n_{\mathrm{B}}(q)] \,, \tag{B.87}$$

so that after the substitution $\omega \to m$ we find

$$\partial_{\mathrm{T}} m_{\mathrm{T}}^2 = -\frac{16 d_{\mathrm{A}} c_\chi g^4 m^2}{\pi^2 f_a^2 T^2} \int_0^\infty \mathrm{d}q\, \mathbb{P} \left\{ \frac{q^4 n_{\mathrm{B}}(q)[1 + n_{\mathrm{B}}(q)]}{\left(q - \frac{m}{2}\right)\left(q + \frac{m}{2}\right)} \right\} \,, \tag{B.88}$$

$$\partial_{\mathrm{T}}^2 m_{\mathrm{T}}^2 = -\frac{16 d_{\mathrm{A}} c_\chi g^4 m^2}{\pi^2 f_a^2 T^3} \int_0^\infty \mathrm{d}q\, \mathbb{P} \left\{ \frac{q^5 n_{\mathrm{B}}(q)[1 + n_{\mathrm{B}}(q)]}{\left(q - \frac{m}{2}\right)\left(q + \frac{m}{2}\right)} \left[ -\frac{2}{q} + \frac{1 + 2 n_{\mathrm{B}}(q)}{T} \right] \right\} \,. \tag{B.89}$$

In the limits (B.85) the expressions in eqs. (B.88) and (B.89) simplify to

$$\partial_{\mathrm{T}} m_{\mathrm{T}}^2 \;\longrightarrow\; \begin{cases} -\frac{16 d_{\mathrm{A}} c_\chi g^4 m^2 T}{3 f_a^2} \,, & m \ll T \\ \frac{\alpha^2 d_{\mathrm{A}} T^3}{15 f_a^2} \,, & m \gg T \end{cases} \,, \tag{B.90}$$

$$\partial_{\mathrm{T}}^2 m_{\mathrm{T}}^2 \;\longrightarrow\; \begin{cases} -\frac{16 d_{\mathrm{A}} c_\chi g^4 m^2}{3 f_a^2} \,, & m \ll T \\ \frac{\alpha^2 d_{\mathrm{A}} T^2}{5 f_a^2} \,, & m \gg T \end{cases} \,. \tag{B.91}$$

# Appendix C

# Gravitational wave production via scatterings

Processes characterized by momenta in the Boltzmann regime, $k/a \sim \pi T$, are fast with respect to the expansion of the universe after the end of inflation. In this regime we thus work in a local Minkowskian frame, and simplify the notation by the redefinition $k/a \to k$. Moreover, in the following we change the signature of the Minkowski metric to the particle physics convention,

$$\eta = \mathrm{diag}(+,-,-,-) \ . \tag{C.1}$$

The production rate of gravitational waves in a local Minkowskian frame is [2]

$$\frac{\mathrm{d}e_{\rm GW}}{\mathrm{d}t\,\mathrm{d}\ln k} \overset{k\sim\pi T}{\approx} \frac{4k^3 n_{\rm B}(k)}{\pi m_{\rm Pl}^2}\ \mathrm{scat}_{2\leftrightarrow 2,1\leftrightarrow 3}(g_1,\varphi,g_2)\ \Theta(\mathcal{P}_{g_1},\mathcal{P}_{\varphi},\mathcal{P}_{g_2}) \ , \tag{C.2}$$

where $\mathrm{scat}_{2\leftrightarrow 2,1\leftrightarrow 3}$ is a phase space operator for all crossed channels, that contains the integration measure, as defined in [128]. In sec. 6.2, the corresponding integrand $\Theta$ is inferred from the matrix elements squared for $3 \to 1$ processes, fig. C.1, which we compute here along the lines of ref. [128]. The advantage of considering $3 \to 1$ processes instead of the kinematically allowed ones (see fig. 6.5) is that the expressions are more symmetric and compact, because non-equilibrium particles and plasma particles are on different sides of the reaction.

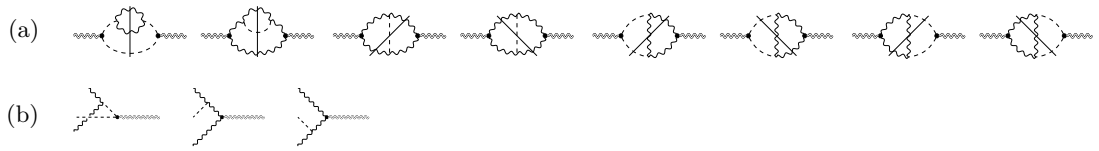


Figure C.1: (a) Matrix elements squared contributing to gravitational wave production in the Boltzmann domain, represented as *cuts* of a 2-point correlator of the energy-momentum tensor $T_{\mu\nu}$. (b) The corresponding $3 \to 1$ amplitudes, which are not kinematically allowed, but can be used for deriving eq. (6.90). Dashed lines denote the inflaton $\varphi$; wiggly lines gauge fields; doubled lines gravitons; blobs the energy-momentum tensor operator.

## C.1 Feynman rules

We derive the Feynman rules from the interaction Lagrangian,

$$\mathcal{L} = \mathcal{L}_0 - \varphi J + \hat{h}^{\mu\nu}\left(\partial_\mu\varphi\,\partial_\nu\varphi - F^c_{\mu\alpha}F^{\alpha c}_{\nu}\right) \ , \qquad J \equiv \frac{\alpha}{16\pi f_a}\epsilon^{\mu\nu\rho\sigma}F^c_{\mu\nu}F^c_{\rho\sigma} \ , \tag{C.3}$$

$$\mathcal{L}_0 \approx \frac{1}{2}\left(\partial^\mu\varphi\partial_\mu\varphi - m^2\varphi^2\right) - \frac{1}{4}F^{c\,\mu\nu}F^c_{\mu\nu} \ , \tag{C.4}$$

following a procedure analogous to the one described in [27, p.123]. The inflaton potential is expanded around the minimum, $V(\varphi) \approx m^2\varphi^2/2$, because we consider late stages after the end of inflation.

**Propagators**

From the free part $\mathcal{L}_0$ of the Lagrangian in eq. (C.3) one derives the needed propagators for

* **scalars** with momentum $\mathcal{P}$ and mass $m$:

$$\text{internal:} \qquad \Delta^{\varphi}(\mathcal{P}) = \frac{i}{\mathcal{P}^2 - m^2} \ . \tag{C.5}$$

* **gauge bosons** with momentum $\mathcal{P}$, helicity $s$ and SU($N_c$) index $a$:

$$\begin{aligned} &\text{internal:} \qquad \Delta^{g,ab}_{\alpha\beta}(\mathcal{P}) = \frac{i}{\mathcal{P}^2}\delta^{ab}\left(-\eta_{\alpha\beta} + \xi\frac{\mathcal{P}_\alpha\mathcal{P}_\beta}{\mathcal{P}^2}\right) \ , \\ &\text{external:} \qquad \hat{g}_\mu(\mathcal{P}, s) \ . \end{aligned} \tag{C.6}$$

  The internal propagator is here in an arbitrary gauge $\xi$.

* **graviton** with momentum $\mathcal{K}$ and helicity $\lambda$:

$$\text{external:} \qquad \hat{h}_{\alpha\beta}(\mathcal{K}, \lambda) \ . \tag{C.7}$$

As a consequence of the Ward identities, gauge boson and graviton helicities obey the sum rules

$$\sum_s \hat{g}_\mu(\mathcal{P}, s)\hat{g}^*_\nu(\mathcal{P}, s) = \mathbb{P}^{\mathrm{T}}_{\mu\nu} \ , \tag{C.8}$$

$$\sum_\lambda \hat{h}_{\alpha\beta}(\mathcal{K}, \lambda)\hat{h}^*_{\mu\nu}(\mathcal{K}, \lambda) = \mathbb{L}_{\alpha\beta;\mu\nu} \ , \tag{C.9}$$

where $\mathbb{L}$ is the projection operator defined in eq. (3.83), while $\mathbb{P}^{\mathrm{T}}$ is defined with respect to the momentum $\mathcal{P}$ of the gauge bosons as

$$\mathbb{P}^{\mathrm{T}}_{\mu\nu} \equiv -\eta_{\mu\nu} + \frac{\mathcal{P}_{\{\mu}\bar{\mathcal{P}}_{\nu\}}}{\mathcal{P}\cdot\bar{\mathcal{P}}} = \eta_{\mu i}\eta_{\nu j}\left(\delta_{ij} - \frac{p_i p_j}{p^2}\right) \qquad \bar{\mathcal{P}}^\mu = (\mathcal{P}^0, -p^i) \ , \tag{C.10}$$

$$\mathcal{P}^\mu\mathbb{P}^{\mathrm{T}}_{\mu\nu} = 0 \ . \tag{C.11}$$

The parentheses $\{ \dots \}$ denote here total symmetrization.

**Vertices**

Denoting $c_\chi \equiv 1/(64\pi^2)$, from eq. (C.3) we find the vertices

$$\varphi \to gg \ : \qquad U_{\alpha\beta}(\mathcal{P}^a_{g_1}, \mathcal{P}^b_{g_2}) = -4i\frac{c_\chi g^2}{f_a}\delta^{ab}\epsilon_{[\alpha\beta]\gamma\delta}\mathcal{P}^\gamma_{g_1}\mathcal{P}^\delta_{g_2} = -8i\frac{c_\chi g^2}{f_a}\delta^{ab}\epsilon_{\alpha\beta\gamma\delta}\mathcal{P}^\gamma_{g_1}\mathcal{P}^\delta_{g_2} \ , \tag{C.12}$$

$$h \to \varphi\varphi \ : \qquad V^{\alpha\beta}(\mathcal{P}_{\varphi_1}, \mathcal{P}_{\varphi_2}) = \ i\mathcal{P}^{\{\alpha}_{\varphi_1}\mathcal{P}^{\beta\}}_{\varphi_2} = 2i\mathcal{P}^\alpha_{\varphi_1}\mathcal{P}^\beta_{\varphi_2} \ , \tag{C.13}$$

$$h \to gg \ : \qquad W^{\alpha\beta\gamma\delta}(\mathcal{P}^c_{g_1}, \mathcal{P}^d_{g_2}) = -i\delta^{cd}\theta^{\{\alpha\beta\}\gamma\delta}(\mathcal{P}_{g_1}, \mathcal{P}_{g_2}) = -2i\delta^{cd}\theta^{\alpha\beta\gamma\delta}(\mathcal{P}_{g_1}, \mathcal{P}_{g_2}) \ , \tag{C.14}$$

with the $h \to gg$ vertex function

$$\theta^{\alpha\beta\gamma\delta}(\mathcal{Q}, \mathcal{P}) \equiv \mathcal{Q}^\alpha\mathcal{P}^\beta\eta^{\gamma\delta} + (\mathcal{Q}\cdot\mathcal{P})\eta^{\gamma\alpha}\eta^{\delta\beta} - \eta^{\alpha\gamma}\mathcal{P}^\beta\mathcal{Q}^\delta - \eta^{\alpha\delta}\mathcal{Q}^\beta\mathcal{P}^\gamma \ . \tag{C.15}$$

## Symmetries and contractions

Let us label the momenta and the helicities of the gauge bosons as

$$\mathcal{P}_1 = \mathcal{P}_{g_1}\ , \quad \mathcal{P}_3 = \mathcal{P}_{g_2}\ , \quad \mathcal{P}_2 = \mathcal{P}_{\varphi}\ , \qquad s_1 = s_{g_1}\ , \quad s_3 = s_{g_2}\ , \tag{C.16}$$

$$\mathcal{P}_1^2 = \mathcal{P}_3^2 = 0\ , \qquad \mathcal{P}_2^2 = m^2\ . \tag{C.17}$$

We also introduce a more compact notation for the internal momenta and their squares

$$\mathcal{Q}_i \equiv \mathcal{K} - \mathcal{P}_i\ , \qquad s_{12} = \mathcal{Q}_3^2\ , \quad s_{13} = \mathcal{Q}_2^2\ , \quad s_{32} = \mathcal{Q}_1^2\ . \tag{C.18}$$

From the definitions one can derive many useful relations among the Mandelstam variables,

$$\mathcal{K}^2 = s_{12} + s_{13} + s_{23} - m^2 \quad \Rightarrow \quad s_{13} - m^2 = \mathcal{K}^2 - (s_{12} + s_{23})\ ,\ \ldots\ , \tag{C.19}$$

that can be further simplified imposing the graviton to be on-shell, $\mathcal{K}^2 \to 0$. For the momenta of the gluons we find the identities

$$\mathcal{P}_g{\cdot}\mathcal{Q}_g = \mathcal{P}_g{\cdot}\mathcal{K}\ , \tag{C.20}$$

$$2\,(\mathcal{P}_g{\cdot}\mathcal{K}) = -(\mathcal{K} - \mathcal{P}_g)^2 + \mathcal{P}_g^2 + \mathcal{K}^2 = \mathcal{K}^2 - \mathcal{Q}_g^2 \quad \overset{\mathcal{K}^2\to 0}{\longrightarrow} \quad -\mathcal{Q}_g^2\ , \tag{C.21}$$

$$2\,(\mathcal{Q}_g{\cdot}\mathcal{K}) = -(\mathcal{K} - \mathcal{Q}_g)^2 + \mathcal{Q}_g^2 + \mathcal{K}^2 = \mathcal{K}^2 + \mathcal{Q}_g^2 = 2(\mathcal{K} - \mathcal{P}_g){\cdot}\mathcal{K} \quad \overset{\mathcal{K}^2\to 0}{\longrightarrow} \quad \mathcal{Q}_g^2\ , \tag{C.22}$$

$$2\,(\mathcal{Q}_{g_1}{\cdot}\mathcal{Q}_{g_2}) = \mathcal{K}^2 + m^2 \quad \overset{\mathcal{K}^2\to 0}{\longrightarrow} \quad m^2\ . \tag{C.23}$$

We define the transverse momentum with respect to the graviton's momentum $\mathcal{K}$ as

$$p_\perp^2 \equiv \mathbb{K}^{\mathrm{T}}_{\alpha\beta}\mathcal{P}^\alpha\mathcal{P}^\beta\ , \tag{C.24}$$

where $\mathbb{K}^{\mathrm{T}}$ is defined like in eq. (C.10) but with $\mathcal{P} \to \mathcal{K}$. Useful relations following from momentum conservation $\mathcal{K} = \mathcal{P}_1 + \mathcal{P}_2 + \mathcal{P}_3$ , with $\mathcal{Q} = \mathcal{K} - \mathcal{P}$, are

$$q_\perp^2 = p_\perp^2\ , \qquad \mathbb{L}_{\alpha\beta;\mu\nu}\mathcal{P}^\alpha\mathcal{P}^\beta\mathcal{P}^\mu\mathcal{P}^\nu = \mathbb{L}_{\alpha\beta;\mu\nu}\mathcal{P}^\alpha\mathcal{P}^\beta\mathcal{Q}^\mu\mathcal{Q}^\nu = \frac{1}{2}p_\perp^4\ , \tag{C.25}$$

$$\mathbb{K}^{\mathrm{T}}_{\alpha\beta}\mathcal{P}^\alpha\mathcal{Q}^\beta = -p_\perp^2\ , \qquad \mathbb{L}_{\alpha\beta;\mu\nu}\mathcal{P}^\alpha\mathcal{P}^\beta\mathcal{P}^\mu\mathcal{Q}^\nu = \mathbb{L}_{\alpha\beta;\mu\nu}\mathcal{P}^\alpha\mathcal{Q}^\beta\mathcal{Q}^\mu\mathcal{Q}^\nu = -\frac{1}{2}p_\perp^4\ . \tag{C.26}$$

Similarly we find relations for the projection operators acting on (all) combinations of momenta,

$$\mathbb{K}^{\mathrm{T}}_{\alpha\beta}\mathcal{P}_1^\alpha\mathcal{P}_2^\beta = \frac{1}{2}(p_{3\perp}^2 - p_{1\perp}^2 - p_{2\perp}^2)\ ,\ \ldots\ , \tag{C.27}$$

$$\mathbb{L}_{\alpha\beta;\mu\nu}\mathcal{P}_1^\alpha\mathcal{P}_1^\beta\mathcal{P}_1^\mu\mathcal{P}_2^\nu = \frac{1}{4}p_{1\perp}^2(p_{3\perp}^2 - p_{1\perp}^2 - p_{2\perp}^2)\ ,\ \ldots\ . \tag{C.28}$$

Using the definition of the projection operator $\mathbb{K}^{\mathrm{T}}$ and choosing $\mathcal{K}^2 = 0$, one can find the following expressions for the transverse momenta,

$$p_{1\perp}^2 = -s_{23}\frac{(\mathcal{P}_1{\cdot}\bar{\mathcal{K}})}{2k^2}\ , \qquad p_{2\perp}^2 = -m^2 - (s_{13} - m^2)\frac{(\mathcal{P}_2{\cdot}\bar{\mathcal{K}})}{2k^2}\ , \qquad p_{3\perp}^2 = -s_{12}\frac{(\mathcal{P}_3{\cdot}\bar{\mathcal{K}})}{2k^2}\ . \tag{C.29}$$

Adding these together it follows the relation

$$\frac{p_{1\perp}^2}{s_{23}} + \frac{p_{2\perp}^2}{s_{13} - m^2} + \frac{p_{3\perp}^2}{s_{12}} = -\frac{s_{13}}{s_{13} - m^2}\ . \tag{C.30}$$

Finally, we introduce a new symbol for a quartic combination of transverse momenta that occurs in multiple computations,

$$P^4 \equiv p_{1\perp}^4 + p_{2\perp}^4 + p_{3\perp}^4 - 2p_{1\perp}^2p_{2\perp}^2 - 2p_{1\perp}^2p_{3\perp}^2 - 2p_{2\perp}^2p_{3\perp}^2\ . \tag{C.31}$$

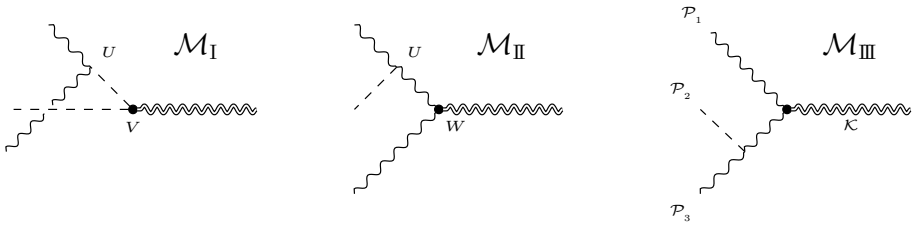


Figure C.2: The same $3 \to 1$ amplitudes as in fig. C.1b, with the notation introduced in eqs. (C.34)–(C.36).

Due to the $\varphi \to gg$ vertex (C.12), contractions of one or two indices of two Levi-Civita tensors may occur. The full uncontracted expression in Minkowskian signature is

$$\begin{aligned}\epsilon^{\gamma\rho\sigma\tau}\epsilon^{\bar\gamma\bar\rho\bar\sigma\bar\tau} = &-\eta^{\gamma[\bar\gamma}\eta^{\bar\rho]\rho}\eta^{\sigma[\bar\sigma}\eta^{\bar\tau]\tau} + \eta^{\gamma[\bar\gamma}\eta^{\bar\sigma]\rho}\eta^{\sigma[\bar\rho}\eta^{\bar\tau]\tau} + \eta^{\gamma[\bar\gamma}\eta^{\bar\tau]\rho}\eta^{\sigma[\bar\sigma}\eta^{\bar\rho]\tau} \\ &- \eta^{\gamma[\bar\sigma}\eta^{\bar\tau]\rho}\eta^{\sigma[\bar\gamma}\eta^{\bar\rho]\tau} + \eta^{\gamma[\bar\sigma}\eta^{\bar\rho]\rho}\eta^{\sigma[\bar\gamma}\eta^{\bar\tau]\tau} + \eta^{\gamma[\bar\tau}\eta^{\bar\rho]\rho}\eta^{\sigma[\bar\sigma}\eta^{\bar\gamma]\tau} \ ,\end{aligned} \tag{C.32}$$

where the parentheses $[\ \dots\ ]$ denote total anti-symmetrization.

## C.2 Matrix elements

### Cuts

We are interested in the contributions to the graviton self-energy from interactions involving two gauge bosons and one scalar field, cf. fig. C.2. To obtain the matrix elements squared for the self-energy diagrams in fig. C.1a, we sum over graviton helicities and gauge bosons' spins,

$$\Theta_{A,B} = \sum_{\lambda}\sum_{s_1,s_3}\ \Big(\ \mathcal{M}_A\mathcal{M}_B^\dagger\ + \mathcal{M}_B\mathcal{M}_A^\dagger\ \Big)\,, \qquad A,B \in \{\text{I},\text{II},\text{III}\}\ . \tag{C.33}$$

Cutting the self-energy diagrams, there are three types of contributing amplitudes,

$$\begin{aligned}\mathcal{M}_{\text{I}}^{cd} &\equiv \hat h^{\alpha\beta}(\mathcal{K},\lambda)V_{\alpha\beta}(\mathcal{Q}_2,\mathcal{P}_2)\ \frac{i}{s_{13}-m^2}\ U^{\gamma\delta}(\mathcal{P}_1^c,\mathcal{P}_3^d)\ \hat g_\gamma(\mathcal{P}_1,s_1)\hat g_\delta(\mathcal{P}_3,s_3) \\ &= \frac{16ic_\chi\delta^{cd}}{f_a}\frac{1}{s_{13}-m^2}\hat h^{\alpha\beta}(\mathcal{K},\lambda)\mathcal{P}_{2\alpha}\mathcal{Q}_{2\beta}\ \varepsilon^{\gamma\delta\rho\sigma}\mathcal{P}_{1\rho}\mathcal{P}_{3\sigma}\hat g_\gamma(\mathcal{P}_1,s_1)\hat g_\delta(\mathcal{P}_3,s_3)\ , \qquad \text{(C.34)}\\ \mathcal{M}_{\text{II}}^{cd} &\equiv \hat h^{\alpha\beta}(\mathcal{K},\lambda)W^{\zeta\delta}_{\alpha\beta}(\mathcal{Q}_3^b,\mathcal{P}_3^d)\ \Delta^{g,ba}_{\zeta\kappa}(\mathcal{Q}_3)\ U^{\kappa\gamma}(\mathcal{Q}_3^a,\mathcal{P}_1^c)\ \hat g_\gamma(\mathcal{P}_1,s_1)\hat g_\delta(\mathcal{P}_3,s_3) \\ &= \frac{16ic_\chi\delta^{cd}}{f_a}\frac{1}{s_{12}}\hat h^{\alpha\beta}(\mathcal{K},\lambda)\theta^{\zeta\delta}_{\alpha\beta}(\mathcal{Q}_3,\mathcal{P}_3)\ (-\eta_{\zeta\rho})\ \varepsilon^{\gamma\rho\sigma\tau}\mathcal{P}_{1\sigma}\mathcal{Q}_{3\tau}\hat g_\gamma(\mathcal{P}_1,s_1)\hat g_\delta(\mathcal{P}_3,s_3)\ , \qquad \text{(C.35)}\\ \mathcal{M}_{\text{III}}^{cd} &\equiv \mathcal{M}_{\text{II}}^{cd}\,|_{1\leftrightarrow 3}\ , \qquad \text{(C.36)}\end{aligned}$$

depicted in fig. C.2.

Note that in the internal gluon propagators $\Delta^g$, the gauge-fixing part proportional to $\xi$ drops out when contracted with the two vertices, such that one can equivalently choose the Feynman gauge $\xi = 0$. We finally add all contributions together, obtaining

$$\Theta(\mathcal{P}_{g_1},\mathcal{P}_\varphi,\mathcal{P}_{g_2}) = \frac{\Theta_{\text{I},\text{I}}}{2} + \frac{\Theta_{\text{II},\text{II}}}{2} + \frac{\Theta_{\text{III},\text{III}}}{2} + \Theta_{\text{I},\text{II}} + \Theta_{\text{I},\text{III}} + \Theta_{\text{II},\text{III}}\ . \tag{C.37}$$

The overall normalization factor $1/2$ is introduced to avoid double-counting of the two identical gluons.

## Matrix elements squared

We introduce the common prefactor

$$\mathcal{N} \equiv \frac{16 c_\chi^2 g^4 d_A}{f_a^2} \ , \tag{C.38}$$

where $d_A = N_c^2 - 1 = \delta^{ab}\delta_{ab}$ for $a = 1, \dots, N_c^2 - 1$, and $c_\chi = 1/(64\pi^2)$.

### Diagonals

Let us denote $p \equiv |\mathbf{p}|$. The simplest contribution is

$$2\sum_\lambda \sum_{s_1,s_3} |\mathcal{M}_{\text{I}}|^2 = \frac{16\mathcal{N}}{(s_{13}-m^2)^2} \underbrace{\mathbb{L}^{\alpha\beta;\bar\alpha\bar\beta}\mathcal{P}_{2\alpha}\mathcal{Q}_{2\beta}\mathcal{P}_{2\bar\alpha}\mathcal{Q}_{2\bar\beta}}_{=\frac{1}{2}p_{2\perp}^4} \underbrace{\varepsilon^{\gamma\delta\rho\sigma}\varepsilon^{\bar\gamma\bar\delta\bar\rho\bar\sigma}\mathbb{P}^{\text{T}}_{1\gamma\bar\gamma}\mathbb{P}^{\text{T}}_{3\delta\bar\delta}\mathcal{P}_{1\rho}\mathcal{P}_{3\sigma}\mathcal{P}_{1\bar\rho}\mathcal{P}_{3\bar\sigma}}_{\text{I}_0} \ . \tag{C.39}$$

Thanks to eq. (C.10), and inserting (C.32), the term $\text{I}_0$ in eq. (C.39) can be simplified to

$$\begin{aligned}\text{I}_0 &= \Big[\eta^{\gamma[\bar\gamma}\eta^{\bar\delta]\delta}\eta^{\rho\bar\sigma}\eta^{\sigma\bar\rho} + \eta^{\gamma\bar\delta}\eta^{\delta\bar\rho}\eta^{\rho\bar\sigma}\eta^{\sigma\bar\gamma} + \eta^{\gamma\bar\sigma}\eta^{\rho\bar\delta}\eta^{\delta[\bar\gamma}\eta^{\bar\rho]\sigma}\Big]\mathbb{P}^{\text{T}}_{1\gamma\bar\gamma}\mathbb{P}^{\text{T}}_{3\delta\bar\delta}\mathcal{P}_{1\rho}\mathcal{P}_{3\sigma}\mathcal{P}_{1\bar\rho}\mathcal{P}_{3\bar\sigma} \\ &= 2(\mathcal{P}_1\cdot\mathcal{P}_3)^2 \ = \frac{s_{13}^2}{2} \, .\end{aligned} \tag{C.40}$$

The result is thus

$$\frac{\Theta_{\text{I,I}}}{2} = 2\mathcal{N} \ \frac{s_{13}^2}{(s_{13}-m^2)^2} \ p_{2\perp}^4 \ . \tag{C.41}$$

The $|\mathcal{M}_{\text{II}}|^2$ and $|\mathcal{M}_{\text{III}}|^2$ contributions have the same structure after the relabelling $\mathcal{P}_1 \leftrightarrow \mathcal{P}_3$ . It is therefore enough to compute one of them. We start from

$$2\sum_\lambda \sum_{s_1,s_3} |\mathcal{M}_{\text{II}}|^2 = \frac{16\mathcal{N}}{s_{12}^2} \underbrace{\mathbb{L}^{\alpha\beta;\bar\alpha\bar\beta}\theta_{\alpha\beta\rho}{}^{\delta}\theta_{\bar\alpha\bar\beta\bar\rho}{}^{\bar\delta}(\mathcal{Q}_3,\mathcal{P}_3)\mathbb{P}^{\text{T}}_{3\delta\bar\delta}}_{\text{II}_1} \underbrace{\varepsilon^{\gamma\rho\sigma\tau}\varepsilon^{\bar\gamma\bar\rho\bar\sigma\bar\tau}\mathbb{P}^{\text{T}}_{1\gamma\bar\gamma}\mathcal{P}_{1\sigma}\mathcal{Q}_{3\tau}\mathcal{P}_{1\bar\sigma}\mathcal{Q}_{3\bar\tau}}_{\text{II}_0} \ , \tag{C.42}$$

and first simplify the $\varphi \to gg$ channel,

$$\begin{aligned}(\text{II}_0)^{\rho\bar\rho} = \big[&\eta^{\gamma[\bar\gamma}\eta^{\bar\rho]\rho}\eta^{\sigma\bar\tau}\eta^{\tau\bar\sigma} + \eta^{\gamma\bar\gamma}\eta^{\rho\bar\sigma}\eta^{\sigma[\bar\rho}\eta^{\bar\tau]\tau} \\ &-\eta^{\gamma[\bar\gamma}\eta^{\bar\tau]\rho}\eta^{\sigma\bar\rho}\eta^{\tau\bar\sigma} + \eta^{\gamma[\bar\rho}\eta^{\bar\tau]\sigma}\eta^{\rho\bar\sigma}\eta^{\tau\bar\gamma}\big]\mathbb{P}^{\text{T}}_{1\gamma\bar\gamma}\mathcal{P}_{1\sigma}\mathcal{Q}_{3\tau}\mathcal{P}_{1\bar\sigma}\mathcal{Q}_{3\bar\tau}\end{aligned} \tag{C.43}$$

$$= -(\mathcal{P}_1\cdot\mathcal{Q}_3)^2\eta^{\rho\bar\rho} - \mathcal{Q}_3^2\mathcal{P}_1^\rho\mathcal{P}_1^{\bar\rho} + (\mathcal{P}_1\cdot\mathcal{Q}_3)\mathcal{P}_1^{\{\rho}\mathcal{Q}_3^{\bar\rho\}} \ . \tag{C.44}$$

We recognise three types of contributions. The last term vanishes due to the symmetries of the $\mathbb{L}$ operator,

$$\begin{aligned}(\text{II}_1)_{\rho\bar\rho}\mathcal{P}_1^{\{\rho}\mathcal{Q}_3^{\bar\rho\}} &= 2\mathbb{L}^{\alpha\beta;\bar\alpha\bar\beta}\theta_{\alpha\beta\rho}{}^{\delta}(\mathcal{Q}_3,\mathcal{P}_3)\mathcal{P}_1^\rho\mathbb{P}^{\text{T}}_{3\delta\bar\delta} \\ &\quad\times\Big[\cancel{\mathcal{Q}_{3\bar\alpha}\mathcal{P}_{3\bar\beta}\mathcal{Q}_3^{\bar\delta}} + \cancel{(\mathcal{P}_3\cdot\mathcal{Q}_3)\mathcal{Q}_{3\bar\alpha}\delta_{\bar\beta}^{\bar\delta}} - \cancel{\mathcal{Q}_{3\bar\alpha}\mathcal{P}_{3\bar\beta}\mathcal{Q}_3^{\bar\delta}} - \cancel{\delta_{\bar\alpha}^{\bar\delta}\mathcal{Q}_{3\bar\beta}(\mathcal{P}_3\cdot\mathcal{Q}_3)}\Big] = 0 \ .\end{aligned} \tag{C.45}$$

The remaining two terms are

$$\begin{aligned}(\text{II}_1)_{\rho\bar\rho}\ \eta^{\rho\bar\rho} &= \mathbb{L}^{\alpha\beta;\bar\alpha\bar\beta}\theta_{\alpha\beta\rho}{}^{\delta}(\mathcal{Q}_3,\mathcal{P}_3) \\ &\quad\times\Big[\mathcal{Q}_{3\bar\alpha}\mathcal{P}_{3\bar\beta}\mathbb{P}^{\text{T}\,\rho}_{3\ \delta} + (\mathcal{P}_3\cdot\mathcal{Q}_3)\delta_{\bar\alpha}^\rho\mathbb{P}^{\text{T}}_{3\delta\bar\beta} - \delta_{\bar\alpha}^\rho\mathcal{P}_{3\bar\beta}\mathbb{P}^{\text{T}}_{3\delta\bar\delta}\mathcal{Q}_3^{\bar\delta} - \mathbb{P}^{\text{T}}_{3\delta\bar\alpha}\mathcal{Q}_{3\bar\beta}\mathcal{P}_3^\rho\Big] \\ &= -\mathbb{L}^{\alpha\beta;\bar\alpha\bar\beta}\Big[2\mathcal{P}_{3\alpha}\mathcal{P}_{3\beta}\mathcal{P}_{3\bar\alpha}\mathcal{P}_{3\bar\beta} + \Big[4(\mathcal{P}_3\cdot\mathcal{Q}_3) + \mathcal{Q}_3^2\Big]\eta_{\alpha\bar\alpha}\mathcal{P}_{3\beta}\mathcal{P}_{3\bar\beta} + (\mathcal{P}_3\cdot\mathcal{Q}_3)^2\eta_{\alpha\bar\alpha}\eta_{\beta\bar\beta}\Big] \\ &\overset{\mathcal{K}^2\to 0}{\longrightarrow} \ -p_{3\perp}^4 - s_{12}p_{3\perp}^2 - \frac{s_{12}^2}{2} \ ,\end{aligned} \tag{C.46}$$

$$
\begin{aligned}
(\mathbb{II}_1)_{\rho\bar\rho}\ \mathcal{P}_1^\rho\mathcal{P}_1^{\bar\rho} &= \mathbb{L}^{\alpha\beta;\bar\alpha\bar\beta}\Big[\mathcal{Q}_{3\alpha}\mathcal{P}_{3\beta}\mathbb{P}^{\mathrm{T}}_{3\delta\bar\delta}\mathcal{P}_1^\delta + (\mathcal{P}_3{\cdot}\mathcal{Q}_3)\mathcal{P}_{1\alpha}\mathbb{P}^{\mathrm{T}}_{3\beta\bar\delta} - \mathcal{P}_{1\alpha}\mathcal{P}_{3\beta}\mathbb{P}^{\mathrm{T}}_{\delta\bar\delta}\mathcal{Q}_3^\delta - \mathbb{P}^{\mathrm{T}}_{3\alpha\bar\delta}\mathcal{Q}_{3\beta}(\mathcal{P}_3{\cdot}\mathcal{P}_1)\Big]\\
&\quad\times\Big[\mathcal{Q}_{3\bar\alpha}\mathcal{P}_{3\bar\beta}\mathcal{P}_1^{\bar\delta} + (\mathcal{P}_3{\cdot}\mathcal{Q}_3)\mathcal{P}_{1\bar\alpha}\delta^{\bar\delta}_{\bar\beta} - \mathcal{P}_{1\bar\alpha}\mathcal{P}_{3\bar\beta}\mathcal{Q}_3^{\bar\delta} - \delta^{\bar\delta}_{\bar\alpha}\mathcal{Q}_{3\bar\beta}(\mathcal{P}_1{\cdot}\mathcal{P}_3)\Big]\\
&= \mathbb{L}^{\alpha\beta;\bar\alpha\bar\beta}\Big[2(\mathcal{P}_3{\cdot}\mathcal{Q}_3)\mathcal{P}_{1\alpha}\mathcal{P}_{1\beta}\mathcal{P}_{3\bar\alpha}\mathcal{P}_{3\bar\beta} - \mathcal{K}^2\mathcal{P}_{1\alpha}\mathcal{P}_{3\beta}\mathcal{P}_{1\bar\alpha}\mathcal{P}_{3\bar\beta}\\
&\quad - 2(\mathcal{P}_1{\cdot}\mathcal{Q}_3)\mathcal{P}_{1\alpha}\mathcal{P}_{3\beta}\mathcal{P}_{3\bar\alpha}\mathcal{P}_{3\bar\beta} - 2(\mathcal{P}_1{\cdot}\mathcal{P}_3)(\mathcal{P}_3{\cdot}\mathcal{Q}_3)\eta_{\alpha\bar\alpha}\mathcal{P}_{1\beta}\mathcal{P}_{3\bar\beta}\\
&\quad -(\mathcal{P}_3{\cdot}\mathcal{Q}_3)^2\eta_{\alpha\bar\alpha}\mathcal{P}_{1\beta}\mathcal{P}_{1\bar\beta} - (\mathcal{P}_1{\cdot}\mathcal{P}_3)^2\eta_{\alpha\bar\alpha}\mathcal{P}_{3\beta}\mathcal{P}_{3\bar\beta}\Big]\\
&\xrightarrow{\mathcal{K}^2\to 0} -\frac{1}{4}\Big[s_{12}(p_{1\perp}^4 - 2p_{1\perp}^2p_{2\perp}^2 + p_{2\perp}^4) + m^2p_{3\perp}^4\\
&\qquad - (s_{12}+m^2)p_{2\perp}^2p_{3\perp}^2 - (s_{12}-m^2)p_{1\perp}^2p_{3\perp}^2\\
&\qquad + s_{12}(s_{23}-m^2)p_{1\perp}^2 + s_{12}s_{13}p_{2\perp}^2 + s_{13}(s_{23}-m^2)p_{3\perp}^2\Big]\ .
\end{aligned}
\tag{C.47}
$$

Denoting $P^4$ as in eq. (C.31), and imposing the graviton to be on-shell $\mathcal{K}^2 = 0$, the final result is

$$
\begin{aligned}
\frac{\Theta_{\mathrm{II},\mathrm{II}}}{2} &= -\frac{8\mathcal{N}}{s_{12}^2}(\mathbb{II}_1)_{\rho\bar\rho}[(\mathcal{P}_1{\cdot}\mathcal{Q}_3)^2\eta^{\rho\bar\rho} + \mathcal{Q}_3^2\mathcal{P}_1^\rho\mathcal{P}_1^{\bar\rho}]\\
&\xrightarrow{\mathcal{K}^2\to 0} 2\mathcal{N}\left\{\frac{(s_{12}-m^2)^2}{2} + P^4 + \frac{m^2}{s_{12}}\left(\frac{m^2}{s_{12}}-1\right)p_{3\perp}^4\right.\\
&\quad + \left(1+\frac{m^2}{s_{12}}\right)p_{1\perp}^2p_{3\perp}^2 + \left(1-\frac{m^2}{s_{12}}\right)p_{2\perp}^2p_{3\perp}^2\\
&\quad \left.+(s_{23}-m^2)p_{1\perp}^2 + s_{13}p_{2\perp}^2 - p_{3\perp}^2\left[s_{23}+m^2-s_{12}+\frac{s_{23}}{s_{12}}(s_{23}-2m^2)\right]\right\}\ .
\end{aligned}
\tag{C.48}
$$

By permuting $1 \leftrightarrow 3$ we obtain the remaining diagonal element,

$$
\begin{aligned}
\frac{\Theta_{\mathrm{III},\mathrm{III}}}{2} &\xrightarrow{\mathcal{K}^2\to 0} 2\mathcal{N}\left\{\frac{(s_{23}-m^2)^2}{2} + P^4 + \frac{m^2}{s_{23}}\left(\frac{m^2}{s_{23}}-1\right)p_{1\perp}^4\right.\\
&\quad + \left(1+\frac{m^2}{s_{23}}\right)p_{1\perp}^2p_{3\perp}^2 + \left(1-\frac{m^2}{s_{23}}\right)p_{1\perp}^2p_{2\perp}^2\\
&\quad \left.+(s_{12}-m^2)p_{3\perp}^2 + s_{13}p_{2\perp}^2 - p_{1\perp}^2\left[s_{12}+m^2-s_{23}+\frac{s_{12}}{s_{23}}(s_{12}-2m^2)\right]\right\}\ .
\end{aligned}
\tag{C.49}
$$

**Interference terms**

Also in this case, it is enough to compute one of the gluon contributions,

$$
\begin{aligned}
\sum_\lambda\sum_{s_1,s_3}\left(\mathcal{M}_{\mathrm{II}}\mathcal{M}_{\mathrm{I}}^\dagger + \mathcal{M}_{\mathrm{I}}\mathcal{M}_{\mathrm{II}}^\dagger\right) &= \frac{-16\mathcal{N}}{s_{12}(s_{13}-m^2)}\underbrace{\mathbb{L}^{\alpha\beta;\bar\alpha\bar\beta}\theta_{\alpha\beta\rho}{}^{\delta}(\mathcal{Q}_3,\mathcal{P}_3)\mathcal{P}_{2\bar\alpha}\mathcal{Q}_{2\bar\beta}\mathbb{P}^{\mathrm{T}}_{3\delta\bar\delta}}_{\mathbb{I}_1}\\
&\quad\times\ \underbrace{\varepsilon^{\gamma\rho\sigma\tau}\varepsilon^{\bar\gamma\bar\delta\bar\rho\bar\sigma}\mathcal{P}_{1\sigma}\mathcal{Q}_{3\tau}\mathcal{P}_{1\bar\rho}\mathcal{P}_{3\bar\sigma}\mathbb{P}^{\mathrm{T}}_{1\gamma\bar\gamma}}_{\mathbb{I}_0}\ ,
\end{aligned}
\tag{C.50}
$$

and symmetrize the final result to obtain $\Theta_{\mathrm{I},\mathrm{III}}$. Thanks to the gluonic projection operators $\mathbb{P}_3^{\mathrm{T}}$ , the double-epsilon expression can be simplified to

$$
\begin{aligned}
(\mathbb{I}_0)^{\rho\bar\delta} &= \Big[\eta^{\gamma\bar\gamma}\eta^{\rho[\bar\delta}\eta^{\bar\sigma]\sigma}\eta^{\tau\bar\rho} + \eta^{\gamma\bar\gamma}\eta^{\rho\bar\rho}\eta^{\sigma[\bar\delta}\eta^{\bar\sigma]\tau} + \eta^{\gamma\bar\delta}\eta^{\rho[\bar\rho}\eta^{\bar\gamma]\tau}\eta^{\sigma\bar\sigma} + \eta^{\gamma\bar\sigma}\eta^{\rho[\bar\gamma}\eta^{\bar\rho]\tau}\eta^{\sigma\bar\delta}\Big]\\
&\quad\times\mathbb{P}^{\mathrm{T}}_{1\gamma\bar\gamma}\mathcal{P}_{1\sigma}\mathcal{Q}_{3\tau}\mathcal{P}_{1\bar\rho}\mathcal{P}_{3\bar\sigma}\\
&= -(\mathcal{P}_1{\cdot}\mathcal{P}_3)(\mathcal{P}_1{\cdot}\mathcal{Q}_3)\eta^{\rho\bar\delta} - (\mathcal{P}_3{\cdot}\mathcal{Q}_3)\mathcal{P}_1^\rho\mathcal{P}_1^{\bar\delta} + (\mathcal{P}_1{\cdot}\mathcal{P}_3)\mathcal{P}_1^\rho\mathcal{Q}_3^{\bar\delta} + (\mathcal{P}_1{\cdot}\mathcal{Q}_3)\mathcal{P}_3^\rho\mathcal{P}_1^{\bar\delta}\ .
\end{aligned}
\tag{C.51}
$$

Contracting term by term in the $\mathcal{K}^2 \to 0$ limit we have

$$\begin{aligned}
(\mathbb{I}_1)_{\rho\bar\delta}\eta^{\rho\bar\delta} \to\ & -\mathbb{L}^{\alpha\beta;\bar\alpha\bar\beta}\mathcal{P}_{3\alpha}\mathcal{P}_{3\beta}\mathcal{P}_{2\bar\alpha}\mathcal{P}_{2\bar\beta}\ ,\\
(\mathbb{I}_1)_{\rho\bar\delta}\mathcal{P}_3^{\rho}\mathcal{P}_1^{\bar\delta} \to\ & -\frac{1}{2}\mathbb{L}^{\alpha\beta;\bar\alpha\bar\beta}\left[s_{12}\mathcal{P}_{1\bar\alpha}\mathcal{P}_{3\bar\beta}+(s_{12}-m^2)\mathcal{P}_{3\bar\alpha}\mathcal{P}_{3\bar\beta}\right]\mathcal{P}_{2\bar\alpha}\mathcal{P}_{2\bar\beta}\ ,\\
(\mathbb{I}_1)_{\rho\bar\delta}\mathcal{P}_1^{\rho}\mathcal{P}_1^{\bar\delta} \to\ & -\frac{1}{2}\mathbb{L}^{\alpha\beta;\bar\alpha\bar\beta}\left[s_{12}\mathcal{P}_{1\alpha}\mathcal{P}_{1\beta}-(s_{13}-s_{12}+m^2)\mathcal{P}_{1\alpha}\mathcal{P}_{3\beta}\right]\mathcal{P}_{2\bar\alpha}\mathcal{P}_{2\bar\beta}\ ,\\
(\mathbb{I}_1)_{\rho\bar\delta}\mathcal{P}_1^{\rho}\mathcal{Q}_3^{\bar\delta} \to\ & -\frac{1}{2}\mathbb{L}^{\alpha\beta;\bar\alpha\bar\beta}\left[s_{12}\mathcal{P}_{1\alpha}\mathcal{P}_{3\beta}-s_{23}\mathcal{P}_{3\alpha}\mathcal{P}_{3\beta}\right]\mathcal{P}_{2\bar\alpha}\mathcal{P}_{2\bar\beta}\ .
\end{aligned} \tag{C.52}$$

Adding together all terms with the corresponding coefficients yields

$$\begin{aligned}
\Theta_{\text{I,II}} \xrightarrow{\mathcal{K}^2\to 0}\ & \frac{4\mathcal{N}}{s_{12}(s_{13}-m^2)}\mathbb{L}^{\alpha\beta;\bar\alpha\bar\beta}\mathcal{P}_{2\bar\alpha}\mathcal{P}_{2\bar\beta}\\
&\qquad\times\left\{[s_{13}^2+(s_{12}-m^2)^2]\mathcal{P}_{3\alpha}\mathcal{P}_{3\beta}+s_{12}(s_{12}-m^2)\mathcal{P}_{1\alpha}\mathcal{P}_{3\beta}+s_{12}^2\mathcal{P}_{1\alpha}\mathcal{P}_{1\beta}\right\}\\
\longrightarrow\ & \mathcal{N}\left\{\frac{1}{s_{12}}\left(s_{13}-m^2+\frac{2m^2s_{13}}{s_{13}-m^2}\right)P^4+2\frac{s_{12}-m^2}{s_{13}-m^2}p_{2_\perp}^4\right.\\
&\left.+\frac{2m^2}{s_{13}-m^2}p_{1_\perp}^2p_{2_\perp}^2+2\left[\frac{1}{s_{12}}\left(s_{13}-m^2+\frac{2m^2s_{13}}{s_{13}-m^2}\right)-\frac{m^2}{s_{13}-m^2}\right]p_{2_\perp}^2p_{3_\perp}^2\right\}\ .
\end{aligned} \tag{C.53}$$

We obtain $\Theta_{\text{I,III}}$ by simply switching the labellings $1 \leftrightarrow 3$. For on-shell gravitons the result is

$$\begin{aligned}
\Theta_{\text{I,III}} \xrightarrow{\mathcal{K}^2\to 0}\ & \mathcal{N}\left\{\frac{1}{s_{23}}\left(s_{13}-m^2+\frac{2m^2s_{13}}{s_{13}-m^2}\right)P^4+2\frac{s_{23}-m^2}{s_{13}-m^2}p_{2_\perp}^4\right.\\
&\left.+\frac{2m^2}{s_{13}-m^2}p_{2_\perp}^2p_{3_\perp}^2+2\left[\frac{1}{s_{23}}\left(s_{13}-m^2+\frac{2m^2s_{13}}{s_{13}-m^2}\right)-\frac{m^2}{s_{13}-m^2}\right]p_{1_\perp}^2p_{2_\perp}^2\right\}\ .
\end{aligned} \tag{C.54}$$

Adding eq. (C.53) and eq. (C.54) one gets

$$\begin{aligned}
\Theta_{\text{I,II}}+\Theta_{\text{I,III}} \to \mathcal{N}\Bigg[ & -\frac{(s_{12}+s_{23})^2+2m^2s_{13}}{s_{12}s_{23}}P^4-2\frac{s_{13}+m^2}{s_{13}-m^2}p_{2_\perp}^4\\
&+2p_{2_\perp}^2\left(\frac{p_{1_\perp}^2}{s_{23}}+\frac{p_{3_\perp}^2}{s_{12}}\right)\left(s_{13}-m^2+\frac{2m^2s_{13}}{s_{13}-m^2}\right)\Bigg]\ .
\end{aligned} \tag{C.55}$$

The remaining contribution is given by

$$\begin{aligned}
\sum_{\lambda}\sum_{s_1,s_3}\left(\mathcal{M}_{\text{III}}\mathcal{M}_{\text{II}}^{\dagger}+\mathcal{M}_{\text{II}}\mathcal{M}_{\text{III}}^{\dagger}\right) = \frac{16\mathcal{N}}{s_{12}s_{23}}\ & \underbrace{\mathbb{L}^{\alpha\beta;\bar\alpha\bar\beta}\theta_{\alpha\beta\rho}{}^{\delta}(\mathcal{Q}_1,\mathcal{P}_1)\mathbb{P}^{\text{T}}_{1\delta\bar\gamma}\theta_{\bar\alpha\bar\beta\bar\rho}{}^{\bar\delta}(\mathcal{Q}_3,\mathcal{P}_3)\mathbb{P}^{\text{T}}_{3\bar\delta\gamma}}_{\mathbb{I}_1}\\
&\times\ \underbrace{\epsilon^{\gamma\rho\sigma\tau}\mathcal{P}_{3\sigma}\mathcal{Q}_{1\tau}\epsilon^{\bar\gamma\bar\rho\bar\sigma\bar\tau}\mathcal{P}_{1\bar\sigma}\mathcal{Q}_{3\bar\tau}}_{\mathbb{I}_0}\ .
\end{aligned} \tag{C.56}$$

The two epsilon-tensors can be treated as

$$\begin{aligned}
(\mathbb{I}_0)^{\gamma\rho\bar\gamma\bar\rho} = & [(\mathcal{P}_1\cdot\mathcal{Q}_1)(\mathcal{P}_3\cdot\mathcal{Q}_3)-(\mathcal{P}_1\cdot\mathcal{P}_3)(\mathcal{Q}_1\cdot\mathcal{Q}_3)]\eta^{\gamma\bar\gamma}\eta^{\rho\bar\rho}\\
&+\eta^{\gamma\bar\gamma}\left[(\mathcal{Q}_1\cdot\mathcal{Q}_3)\mathcal{P}_1^{\rho}\mathcal{P}_3^{\bar\rho}-(\mathcal{P}_3\cdot\mathcal{Q}_3)\mathcal{P}_1^{\rho}\mathcal{Q}_1^{\bar\rho}-(\mathcal{P}_1\cdot\mathcal{Q}_1)\mathcal{Q}_3^{\rho}\mathcal{P}_3^{\bar\rho}+(\mathcal{P}_1\cdot\mathcal{P}_3)\mathcal{Q}_3^{\rho}\mathcal{Q}_1^{\bar\rho}\right]\\
&-\eta^{\rho\bar\gamma}\left[(\mathcal{Q}_1\cdot\mathcal{Q}_3)\mathcal{P}_1^{\gamma}\mathcal{P}_3^{\bar\rho}-(\mathcal{P}_3\cdot\mathcal{Q}_3)\mathcal{P}_1^{\gamma}\mathcal{Q}_1^{\bar\rho}-(\mathcal{P}_1\cdot\mathcal{Q}_1)\mathcal{Q}_3^{\gamma}\mathcal{P}_3^{\bar\rho}+(\mathcal{P}_1\cdot\mathcal{P}_3)\mathcal{Q}_3^{\gamma}\mathcal{Q}_1^{\bar\rho}\right]\\
&+\mathcal{P}_1^{\gamma}\mathcal{Q}_1^{\bar\gamma}\mathcal{Q}_3^{\rho}\mathcal{P}_3^{\bar\rho}-\mathcal{P}_1^{\rho}\mathcal{Q}_1^{\bar\gamma}\mathcal{Q}_3^{\gamma}\mathcal{P}_3^{\bar\rho}\ -\ \bar\rho\leftrightarrow\bar\gamma\ .
\end{aligned} \tag{C.57}$$

After anti-symmetrization, the first row of eq. (C.57) gives

$$\begin{aligned}(\mathbb{I}_1)_{\gamma\rho\bar\gamma\bar\rho}\,\eta^{\gamma[\bar\gamma}\eta^{\bar\rho]\rho} = \mathbb{L}^{\alpha\beta;\bar\alpha\bar\beta}\big\{&(\mathcal{P}_1{\cdot}\mathcal{Q}_1)(\mathcal{P}_3{\cdot}\mathcal{Q}_3)\eta_{\alpha\bar\alpha}\eta_{\beta\bar\beta} + [(\mathcal{P}_1{\cdot}\mathcal{P}_3)+(\mathcal{Q}_1{\cdot}\mathcal{Q}_3)]\eta_{\alpha\bar\alpha}\mathcal{P}_{1\beta}\mathcal{P}_{3\bar\beta}\\ &+2(\mathcal{P}_1{\cdot}\mathcal{Q}_1)\eta_{\alpha\bar\alpha}\mathcal{P}_{3\beta}\mathcal{P}_{3\bar\beta}+2(\mathcal{P}_3{\cdot}\mathcal{Q}_3)\eta_{\alpha\bar\alpha}\mathcal{P}_{1\beta}\mathcal{P}_{1\bar\beta}\\ &-2\mathcal{P}_{1\alpha}\mathcal{P}_{1\beta}\mathcal{P}_{3\bar\alpha}\mathcal{P}_{3\bar\beta}+2\mathcal{P}_{1\alpha}\mathcal{P}_{3\beta}\mathcal{P}_{1\bar\alpha}\mathcal{P}_{3\bar\beta}\big\}\\ \overset{\mathcal{K}^2\to0}{\longrightarrow}\ \mathbb{L}^{\alpha\beta;\bar\alpha\bar\beta}\Big\{&-2\mathcal{P}_{1\alpha}\mathcal{P}_{1\beta}\mathcal{P}_{3\bar\alpha}\mathcal{P}_{3\bar\beta}+2\mathcal{P}_{1\alpha}\mathcal{P}_{3\beta}\mathcal{P}_{1\bar\alpha}\mathcal{P}_{3\bar\beta}+\frac{s_{12}s_{23}}{4}\eta_{\alpha\bar\alpha}\eta_{\beta\bar\beta}\\ &\eta_{\alpha\bar\alpha}\mathcal{P}_{1\beta}\mathcal{P}_{3\bar\beta}\frac{s_{13}+m^2}{2}-s_{23}\eta_{\alpha\bar\alpha}\mathcal{P}_{3\beta}\mathcal{P}_{3\bar\beta}-s_{12}\eta_{\alpha\bar\alpha}\mathcal{P}_{1\beta}\mathcal{P}_{1\bar\beta}\Big\}\ .\end{aligned}\tag{C.58}$$

The corresponding coefficient in the limit $\mathcal{K}^2\to0$ is $(s_{12}s_{23}-m^2s_{13})/4$. We now proceed to summing together the terms with the same coefficient first. Starting with the first terms in eq. (C.57), with the coefficient $(\mathcal{Q}_1{\cdot}\mathcal{Q}_3)=(\mathcal{K}^2+m^2)/2\to m^2/2$, they give

$$\begin{aligned}(\mathbb{I}_1)_{\gamma\rho\bar\gamma\bar\rho}\,\mathcal{P}_1^{[\rho}\eta^{\gamma][\bar\gamma}\mathcal{P}_3^{\bar\rho]}\to\ \mathbb{L}^{\alpha\beta;\bar\alpha\bar\beta}\Big\{&\frac{m^2}{2}\mathcal{P}_{1\alpha}\mathcal{P}_{1\beta}\mathcal{P}_{3\bar\alpha}\mathcal{P}_{3\bar\beta}+\frac{2s_{13}+m^2}{2}\mathcal{P}_{1\alpha}\mathcal{P}_{3\beta}\mathcal{P}_{1\bar\alpha}\mathcal{P}_{3\bar\beta}\\ &-s_{23}\mathcal{P}_{1\alpha}\mathcal{P}_{3\beta}\mathcal{P}_{3\bar\alpha}\mathcal{P}_{3\bar\beta}-s_{12}\mathcal{P}_{1\alpha}\mathcal{P}_{1\beta}\mathcal{P}_{1\bar\alpha}\mathcal{P}_{3\bar\beta}\\ &+\frac{s_{12}(s_{23}-m^2)}{4}\eta_{\alpha\bar\alpha}\mathcal{P}_{1\beta}\mathcal{P}_{1\bar\beta}+\frac{s_{23}(s_{12}-m^2)}{4}\eta_{\alpha\bar\alpha}\mathcal{P}_{3\beta}\mathcal{P}_{3\bar\beta}\\ &+\frac{3s_{12}s_{23}+m^2s_{13}}{4}\eta_{\alpha\bar\alpha}\mathcal{P}_{1\beta}\mathcal{P}_{3\bar\beta}\Big\}\ .\end{aligned}\tag{C.59}$$

We now repeat the same procedure for the other terms. The two $(\mathcal{P}_3{\cdot}\mathcal{Q}_3)=(\mathcal{K}^2-\mathcal{Q}_3^2)/2\to-s_{12}/2$ terms yield

$$\begin{aligned}(\mathbb{I}_1)_{\gamma\rho\bar\gamma\bar\rho}\,\mathcal{P}_1^{[\rho}\eta^{\gamma][\bar\gamma}\mathcal{Q}_1^{\bar\rho]}\to\ \mathbb{L}^{\alpha\beta;\bar\alpha\bar\beta}\Big\{&\frac{s_{23}}{2}\mathcal{P}_{1\alpha}\mathcal{P}_{1\beta}\mathcal{P}_{3\bar\alpha}\mathcal{P}_{3\bar\beta}-(s_{13}+m^2)\mathcal{P}_{1\alpha}\mathcal{P}_{1\beta}\mathcal{P}_{1\bar\alpha}\mathcal{P}_{3\bar\beta}\\ &+s_{12}\mathcal{P}_{1\alpha}\mathcal{P}_{1\beta}\mathcal{P}_{1\bar\alpha}\mathcal{P}_{1\bar\beta}+\frac{s_{23}(s_{12}-s_{23})}{4}\eta_{\alpha\bar\alpha}\mathcal{P}_{1\beta}\mathcal{P}_{3\bar\beta}\Big\}\ .\end{aligned}\tag{C.60}$$

For the $(\mathcal{P}_1{\cdot}\mathcal{Q}_1)=(\mathcal{K}^2-\mathcal{Q}_1^2)/2\to-s_{23}/2$ terms we have

$$\begin{aligned}(\mathbb{I}_1)_{\gamma\rho\bar\gamma\bar\rho}\,\mathcal{Q}_3^{[\rho}\eta^{\gamma][\bar\gamma}\mathcal{P}_3^{\bar\rho]}\to\ \mathbb{L}^{\alpha\beta;\bar\alpha\bar\beta}\big\{&s_{12}\mathcal{P}_{1\alpha}\mathcal{P}_{1\beta}\mathcal{P}_{3\bar\alpha}\mathcal{P}_{3\bar\beta}-\left(s_{13}+m^2\right)\mathcal{P}_{1\alpha}\mathcal{P}_{3\beta}\mathcal{P}_{3\bar\alpha}\mathcal{P}_{3\bar\beta}\\ &+s_{23}\mathcal{P}_{3\alpha}\mathcal{P}_{3\beta}\mathcal{P}_{3\bar\alpha}\mathcal{P}_{3\bar\beta}+\frac{s_{12}(s_{23}-s_{12})}{4}\eta_{\alpha\bar\alpha}\mathcal{P}_{1\beta}\mathcal{P}_{3\bar\beta}\Big\}\ .\end{aligned}\tag{C.61}$$

The last two terms with the coefficient $(\mathcal{P}_1{\cdot}\mathcal{P}_3)=s_{13}/2$ are

$$\begin{aligned}(\mathbb{I}_1)_{\gamma\rho\bar\gamma\bar\rho}\,\mathcal{Q}_3^{[\rho}\eta^{\gamma][\bar\gamma}\mathcal{Q}_1^{\bar\rho]}\to\ \mathbb{L}^{\alpha\beta;\bar\alpha\bar\beta}\Big\{&-\frac{m^2}{2}\mathcal{P}_{1\alpha}\mathcal{P}_{1\beta}\mathcal{P}_{3\bar\alpha}\mathcal{P}_{3\bar\beta}+\frac{s_{13}+2m^2}{2}\mathcal{P}_{1\alpha}\mathcal{P}_{3\beta}\mathcal{P}_{1\bar\alpha}\mathcal{P}_{3\bar\beta}\\ &-\frac{s_{23}}{2}\mathcal{P}_{1\alpha}\mathcal{P}_{3\beta}\mathcal{P}_{3\bar\alpha}\mathcal{P}_{3\bar\beta}-\frac{s_{12}}{2}\mathcal{P}_{1\alpha}\mathcal{P}_{1\beta}\mathcal{P}_{1\bar\alpha}\mathcal{P}_{3\bar\beta}\\ &+\frac{3s_{12}s_{23}+m^2s_{13}}{4}\eta_{\alpha\bar\alpha}\mathcal{P}_{1\beta}\mathcal{P}_{3\bar\beta}\\ &+\frac{s_{23}(s_{23}-m^2)}{4}\eta_{\alpha\bar\alpha}\mathcal{P}_{1\beta}\mathcal{P}_{1\bar\beta}+\frac{s_{12}(s_{12}-m^2)}{4}\eta_{\alpha\bar\alpha}\mathcal{P}_{3\beta}\mathcal{P}_{3\bar\beta}\Big\}\ .\end{aligned}\tag{C.62}$$

Finally, the fourth row of eq. (C.57) contains two terms that together yield

$$
\begin{aligned}
(\mathbb{I}_1)_{\gamma\rho\bar\gamma\bar\rho}\ \mathcal{Q}_3^{[\rho}\mathcal{P}_1^{\gamma]}\mathcal{Q}_1^{[\bar\gamma}\mathcal{P}_3^{\bar\rho]} \to\ \mathbb{L}^{\alpha\beta;\bar\alpha\bar\beta}\Big\{&\frac{1}{4}\big[(s_{12}-s_{23})^2-m^2(s_{12}+s_{23})-s_{12}s_{23}\big]\mathcal{P}_{1\alpha}\mathcal{P}_{1\beta}\mathcal{P}_{3\bar\alpha}\mathcal{P}_{3\bar\beta}\\
&-\frac{1}{4}\big[(s_{12}+s_{23})^2+2s_{12}s_{23}+4m^2s_{13}\big]\mathcal{P}_{1\alpha}\mathcal{P}_{3\beta}\mathcal{P}_{1\bar\alpha}\mathcal{P}_{3\bar\beta}\\
&+\frac{s_{23}}{4}(s_{13}-2s_{12}+4m^2)\mathcal{P}_{1\alpha}\mathcal{P}_{3\beta}\mathcal{P}_{3\bar\alpha}\mathcal{P}_{3\bar\beta}\\
&+\frac{s_{12}}{4}(s_{13}-2s_{23}+4m^2)\mathcal{P}_{1\alpha}\mathcal{P}_{1\beta}\mathcal{P}_{1\bar\alpha}\mathcal{P}_{3\bar\beta}\\
&-\frac{s_{23}^2}{4}\mathcal{P}_{3\alpha}\mathcal{P}_{3\beta}\mathcal{P}_{3\bar\alpha}\mathcal{P}_{3\bar\beta}-\frac{s_{12}^2}{4}\mathcal{P}_{1\alpha}\mathcal{P}_{1\beta}\mathcal{P}_{1\bar\alpha}\mathcal{P}_{1\bar\beta}\Big\}\ ,
\end{aligned}
\tag{C.63}
$$

in the $\mathcal{K}^2\to 0$ limit. Adding eqs. (C.58)–(C.63) one obtains

$$
\begin{aligned}
\Theta_{\text{II,III}}\to\frac{16\mathcal{N}}{s_{12}s_{23}}\mathbb{L}^{\alpha\beta;\bar\alpha\bar\beta}\Big\{&\frac{s_{12}s_{23}}{4}\frac{s_{12}s_{23}-m^2s_{13}}{4}\eta_{\alpha\bar\alpha}\eta_{\beta\bar\beta}+\frac{s_{12}s_{23}}{2}(m^2+s_{13})\eta_{\alpha\bar\alpha}\mathcal{P}_{1\beta}\mathcal{P}_{3\bar\beta}\\
&-\frac{s_{23}^2}{8}(3s_{12}+s_{23})\eta_{\alpha\bar\alpha}\mathcal{P}_{3\beta}\mathcal{P}_{3\bar\beta}-\frac{s_{12}^2}{8}(3s_{23}+s_{12})\eta_{\alpha\bar\alpha}\mathcal{P}_{1\beta}\mathcal{P}_{1\bar\beta}\\
&+\frac{1}{2}\left(\frac{(s_{12}-s_{23})^2}{2}+m^2s_{13}\right)\mathcal{P}_{1\alpha}\mathcal{P}_{1\beta}\mathcal{P}_{3\bar\alpha}\mathcal{P}_{3\bar\beta}\\
&+\frac{s_{23}}{2}(s_{12}-m^2)\mathcal{P}_{1\alpha}\mathcal{P}_{3\beta}\mathcal{P}_{3\bar\alpha}\mathcal{P}_{3\bar\beta}\\
&+\frac{s_{12}}{2}(s_{23}-m^2)\mathcal{P}_{1\alpha}\mathcal{P}_{1\beta}\mathcal{P}_{1\bar\alpha}\mathcal{P}_{3\bar\beta}\\
&+\frac{s_{23}^2}{4}\mathcal{P}_{3\alpha}\mathcal{P}_{3\beta}\mathcal{P}_{3\bar\alpha}\mathcal{P}_{3\bar\beta}+\frac{s_{12}^2}{4}\mathcal{P}_{1\alpha}\mathcal{P}_{1\beta}\mathcal{P}_{1\bar\alpha}\mathcal{P}_{1\bar\beta}\Big\}\ .
\end{aligned}
\tag{C.64}
$$

Separating the term that contains $P^4$, the result can be written as

$$
\begin{aligned}
\Theta_{\text{II,III}}\ \to\ \mathcal{N}\Big\{&2(s_{12}s_{23}-m^2s_{13})+\frac{(s_{12}-s_{23})^2+2m^2s_{13}}{s_{12}s_{23}}P^4-4p_{2\perp}^2(s_{13}+m^2)\\
&+2p_{1\perp}^2\left(\frac{s_{12}^2}{s_{23}}+s_{12}-2s_{23}+4m^2\right)+2p_{3\perp}^2\left(\frac{s_{23}^2}{s_{12}}+s_{23}-2s_{12}+4m^2\right)\\
&+2m^2\left(\frac{p_{1\perp}^4}{s_{23}}+\frac{p_{1\perp}^4}{s_{12}}\right)-p_{1\perp}^2p_{3\perp}^2\left[4+2m^2\left(\frac{1}{s_{12}}+\frac{1}{s_{23}}\right)-\frac{4m^4}{s_{12}s_{23}}\right]\\
&+2p_{1\perp}^2p_{2\perp}^2\frac{s_{12}-m^2}{s_{23}}+2p_{2\perp}^2p_{3\perp}^2\frac{s_{23}-m^2}{s_{12}}\Big\}\ .
\end{aligned}
\tag{C.65}
$$

**Final result**

The different contributions can now be added together as described in eq. (C.37). For this, it is worth to proceed in steps. First we compute the total $p_\perp$-independent contribution,

$$
\Theta|_1=s_{12}^2-2m^2s_{12}+m^4+s_{23}^2-2m^2s_{23}+m^4+2s_{12}s_{23}-2m^2s_{13}=(s_{13}-m^2)^2\ . \tag{C.66}
$$

On the other hand, the coefficients of the $P^4$ terms add to

$$
\Theta|_{P^4}=4-\frac{(s_{12}+s_{23})^2+2m^2s_{13}}{s_{12}s_{23}}+\frac{(s_{12}-s_{23})^2+2m^2s_{13}}{s_{12}s_{23}}=0\ . \tag{C.67}
$$

Similarly, we compute the total coefficients for the $p_\perp^2$ contributions,

$$\begin{aligned}
\Theta|_{p_{1\perp}^2} &= -2s_{12} - 4m^2 + 4s_{23} - 2\frac{s_{12}}{s_{23}}(s_{12} - 2m^2) + 2\frac{s_{12}^2}{s_{23}} + 2s_{12} - 4s_{23} + 8m^2 \\
&= 4m^2\left(1 + \frac{s_{12}}{s_{23}}\right) , \\
\Theta|_{p_{2\perp}^2} &= 4s_{13} - 4(s_{13} + m^2) = -4m^2 , \\
\Theta|_{p_{3\perp}^2} &= 4m^2\left(1 + \frac{s_{23}}{s_{12}}\right) ,
\end{aligned} \tag{C.68}$$

such that together they yield

$$\frac{\Theta|_{p_\perp^2}}{-4m^2(s_{13} - m^2)} = \frac{p_{1\perp}^2}{s_{23}} + \frac{p_{2\perp}^2}{s_{13} - m^2} + \frac{p_{3\perp}^2}{s_{12}} \overset{(C.30)}{=} -\frac{s_{13}}{s_{13} - m^2} . \tag{C.69}$$

The remaining $p_\perp^4$-contributions are

$$\begin{aligned}
\Theta|_{p_{1\perp}^4} &= \frac{2m^4}{s_{23}^2} - \frac{2m^2}{s_{23}} + \frac{2m^2}{s_{23}} = \frac{2m^4}{s_{23}^2} , \\
\Theta|_{p_{2\perp}^4} &= \frac{2s_{13}^2}{(s_{13} - m^2)^2} - 2\frac{s_{13} + m^2}{s_{13} - m^2} = \frac{2m^4}{(s_{13} - m^2)^2} , \\
\Theta|_{p_{3\perp}^4} &= \frac{2m^4}{s_{12}^2} - \frac{2m^2}{s_{12}} + \frac{2m^2}{s_{12}} = \frac{2m^4}{s_{12}^2} , \\
\Theta|_{p_{1\perp}^2 p_{2\perp}^2} &= 2 - \frac{2m^2}{s_{23}} + 2\frac{s_{13} - m^2}{s_{23}} + \frac{4m^2 s_{13}}{s_{23}(s_{13} - m^2)} - 2 - \frac{2s_{13}}{s_{23}} = \frac{4m^4}{s_{23}(s_{13} - m^2)} , \\
\Theta|_{p_{1\perp}^2 p_{3\perp}^2} &= 4 + 2m^2\frac{s_{12} + s_{23}}{s_{12}s_{23}} - 4 - 2m^2\frac{s_{12} + s_{23}}{s_{12}s_{23}} + \frac{4m^4}{s_{12}s_{23}} = \frac{4m^4}{s_{12}s_{23}} , \\
\Theta|_{p_{2\perp}^2 p_{3\perp}^2} &= \frac{4m^4}{s_{12}(s_{13} - m^2)} ,
\end{aligned} \tag{C.70}$$

such that they add to

$$\frac{\Theta|_{p_\perp^4}}{2m^4} = \left(\frac{p_{1\perp}^2}{s_{23}} + \frac{p_{2\perp}^2}{s_{13} - m^2} + \frac{p_{3\perp}^2}{s_{12}}\right)^2 \overset{(C.30)}{=} \left(\frac{s_{13}}{s_{13} - m^2}\right)^2 . \tag{C.71}$$

Therefore from eqs. (C.66), (C.69) and (C.71), the final result for massless gravitons reduces to

$$\begin{aligned}
\Theta(\mathcal{P}_{g_1}, \mathcal{P}_\varphi, \mathcal{P}_{g_2}) &= \mathcal{N}\frac{(s_{13} - m^2)^4 + 4m^2 s_{13}(s_{13} - m^2)^2 + 2m^4 s_{13}^2}{(s_{13} - m^2)^2} \\
&= \mathcal{N}\frac{s_{13}^4 + m^8}{(s_{13} - m^2)^2} \overset{m^2 \ll s_{13}}{\longrightarrow} \frac{16g^4 d_A c_\chi^2}{f_a^2} s_{13}^2 .
\end{aligned} \tag{C.72}$$

Given that the thermal average in eq. (C.2) sets the average magnitude of the Mandelstam invariant (or its crossing) to be $s_{13} \sim T^2$, in the regime $T \gg m$ the dependence on the inflaton mass $m$ can be neglected, and the result is free from poles.

# Bibliography


[1] M. Laine and S. Procacci, *Minimal warm inflation with complete medium response*, JCAP 06 (2021), 031 [2102.09913].

[2] P. Klose, M. Laine and S. Procacci, *Gravitational wave background from non-Abelian reheating after axion-like inflation*, JCAP 05 (2022), 021 [2201.02317].

[3] M. Laine, L. Niemi, S. Procacci and K. Rummukainen, *Shape of the hot topological charge density spectral function*, JHEP 11 (2022), 126 [2209.13804].

[4] P. Klose, M. Laine and S. Procacci, *Gravitational wave background from vacuum and thermal fluctuations during axion-like inflation*, JCAP 12 (2022), 020 [2210.11710].

[5] H. Kolesova, M. Laine and S. Procacci, *Maximal temperature of strongly-coupled dark sectors*, JHEP 05 (2023), 239 [2303.17973].

[6] V. Mukhanov and S. Winitzki, *Introduction to quantum effects in gravity*, Cambridge University Press, 2007.

[7] A. R. Liddle and D. H. Lyth, *Cosmological inflation and large scale structure*, Cambridge University Press, 2000.

[8] D. J. Schwarz, *The first second of the universe*, Annalen Phys. 12 (2003), 220 [astro-ph/0303574].

[9] V. A. Rubakov and D. S. Gorbunov, *Introduction to the Theory of the Early Universe: Hot big bang theory*, World Scientific, 2017.

[10] G. F. Smoot *et al.* [COBE], *Structure in the COBE differential microwave radiometer first year maps*, Astrophys. J. Lett. 396 (1992), L1.

[11] N. Aghanim *et al.* [Planck], *Planck 2018 results. I. Overview and the cosmological legacy of Planck*, Astron. Astrophys. 641 (2020), A1 [1807.06205].

[12] D. S. Gorbunov and V. A. Rubakov, *Introduction to the theory of the early universe: Cosmological perturbations and inflationary theory*, World Scientific, 2011.

[13] H. Kurki-Suonio, *Cosmological Perturbation Theory*, lecture notes, 2022.

[14] K. A. Malik and D. Wands, *Evolution of second-order cosmological perturbations*, Class. Quant. Grav. 21 (2004), L65 [astro-ph/0307055].

[15] R. L. Arnowitt, S. Deser and C. W. Misner, *The Dynamics of general relativity*, Gen. Rel. Grav. 40 (2008), 1997 [gr-qc/0405109].

[16] J. M. Bardeen, *Gauge Invariant Cosmological Perturbations*, Phys. Rev. D 22 (1980), 1882.

[17] G. B. Arfken and H. J. Weber, *Mathematical methods for physicists*, Elsevier Academic Press, 2005.

[18] S. Weinberg, *Cosmology*, Oxford University Press, 2008.

[19] C. P. Ma and E. Bertschinger, *Cosmological perturbation theory in the synchronous and conformal Newtonian gauges*, Astrophys. J. 455 (1995), 7 [astro-ph/9506072].

[20] A. A. Starobinsky, *Spectrum of relict gravitational radiation and the early state of the universe*, JETP Lett. 30 (1979), 682.

[21] R. Flauger, N. Karnesis, G. Nardini, M. Pieroni, A. Ricciardone and J. Torrado, *Improved reconstruction of a stochastic gravitational wave background with LISA,* JCAP 01 (2021) 059 [2009.11845].

[22] J. Martin, C. Ringeval and V. Vennin, *Encyclopædia Inflationaris*, Phys. Dark Univ. 5 (2014), 75 [1303.3787].

[23] A. H. Guth, *The Inflationary Universe: A Possible Solution to the Horizon and Flatness Problems*, Phys. Rev. D 23 (1981), 347.

[24] A.D. Linde, *Chaotic Inflation,* Phys. Lett. B 129 (1983) 177.

[25] D. Baumann, *TASI Lectures on Inflation*, [0907.5424].

[26] M. P. Hertzberg, *On Inflation with Non-minimal Coupling*, JHEP 11 (2010), 023 [1002.2995].

[27] M. E. Peskin and D. V. Schroeder, *An Introduction to quantum field theory*, Addison-Wesley, 1995.

[28] M. Sasaki, Y. Nambu and K. i. Nakao, *Classical Behavior of a Scalar Field in the Inflationary Universe*, Nucl. Phys. B 308 (1988), 868.

[29] M. Matsumiya, M. Sasaki and J. Yokoyama, *Cosmic inversion: Reconstructing primordial spectrum from CMB anisotropy*, Phys. Rev. D 65 (2002), 083007 [astro-ph/0111549].

[30] N. Kogo, M. Sasaki and J. Yokoyama, *Reconstructing the primordial spectrum with CMB temperature and polarization*, Phys. Rev. D 70 (2004), 103001 [astro-ph/0409052].

[31] R. Durrer, *The Cosmic Microwave Background*, Cambridge University Press, 2008.

[32] R. K. Sachs and A. M. Wolfe, *Perturbations of a cosmological model and angular variations of the microwave background*, Astrophys. J. 147 (1967), 73.

[33] E. Pajer and S. Jazayeri, *Systematics of Adiabatic Modes: Flat Universes*, JCAP 03 (2018), 013 [1710.02177].

[34] K. Enqvist and H. Kurki-Suonio, *Constraining isocurvature fluctuations with the Planck surveyor*, Phys. Rev. D 61 (2000), 043002 [astro-ph/9907221].

[35] H. Kurki-Suonio, *Physics of the Cosmic Microwave Background and the Planck Mission*, lecture notes, 2010.

[36] S. Scodeller, M. Kunz and R. Durrer, *CMB anisotropies from acausal scaling seeds*, Phys. Rev. D 79 (2009), 083515 [0901.1845].

[37] J. Silk, *Cosmic black body radiation and galaxy formation*, Astrophys. J. 151 (1968), 459.

[38] Y. Akrami *et al.* [Planck], *Planck 2018 results. X. Constraints on inflation*, Astron. Astrophys. 641 (2020), A10 [1807.06211].

[39] M. Zaldarriaga and U. Seljak, *An all sky analysis of polarization in the microwave background*, Phys. Rev. D 55 (1997), 1830 [astro-ph/9609170].

[40] P. A. R. Ade *et al.* [Planck], *Planck 2013 results. XV. CMB power spectra and likelihood*, Astron. Astrophys. 571 (2014), A15 [1303.5075].

[41] N. Bartolo, C. Caprini, V. Domcke, D. G. Figueroa, J. Garcia-Bellido, M. C. Guzzetti, M. Liguori, S. Matarrese, M. Peloso and A. Petiteau, *et al. Science with the space-based interferometer LISA. IV: Probing inflation with gravitational waves*, JCAP 12 (2016), 026 [1610.06481].

[42] P. Amaro-Seoane *et al.* [LISA], *Laser Interferometer Space Antenna*, [1702.00786].

[43] P. Auclair *et al.* [LISA Cosmology Working Group], *Cosmology with the Laser Interferometer Space Antenna*, [2204.05434].

[44] S. Babak, A. Petiteau and M. Hewitson, *LISA Sensitivity and SNR Calculations*, [2108.01167].

[45] R. A. Alpher, H. Bethe and G. Gamow, *The origin of chemical elements*, Phys. Rev. 73 (1948), 803.

[46] R. H. Cyburt, B. D. Fields, K. A. Olive and T. H. Yeh, *Big Bang Nucleosynthesis: 2015*, Rev. Mod. Phys. 88 (2016), 015004 [1505.01076].

[47] M. Escudero Abenza, *Precision early universe thermodynamics made simple: $N_{\rm eff}$ and neutrino decoupling in the Standard Model and beyond*, JCAP 05 (2020), 048 [2001.04466].

[48] M. Cielo, M. Escudero, G. Mangano and O. Pisanti, *Neff in the Standard Model at NLO is 3.043*, [2306.05460].

[49] T. Kahniashvili, E. Clarke, J. Stepp and A. Brandenburg, *Big Bang Nucleosynthesis Limits and Relic Gravitational-Wave Detection Prospects*, Phys. Rev. Lett. 128 (2022), 22 [2111.09541].

[50] B. D. Fields, K. A. Olive, T. H. Yeh and C. Young, *Big-Bang Nucleosynthesis after Planck*, JCAP 03 (2020), 010 [erratum: JCAP 11 (2020), E02], [1912.01132].

[51] K.D. Lozanov, *Lectures on Reheating after Inflation*, [1907.04402].

[52] L. Kofman, A. D. Linde and A. A. Starobinsky, *Towards the theory of reheating after inflation*, Phys. Rev. D 56 (1997), 3258 [hep-ph/9704452].

[53] A. Berera, *Warm inflation*, Phys. Rev. Lett. 75 (1995) 3218 [astro-ph/9509049].

[54] J. Yokoyama and A.D. Linde, *Is warm inflation possible?*, Phys. Rev. D 60 (1999) 083509 [hep-ph/9809409].

[55] R. Rangarajan, *Current Status of Warm Inflation,* [1801.02648].

[56] V. Kamali, M. Motaharfar and R. O. Ramos, *Recent Developments in Warm Inflation*, Universe 9 (2023) 124 [2302.02827].

[57] M. Laine and A. Vuorinen, *Basics of Thermal Field Theory*, Lect. Notes Phys. 925 (2016) 1 [1701.01554].

[58] Y. Fu, J. Ghiglieri, S. Iqbal and A. Kurkela, *Thermalization of non-Abelian gauge theories at next-to-leading order*, Phys. Rev. D 105 (2022) 054031 [2110.01540].

[59] K.V. Berghaus, P.W. Graham and D.E. Kaplan, *Minimal Warm Inflation*, JCAP 03 (2020) 034 [1910.07525].

[60] K.V. Berghaus and T. Karwal, *Thermal Friction as a Solution to the Hubble Tension*, Phys. Rev. D 101 (2020) 083537 [1911.06281].

[61] G. Goswami and C. Krishnan, *Swampland, Axions and Minimal Warm Inflation*, Phys. Rev. D 101 (2020) 10 [1911.00323].

[62] Y. Reyimuaji and X. Zhang, *Warm-assisted natural inflation*, JCAP 04 (2021), 077 [2012.07329].

[63] J. Ignatius, K. Kajantie, H. Kurki-Suonio and M. Laine, *The growth of bubbles in cosmological phase transitions*, Phys. Rev. D 49 (1994) 3854 [astro-ph/9309059].

[64] W. DeRocco, P.W. Graham and S. Kalia, *Warming up cold inflation,* JCAP 11 (2021) 011 [2107.07517].

[65] E. Papantonopoulos, T. Uematsu and T. Yanagida, *Natural chaotic inflation*, Phys. Lett. B 183 (1987), 282.

[66] K. Freese, J.A. Frieman and A.V. Olinto, *Natural inflation with pseudo Nambu-Goldstone bosons*, Phys. Rev. Lett. 65 (1990) 3233.

[67] M. S. Turner and F. Wilczek, *Inflationary axion cosmology*, Phys. Rev. Lett. 66 (1991), 5.

[68] E. Dimastrogiovanni, M. Fasiello and T. Fujita, *Primordial Gravitational Waves from Axion-Gauge Fields Dynamics*, JCAP 01 (2017), 019 [1608.04216].

[69] F. Takahashi and W. Yin, *Challenges for heavy QCD axion inflation*, JCAP 10 (2021), 057 [2105.10493].

[70] E. Pajer and M. Peloso, *A review of Axion Inflation in the era of Planck*, Class. Quant. Grav. 30 (2013), 214002 [1305.3557].

[71] L. Visinelli, *Natural Warm Inflation*, JCAP 09 (2011), 013 [1107.3523].

[72] H. Mishra, S. Mohanty and A. Nautiyal, *Warm natural inflation*, Phys. Lett. B 710 (2012) 245 [1106.3039].

[73] A. Hook and G. Marques-Tavares, *Relaxation from particle production*, JHEP 12 (2016) 101 [1607.01786].

[74] R.Z. Ferreira and A. Notari, *Thermalized Axion Inflation*, JCAP 09 (2017), 007 [1706.00373].

[75] R.Z. Ferreira and A. Notari, *Thermalized axion inflation: natural and monomial inflation with small r*, Phys. Rev. D 97 (2018) 063528 [1711.07483].

[76] V. Kamali, *Warm pseudoscalar inflation*, Phys. Rev. D 100 (2019) 043520 [1901.01897].

[77] R. D. Peccei and H. R. Quinn, *CP Conservation in the Presence of Instantons*, Phys. Rev. Lett. 38 (1977), 1440.

[78] A. Ringwald, *Axions and Axion-Like Particles*, [1407.0546].

[79] M. M. Anber and L. Sorbo, *Naturally inflating on steep potentials through electromagnetic dissipation*, Phys. Rev. D 81 (2010), 043534 [0908.4089].

[80] G. 't Hooft, *Computation of the Quantum Effects Due to a Four-Dimensional Pseudoparticle*, Phys. Rev. D 14 (1976), 3432 [erratum: Phys. Rev. D 18 (1978), 2199].

[81] C. G. Callan, Jr., R. F. Dashen and D. J. Gross, *A Theory of Hadronic Structure*, Phys. Rev. D 19 (1979), 1826.

[82] M. Gockeler, A. S. Kronfeld, M. L. Laursen, G. Schierholz and U. J. Wiese, *Topology in SU(3) Lattice Gauge Theory: First Calculation of the Topological Susceptibility*, Nucl. Phys. B 292 (1987), 349.

[83] D. J. Gross, R. D. Pisarski and L. G. Yaffe, *QCD and Instantons at Finite Temperature*, Rev. Mod. Phys. 53 (1981), 43.

[84] S. Caron-Huot, *Asymptotics of thermal spectral functions*, Phys. Rev. D 79 (2009) 125009 [0903.3958].

[85] M. Laine, A. Vuorinen and Y. Zhu, *Next-to-leading order thermal spectral functions in the perturbative domain*, JHEP 09 (2011) 084 [1108.1259].

[86] G.D. Moore and M. Tassler, *The Sphaleron Rate in SU(N) Gauge Theory*, JHEP 02 (2011) 105 [1011.1167].

[87] M. Cè, C. Consonni, G. P. Engel and L. Giusti, *Non-Gaussianities in the topological charge distribution of the SU(3) Yang–Mills theory*, Phys. Rev. D 92 (2015) 074502 [1506.06052].

[88] L. Giusti and M. Lüscher, *Topological susceptibility at $T > T_c$ from master-field simulations of the SU(3) gauge theory*, Eur. Phys. J. C 79 (2019) 207 [1812.02062].

[89] G. Cuniberti, E. De Micheli and G. A. Viano, *Reconstructing the thermal Green functions at real times from those at imaginary times*, Commun. Math. Phys. 216 (2001), 59 [cond-mat/0109175].

[90] Y. Burnier, M. Laine and L. Mether, *A Test on analytic continuation of thermal imaginary-time data*, Eur. Phys. J. C 71 (2011), 1619 [1101.5534].

[91] L. Altenkort, A.M. Eller, O. Kaczmarek, L. Mazur, G.D. Moore and H.T. Shu, *Sphaleron*

*rate from Euclidean lattice correlators: An exploration*, Phys. Rev. D 103 (2021) 114513 [2012.08279].

[92] M. Barroso Mancha and G.D. Moore, *The sphaleron rate from 4D Euclidean lattices*, JHEP 01 (2023) 155 [2210.05507].

[93] J. C. Collins, *Renormalization*, Cambridge University Press (1986).

[94] A. Francis, O. Kaczmarek, M. Laine, T. Neuhaus and H. Ohno, *Critical point and scale setting in SU(3) plasma: An update*, Phys. Rev. D 91 (2015) 096002 [1503.05652].

[95] M. Kitazawa, T. Iritani, M. Asakawa, T. Hatsuda and H. Suzuki, *Equation of state for SU(3) gauge theory via the energy-momentum tensor under gradient flow*, Phys. Rev. D 94 (2016) 114512 [1610.07810].

[96] L. Giusti and M. Pepe, *Equation of state of the SU(3) Yang-Mills theory: A precise determination from a moving frame*, Phys. Lett. B 769 (2017) 385 [1612.00265].

[97] H.B. Meyer, *High-precision thermodynamics and Hagedorn density of states*, Phys. Rev. D 80 (2009) 051502 [0905.4229].

[98] A. Ringwald, K. Saikawa and C. Tamarit, *Primordial gravitational waves in a minimal model of particle physics and cosmology*, JCAP 02 (2021), 046 [2009.02050].

[99] A. Ringwald and C. Tamarit, *Revealing the cosmic history with gravitational waves*, Phys. Rev. D 106 (2022) 063027 [2203.00621].

[100] R. Easther and E. A. Lim, *Stochastic gravitational wave production after inflation*, JCAP 04 (2006), 010 [astro-ph/0601617].

[101] J. L. Cook and L. Sorbo, *Particle production during inflation and gravitational waves detectable by ground-based interferometers*, Phys. Rev. D 85 (2012), 023534 [erratum: Phys. Rev. D 86 (2012), 069901] [1109.0022].

[102] N. Barnaby, E. Pajer and M. Peloso, *Gauge Field Production in Axion Inflation: Consequences for Monodromy, non-Gaussianity in the CMB, and Gravitational Waves at Interferometers*, Phys. Rev. D 85 (2012), 023525 [1110.3327].

[103] M. M. Anber and L. Sorbo, *Non-Gaussianities and chiral gravitational waves in natural steep inflation*, Phys. Rev. D 85 (2012), 123537 [1203.5849].

[104] P. Adshead, J. T. Giblin, T. R. Scully and E. I. Sfakianakis, *Gauge-preheating and the end of axion inflation*, JCAP 12 (2015), 034 [1502.06506].

[105] D. Jiménez, K. Kamada, K. Schmitz and X. J. Xu, *Baryon asymmetry and gravitational waves from pseudoscalar inflation*, JCAP 12 (2017), 011 [1707.07943].

[106] P. Adshead, J. T. Giblin, M. Pieroni and Z. J. Weiner, *Constraining axion inflation with gravitational waves from preheating*, Phys. Rev. D 101 (2020) 083534 [1909.12842].

[107] R. O. Ramos and L. A. da Silva, *Power spectrum for inflation models with quantum and thermal noises*, JCAP 03 (2013), 032 [1302.3544].

[108] Y. Qiu and L. Sorbo, *Spectrum of tensor perturbations in warm inflation*, Phys. Rev. D 104 (2021) 083542 [2107.09754].

[109] L. Ji, D. E. Kaplan, S. Rajendran and E. H. Tanin, *Thermal perturbations from cosmological constant relaxation*, Phys. Rev. D 105 (2022) 015025 [2109.05285].

[110] C. Graham and I. G. Moss, *Density fluctuations from warm inflation*, JCAP 07 (2009), 013 [0905.3500].

[111] L. Visinelli, *Cosmological perturbations for an inflaton field coupled to radiation*, JCAP 01 (2015), 005 [1410.1187].

[112] M. Benetti and R. O. Ramos, *Warm inflation dissipative effects: predictions and constraints*

*from the Planck data*, Phys. Rev. D 95 (2017) 023517 [1610.08758].

[113] M. Bastero-Gil, A. Berera and J. R. Calderón, *Reexamination of the warm inflation curvature perturbations spectrum*, JCAP 07 (2019), 019 [1904.04086].

[114] E.M. Lifshitz and L.P. Pitaevskii, *Statistical Physics, Part 2*, Butterworth-Heinemann (1980).

[115] L.D. Landau and E.M. Lifshitz, *Fluid Mechanics*, Pergamon Press (1987).

[116] J.I. Kapusta, B. Müller and M. Stephanov, *Relativistic theory of hydrodynamic fluctuations with applications to heavy-ion collisions*, Phys. Rev. C 85 (2012) 054906 [1112.6405].

[117] P. B. Arnold, G. D. Moore and L. G. Yaffe, *Transport coefficients in high temperature gauge theories. 1. Leading log results*, JHEP 11 (2000), 001 [hep-ph/0010177].

[118] A. Buonanno, *Gravitational waves*, [0709.4682].

[119] S. Weinberg, *Damping of tensor modes in cosmology*, Phys. Rev. D 69 (2004), 023503 [astro-ph/0306304].

[120] Y. Watanabe and E. Komatsu, *Improved calculation of the primordial gravitational wave spectrum in the standard model*, Phys. Rev. D 73 (2006) 123515 [astro-ph/0604176].

[121] K. Saikawa and S. Shirai, *Primordial gravitational waves, precisely: the role of thermodynamics in the Standard Model*, JCAP 05 (2018) 035 [1803.01038].

[122] M. Laine and M. Meyer, *Standard Model thermodynamics across the electroweak crossover*, JCAP 07 (2015), 035 [1503.04935].

[123] `http://www.laine.itp.unibe.ch/eos15/`

[124] M. Laine and Y. Schröder, *Quark mass thresholds in QCD thermodynamics*, Phys. Rev. D 73 (2006), 085009 [hep-ph/0603048].

[125] J. Ghiglieri and M. Laine, *Gravitational wave background from Standard Model physics: Qualitative features*, JCAP 07 (2015), 022 [1504.02569].

[126] J. Ghiglieri, G. Jackson, M. Laine and Y. Zhu, *Gravitational wave background from Standard Model physics: Complete leading order*, JHEP 07 (2020) 092 [2004.11392].

[127] D. Bödeker, M. Sangel and M. Wörmann, *Equilibration, particle production, and self-energy*, Phys. Rev. D 93 (2016) 045028 [1510.06742].

[128] G. Jackson and M. Laine, *Efficient numerical integration of thermal interaction rates*, JHEP 09 (2021) 125 [2107.07132].

[129] P. Schwaller, *Gravitational Waves from a Dark Phase Transition*, Phys. Rev. Lett. 115 (2015) 181101 [1504.07263].

[130] T. Hambye and M.H.G. Tytgat, *Confined hidden vector dark matter*, Phys. Lett. B 683 (2010) 39 [0907.1007].

[131] A. Soni and Y. Zhang, *Hidden SU(N) glueball dark matter*, Phys. Rev. D 93 (2016) 115025 [1602.00714].

[132] C. Gross, S. Karamitsos, G. Landini and A. Strumia, *Gravitational vector Dark Matter*, JHEP 03 (2021) 174 [2012.12087].

[133] K. A. Malik and D. Wands, *Cosmological perturbations*, Phys. Rept. 475 (2009), 1 [0809.4944].

[134] K. A. Malik and D. R. Matravers, *A Concise Introduction to Perturbation Theory in Cosmology*, Class. Quant. Grav. 25 (2008), 193001 [0804.3276].

[135] M. Laine, M. Vepsäläinen and A. Vuorinen, *Ultraviolet asymptotics of scalar and pseudoscalar correlators in hot Yang-Mills theory*, JHEP 10 (2010), 010 [1008.3263].

[136] `https://oeis.org/A001620`

# Acknowledgements


* **Thank you**
  Mikko, especially for the always precious and precise feedbacks, the great availability and support, and the kind guidance throughout these years.
  Helena for plenty of inspiring and helpful discussions.
  Hannu Kurki-Suonio for providing your excellent lecture notes online.
  Chiara and Alberto for your time and engagement.
  Jorinde for the perseverance explaining this and that to me during your visit.
  Greg for the help with your code, and inspiring me to pursue a PhD.
  Andrea and Léo for cheerful company and interesting discussions at CERN.
  Dietrich, Dominik, Susi and Irene for welcoming me in Bielefeld.
  Guilherme, Enrico, Adrien, Marco, Francesco, Tom, and Craig for having me in Pisa.
  Admir for stimulating and candid conversations.
  Philipp and Seyong for actively participating in our group meetings.
  Rafael, Jakub and Ajdin for fun hours together as teaching assistants.
  To the students, in particular Armando, Daniil, Fabio, Federico, Ivan, Jan, Lara, Lukas, Rebecca and Valentin for insightful conversations about physics.
  To Nicolas, Samuel, Sebastian and the other fellow PhD students and postdocs for sharing moments not only at the ITP.

* **Danke**
  Matthias und Uwe-Jens für das Vorbild und für die Unterstützung.
  Binia für den frischen Wind durch das Institut.
  Esther für den Unternehmergeist betreffend meiner Steuersituation.
  Markus für eine sympatische Bürogemeinschaft.
  Res und Rolf für dieses Reich und die Freundschaft.

* **Grazie**
  Martina soprattutto per i pranzi spensierati, le ore sportive e i gelati.
  Fadua per aver pulito giosamente il nostro ufficio ogni mercoledì.
  Simone per una lieta collaborazione che spero continui a lungo.
  Michael per le estese chiacchere di fisica in Francia.
  Germano per la stimolante e simpatica visita a Stavanger.
  Martina Gerbino per la pazienza a rispondere alle mie domande durante la scuola al GGI.
  Gilberto per quella discussione aperta che mi ha parzialmente messo a posto la coscienza.
  Alla mia famiglia in senso lato, e agli amici, per aver contribuito quotidianamente ad uno scambio interdisciplinare e per aver sopportato me e le mie assenze.
  Phil che quando i miei conti non tornavano mai tu preparavi le lasagne e riparavi la bici...

* **Obrigada**
  Mestre Matias e toda a família da Brasil Capoeira pela melhor distração.

This work was supported by the Swiss National Science Foundation under grant 200020B–188712.

# Declaration of consent

on the basis of Article 18 of the PromR Phil.-nat. 19

Name/First Name: Procacci Simona

Registration Number: 15 - 130 - 347

Study program: Physics

Bachelor ☐ Master ☐ Dissertation ☑

Title of the thesis: Towards a thermally complete study of inflationary predictions

Supervisor: Mikko Laine

I declare herewith that this thesis is my own work and that I have not used any sources other than those stated. I have indicated the adoption of quotations as well as thoughts taken from other authors as such in the thesis. I am aware that the Senate pursuant to Article 36 paragraph 1 litera r of the University Act of September 5th, 1996 and Article 69 of the University Statute of June 7th, 2011 is authorized to revoke the doctoral degree awarded on the basis of this thesis.
For the purposes of evaluation and verification of compliance with the declaration of originality and the regulations governing plagiarism, I hereby grant the University of Bern the right to process my personal data and to perform the acts of use this requires, in particular, to reproduce the written thesis and to store it permanently in a database, and to use said database, or to make said database available, to enable comparison with theses submitted by others.

Place/Date Bern, 28.06.2023
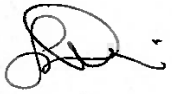
Signature